NOVA SCHOOL OF SCIENCE & TECHNOLOGY

DEPARTAMENT OF CHEMISTRY

Beatriz Isabel Serrano Garcia

BSc in Applied Chemistry

Molybdenum(0) Triazolylidenes as Catalysts for Borrowing Hydrogen Processes

Supervisor: Dr. Beatriz Royo, Principal Investigator, ITQB NOVA

DISSERTATION PRESENTED TO OBTAIN THE MASTER DEGREE IN BIOORGANIC CHEMISTRY

NOVA University Lisbon
September, 2023

NOVA SCHOOL OF SCIENCE & TECHNOLOGY

DEPARTAMENT OF CHEMISTRY

Molybdenum(0) Triazolylidenes as Catalysts for Borrowing Hydrogen Processes

Beatriz Isabel Serrano Garcia

BSc in Applied Chemistry

Supervisor: Dr. Beatriz Royo

Principal Investigator, ITQB NOVA

DISSERTATION PRESENTED TO OBTAIN THE MASTER DEGREE IN BIOORGANIC CHEMISTRY

NOVA University Lisbon
September, 2023

Molybdenum(0) Triazolylidenes as Catalysts for Borrowing Hydrogen Processes

Table of contents

Acknowledgments

I would like to express my sincere gratitude and appreciation to the following people and institutions who have played a significant role in the completion of this thesis.

Firstly, I would like to express my deepest gratitude to my supervisor Dra. Beatriz Royo for her unwavering guidance, invaluable insights, and endless support throughout this research. I am deeply thankful to her for giving me the opportunity to present my work at the XXV Conference on Organometallic Chemistry (EuCOMC XXV) held at the University of Alcalá. This experience not only enriched my knowledge but also allowed me to connect with experts in the field and gain valuable insights into international opportunities.

I would like to acknowledge FC&T (Fundação para a Ciência e Tecnologia) for providing financial support PTDC/QUI-QIN/0359/2021, PTDC/QUI-QOR/0712/2020, MOSTMICRO-ITQB, UIDB/04612/20220 and UIPD/04612/2020, which made this research possible. Furthermore, I would like to recognize NOVA University, the institution where I spent the past five years, for providing me with the necessary knowledge to complete this thesis. I would also like to extend my appreciation to ITQB, the institution that facilitated the execution of this thesis.

I would like to thank Helena Matias for all availability and help on the NMR service, especially with the ^{95}Mo NMR spectra. I extend my thanks to M. Conceição Almeida and Dra. Clara Gomes for the elemental analysis and structural determination of the compounds.

I am also grateful to all of my laboratory colleagues, Sofia, Dr. Luís Lima, Daniel, Henrique, and Maria, for always being available to provide all of the support and guidance necessary to overcome all of the challenges that have emerged over time. I have to express a special appreciation to Sofia for welcoming me into the lab from the beginning and teaching me all of the lab's methodologies and techniques, but also for being an amazing friend. To Dr. Luís Lima I have to express my deepest gratitude for all of the help, patience, and motivational words. The discussions and debates have enriched my knowledge and perspective.

To my friends, some of them Daniela, Bia, Margarida, Bárbara, Marta, Guilherme, João, and David, who have been a constant source of encouragement and support, I thank you for your patience, understanding, and unwavering belief in me throughout this challenging journey. I would like to express a special thanks to Daniela, Bia, and Margarida in particular for providing the emotional strength I needed to persevere through the long hours of research and writing. Finally, I would like to express my gratitude to my parents whose support made everything achievable.

A thesis cannot be done alone, and I am truly grateful for the role each of you has played in this achievement.

Thank you!

Resumo

Esta tese descreve a síntese e caracterização de complexos de molibdénio(0) com ligandos bidentados contendo fragmentos de triazolilideno/piridina/triazole, bem como a sua aplicação catalítica em processos de *borrowing hydrogen* (BH) e *acceptorless dehydrogenative coupling* (ADC), e na oxidação de aminas primárias a amidas.

O manuscrito da tese está organizado em quatro capítulos. O Capítulo 1 apresenta uma introdução geral aos carbenos N-heterocíclicos (NHCs) e mesoiónicos (MICs), incluindo uma discussão sobre as suas propriedades eletrónicas e os métodos sintéticos utilizados para a preparação de 1,2,3-triazolilidenos (trz). Além disso, está incluído o estado da arte dos complexos de molibdénio contendo ligandos bidentados NHC e a sua aplicação catalítica em processos BH e ADC. Por fim, são apresentados o objetivo principal da tese e os objetivos específicos.

O Capítulo 2 descreve a síntese e caracterização de uma nova família de complexos Mo(0) tetracarbonilo contendo ligandos bidentados 1,2,3-triazolilideno. Todos os complexos foram caracterizados por espectroscopia de RMN (^{1}H, ^{13}C e ^{95}Mo) e IR, e por análise elementar. Além disso, a estrutura molecular do complexo Mo contendo o ligando piridil-triazolilideno foi determinada por estudos de difração de raios-X de cristal único. A capacidade doadora dos ligandos NHC e MIC também é discutida.

O Capítulo 3 descreve a aplicação dos novos complexos de molibdénio(0) descritos no Capítulo 2 na síntese de quinolinas, *N*-alquilação de aminas com álcoois, α-alquilação de cetonas com álcoois, β-alquilação entre álcoois e oxidação de aminas. Entre os diferentes complexos [$Mo(CO)_4$(trz)], o complexo com o grupo Et como substituinte apresentou a maior atividade catalítica na síntese de quinolinas e na oxidação de aminas. Em contraste, o complexo Mo contendo o ligando triazolilideno com grupos fenil nas posições N3 foi mais ativo na α-alquilação de cetonas com álcoois.

Por fim, no Capítulo 4, são apresentadas as conclusões da tese.

Termos chave: molibdénio; ligandos triazolilidenos; borrowing hydrogen; quinolinas

Summary

This thesis describes the synthesis and characterization of a new family of molybdenum(0) complexes with bidentate ligands containing triazolylidene/pyridine/triazole fragments and different wingtips, as well as their catalytic application in borrowing hydrogen (BH) and acceptorless dehydrogenative coupling (ADC) processes, and in the oxidation of primary amines to amides.

The manuscript of the thesis is organized in four chapters. Chapter 1 presents a general introduction to N-heterocyclic (NHCs) and mesoionic carbenes (MICs), including a discussion of their electronic properties and the synthetic methods used for the preparation of 1,2,3-triazolylidenes (trz). In addition, the state-of-the-art of molybdenum complexes bearing bidentate NHC and their catalytic application in BH and ADC processes are included. Finally, the main goal of the thesis and the specific objectives are presented.

Chapter 2 describes the synthesis and characterization of a new family of Mo(0) tetracarbonyl complexes containing bis-chelating 1,2,3-triazolylidene ligands. All complexes were characterized by NMR (^{1}H, ^{13}C, and ^{95}Mo) and IR spectroscopy, and by elemental analysis. In addition, the molecular structure of the Mo complex containing the mixed pyridyl-triazolylidene ligand was determined by single-crystal X-ray diffraction studies. The donor capacity of the NHC and MIC ligands is also discussed.

Chapter 3 describes the application of the novel molybdenum(0) complexes described in Chapter 2 in the synthesis of quinolines, *N*-alkylation of amines with alcohols, α-alkylation of ketones with alcohols, β-alkylation between alcohols, and in the oxidation of amines. Among the different [Mo(CO)$_4$(trz)] complexes, the ethyl wingtip-substituted complex showed the highest catalytic activity in the synthesis of quinolines and the oxidation of amines. In contrast, the Mo complex bearing the triazolylidene ligand with phenyl groups at N3 positions was more active in the α-alkylation of ketones with alcohols.

Finally, in Chapter 4, the conclusions of the thesis are presented.

Keywords*:* molybdenum; triazolylidene ligands; borrowing hydrogen; quinolines

List of Publications and Communications

Publication: Beatriz Garcia, Beatriz Royo, Molybdenum Triazolylidenes for the Dehydrogenative Synthesis of Quinolines, *Catal. Sci. Technol*., manuscript under preparation to be submitted in Nov. 2023.

Communication: Beatriz Garcia, Beatriz Royo, Mesoionic Carbenes of Molybdenum(0) as Catalysts for Acceptorless Dehydrogenative Coupling Reactions, XXV Conference on Organometallic Chemistry, EuCOMC XXV, University of Alcalá, Madrid, Spain, September 4th-8th 2023. Poster communication presented by Beatriz Garcia (PA70).

Oral presentation: Beatriz Garcia, Beatriz Royo, Molybdenum(0) Triazolylidenes as Catalysts for Borrowing Hydrogen Processes, Jornadas Intercalares das Dissertações Anuais dos Mestrados dos Departamentos de Química e de Ciências da Vida 2023, JIM2023, NOVA University, Lisbon, March 1st 2023. Oral communication presented by Beatriz Garcia.

List of Abbreviations and Symbols

Å	Angström
ADC	Acceptorless Dehydrogenative Coupling
bis-NHC	bis(N-Heterocyclic Carbene)
bis-trz	bis(1,2,3-Triazolylidene)
BH	Borrowing Hydrogen
Bu	Butyl
BuOH	Butanol
CuAAC	Copper(I)- Catalyzed Azide-Alkyne Cycloaddition
Et	Ethyl
IR	Infrared Spectroscopy
$KOBu^t$	Potassium *tert*-Butoxide
m	*meta*-
Me	Methyl
MeI	Methyl Iodide
MeOTf	Methyl Trifluoromethanesulfonate
MIC	Mesoionic Carbene
NHC	N-Heterocyclic Carbene
NMR	Nuclear Magnetic Resonance
o	*ortho*-
OTf	Triflate
p	*para*-
Ph	Phenyl
py	Pyridine
t	*tert*
TBAB	Tetrabutylammonium bromide
THF	Tetrahydrofuran
trz	1,2,3-Triazolylidene
X	Generalized Anionic Ligand (usually halogen)
σ	sigma
π	pi
α	alpha
γ	gamma
β	beta
J	Coupling Constant
δ	Chemical Shift in ppm (NMR)
Hz	Hertz
v	Wavenumber (cm^{-1})

List of Figures

Chapter 1

Chapter 2

List of Schemes

Chapter 1

Chapter 2

Chapter 3

List of Tables

Chapter 2

Chapter 3

Chapter 1

Introduction and Objectives

1.1. N-Heterocyclic and Mesoionic Carbene Ligands

1.1.1. General Aspects

1.1.2. Preparation of Triazolylidenes: Click Chemistry

1.2. Molybdenum NHC and MIC Complexes

1.3. Molybdenum Complexes in Borrowing Hydrogen (BH) Reactions

1.4. Objective of the Thesis

1.5. References

1.1. N-Heterocyclic and Mesoionic Carbene Ligands

1.1.1. General Aspects

N-Heterocyclic carbenes (NHCs), first reported by Öfele and Wanzlick and later isolated in the free form by Arduengo, have become one of the most exciting and popular species in modern organometallic chemistry due to their ease of preparation and modularity in stereoelectronic properties. In addition, their superior σ-donation ability compared to conventional two-electron donors such as phosphines has led to numerous breakthroughs in a range of catalytic transformations.[1-4]

NHCs are electron-rich nucleophilic species that provide metal-NHC complexes with strong metal-carbon bonds. NHCs are defined as singlet carbenes in which the divalent carbenic centre is directly bonded to at least one nitrogen atom within the heterocycle. Many different types of carbene compounds with various substitution patterns, ring sizes, and degrees of heteroatom stabilization fall under these criteria. The most common ones are based on either imidazol-2-ylidenes or on 1,2,4-triazol-5-ylidenes, derived from imidazolium and 1,2,4-triazolium salts, respectively (Figure 1.1). However, imidazolium salts can also be deprotonated at the C4 position leading to imidazol-4-ylidenes, a compound class known as abnormal carbenes (aNHCs) or mesoionic carbenes (MICs) because it is not possible to formulate a localized Lewis structure of these compounds without charge separation while following the octet rule. On the other hand, 1,4-substituted 1,2,3-triazoles can be selectively methylated or arylated at the N3 atom to generate the corresponding 1,2,3-triazolium salts, which can subsequently be deprotonated to produce 1,2,3-triazol-5-ylidenes, another class of MIC ligands.[1-8] A representation of selected structures of NHCs and MICs is shown in **Figure 1.1**.

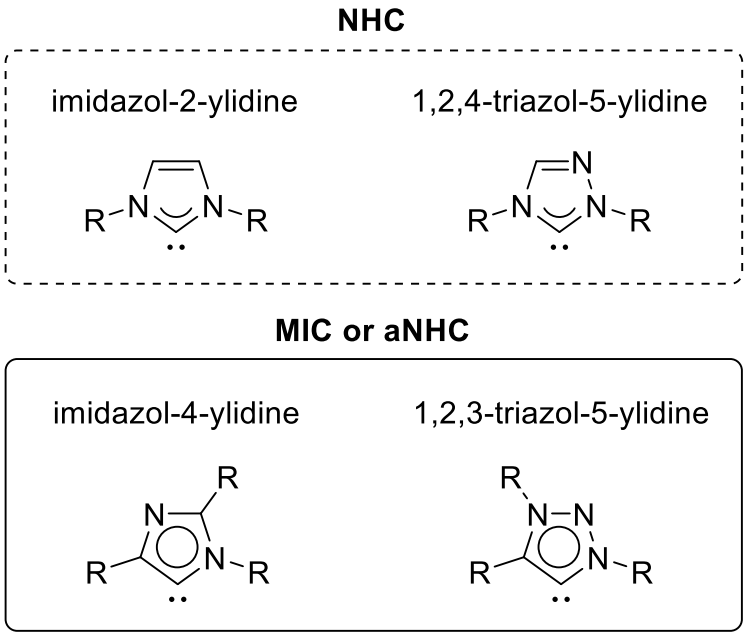

Figure 1.1. Selected structures of NHCs and mesoionic carbenes (MICs).

The unusual stability of NHCs is due to the electronic stabilization provided by the nitrogen atoms. That is, NHCs exhibit a singlet ground-state electronic configuration with a sp^2-hybridized lone pair and an unoccupied *p*-orbital at the C2 carbon. The adjacents σ-electron-withdrawing and π-electron-

donating nitrogen atoms stabilize this structure both inductively by lowering the energy of the occupied σ-orbital and mesomerically by donating electron density into the empty *p*-orbital (**Figure 1.2**).[1,2]

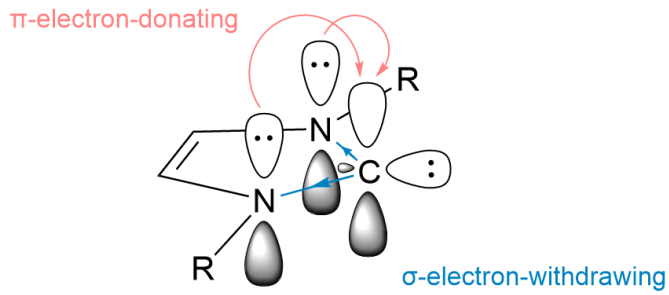

Figure 1.2. Mesomeric interaction in the stabilization of NHCs.

Mesoionic carbenes (MICs), on the other hand, are becoming increasingly popular and, in terms of electron donation, outperform their classic counterparts (NHCs) (**Figure 1.3**). In particular, 1,2,3-triazol-5-ylidenes have a significantly higher σ-donor strength than the commonly used classical imidazol-2-ylidenes with an almost unlimited synthetic access of the ligand precursors through the copper-catalyzed azide-alkyne cycloaddition reaction (CuAAC). The strong ligand donor properties directly affect the strength of the metal-carbon bond in metal-NHC and metal-MIC complexes and, consequently, the catalytic activity of the metal center. Therefore, the observed high catalytic activity of metal complexes containing 1,2,3-triazol-5-ylidene ligands is often attributed to their strong overall electron-donating properties.[5-8]

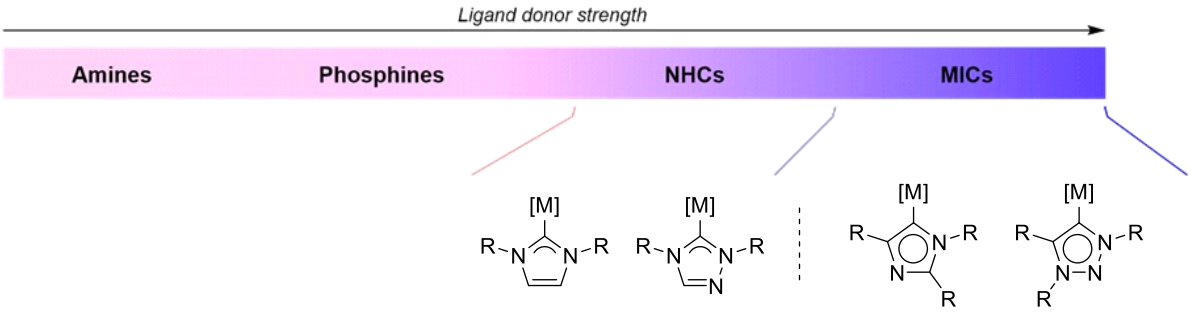

Figure 1.3. Schematic donor ability scale illustrating the donor ability of different NHC and MIC ligands.

Several chelating triazolylidene transition metal complexes have been described in catalytic, spectroscopic, and electrochemical reports, and several experimental approaches for studying their electronic properties have been proposed in order to rationalize the reactivities observed.[3] For example, in carbonyl complexes, the donor abilities of NHCs and MICs can be determined by analyzing the C–O stretching frequency of the carbonyl ligands in infrared spectroscopy. The more electron-donating character of the ligand of interest, the more electron-rich the metal center becomes, increasing the degree of π-backbonding into the carbonyl ligands and therefore reducing their bond order and infrared stretching frequency. The "asymmetric" (*trans*-CO) band is used for comparison, since it is supposedly more affected by the NHC or MIC ligands. In addition to this approach, the carbenic C5 resonance in the ^{13}C NMR spectra of metal complexes containing NHCs or MICs ligands can also be used to probe their donor properties.

1.1.2. Preparation of Triazolylidenes: Click Chemistry

As previously mentioned, 1,2,3-triazoles are the precursors of 1,2,3-triazolylidene ligands and can be synthesized via the well-known copper-catalyzed click [3 + 2] cycloaddition reaction between an alkyne and an organic azide. Since the structure of 1,2,3-1*H*-triazole has three substitution centers in positions 1, 4, and 5, it has two regioisomers when disubstituted: 1,4- and 1,5- regioisomer.[9-12] The Cu(I) catalyst strongly activates alkynes toward the 1,3-dipole of organic azides, leading to the regiospecific formation of the 1,4-regioisomer (**Scheme 1.1**). On the other hand, a more recent approach for synthesizing exclusively the 1,5-regioisomer has been discovered, which involves a base-catalyzed cycloaddition reaction using NMe_4OH as a catalyst (**Scheme 1.1**).[13-15]

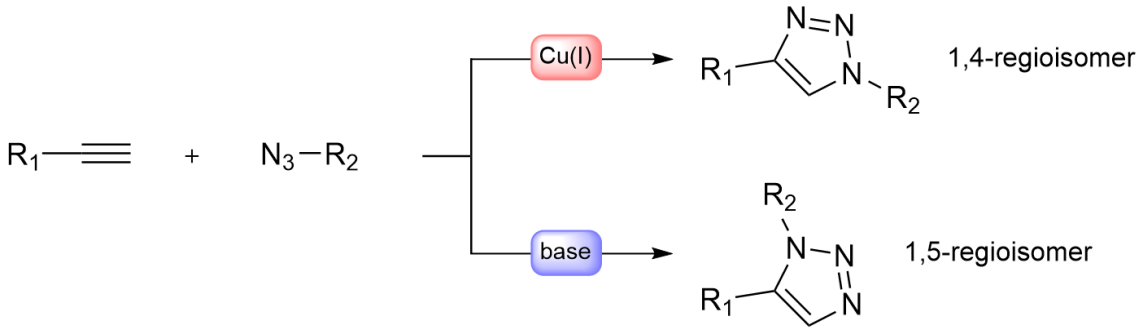

Scheme 1.1. Copper and base-catalyzed versions of the azide-alkyne cycloaddition reaction.

Different copper sources can be used as pre-catalysts for the "click" reaction, but one of the most efficient methods involves the *in situ* reduction of stable Cu(II) salts, such as $CuSO_4$, with sodium ascorbate. In this case, the interference from atmospheric oxygen is avoided because any dissolved oxygen is quickly reduced. The absence of a reductant in the medium can result in the formation of oxygen-favored byproducts. This methodology was developed in an aqueous medium because $CuSO_4$ and the reducing agent are water-soluble and it is important to preserve copper acetylide in its reactive state; however, it is also possible to use a variety of solvents or solvent mixtures, depending on the properties of the reagents. It is worth noting that organic azides can be isolated or generated *in situ*, depending on their stability (**Scheme 1.2**).

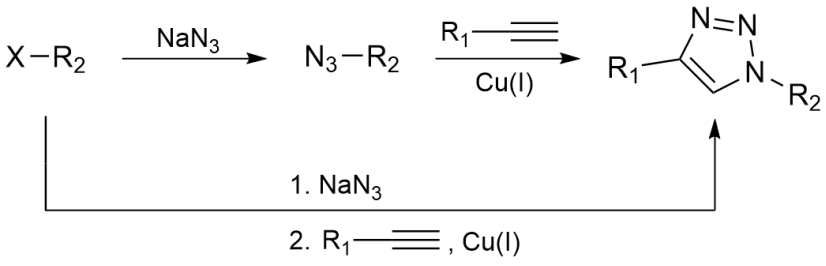

Scheme 1.2. Formation of 1,2,3-triazoles via a copper-catalyzed “click” reaction i) isolating the organic azide; and ii) generating the organic azide *in situ*. X = I, Cl, Br, NH_2, etc.

The CuAAC reaction is a very versatile procedure, offering the possibility of introducing different substituents as a wingtip. Considering the 1,4- regioisomer, it is possible to introduce additional donor substituents at the C4 and N1 positions. Therefore, the introduction of another 1,2,3-triazole group at C4 leads to a bidentate ligand of the 1,1'-R-4,4'-bis-(1,2,3-triazole) type, which allows functionalization

with several organic substituents on N1 forming bidentate ligands with strong donor abilities. Then, alkylation of the N3 position of such bis-triazoles generates the corresponding bis-triazolium salts, which when deprotonated deliver the bis-1,2,3-triazol-5-ylidene ligands[16] (**Scheme 1.3**), which have even stronger donor properties and remarkable stability toward various oxidation states in transition metal complexes. On the other hand, the N3-alkylation of the 1,5-regioisomer yields the corresponding 1,2,3-triazolium salt, which is transformed by deprotonation to 1,2,3-triazol-4-ylidene[7]. Using a bridging alkylation agent, a bis-1,2,3-triazol-4-ylidene ligand can be obtained (**Scheme 1.3**).

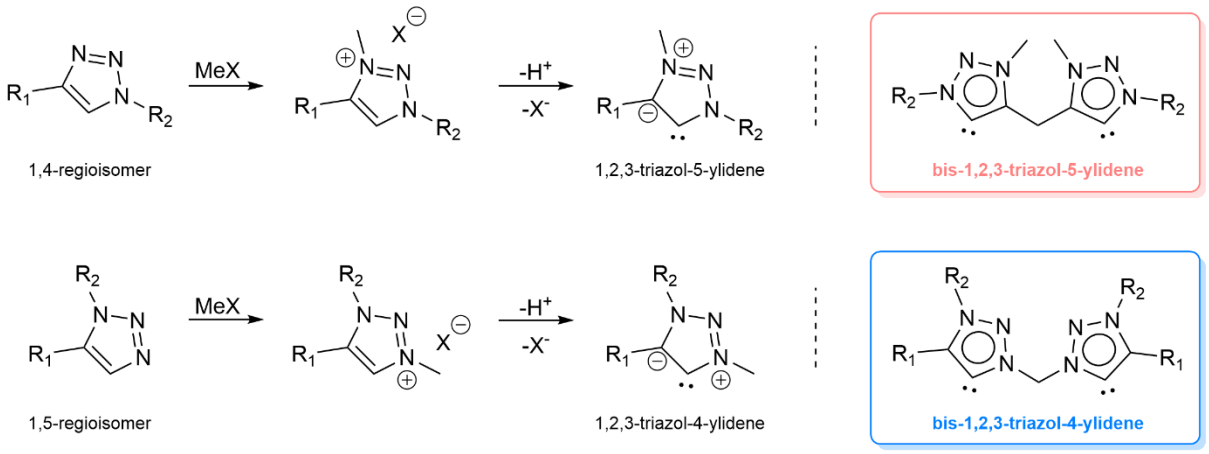

Scheme 1.3. Synthesis of triazolylidenes from the 1,4- and 1,5- regioisomers of 1,2,3-triazoles; X = I, OTf, etc.

1.2. Molybdenum NHC and MIC Complexes

N-Heterocyclic (NHCs) and mesoionic (MICs) carbenes are currently extensively used as ligands in organometallic chemistry and homogeneous catalysis. A wide variety of metal catalysts, incorporating these ligands, have been developed for a variety of applications including small molecule activation, and photo- and electrochemical catalysis.[4] The extraordinary performance of NHC and MIC ligands in transition metal-catalyzed processes has been attributed to their excellent σ-donor abilities, forming strong metal-carbon bonds, and providing high stability to their metal complexes. In addition, the facile modulation of the NHC wingtip substituents, allows the easy tunning of the steric and electronic properties of their metal complexes.

Initially, most of the studies using NHC and MIC ligands focused on complexes with noble metals (Ir, Ru, Re, Pd). However, due to the need of replacing expensive metals by earth-abundant cheap metals, the focus recently shifted to 3d metals such as Mn, Fe, Co, and Ni.[17] Molybdenum complexes with NHCs and MICs, on the other hand, are still rare, particularly with bidentate ligands.

Molybdenum is a group 6 transition metal element used in a variety of catalytic processes in both natural and industrial settings; the selective oxidation of hydrocarbons and the reduction of N_2 to ammonia, are two illustrative examples. Indeed, Nishibayashi and co-workers[18] described the catalytic production of ammonia from dinitrogen employing molybdenum complexes bearing NHC-based PCP-type pincer ligands earlier this year. Furthermore, Mo is an essential trace element for all living organisms and constitutes a relatively non-toxic and a rather inexpensive metal. In homogeneous

catalysis, Mo has been used for a variety of reactions ranging from olefin metathesis and allylic alkylations to oxidation of different functional groups with hydroperoxides.

Group 6 metal-based complexes are particularly attractive due to their low cost and high coordination number enabling great flexibility in the design of the ligand sphere. In particular, group 6 carbonyl complexes play an important role as catalysts or precatalysts in many organic transformations, and most of these complexes are readily available from the corresponding hexacarbonyl complexes. In the last decades, several applications have been explored for carbonyl molybdenum complexes supported by monodentate NHC ligands, including saturated and unsaturated backbone NHCs with or without substituents in the backbone, *N*-alkyl and *N*-aryl NHCs, and five- and six-membered ring NHCs. However, the use of bidentate ligands containing NHCs allowed the preparation of new complexes whose stability is entropically improved by the chelate effect. In contrast to the numerous reports on late transition metal complexes with bidentate NHC ligands, only a limited number of reports on group 6 transition metal complexes bearing bidentate NHC ligands have been published. **Figure 1.4** depicts all molybdenum carbonyl complexes containing bidentate NHC ligands that have been reported in the literature. In 2010, Royo and co-workers[19] described the synthesis of a Mo(II) η^3-allyl dicarbonyl complex bearing a bidentate NHC ligand [Mo(η^3-C_3H_5)Cl(CO)$_2$(bis-NHC^{Bz})] (**1**) (bis-NHC^{Bz} = 1,1'-dibenzyl-3,3'-methylenediimidazoline-2,2'-diylidene) and its catalytic performance in the epoxidation of *cis*-cyclooctene using H_2O_2 as oxidant, showing that complex **1** achieved 100% selectivity in the formation of cyclooctene oxide. Soon later, bis-NHC ligands bearing *o*-xylylene, propylene, and ethylene linkers were coordinated to molybdenum by Ito and co-workers[20], affording [Mo(CO)$_4$(bis-NHC)] (**2**) complexes. In complexes **2**, the bis-NHC ligands adopt a twisted conformation in an octahedral geometry, thus resulting in Mo(0) complexes with a C_2-symmmetric structure. In 2014, Tuczek and co-workers[21] synthesized and characterized two molybdenum(0) tetracarbonyl complexes with bidentate NHC/phosphine ligands, [Mo(CO)$_4$(Benz-CC)] (**3**) and [Mo(CO)$_4$(Benz-CP)] (**4**) (Benz-CC = di(1-ethylbenzimidazol-2-ylidene)methane, Benz-CP = 3-(2-diphenylphosphanylethyl)-1-ethylbenzimidazol-2-ylidene). In 2015, Tang and co-workers[22] studied the catalytic activity of two azaaryl-functionalized NHC molybdenum carbonyl complexes (**5** and **6**) in the oxidation of styrene, giving 2,5-diphenyl-1,4-dioxane as a sole product albeit with low yield. The azaaryl-functionalized NHCs act as chelating N,C-bidentate ligands in these complexes. In addition, Hor and co-workers investigated the coordination properties of a benzothiazole-carbene ligand with molybdenum.[23] Cyclopentadienyl Mo(II) N,C-chelating benzothiazole-NHC complex **7** was easily prepared from the corresponding benzothiazolylimidazolium salts and applied with success in cyclooctene epoxidation catalysis. In 2018, the same group synthesized Mo(0) tricarbonyl complexes (**8**) containing the N,C-chelating benzothiazole-NHC ligand, and these complexes showed good catalytic activity for the epoxidation of *cis*-cyclooctene in the presence of TBHP. The oxidative addition of I_2 to these complexes afforded Mo(II) complexes (**9**), which were the first isolable and crystallographically elucidated seven-coordinate diiodo-Mo(II)-carbonyl complexes with NHC ligands.[24] Other interesting examples of Mo(0)-NHC tetracarbonyl complexes were reported in 2021 by Ke and co-workers[25], which were applied as catalysts for the direct *N*-alkylation of anilines or nitroarenes with alcohols (complexes **10** and **11** in **Figure 1.4**).

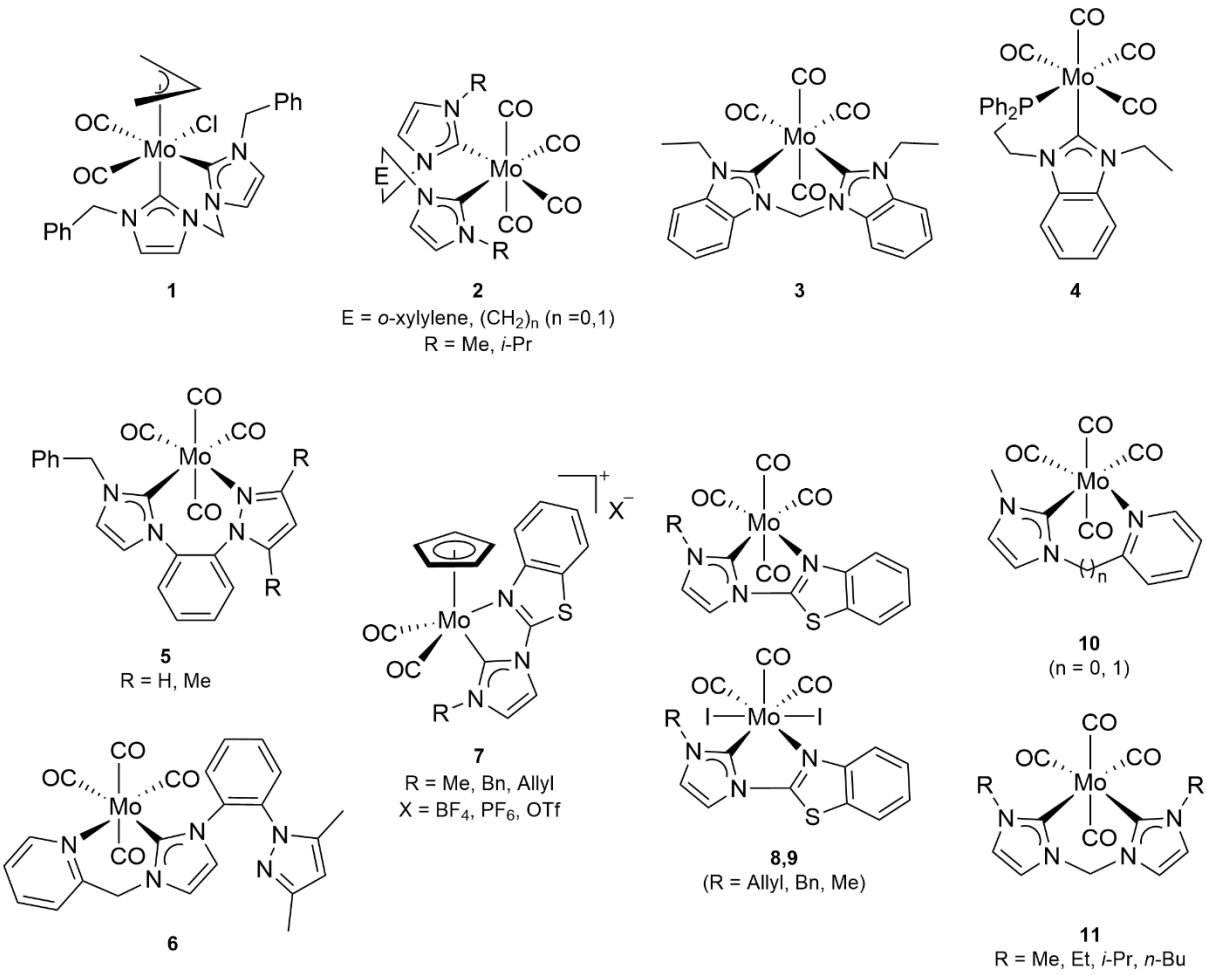

Figure 1.4. Molybdenum carbonyl complexes **1**-**11** bearing bidentate NHC ligands described in the literature.

Metal complexes of 1,2,3-triazole-derived mesoionic carbenes (1,2,3-triazolylidenes), on the other hand, have shown remarkable properties and unique catalytic potential towards various transformations in the last years.[7] The advantages of triazole-based ligands include the availability of both N- and C-centered coordination sites, as well as their easy steric and electronic modulation based on the "click synthesis". The interest in using MICs as ligands for catalytically active metal centers lies primarily from the fact that these ligands are strong σ-donors, outperforming their normal analogues (NHCs) and thus providing access to exceptionally high donor systems that may stabilize their metal complexes. Regarding the studies of molybdenum complexes bearing MIC ligands, these are scarce, as stated in the Introduction of Chapter 2.

Besides the given properties of supporting ligands in organometallic catalysis, an important prerequisite is that the desired catalytically active complexes are synthetically easily accessible; therein lies a pivotal element to the success of NHC- and MIC-based catalysts. Molybdenum NHC and MIC complexes are simply and easily prepared by ligand substitution of a suitable Mo precursor with NHCs. However, due to the highly reactive nature of NHCs toward air and moisture, it is often difficult to manipulate free NHCs or MICs. Therefore, the formation of free NHCs or MICs *in situ* by deprotonation of the corresponding imidazolium or triazolium salts with a strong base (e.g., *t*-BuOK), and subsequent reaction with the appropriate Mo precursor is one of the most common and broadly applicable methods

for accessing the target metal carbene complexes that circumvent the isolation of free carbenes. Apart from this approach, these complexes are also accessible by other synthetic routes that do not require the isolation of the free carbene, such as the use of carbene transfer reagents (e.g., Ag(I) or BEt_3 adducts).[1,2,7] The use of NHC adducts as protected forms of free NHC is a viable alternative for the synthesis of NHC complexes. In the Ag-transmetalation route, Ag_2O is reacted with the appropriate azolium salts to form an Ag-NHC complex capable of transferring the NHC to another metal centre. This Ag(I) adduct is usually not isolated but is reacted further with an appropriate metal precursor to generate the metal complex of interest. It is normally assumed that a mononuclear, linearly coordinated silver(I) complex is generated *in situ*, but different silver adducts could be formed depending on the wingtip present in the azolium salt and the corresponding couterions, since Ag(I) complexes are known to be prone to form polynuclear structures.[1,2,7] The BEt_3-adduct of NHC, which is prepared by the reaction of the appropriate azolium salts with $LiBEt_3H$, is another efficient NHC transfer reagent.[20] These three main synthetic approaches are illustrated in **Scheme 1.4**.

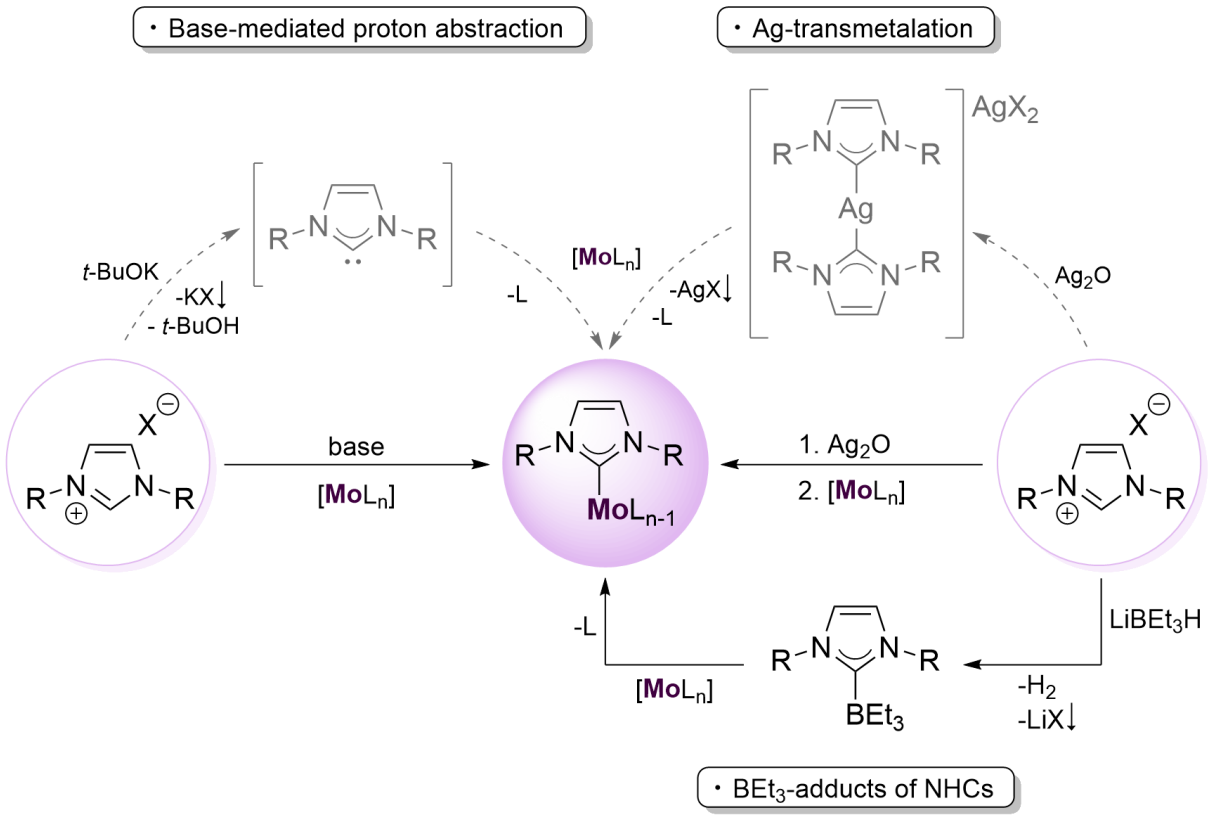

Scheme 1.4. Synthesis of Mo-NHC complexes through i) the base-mediated route; ii) transmetalation with silver; iii) the preparation of BEt_3-NHC adducts. X = Br, PF_6, etc. L = CO, NCMe.

1.3. Molybdenum Complexes in Borrowing Hydrogen (BH) Reactions

Homogeneous transition-metal-catalyzed C-C and C-N bond formation reactions are among the most promising and sustainable organic synthesis methods for high-value compounds, such as alkylated amines, imines, amides, and *N*-heterocycles, which play a pivotal role in pharmaceutical and medicinal chemistry. In particular, nitrogen-containing heterocycles are ubiquitous substructures of a wide range of important compounds that play crucial roles in biological systems and processes. Therefore, they are used as fundamental building blocks for biologically active natural products.[26]

One of the primary goals of the current research on synthetic chemistry is to replace toxic and waste-generating reagents by greener and more sustainable feedstocks. Alcohols are considered as suitable and environmentally friendly reagents, since they can be easily obtained from a variety of natural resources. Therefore, using alcohols as alkylating agents for the construction of new C-C and C-N bonds is highly desirable. In this regard, Borrowing Hydrogen (BH) and Acceptorless Dehydrogenative Coupling (ADC), reactions are prominent synthetic strategies for the preparation of functionalized compounds and heterocycles that have received significant attention in the last decade. Indeed, a large number of transition metal-catalyzed systems for these processes have recently reported in the literature.[26-31] The BH and ADC processes are very attractive because the only byproducts generated in these reactions are water and/or hydrogen. In the BH process, alcohols are first dehydrogenated to form reactive carbonyl intermediates, aldehydes or ketones, that undergo further transformations, such as condensations with nucleophiles, to give unsaturated compounds (imines or alkenes). Further reduction of the unsaturated compounds afford the desired saturated products – amines or alkanes (**Scheme 1.5A**). The key concept here is that the metal catalyst is capable to "borrow" the hydrogen from the alcohol that will be later released in a final hydrogenation step. In ADC coupling processes, instead of occurring the last hydrogenation step, H_2 is released (**Scheme 1.5B**). Therefore, these strategies allow the direct conversion of alcohols into amines, imines, *N*-heterocycles, and various aldol condensation products.[26-31]

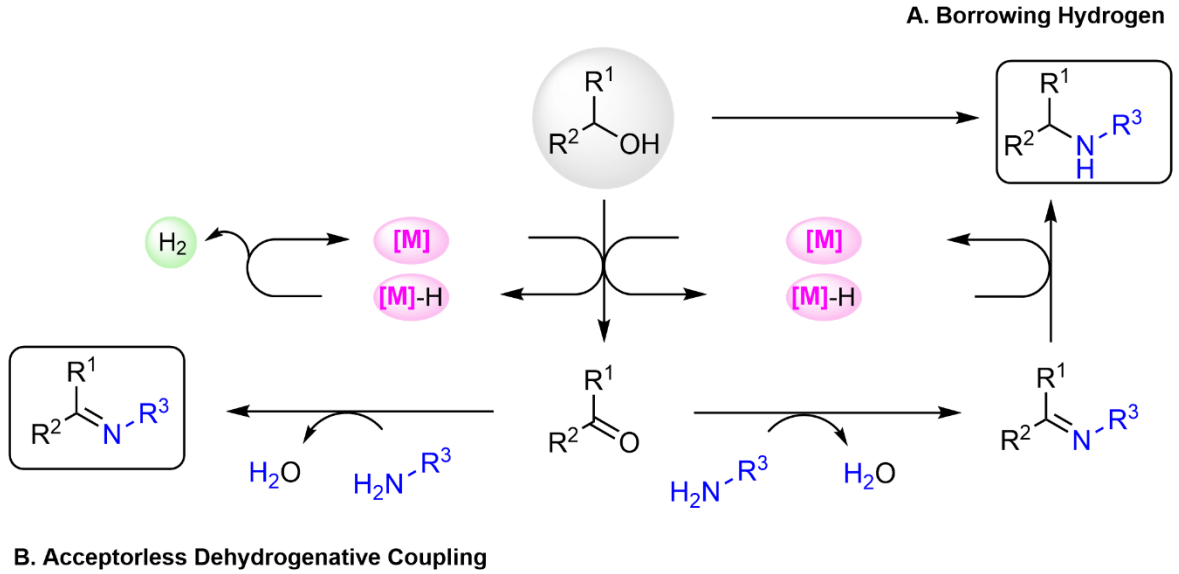

Scheme 1.5. General pathways of the (**A**) BH and (**B**) ADC reactions mediated by transition-metal catalysts [M].

Various catalytic systems using this BH/ADC methodology have been developed, including molybdenum-containing systems (**Scheme 1.6**). In 2018, Madsen and Azizi[32] described the first example of a homogeneous molybdenum-catalyzed acceptorless dehydrogenation coupling (ADC) of alcohols for the synthesis of imines. The Mo catalyst is generated *in situ* from $Mo(CO)_6$, 1,3-dicyclohexylimidazolium chloride and potassium *tert*-butoxide, and is further stabilized by the phosphine ligand dppe. In 2021, Liu and co-workers[33] described the use of $Mo(CO)_6$ in combination with an organocatalyst (A in Scheme 1.6) as a binary catalytic system for the *N*-alkylation of alcohols with amines. Using this catalytic system, both amines (BH product) and imines (ADC product) can be selectively achieved under different reaction temperature. Furthermore, in the same year, Ke and co-workers[25] reported the catalytic use of a Mo(0) tetracarbonyl complex with a bis-NHC ligand in the direct *N*-alkylation of anilines or nitroarenes with alcohols, as already mentioned (complex **11** in Figure 1.4). Later, they applied complex **11** in the efficient β-alkylation of secondary alcohols via BH, which represented the first implementation of molybdenum catalysts in this type of transformation.[34]

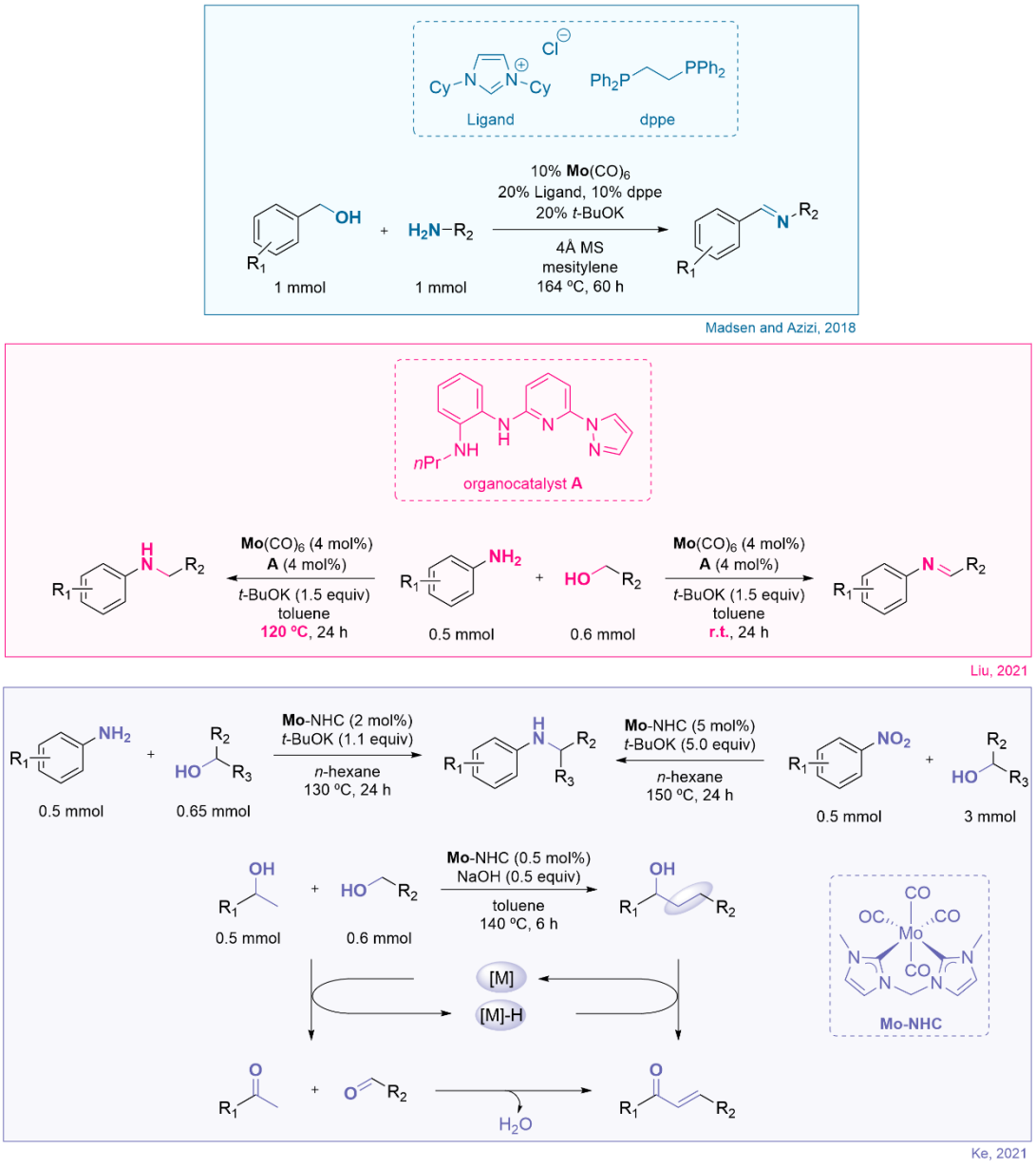

Scheme 1.6. Molybdenum-catalyzed BH and ADC processes described in the literature.

1.4. Objective of the Thesis

The main goal of this thesis was the synthesis and characterization of a new family of molybdenum complexes bearing mesoionic carbene ligands and their application as catalysts for BH and ADC processes. To meet this goal, the following specific objectives were proposed:

- ✓ Synthesis of bidentate ligands containing the combinations of triazolylidene/pyridine/triazole using already reported and/or novel synthetic protocols.
- ✓ Development of effective synthetic protocols for the preparation of Mo complexes bearing the synthesized bidentate ligands.
- ✓ Characterization of the new family of Mo triazolylidene complexes by NMR (^{1}H, ^{13}C, and ^{95}Mo) and IR spectroscopy, and by elemental analysis.
- ✓ Determination of the donor properties of the chelating ligands using ^{13}C and ^{95}Mo NMR, and IR spectroscopic data.
- ✓ Investigation of the catalytic activity of the Mo-triazolylidene complexes in borrowing hydrogen (BH) and acceptorless dehydrogenative coupling (ADC) processes. In particular in (i) synthesis of quinolines; (ii) *N*-alkylation of amines; (iii) α-alkylation of ketones with alcohols; (iv) β-alkylation of alcohols.
- ✓ Investigation of the catalytic activity of Mo-triazolylidenes in the aerobic oxidation of primary amines to amides.

1.5. References

1. Hopkinson, M. N., Richter, C., Schedler, M., Glorius, F. (**2014**). An overview of N-heterocyclic carbenes. *Nature*, 510(7506), 485–496. https://doi.org/10.1038/nature13384

2. Hahn, F. E., Jahnke, M. C. (**2008**). Heterocyclic carbenes: Synthesis and coordination chemistry. *Angew. Chem. Int. Ed.,* 47(17), 3122–3172. https://doi.org/10.1002/anie.200703883

3. Huynh, H. V. (**2018**). Electronic Properties of N-Heterocyclic Carbenes and Their Experimental Determination. *Chem. Rev.*, 118(19), 9457–9492. https://doi.org/10.1021/acs.chemrev.8b00067

4. Peris, E. (**2018**). Smart N-Heterocyclic Carbene Ligands in Catalysis. *Chem. Rev.*, 118(19), 9988–10031. https://doi.org/10.1021/acs.chemrev.6b00695

5. Phukan, A. K., Guha, A. K., Sarmah, S., Dewhurst, R. D. (**2013**). Electronic and ligand properties of annelated normal and abnormal (mesoionic) N-heterocyclic carbenes: A theoretical study. *J. Org. Chem.*, 78(21), 11032–11039. https://doi.org/10.1021/jo402057g

6. Krüger, A., Albrecht, M. (**2011**). Abnormal N-heterocyclic carbenes: More than just exceptionally strong donor ligands. *Aust. J. Chem.*, 64(8), 1113–1117. https://doi.org/10.1071/CH11265

7. Schweinfurth, D., Hettmanczyk, L., Suntrup, L., Sarkar, B. (**2017**). Metal Complexes of Click-Derived Triazoles and Mesoionic Carbenes: Electron Transfer, Photochemistry, Magnetic Bistability, and Catalysis. *Z. Anorg. Allg. Chem.*, 643(9), 554–584. https://doi.org/10.1002/zaac.201700030

8. Albrecht, M. (**2014**). Normal and abnormal N-heterocyclic carbene ligands. Similarities and differences of mesoionic C-donor complexes. *Adv. Organomet. Chem.*, 62, 111–158. https://doi.org/10.1016/B978-0-12-800976-5.00002-3

9. Friães, S., Realista, S., Gomes, C. S. B., Martinho, P. N., Royo, B. (**2021**). Click-derived triazoles and triazolylidenes of manganese for electrocatalytic reduction of CO_2. *Molecules*, 26(21). https://doi.org/10.3390/molecules26216325

10. Maity, R., Sarkar, B. (**2022**). Chemistry of Compounds Based on 1,2,3-Triazolylidene-Type Mesoionic Carbenes. *JACS Au*, 2(1), 22–57. https://doi.org/10.1021/jacsau.1c00338

11. Guisado-Barrios, G., Soleilhavoup, M., Bertrand, G. (**2018**). 1 H-1,2,3-Triazol-5-ylidenes: Readily Available Mesoionic Carbenes. *Acc. Chem. Res.*, 51(12), 3236–3244. https://doi.org/10.1021/acs.accounts.8b00480

12. Sharpless, W. D., Wu, P., Vidar Hansen, T., Lindberg, J. G. (**2005**). Just Click It: Undergraduate Procedures for the Copper(I)-Catalyzed Formation of 1,2,3-Triazoles from Azides and Terminal Acetylenes. *J. Chem. Educ.*, 82(12), 1833. https://doi.org/10.1021/ed082p1833

13. Kwok, S. W., Fotsing, J. R., Fraser, R. J., Rodionov, V. O., Fokin, V. v. (**2010**). Transition-metal-free catalytic synthesis of 1,5-diaryl-1,2,3-triazoles. *Org. Lett.*, *12*(19), 4217–4219. https://doi.org/10.1021/ol101568d

14. Badawi, M. A. A. H., Abu-Orabi, S. T. (**2021**). Quantum mechanical investigations of base-catalyzed cycloaddition reaction between phenylacetylene and azidobenzene. *J. Chem. Res.*, *45*(5–6), 519–525. https://doi.org/10.1177/1747519820946253

15. Suntrup, L., Hohloch, S., Sarkar, B. (**2016**). Expanding the Scope of Chelating Triazolylidenes: Mesoionic Carbenes from the 1,5-"Click"-Regioisomer and Catalytic Synthesis of Secondary Amines from Nitroarenes. *Chem. Eur. J.*, *22*(50), 18009–18018. https://doi.org/10.1002/chem.201603901

16. Monkowius, U., Ritter, S., König, B., Zabel, M., Yersin, H. (**2007**). Synthesis, characterisation and ligand properties of novel Bi-1,2,3-triazole ligands. *Eur. J. Inorg. Chem.*, 29, 4597–4606. https://doi.org/10.1002/ejic.200700479

17. Romain, C., Bellemin-Laponnaz, S., Dagorne, S. (**2020**). Recent progress on NHC-stabilized early transition metal (group 3–7) complexes: Synthesis and applications. *Coord. Chem. Rev.*, 422. https://doi.org/10.1016/j.ccr.2020.213411

18. Ashida, Y., Mizushima, T., Arashiba, K., Egi, A., Tanaka, H., Yoshizawa, K., Nishibayashi, Y. (**2023**). Catalytic production of ammonia from dinitrogen employing molybdenum complexes bearing N-heterocyclic carbene-based PCP-type pincer ligands. *Nature Synthesis*, 2, 635–644 https://doi.org/10.1038/s44160-023-00292-9

19. Krishna Mohan Kandepi, V. v., Cardoso, J. M. S., Royo, B. (**2010**). N-heterocyclic carbene-based molybdenum and tungsten complexes as efficient epoxidation catalysts with H2O2 and tert-butyl hydroperoxide. *Catalysis Letters*, 136(3–4), 222–227. https://doi.org/10.1007/s10562-010-0332-1

20. Ogata, K., Yamaguchi, Y., Kurihara, Y., Ueda, K., Nagao, H., Ito, T. (**2012**). Twisted coordination mode of bis(N-heterocyclic carbene) ligands in octahedral geometry of group 6 transition metal complexes: Synthesis, structure, and reactivity. *Inorganica Chim. Acta*, 390, 199–209. https://doi.org/10.1016/j.ica.2012.04.027

21. Gradert, C., Krahmer, J., Sönnichsen, F. D., Näther, C., Tuczek, F. (**2014**). Molybdenum(0)-carbonyl complexes supported by mixed benzimidazol-2-ylidene/ phosphine ligands: Influence of benzannulation on the donor properties of the NHC groups. *J. Organomet. Chem.*, 770, 61–68. https://doi.org/10.1016/j.jorganchem.2014.08.010

22. Cheng, C. H., Guo, R. Y., Cui, Q., Song, H., Tang, L. F. (**2015**). Synthesis and catalytic activity of N-heterocyclic carbene metal carbonyl complexes based on 1-[2-(pyrazol-1-yl)phenyl]imidazole. *Transition Met. Chem.*, 40(3), 297–304. https://doi.org/10.1007/s11243-015-9917-2

23. Wang, Z., Ng, S. W. B., Jiang, L., Leong, W. J., Zhao, J., Hor, T. S. A. (**2014**). Cyclopentadienyl molybdenum(II) N,C-chelating benzothiazole-carbene complexes: Synthesis, structure, and application in cyclooctene epoxidation catalysis. *Organometallics*, 33(10), 2457–2466. https://doi.org/10.1021/om401128z

24. Wang, Z., Song, X., Jiang, L., Lin, T. T., Schreyer, M. K., Zhao, J., & Hor, T. S. A. (**2018**). Seven-Coordinate MoII−Diiodo Complexes with Benzothiazole−N-Heterocyclic-Carbene Ligands and Their

Mo0 Precursors: Synthesis, Structures, and Catalytic Application in the Epoxidation of cis-Cyclooctene. *Asian J. Org. Chem.*, 7(2), 395–403. https://doi.org/10.1002/ajoc.201700583

25. Li, W., Huang, M., Liu, J., Huang, Y. L., Lan, X. B., Ye, Z., Zhao, C., Liu, Y., & Ke, Z. (**2021**). Enhanced Hydride Donation Achieved Molybdenum Catalyzed Direct N-Alkylation of Anilines or Nitroarenes with Alcohols: From Computational Design to Experiment. *ACS Catalysis*, 11, 10377–10382. https://doi.org/10.1021/acscatal.1c02956

26. Hofmann, N., & Hultzsch, K. C. (**2021**). Borrowing Hydrogen and Acceptorless Dehydrogenative Coupling in the Multicomponent Synthesis of N-Heterocycles: A Comparison between Base and Noble Metal Catalysis. *Eur. J. Org. Chem.*, 2021(46), 6206–6223. https://doi.org/10.1002/ejoc.202100695

27. Ding, K. (**2021**). Switching between borrowing hydrogen and acceptorless dehydrogenative coupling by base transition-metal catalysts. *Tetrahedron*, 99. https://doi.org/10.1016/j.tet.2021.132451

28. Paul, B., Maji, M., Chakrabarti, K., & Kundu, S. (**2020**). Tandem transformations and multicomponent reactions utilizing alcohols following dehydrogenation strategy. *Org. Biomol. Chem.*, 18(12), 2193–2214. https://doi.org/10.1039/c9ob02760b

29. Hakim Siddiki, S. M. A., Toyao, T., & Shimizu, K. I. (**2018**). Acceptorless dehydrogenative coupling reactions with alcohols over heterogeneous catalysts. *Green Chem.*, 20(13), 2933–2952. https://doi.org/10.1039/c8gc00451j

30. Wang, Y., Wang, M., Li, Y., & Liu, Q. (**2021**). Homogeneous manganese-catalyzed hydrogenation and dehydrogenation reactions. *Chem*, 7(5), 1180–1223. https://doi.org/10.1016/j.chempr.2020.11.013

31. Corma, A., Navas, J., & Sabater, M. J. (**2018**). Advances in One-Pot Synthesis through Borrowing Hydrogen Catalysis. *Chem. Rev.*, 118(4), 1410–1459. https://doi.org/10.1021/acs.chemrev.7b00340

32. Azizi, K., & Madsen, R. (**2018**). Molybdenum-Catalyzed Dehydrogenative Synthesis of Imines from Alcohols and Amines. *ChemCatChem*, 10(17), 3703–3708. https://doi.org/10.1002/cctc.201800677

33. Wu, D., Bu, Q., Guo, C., Dai, B., & Liu, N. (**2021**). Cooperative catalysis of molybdenum with organocatalysts for distribution of products between amines and imines. *Molecular Catalysis*, 503. https://doi.org/10.1016/j.mcat.2021.111415

34. Liu, J., Li, W., Li, Y., Liu, Y., & Ke, Z. (**2021**). Selective C-alkylation Between Alcohols Catalyzed by N-Heterocyclic Carbene Molybdenum. *Chem. Asian J.*, 16(20), 3124–3128. https://doi.org/10.1002/asia.202100959

Chapter 2

Synthesis and Characterization of Molybdenum(0) Complexes with Triazolylidene Ligands

2.1. Summary

In this chapter new molybdenum complexes bearing 1,2,3-triazolylidene (trz) ligands are described. A series of Mo(0) tetracarbonyl complexes with general formula $[Mo(CO)_4(trz)]$ containing bis-1,2,3-triazol-5-ylidene and pyridyl-1,2,3-triazol-4-ylidene ligands were prepared via *in situ* deprotonation of the corresponding triazolium salts with *t*-BuOK. In addition, a Mo complex containing a chelating N-based ligand, $[Mo(CO)_4(N^N)]$ (N^N = bis-1,2,3-triazole), was prepared by direct reaction of $Mo(CO)_6$ with a bis-triazole ligand. All complexes were characterized by NMR (^1H, ^{13}C, and ^{95}Mo) and IR spectroscopy, and by elemental analysis. In addition, the molecular structure of the Mo complex containing the mixed pyridyl-triazolylidene ligand was determined by single-crystal X-ray diffraction studies. The crystal structure revealed a slightly distorted octahedral geometry around the Mo(0) centre, with the chelating ligand situated in *trans* position to the two CO ligands in the equatorial plane, and two axial CO ligands. Furthermore, a comparison of the donor capacity of the bidentate mesoionic ligands has been established using IR, ^{13}C and ^{95}Mo NMR spectroscopy.

2.2. Introduction

Mesoionic carbenes (MICs) of the 1,2,3-triazol-5-ylidene type (trz) have become popular ligands in organometallic chemistry owing to their strong σ-donor properties, which make them excellent candidates as supporting ligands for transition metals.[1-3] Another interesting feature of MICs is their modular synthesis through Cu(I) catalyzed click reactions, which allows for tailoring them to specific functions. The copper(I)-catalyzed azide-alkyne cycloaddition (CuAAC) reaction exclusively yields the 1,4-substituted 1,2,3-triazole,[4-6] while the use of bases such as NMe_4OH results in the formation of the 1,5-regioisomer.[7-9] The 1,4-substituted 1,2,3-triazoles can be selectively methylated or arylated at the N3 atom, due to the most nucleophilic nature of the N3 site, to generate the corresponding triazolium salts in near quantitative yield.[6] The N3-aryl substitution is facilitated via copper-catalyzed reaction with an aryl iodonium salt.[10] 1,2,3-triazol-5-ylidenes (trz) are usually synthesized from the corresponding triazolium salts, and their transition metal complexes have shown excellent activities in a wide variety of catalytic reactions, e.g. water oxidation[11,12] and transfer hydrogenation,[13,14] as well as in other fields such as photochemistry,[15,16] supramolecular chemistry,[17,18] and electrocatalysis.[19] It is also possible to synthesize MICs from 1,5-substituted 1,2,3-triazoles, such as the mixed bidentate pyridyl-triazolylidene (py-trz) ligands that have been explored independently by the groups of Sarkar[20] and Piers[21] for the electrocatalytic reduction of CO_2.

Up to date, the chemistry of 1,2,3-triazolylidenes (trz) with molybdenum remains poorly developed. The only five examples reported in the literature are depicted in **Figure 2.1**. In 2013, Kühn and co-workers[22,23] described the synthesis of the first Mo compound containing a triazolylidene ligand, a half-sandwich Mo(II) dicarbonyl complex, and its catalytic activity in the epoxidation of alkenes. In 2017, Buchmeiser and co-workers[24] reported the synthesis of Mo(VI) imido alkylidene triazolylidene complexes and their application as catalysts for the polymerization of dicyclopentadiene (DCPD). Soon later, a bis-phenolate mesoionic carbene (MIC) ligand was coordinated to molybdenum by Hohloch and co-workers.[25] In 2020, Sarkar and co-workers[26] reported the synthesis, and the electrochemical and photochemical properties of the first example of a molybdenum(0) complex with a mixed bidentate C-N linked pyridyl-MIC ligand of the 1,2,3-triazol-4-ylidene type and carbonyl co-ligands (powerful markers for IR spectroscopy). This year, the same group compared the photophysical and photochemical properties of a new Mo(0) complex bearing a C-C linked pyridyl-MIC ligand with those of its analogous complex bearing the constitutional isomer of the C-N type.[27]

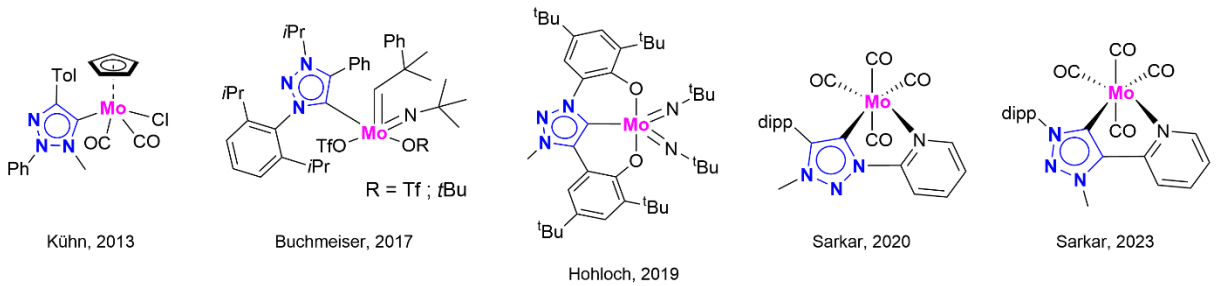

Kühn, 2013 | Buchmeiser, 2017 | Hohloch, 2019 | Sarkar, 2020 | Sarkar, 2023

Figure 2.1. Molybdenum triazolylidene complexes reported in the literature.

In continuation with the interest of our group in developing Earth-abundant metals for catalysis, we decided to synthesize a new family of Mo(0) tetracarbonyl complexes bearing 1,2,3-triazolylidene ligands and explore their catalytic activity in dehydrogenative coupling reactions. In this thesis, we describe the synthesis of [$Mo(CO)_4$(trz)] complexes, a new family of Mo(0) tetracarbonyl complexes containing chelating bis-1,2,3-triazole (**L1**), bis-1,2,3-triazol-5-ylidene (**L2** and **L3**), and pyridyl-1,2,3-triazol-4-ylidene (**L4**) ligands (**Figure 2.2**). Ligands **L2-L4** were coordinated to $Mo(CO)_6$ via *in situ* deprotonation of the corresponding triazolium salts with *t*-BuOK. On the other hand, coordination of **L1** was accomplished by its direct reaction with $Mo(CO)_6$. NMR (^1H,^{13}C, and ^{95}Mo) and IR spectroscopy proved useful to fully characterize our novel molybdenum complexes, allowing us to compare the donor capacity of the bidentate ligands (**L1-L4**), and get insights into the electronic density at the Mo(0) center of all complexes. The molecular structure of the Mo complex containing the mixed C-N linked pyridyl-triazolylidene ligand was determined by single-crystal X-ray diffraction studies.

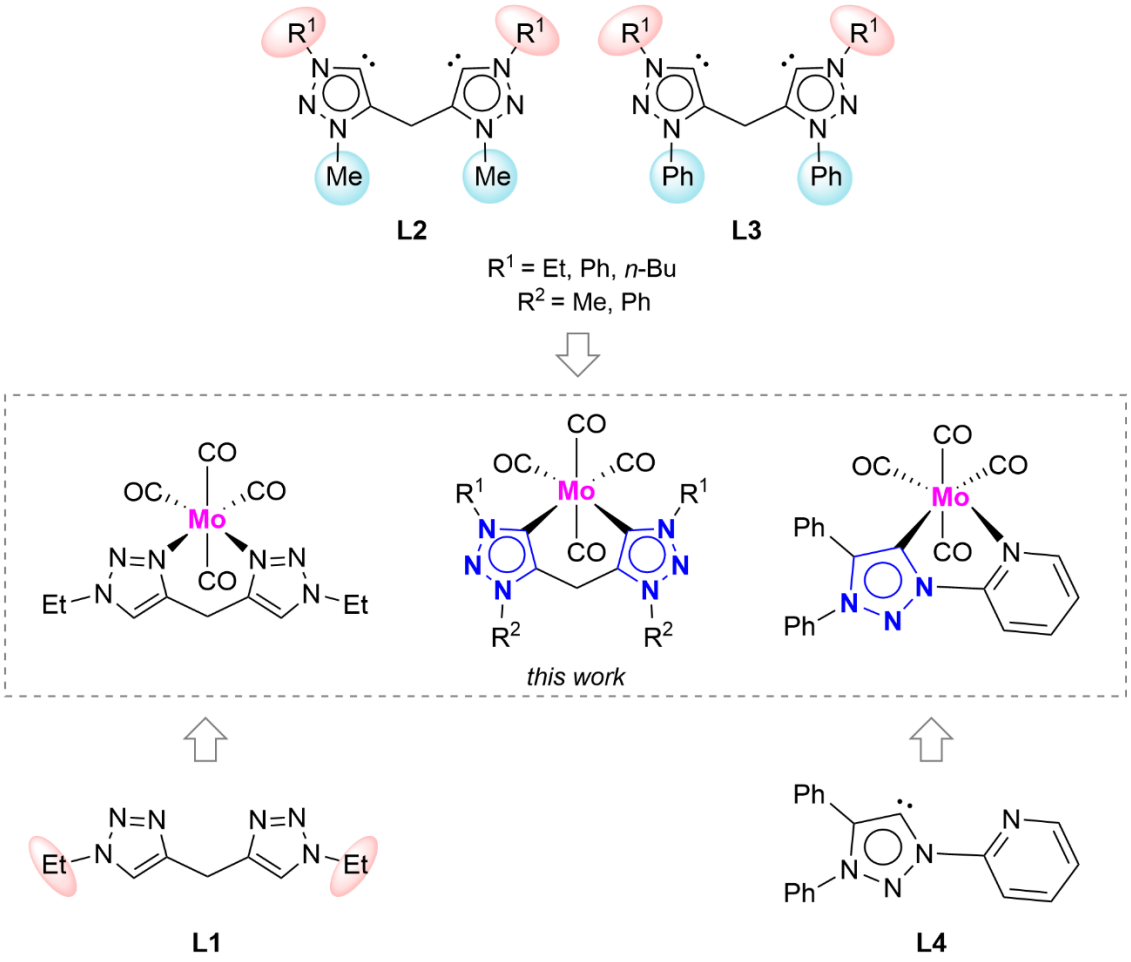

Figure 2.2. Mo(0) complexes synthesized in this work.

2.3. Results and Discussion

2.3.1. Synthesis and Characterization of Bis-triazolium Salts

The new bis-triazoles **L1b** and **L1c** were synthesized following the same protocol that has been reported in the literature for the preparation of **L1a**.[13,28] The synthetic method consists in the well-established copper-catalyzed "click" [3 + 2] cycloaddition of an organic azide to a commercially available dialkyne catalyzed by Cu(I) (CuAAC) (**Scheme 2.1**).

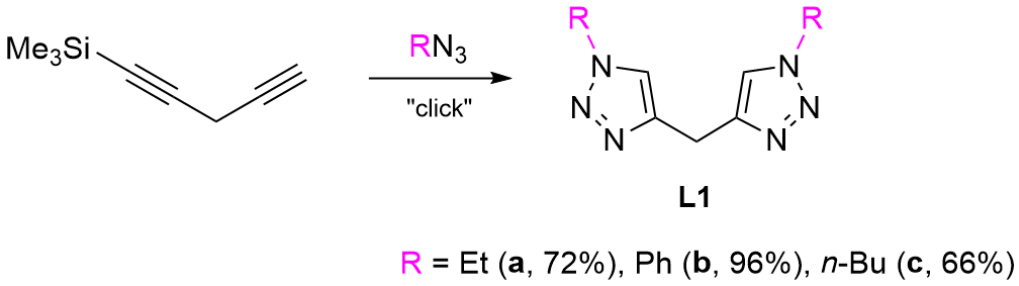

Scheme 2.1. Synthesis of bis-triazoles **L1a-c**.

The preparation of phenyl azide was performed following the procedure described in the literature[29] by reaction of aniline with sodium nitrite and hydrochloric acid followed by addition of sodium azide in water as shown in **Scheme 2.2**. The organic azides used for the preparation of **L1a** and **L1c** were not isolated; they were generated *in situ* from the corresponding alkyl halides (**Scheme 2.2**) and reacted with the dialkyne to yield the corresponding bis-triazoles. In contrast, phenyl azide was isolated (in 56% yield) through liquid-liquid extraction in diethyl ether. Its identity was confirmed by ^{1}H NMR spectroscopy, by comparison with the data reported in the literature.[29]

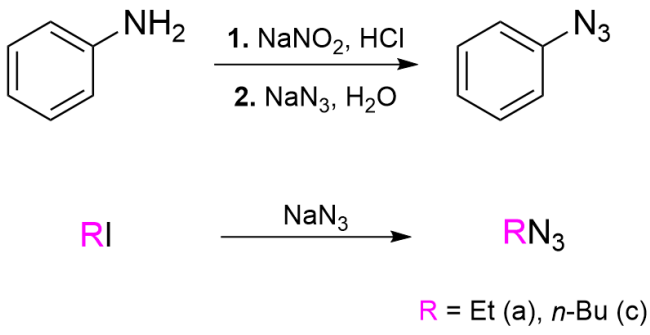

Scheme 2.2. Synthesis of organic azides.

Compounds **L1a-c** were characterized by ^{1}H NMR spectroscopy. The success of the "click" reaction was unequivocally confirmed by the appearance of a singlet resonance at approx. 7.00-8.00 ppm, which corresponds to the protons of the CH groups of the triazole rings. The presence of the CH_2 bridge was also confirmed by the singlet resonance at around 4.00-5.00 ppm.

Subsequent alkylation or arylation of the isolated bis-triazoles **L1**, followed by anion exchange with tetra-*n*-butylammonium bromide (TBAB), afforded the bis-triazolium bromide salts **L2[Br]$_2$** and **L3[Br]$_2$**, respectively, in good yields (**Scheme 2.3**).

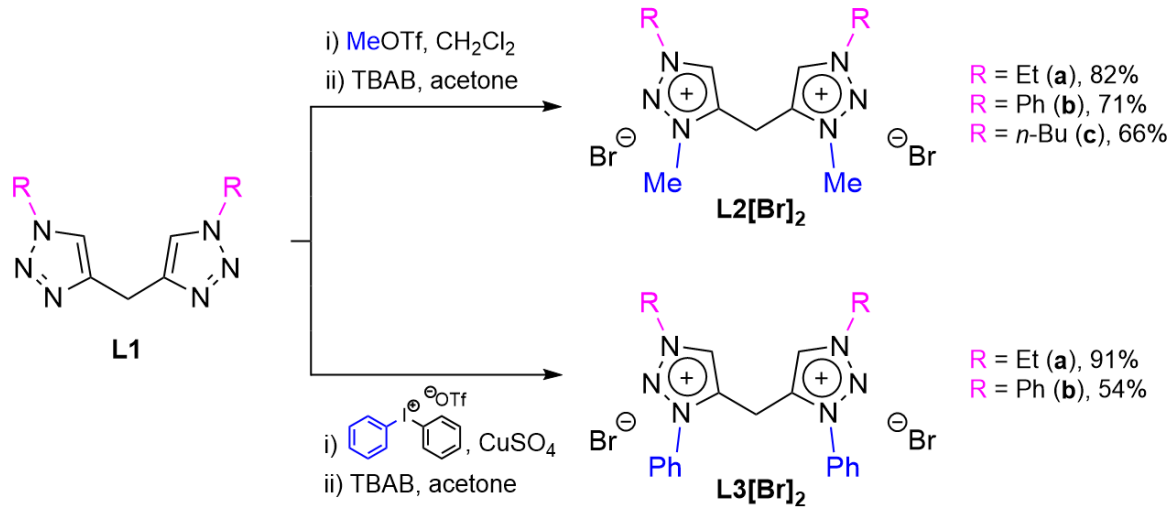

Scheme 2.3. Synthesis of bis-triazolium bromide salts **L2[Br]$_2$** and **L3[Br]$_2$**.

Following the protocol reported for the alkylation of **L1a**,[13,28] the methylating agent used to proceed with the methylation of **L1b** and **L1c** was methyl triflate due to its high reactivity, as it has the ability to delocalize the negative charge along its three oxygen atoms, resulting in resonance structures, after the loss of the methyl group that is bonded to one of these three atoms. The N3 atom, being the most basic, is the one that undergoes methylation in the presence of the methylating agent through the nucleophilic attack of this nitrogen atom on the carbon of the methyl group of MeOTf. The resulting bis-triazolium triflate salt is stabilized by resonance because the positive charge formed on the nitrogen atom is delocalized along the triazole rings. Then, the bis-triazolium triflate salt is subjected to anion exchange for bromide by its reaction with *n*-tetrabutylammonium bromide (TBAB) to yield **L2[Br]$_2$** in good yield (66-82%). The successful N3 methylation is confirmed by ^{1}H NMR spectroscopy. The ^{1}H NMR spectrum of **L2[OTf]$_2$** shows a new singlet at around 4.00-5.00 ppm, which corresponds to the protons of the CH_3 groups attached to the N3 atoms of the triazole rings. The ^{1}H NMR spectrum of **L2[Br]$_2$** displays the resonances slightly deshielded compared to those of **L2[OTf]$_2$**, as expected due to the increase in the electronegativity of the counterion.

For the N3 arylation of **L1a-b**, a new protocol was developed using diaryliodonium salts in the presence of a copper catalyst. First, the diphenyliodonium triflate salt was synthesized from the reaction of iodobenzene with benzene, in the presence of *meta*-chloroperoxybenzoic acid (*m*-CPBA) and triflic acid[10], as shown in **Scheme 2.4**.

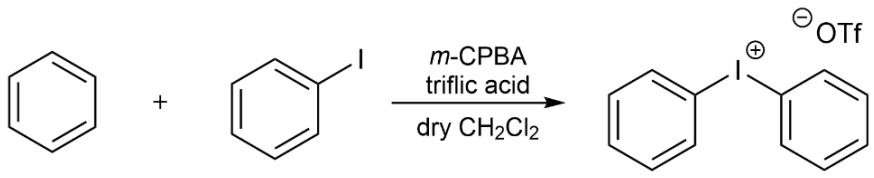

Scheme 2.4. Synthesis of diphenyliodonium triflate salt.

Proposed mechanism for this reaction is outlined in **Scheme 2.5**. Initially, *m*-CPBA oxidizes iodobenzene *in situ* to generate electrophilic hypervalent iodine(III) species PhI(OH). Addition of triflic acid forms the electrophilic hypervalent iodine(V) species PhI(OH)(OTf) through formation of 3-chlorobenzoic acid. Then, the nucleophilic attack of benzene to the electrophilic iodine(V) centre of PhI(OH)(OTf) produces species **A**. After the attack, the transfer of the hydroxyl group from the iodine(V) centre to the ring occurs, generating species **B**, so that, with the loss of water, the ring can recover its aromaticity, to obtain the diphenyliodonium triflate salt, a hypervalent iodine(III) reagent. The conjugate base of triflic acid (triflate) is non-nucleophilic, so it remains a counterion.[30]

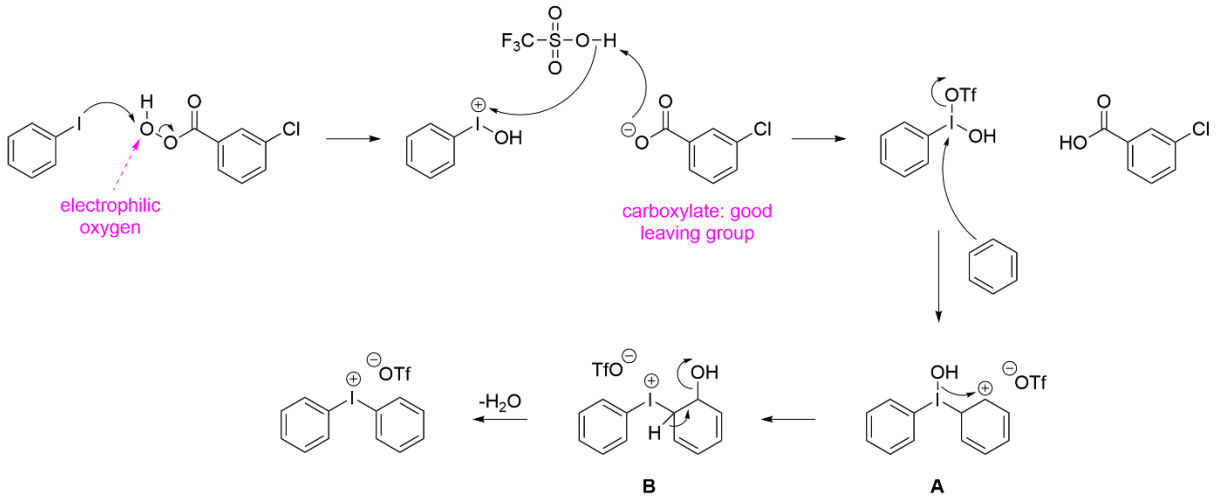

Scheme 2.5. Proposed reaction mechanism for the formation of diphenyliodonium triflate.

The diphenyliodonium triflate was obtained in 51% yield, and its identity was confirmed by ^{1}H NMR spectroscopy, by comparison with the data reported in the literature.[10] Having synthesized the diphenyliodonium triflate salt, it was possible to carry out the arylation of bis-triazoles **L1a-b** (as shown in **Scheme 2.3**) to obtain the desired bis-triazolium salts **L3[OTf]$_2$** with a high level of purity and without the need for purification by column chromatography. Subsequently, the triflate ion was easily exchanged for bromide to yield **L3[Br]$_2$**, using the same reaction conditions previously discussed. Compound **L3[OTf]$_2$** was characterized by ^{1}H NMR spectroscopy. Its spectrum displays a resonance at 7.00-9.00 ppm, which corresponds to the resonances of the Ph protons attached to the N3 atoms of the triazole rings, indicating that arylation has occurred on both sides of the molecule. After the ion exchange, the ^{1}H NMR spectrum of **L3[Br]$_2$** shows a slight deshielding of all resonances, as observed in **L2[Br]$_2$**.

2.3.2. Synthesis of the Pyridyl-triazolium Salt L4[Br]

The 1,5-diphenyl-1*H*-1,2,3-triazole (1,5-triazole^{Ph}, **A**) was synthesized from phenyl azide and phenylacetylene as illustrated in **Scheme 2.6**, following the procedure reported in the literature.[4]

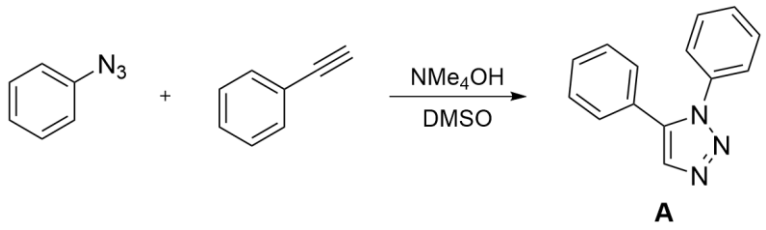

Scheme 2.6. Synthesis of 1,5-triazole^{Ph} (**A**).

The mechanism shown in **Scheme 2.7** for the base-catalyzed cycloaddition reaction between phenylacetylene and phenyl azide has been proposed by Kwok et al.[7] and investigated with density functional theory (DFT) by Badawi et al.[8] Initially, NMe_4OH catalyzes the reversible deprotonation of phenylacetylene generating the phenyl acetylide **I**, which acts as a nucleophile to attack the terminal nitrogen of phenyl azide to form the triazenide intermediate **II**. Afterwards, this intermediate undergoes either 6π-electrocyclization or 5-*endo-dig* cyclization to form 1,5-diphenyl-1,2,3-triazolyl anion **III** and the catalytic cycle is then completed by deprotonation of a molecule of water, DMSO, or phenylacetylene to obtain the respective triazole.[7,8] In this reaction, the solvent appears to be of great importance, due to the high acidity of phenyl acetylene in DMSO, which allows the formation of reactive acetylide species (intermediates **II** and **III**) and their stabilization. Furthermore, by carrying out the reaction in d_6-DMSO, it was proven that it participates in several necessary proton-relay events, which was evidenced by the incorporation of deuterium into the product.[7]

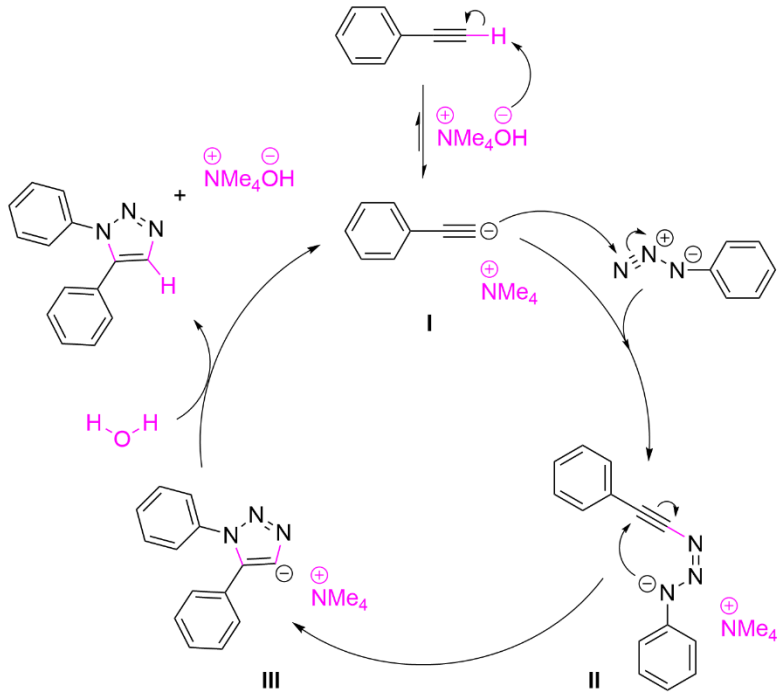

Scheme 2.7. Currently proposed mechanism for the base-catalyzed cycloaddition reaction to form 1,5-triazole^{Ph}.

The reaction for the preparation of **A** is not sensitive to atmospheric oxygen and moisture, so it can be carried out without an inert atmosphere, and the desired product precipitated upon addition of water, and was isolated by simple vacuum filtration. Compound **A** was isolated in 71% yield, and its identity was confirmed by ^{1}H NMR spectroscopy, which was in accord with the data reported in the literature.[7]

The pyridyl-triazolium bromide salt **L4[Br]** was then obtained from the condensation of 1,5-triazole^{Ph} with 2-bromopyridine in a solvent-free reaction at 160°C as shown in **Scheme 2.8**.[9] The N3 atom of 1,5-triazole^{Ph} is the most basic donor atom of the triazole ring and, for this reason, in the presence of 2-bromopyridine it acts as a nucleophile, attacking the electrophilic 2-position of this molecule and breaking the C–Br bond to give the respective pyridyl-triazolium salt **L4[Br]**. The reaction was carried out in a closed ampoule at 160 °C to ensure that the 1,5-triazole^{Ph} melts (mp 113–114°C), achieving a yield of 66% of **L4[Br]**. The identity of **L4[Br]** was confirmed by ^{1}H NMR spectroscopy, which compared well with the data reported in the literature.

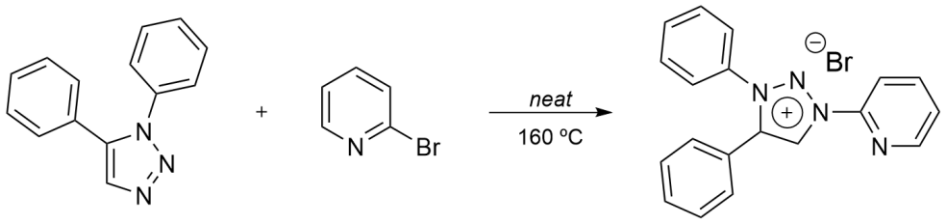

Scheme 2.8. Synthesis of pyridyl-triazolium bromide salt **L4[Br]**.

2.3.2. Synthesis and Characterization of Molybdenum(0) Complexes Bearing Triazolylidenes

Complex **Mo1** was easily prepared by direct reaction of $Mo(CO)_6$ with the bis-triazole ligand **L1a** as shown in **Scheme 2.9**, and it was characterized by ^{1}H NMR and IR spectroscopy. The characteristic pattern of a tetracarbonyl complex in the IR spectrum of **Mo1** (υ_{CO} 1933 (vs), 1883 (vs), 1819 (vs), and 2013 (w) cm^{-1}) confirmed the successful coordination of **L1a** to the molybdenum metal center.

The novel bis-triazolylidene molybdenum(0) complexes **Mo2**-**Mo6** and the mixed pyridine-triazolylidene complex **Mo7** were obtained by reaction of $Mo(CO)_6$ with the appropriate triazolium salts in the presence of *t*-BuOK (**Scheme 2.9**). All complexes were isolated in good to high yields (51-97%), as crystalline solids, and were fully characterized by NMR (^{1}H, ^{13}C, ^{95}Mo) and IR spectroscopy, and by elemental analysis. The disappearance of the signal of the corresponding triazolium protons ca. 8.97-10.02 ppm in the ^{1}H NMR spectra of **Mo2**-**Mo7** complexes, and the appearance of the characteristic resonance of the metalated carbons at ca. 175-185 ppm in their ^{13}C NMR spectra confirmed that coordination of the triazolylidene ligands occurred. The carbonyl ligands in all complexes showed the expected pattern for tetracarbonyl Mo complexes in their IR spectra, displaying four bands in the region of the carbonyl stretching vibrations. In addition, as expected, two characteristic resonances for the axial and equatorial CO ligands in the ^{13}C NMR spectra of the complexes **Mo2**-**Mo6** was observed, while the

carbonyl ligands in **Mo7** showed three characteristic resonances at 208.25 (axial CO), 221.56 (equatorial CO), and 225.69 ppm (equatorial CO), reflecting the asymmetry of the complex.

Moreover, ^{95}Mo NMR spectra were recorded in solution (CD_3CN) at room temperature for all newly synthesized Mo complexes. In all cases, a singlet resonance was observed in their ^{95}Mo NMR spectra, covering a range from -1677.36 to -1741.33 ppm.

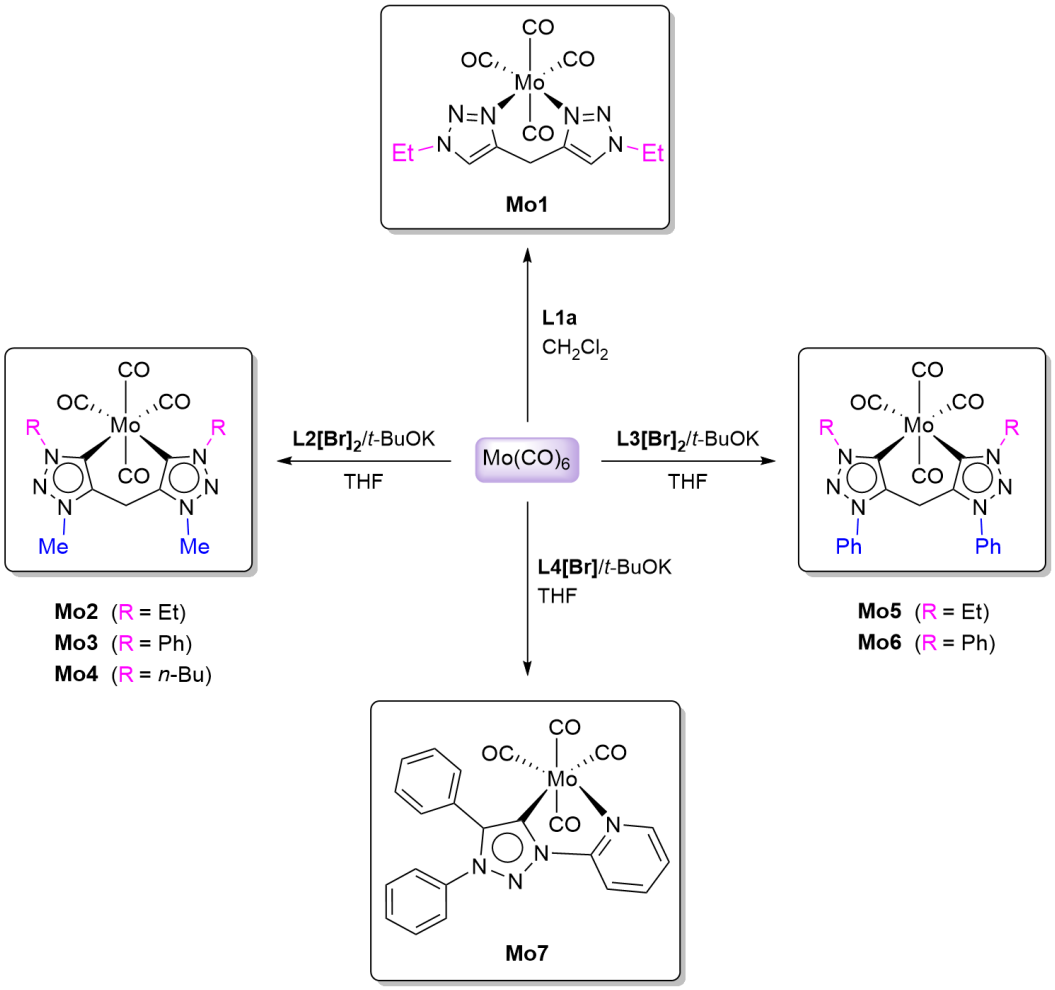

Scheme 2.9. Synthesis of new molybdenum complexes **Mo1**-**Mo7**.

The presence of the four CO groups in a $Mo(CO)_4$ arrangement makes the use of IR spectroscopy for characterization of complexes **Mo1**-**Mo7** very useful. The pattern of the bands observed in IR give a perfect indication of the local symmetry of the complexes while their position provide valuable information on the donor capacity of the bidentate mesoionic ligands. The totally symmetric CO stretching vibration $A_{1(1)}$ or $A`_{(1)}$ is a sensitive probe for density at the metal center. Carbonyl Mo complexes containing stronger electron donor ligands, triazolylidenes *vs* imidazolylidenes, are expected to display the CO stretching vibration $A_{1(1)}$ at lower wavelength numbers. As expected, **Mo1** bearing a chelating N^N ligand, a less σ-electron donor ligand than the triazolylidenes, displays the CO stretching vibration $A_{1(1)}$ at the highest wavelength numbers (υ_{CO} 2013 cm^{-1}). In comparison, complexes **Mo2**-**Mo6** containing a chelating bis-triazolylidene ligand show resonances at lower

wavelength numbers than **Mo1**. Increasing electron density at the metal center results in additional carbonyl π-back-bonding that weakens the C≡O bond and reduces the stretching frequency. Following similar trend, the CO stretching band of **Mo7** appear at higher wavenumber than those observed in complexes **Mo2**-**Mo6**, reflecting the weaker donor capacity of the pyridyl-triazolylidene ligand **L4** compared to the bis-triazolylidene ligands **L2** and **L3** (**Table 2.1**). **Mo2** and **Mo4** bearing N1-Et and N1-*n*Bu displayed a CO stretching band at 1991 and 1992 cm^{-1}, respectively, showing that the replacement of the Et substituent by a *n*-Bu has no impact in the electronic situation of the metal. Unexpectedly, complexes **Mo5** and **Mo6** showed a CO stretching band at 1989 cm^{-1} slightly lower than **Mo2** and **Mo4** (1992 cm^{-1}). The shift to lower frequency is counterintuitive when considering the electron-withdrawing character of aryl groups. These observations may indicate that the donor ligand properties might be affected for other electronic contributions that are not been taken into consideration.

Table 2.1. Selected NMR and IR data of Mo(0) complexes **Mo1**-**Mo7**.

Complex	IR υ CO (cm^{-1})	^{13}C NMR-$C_{carbene}$ δ (ppm)	^{95}Mo NMR δ (ppm)
Mo1	2013, 1933, 1883, 1819	--	--
Mo2	1991, 1872, 1849, 1785	175.87	-1741.33
Mo3	1989, 1858, 1781	179.59	-1681.05
Mo4	1992, 1881, 1840, 1780	175.98	-1735.84
Mo5	1988, 1869, 1842, 1791	177.65	--
Mo6	1988, 1925, 1873, 1827	181.40	-1677.36
Mo7	2010, 1918, 1861, 1816	185.42	--
Mo(bis-NHC^{Me})(CO)$_4$	1991, 1855, 1820	194.32	--

Comparison of the carbenic C5 resonance in the ^{13}C NMR spectra of **Mo2**-**Mo6** complexes provides also interesting trends. Mo complexes with alkyl wingtip substituents on N1 showed similar resonances (at *ca* 175 ppm), indicating that the alkyl chain length (**Mo2** vs **Mo4**) has no detectable impact on the resonance frequency, which is in accord with the trend observed in their IR wavelength numbers. Replacing the N1-alkyl group with a phenyl substituent (**Mo3**) decreases the shielding of the carbene resonance (179.59 ppm). The downfield shift is expected considering the +I effect of the alkyl groups vs aryl groups. Similar trend is observed when comparing **Mo3** and **Mo6**, having a N3-methyl or N3-phenyl substituent (carbene resonance at 179.59 and 181.40 ppm, respectively). Interestingly, the ^{13}C NMR frequencies correlate well with the ligand donor properties expected for **L2**-**L3** (**Figure 2.3**), while the IR in this case shows a different trend.

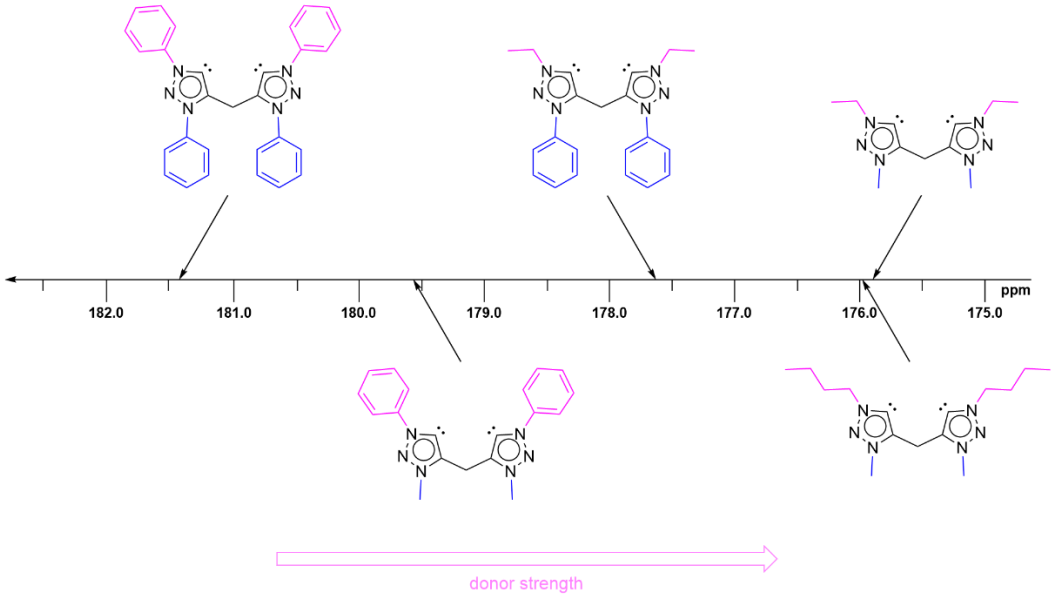

Figure 2.3. Donor abilities of bis-triazolylidene ligands **L2** and **L3** based on 13C NMR data.

The chemical shifts observed in the ^{95}Mo NMR spectra of complexes **Mo2**-**Mo6** cover a range *ca* 64 ppm (from -1677 to -1741 ppm) and showed interesting trends. As shown in **Table 2.1** and **Figure 2.4**, an increase in shielding of the ^{95}Mo nucleus in the order **Mo6**<**Mo3**<<**Mo4**<**Mo2** is observed. The variations in the chemical shifts are most probably related to the electron density localized at the metal center. Thus, the observed trend can be rationalized by the more electron donating capacity of triazolylidenes containing N-alkyl substituents *vs* those with N-aryl substituents considering the +I effect. These observations are consistent with the variations observed in the chemical shifts of $C_{carbene}$ of **Mo2**-**Mo6** complexes in their ^{13}C NMR spectra.

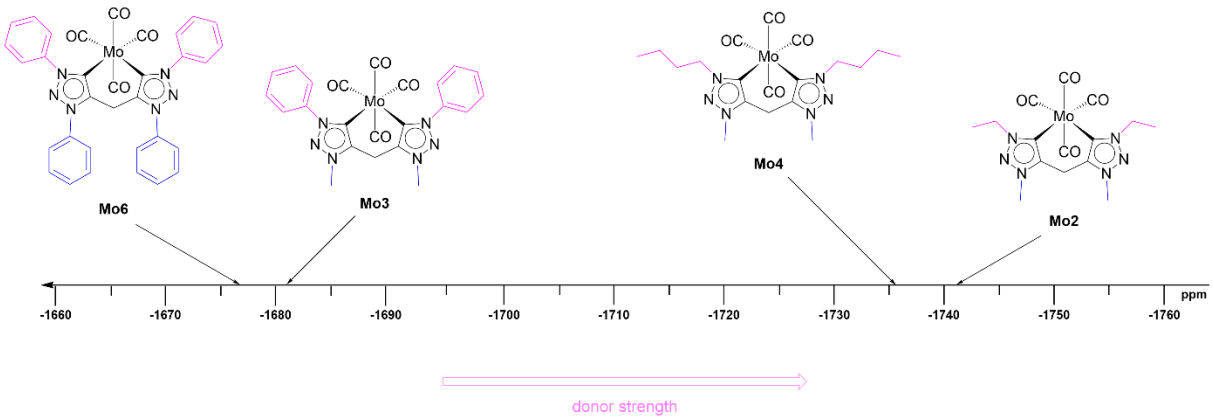

Figure 2.4. ^{95}Mo NMR data of complexes **Mo2**-**Mo6**.

The molecular structure of complex **Mo7** was established by single crystal X-ray diffraction studies. **Figure 2.5** shows the ORTEP-3 diagram, with the most relevant bond distances reported in the corresponding caption. The geometry around the Mo(0) center is that of a slightly distorted octahedron, containing a chelating pyridyl-triazolylidene ligand, two axial CO ligands, and two equatorial CO ligands.

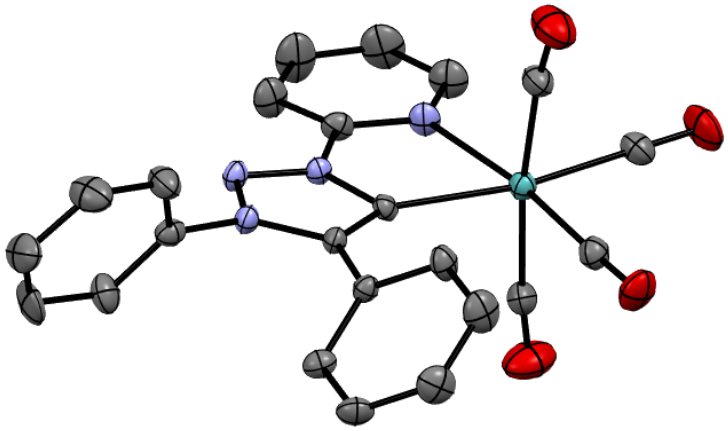

Figure 2.5. ORTEP-3 diagram of complex **Mo7** (asymmetric unit), using 50% probability level ellipsoids. All hydrogen atoms were omitted for clarity. Selected bond lengths: Mo1–C1 2.215(6) Å, Mo1–N4 2.288(6) Å, Mo1–C20 2.035(8) Å, Mo1–C21 1.959(8) Å, Mo1–C22 2.011(9) Å, Mo1–C23 2.051(9) Å.

The Mo-$C_{carbene}$ and Mo-N distances in **Mo7** are 2.215(6) Å and 2.288(6) Å, respectively, which are comparable to the reported values for [Mo(bis-NHC^{Me})$(CO)_4$] (2.260(3) Å and 2.246(3) Å). A short Mo-CO distance with a simultaneously elongated C≡O bond indicates an increased donor strength of the chelating ligand. This impact is more significant for the carbonyl ligands *trans* to the respective donor atoms (CO_{eq}). The Mo-CO_{eq} distances in **Mo7** are 1.959(8) Å and 2.011(9) Å, shorter than those observed for [Mo(bis-NHC^{Me})$(CO)_4$] (1.984(3) Å and 2.034(3) Å), indicating that the bis-imidazolylidene ligand has a lower donor capacity than the pyridyl-triazolylidene ligand.

2.4. Conclusions

In this Chapter, we have presented the synthesis and characterization of a new family of molybdenum(0) complexes with mesoionic carbene (MIC) ligands. These complexes, of general formula $[Mo(CO)_4(trz)]$, contained a variety of chelating bidentate ligands with different wingtips, including bis-1,2,3-triazol-5-ylidene (**L2** and **L3**), and pyridyl-1,2,3-triazol-4-ylidene (**L4**) ligands. The synthesis of these complexes was achieved through *in situ* deprotonation of the corresponding triazolium salts. In addition, a $[Mo(CO)_4(N^N)]$ complex, containing a bis-1,2,3-triazole (**L1**) ligand was synthesized by direct reaction of the bis-triazole ligand with $Mo(CO)_6$.

All Mo complexes were fully characterized by IR and NMR (^1H, ^{13}C, and ^{95}Mo) spectroscopy and by elemental analysis. The IR and NMR data of all complexes provided valuable insights of the donor capacity of the bidentate mesoionic ligands. As expected, bis-triazoly-5-lidene ligands exhibited higher σ-donor ability compared to pyridyl-triazoly-4-lidene and bis-triazole. In addition, the introduction of aromatic groups at the N3 and N1 positions of the triazolylidene rings decreased the overall donor capacity of the bis-triazolylidene ligands.

These newly synthesized complexes contribute to the development of molybdenum chemistry with 1,2,3-triazolylidene ligands, an area that has remained almost unexplored.

2.5. Experimental Details

2.5.1. General Considerations

The reagents and solvents used were commercially acquired and used without further purification. All reactions and manipulations, except the formation of phenyl azide and 1,2,3-triazole compounds, were carried out under nitrogen atmosphere using standard Schlenk techniques, and solvents were purified from appropriate drying agents, as reported in the literature. Compounds containing azides are potentially explosive. Thus, azides should be prepared in small quantities and handled with great care. Preparation of phenyl azide[28], diphenyliodonium salt,[10] and 1,5-diphenyl-1*H*-1,2,3-triazole (1,5-triazole^{Ph})[7] was performed following the procedure described in the literature.

^{1}H, ^{13}C and ^{95}Mo NMR spectra were recorded on a Bruker Avance III 400 MHz. In the description of each spectrum, the data are described as follows: deuterated solvent; chemical shift δ (in ppm); signal multiplicity [singlet (*s*), broad singlet (*br s*), doublet (*d*), triplet (*t*), quartet (*q*), quintet (*quint.*), sextet (*sext.*), multiplet (*m*)]; coupling constant value (*J*, in Hz); relative area (nH, number of protons); assignment to protons of the molecule. The signal of the deuterated solvent itself was used as a reference. For the characterization of the metal complexes, Infrared Spectroscopy (FT-IR) was also used and all spectra were recorded on a Bruker IFS 66v/S spectrophotometer. Only the most relevant frequencies are presented in the description and the data are presented in the following order: physical state of the sample [KBr (in potassium bromide tablets)]; maximum absorption frequency υ_{max} (in cm^{-1}); assignment to a group of atoms in the molecule. Elemental analyses were performed in our ITQB laboratory services.

2.5.2. Synthetic Procedures

2.5.2.1. General Procedure for the Preparation of L1a and L1c

A mixture of RI (R = Et, *n*-Bu) (6.4 mmol) and NaN_3 (1.40 g, 21.2 mmol) in THF/H_2O (40 mL, 1:1 v/v) was stirred at room temperature for 5 h. Then, 1-trimethylsilyl-1,4-pentadiyne (0.52 mL, 3.0 mmol), pyridine (0.28 mL, 3.4 mmol), K_2CO_3 (830 mg, 6.0 mmol), $CuSO_4$ (104 mg, 0.65 mmol), and sodium ascorbate (840 mg, 4.2 mmol) were added, and the reaction mixture was refluxed for 16 h. After cooling to room temperature, the solvent was removed under vacuum, and the residue was extracted with dichloromethane (3 x 80 mL). The combined organic layers were washed with 10% ammonium hydroxide solution (2 x 80 mL), water (2 x 80 mL), and brine (2 x 80 mL), dried over Na_2SO_4, and filtered. All volatiles were removed from the filtrate under reduced pressure to yield the corresponding bis-triazoles **L1a** and **L1c**.

L1a: Beige solid (446 mg, 72%). ^{1}H NMR (400 MHz, DMSO-d_6) δ (ppm): 7.88 (*s*, 2H, C$\underline{H}_{trz}$), 4.33 (*q*, $^{3}J_{HH}$ = 7.3 Hz, 4H, NC$\underline{H}_2$), 4.02 (*s*, 2H, $C_{trz}C\underline{H}_2$), 1.40 (*t*, $^{3}J_{HH}$ = 7.2 Hz, 6H, $NCH_2C\underline{H}_3$).

L1c: Brown solid 520 mg (66%). ^{1}H NMR (400 MHz, $CDCl_3$) δ (ppm): 7.43 (*s*, 2H, C<u>H</u>$_{trz}$), 4.34-4.27 (*m*, 4H, NC<u>H</u>$_2$), 4.17 (*s*, 1H, C_{trz}C<u>H</u>$_2$), 3.72 (*s*, 1H, C_{trz}C<u>H</u>$_2$), 1.89-1.81 (*m*, 4H, $NCH_2C\underline{H}_2$), 1.35-1.30 (*m*, 4H, $NCH_2CH_2C\underline{H}_2$), 0.96-0.90 (*m*, 6H, $NCH_2CH_2CH_2C\underline{H}_3$).

2.5.2.2. Procedure for the Preparation of L1b

In a Schlenk flask containing a solution of phenyl azide (715 mg, 6.0 mmol) in *tert*-butanol/H_2O (20 mL, 1:1 v/v) was added 1-trimethylsilyl-1,4-pentadiyne (0.52 mL, 3.0 mmol), pyridine (0.24 mL, 3.0 mmol), K_2CO_3 (746 mg, 5.4 mmol), $CuSO_4$ (67 mg, 0.42 mmol), and sodium ascorbate (832 mg, 4.2 mmol). The reaction mixture was refluxed for 24 h. After cooling to room temperature, the solvent was removed under vacuum, and the residue was extracted with dichloromethane (3 x 80 mL). The combined organic layers were washed with 10% ammonium hydroxide solution (2 x 80 mL), water (2 x 80 mL), and brine (2 x 80 mL), dried over Na_2SO_4, and filtered. All volatiles were removed from the filtrate under reduced pressure to yield the corresponding bis-triazole **L1b** as a brown solid.

L1b: Yield: 873 mg (96%). ^{1}H NMR (400 MHz, $CDCl_3$) δ (ppm): 7.97 (*s*, 2H, C<u>H</u>$_{trz}$), 7.71 (*d*, $^3J_{HH}$ = 7.9 Hz, 4H, C<u>H</u>$_{orto}$), 7.49 (*t*, $^3J_{HH}$ = 7.7 Hz, 4H, C<u>H</u>$_{meta}$), 7.41 (*t*, $^3J_{HH}$ = 7.4 Hz, 2H, C<u>H</u>$_{para}$), 4.36 (*s*, 2H, C_{trz}C<u>H</u>$_2$).

2.5.2.3. General Procedure for the Synthesis of L2a-c[OTf]$_2$

In a closed ampoule, the appropriate bis-triazole **L1** (1 equiv.) was dissolved in dry dichloromethane (5 mL), and MeOTf (4 equiv.) was added at 0 °C. The reaction mixture was stirred at 60 °C for 24h. Then, diethyl ether was added to the mixture to obtain a precipitate that was collected by filtration, and dried under vacuum to yield the corresponding bis-triazolium triflate salts **L2a[OTf]$_2$-L2c[OTf]$_2$**.

L2a[OTf]$_2$: White solid (516 mg, 100%). ^{1}H NMR (400 MHz, DMSO-d_6) δ (ppm): 8.84 (*s*, 2H, C<u>H</u>$_{trz}$), 4.74 (*s*, 2H, C_{trz}C<u>H</u>$_2$), 4.63 (*q*, $^3J_{HH}$ = 7.3 Hz, 4H, NC<u>H</u>$_2$), 4.26 (*s*, 6H, NC<u>H</u>$_3$), 1.53 (*t*, $^3J_{HH}$ = 7.4 Hz, 6H, $NCH_2C\underline{H}_3$).

L2b[OTf]$_2$: White solid (530 mg, 84%). ^{1}H NMR (400 MHz, DMSO-d_6) δ (ppm): 9.51 (*s*, 2H, C<u>H</u>$_{trz}$), 8.01-7.98 (*m*, 4H, C<u>H</u>$_{Ph}$), 7.81-7.76 (*m*, 6H, C<u>H</u>$_{Ph}$), 4.96 (*s*, 2H, C_{trz}C<u>H</u>$_2$), 4.47 (*s*, 6H, NC<u>H</u>$_3$).

L2c[OTf]$_2$: Brown solid (506 mg, 96%). ^{1}H NMR (400 MHz, DMSO-d_6) δ (ppm): 8.84 (*s*, 2H, C<u>H</u>$_{trz}$), 4.73 (*s*, 2H, C_{trz}C<u>H</u>$_2$), 4.61 (*t*, $^3J_{HH}$ = 7.1 Hz, 4H, NC<u>H</u>$_2$), 4.25 (*s*, 6H, NC<u>H</u>$_3$), 1.88 (*quint.*, $^3J_{HH}$ = 7.3 Hz, 4H, $NCH_2C\underline{H}_2$), 1.33 (*sext.*, $^3J_{HH}$ = 7.4 Hz, 4H, $NCH_2CH_2C\underline{H}_2$), 0.92 (*t*, $^3J_{HH}$ = 7.3 Hz, 6H, $NCH_2CH_2CH_2C\underline{H}_3$).

2.5.2.4. General Procedure for the Synthesis of L2a-c[Br]$_2$

In a Schlenk flask, the appropriate bis-triazolium triflate salt **L2** (1 equiv.) was dissolved in the minimum amount of acetone, and the solution was treated with tetra-*n*-butyl ammonium bromide (4

equiv.). After stirring for 30 min at room temperature, the formed precipitate was isolated by filtration through a celite cannula, washed with acetone and diethyl ether, and dried under vacuum to yield the corresponding bis-triazolium bromide salts **L2a[Br]$_2$-L2c[Br]$_2$**.

L2a[Br]$_2$: White solid (314 mg, 82%). ^{1}H NMR (400 MHz, DMSO-d$_6$) δ (ppm): 8.97 (*s*, 2H, C$\underline{H}_{trz}$), 4.83 (*s*, 2H, $C_{trz}C\underline{H}_2$), 4.65 (*q*, $^3J_{HH}$ = 7.3 Hz, 4H, NC$\underline{H}_2$), 4.30 (*s*, 6H, NC$\underline{H}_3$), 1.54 (*t*, $^3J_{HH}$ = 7.4 Hz, 6H, $NCH_2C\underline{H}_3$).

L2b[Br]$_2$: White solid (347 mg, 84%). ^{1}H NMR (400 MHz, DMSO-d$_6$) δ (ppm): 9.71 (*s*, 2H, C$\underline{H}_{trz}$), 8.06-8.04 (*m*, 4H, C$\underline{H}_{Ph}$), 7.80-7.74 (*m*, 6H, C$\underline{H}_{Ph}$), 5.07 (*s*, 2H, $C_{trz}C\underline{H}_2$), 4.52 (*s*, 6H, NC$\underline{H}_3$).

L2c[Br]$_2$: Brown solid (412 mg, 69%). ^{1}H NMR (400 MHz, DMSO-d$_6$) δ (ppm): 8.93 (*s*, 2H, C$\underline{H}_{trz}$), 4.79 (*s*, 2H, $C_{trz}C\underline{H}_2$), 4.62 (*t*, $^3J_{HH}$ = 7.1 Hz, 4H, NC$\underline{H}_2$), 4.27 (*s*, 6H, NC$\underline{H}_3$), 1.89 (*quint.*, $^3J_{HH}$ = 7.3 Hz, 4H, $NCH_2C\underline{H}_2$), 1.33 (*sext.*, $^3J_{HH}$ = 7.4 Hz, 4H, $NCH_2CH_2C\underline{H}_2$), 0.92 (*t*, $^3J_{HH}$ = 7.4 Hz, 6H, $NCH_2CH_2CH_2C\underline{H}_3$).

2.5.2.5. General Procedure for the Synthesis of L3a-b[OTf]$_2$

In a closed ampoule under N_2, the appropriate bis-triazole **L1** (1 equiv.), diphenyliodonium triflate salt (3 equiv.) and $CuSO_4$ (10 mol%) were added. The reaction mixture was stirred for 17 h at 130 °C. After cooling down to ambient temperature, the crude product was dissolved in acetone and triturated with petroleum ether to yield the corresponding bis-triazolium triflate salts **L3a[OTf]$_2$** and **L3b[OTf]$_2$**.

L3a[OTf]$_2$: Yellowish-purple solid (897 mg, 94% yield). ^{1}H NMR (400 MHz, DMSO-d$_6$) δ (ppm): 8.97 (*s*, 2H, C$\underline{H}_{trz}$), 7.80-7.66 (*m*, 10H, C$\underline{H}_{Ph}$), 4.75 (*q*, $^3J_{HH}$ = 7.3 Hz, 4H, NC$\underline{H}_2$), 4.66 (*s*, 2H, $C_{trz}C\underline{H}_2$), 1.57 (*t*, $^3J_{HH}$ = 7.2 Hz, 6H, $NCH_2C\underline{H}_3$).

L3b[OTf]$_2$: Brown solid (733 mg, 73% yield). ^{1}H NMR (400 MHz, DMSO-d$_6$) δ (ppm): 9.71 (*s*, 2H, C$\underline{H}_{trz}$), 8.12-8.09 (*m*, 3H, C$\underline{H}_{Ph}$), 7.88-7.75 (*m*, 17H, C$\underline{H}_{Ph}$), 4.80 (*s*, 2H, $C_{trz}C\underline{H}_2$).

2.5.2.6. General Procedure for the Synthesis of L3a-b[Br]$_2$

In a Schlenk flask, the appropriate bis-triazolium triflate salt **L3** (1 equiv.) was dissolved in the minimum amount of acetone, and the solution was treated with tetra-*n*-butyl ammonium bromide (4 equiv.). After stirring for 2 h at room temperature, the formed precipitate was isolated by filtration through a celite cannula, washed with acetone and diethyl ether, and dried under vacuum to yield the corresponding bis-triazolium bromide salts **L3a[Br]$_2$** and **L3b[Br]$_2$**.

L3a[Br]$_2$: Orange-purple solid (472 mg, 97% yield). ^{1}H NMR (400 MHz, DMSO-d$_6$) δ (ppm): 9.11 (*s*, 2H, C$\underline{H}_{trz}$), 7.80-7.70 (*m*, 10H, C$\underline{H}_{Ph}$), 4.76 (*q*, $^3J_{HH}$ = 7.2 Hz, 4H, NC$\underline{H}_2$), 4.67 (*s*, 2H, $C_{trz}C\underline{H}_2$), 1.58 (*t*, $^3J_{HH}$ = 7.2 Hz, 6H, $NCH_2C\underline{H}_3$).

L3b[Br]$_2$: Brown solid (442 mg, 74%yield). ^{1}H NMR (400 MHz, DMSO-d$_6$) δ (ppm): 10.02 (*s*, 2H, C$\underline{H}_{trz}$), 8.17-8.14 (*m*, 4H, C$\underline{H}_{Ph}$), 7.93-7.91 (*m*, 4H, C$\underline{H}_{Ph}$), 7.85-7.75 (*m*, 12H, C$\underline{H}_{Ph}$), 4.80 (*s*, 2H, $C_{trz}C\underline{H}_2$).

2.5.2.7. Procedure for the Preparation of L4[Br]

In a closed ampoule, 1,5-triazole^{Ph} (500 mg, 2.24 mmol) and 2-bromopyridine (0.18 mL, 1.87 mmol) were added and the mixture was stirred for 42 h at 160 ºC, during which the clear melt slowly turned into a dark solid. After cooling down to room temperature, the solid was dissolved in dichloromethane (10 mL), and Et_2O was added to induce precipitation of the corresponding pyridyl-triazolium bromide salt **L4[Br]** as a brown solid.

L4[Br]: Brown solid (467 mg, 66% yield). ^{1}H NMR (400 MHz, DMSO-d_6) δ (ppm): 10.23 (*s*, 1H, C$\underline{H}_{trz}$), 8.86 (*d*, $^3J_{HH}$ = 4.4 Hz, 1H, NC$\underline{H}_{Py}$), 8.37 (*d*, $^3J_{HH}$ = 3.2 Hz, 2H, C$\underline{H}_{Py}$), 7.92-7.88 (*td*, $^3J_{HH}$ = 4.3, 4.6 Hz, 1H, C$\underline{H}_{Py}$), 7.76-7.70 (*m*, 5H, NC$\underline{H}_{Ph}$), 7.59-7.48 (*m*, 5H, C$\underline{H}_{Ph}$).

2.5.2.8. Procedure for the Synthesis of Complex Mo1

In a Schlenk flask, **L1a** (100 mg, 0.48 mmol) was dissolved in dry dichloromethane (10 mL) and $Mo(CO)_6$ (128 mg, 0.48 mmol) was added under nitrogen atmosphere. The reaction mixture was refluxed for 24 h. After cooling to room temperature, the solution was filtered over celite. Then, the solvent was removed under vacuum, and the residue was washed with dry *n*-hexane to yield the corresponding complex **Mo1** as a yellow solid.

Mo1: Yield: 178 mg (88%). IR (KBr) υ CO (cm^{-1}): 2013, 1933, 1883, 1819. ^{1}H NMR (400 MHz, CD_3CN) δ (ppm): 7.58 (*s*, 2H, C$\underline{H}_{trz}$), 4.33 (*q*, $^3J_{HH}$ = 7.3 Hz, 4H, NC$\underline{H}_2$), 4.07 (*s*, 2H, $C_{trz}C\underline{H}_2$), 1.44 (*t*, $^3J_{HH}$ = 7.2 Hz, 6H, $NCH_2C\underline{H}_3$).

2.5.2.9. General Procedure for the Synthesis of Complexes Mo2-Mo7

In a closed ampoule, the appropriate bis-triazolium bromide salt, $Mo(CO)_6$, KO^{t}Bu and dry THF (10 mL) were added in this order. The reaction mixture was stirred, in the absence of light, at 90 °C for 19 h. After cooling to room temperature, the solution was filtered through a pad of celite. The filtrate was concentrated under vacuum and *n*-hexane (50 mL) was added. The solution was cooled at 0 ºC to yield pure samples of the corresponding molybdenum complexes.

Mo2: L2a[Br]$_2$ (314 mg, 0.79 mmol), $Mo(CO)_6$ (272 mg, 1.03 mmol), KO^{t}Bu (205 mg, 1.83 mmol). Yellow solid (339 mg, 97% yield). IR (KBr) υ CO (cm^{-1}): 1991, 1872, 1849, 1785. ^{1}H NMR (400 MHz, CD_3CN) δ (ppm): 4.65 (*q*, $^3J_{H\text{-}H}$ = 7.3 Hz, 4H, NC$\underline{H}_2$), 4.04 (*s*, 6H, NC$\underline{H}_3$), 4.01 (*s*, 2H, $C_{trz}C\underline{H}_2$), 1.52 (*t*, $^3J_{H\text{-}H}$ = 7.4 Hz, 6H, $NCH_2C\underline{H}_3$). ^{13}C NMR (100 MHz, CD_3CN) δ (ppm): 223.19 (C$\underline{O}$), 212.82 (C$\underline{O}$), 175.87 ($\underline{C}_{trz}$-Mo), 142.63 ($\underline{C}_{trz}CH_2$), 66.22 ($C_{trz}\underline{C}H_2$), 49.93 (N$\underline{C}H_2$), 36.59 (N$\underline{C}H_3$), 16.35 ($NCH_2\underline{C}H_3$), 15.57 ($NCH_2\underline{C}H_3$). ^{95}Mo NMR (26 MHz, CD_3CN) δ (ppm): -1741.33. Elem. anal. calcd. for $C_{15}H_{18}MoN_6O_4$: C 40.73; H 4.10; N 19.00%. Found: C 40.51; H 4.00; N 19.21%.

Mo3: L2b[Br]$_2$ (100 mg, 0.20 mmol), $Mo(CO)_6$ (70 mg, 0.26 mmol), KO^{t}Bu (52 mg, 0.46 mmol). Orange solid (92 mg, 84% yield). IR (KBr) υ CO (cm^{-1}): 1989, 1858, 1781. ^{1}H NMR (400 MHz, CD_3CN) δ (ppm): 7.61-7.58 (*m*, 4H, C$\underline{H}_{Ph}$), 7.55-7.53 (*m*, 6H, C$\underline{H}_{Ph}$), 4.23 (*s*, 2H, $C_{trz}C\underline{H}_2$), 4.18 (*s*, 6H, NC$\underline{H}_3$). ^{13}C NMR

(100 MHz, CD_3CN) δ (ppm): 221.44 (<u>C</u>O), 213.80 (<u>C</u>O), 179.59 (<u>C</u>$_{trz}$-Mo), 142.33 (<u>C</u>$_{trz}$CH$_2$), 141.98 (<u>C</u>$_{Ph}$), 131.37 (<u>C</u>H$_{Ph}$), 130.38 (<u>C</u>H$_{Ph}$), 129.67 (<u>C</u>H$_{Ph}$), 127.75 (<u>C</u>H$_{Ph}$), 122.82 (<u>C</u>H$_{Ph}$), 79.12 (C$_{trz}$<u>C</u>H$_2$), 68.23 (C$_{trz}$<u>C</u>H$_2$), 36.88 (N<u>C</u>H$_3$). ^{95}Mo NMR (26 MHz, CD_3CN) δ (ppm): -1681.05 . Elem. anal. calcd. for $C_{23}H_{18}MoN_6O_4$: C 51.31; H 3.37; N 15.61%. Found: C 51.20; H 3.13; N 15.71%.

Mo4: L2c[Br]$_2$ (412 mg, 0.91 mmol), $Mo(CO)_6$ (313 mg, 1.18 mmol), KO^{t}Bu (235 mg, 2.09 mmol). Orange solid (365 mg, 80% yield). IR (KBr) υ CO (cm^{-1}): 1992, 1881, 1840, 1780. ^{1}H NMR (400 MHz, CD_3CN) δ (ppm): 4.60 (*t*, $^3J_{H\text{-}H}$ = 7.6 Hz, 4H, NC<u>H</u>$_2$), 4.03 (*s*, 6H, NC<u>H</u>$_3$), 4.00 (*s*, 2H, C$_{trz}$C<u>H</u>$_2$), 1.97-1.89 (*m*, 4H, NCH$_2$C<u>H</u>$_2$), 1.43 (*sext.*, $^3J_{H\text{-}H}$ = 7.5 Hz, 4H, NCH$_2$CH$_2$C<u>H</u>$_2$), 0.96 (*t*, $^3J_{H\text{-}H}$ = 7.4 Hz, 6H, NCH$_2$CH$_2$CH$_2$C<u>H</u>$_3$). ^{13}C NMR (100 MHz, CD_3CN) δ (ppm): 223.13 (<u>C</u>O), 212.88 (<u>C</u>O), 175.98 (<u>C</u>$_{trz}$-Mo), 142.57 (<u>C</u>$_{trz}$CH$_2$), 79.34 (C$_{trz}$<u>C</u>H$_2$), 79.10 (C$_{trz}$<u>C</u>H$_2$), 54.99 (N<u>C</u>H$_2$), 36.55 (NCH$_2$<u>C</u>H$_2$), 33.37 (NCH$_2$<u>C</u>H$_2$), 20.44 (NCH$_2$CH$_2$<u>C</u>H$_2$), 13.90 (NCH$_2$CH$_2$CH$_2$<u>C</u>H$_3$). ^{95}Mo NMR (26 MHz, CD_3CN) δ (ppm): -1735.84. Elem. anal. calcd. for $C_{19}H_{26}MoN_6O_4$: C 45.79; H 5.26; N 16.86%. Found: C 45.60; H 5.02; N 16.99%.

Mo5: L3a[Br]$_2$ (259 mg, 0.50 mmol), $Mo(CO)_6$ (171 mg, 0.65 mmol), KO^{t}Bu (128 mg, 1.14 mmol). Yellow solid (159 mg, 56% yield). IR (KBr) υ CO (cm^{-1}): 1988, 1869, 1842, 1791. ^{1}H NMR (400 MHz, CD_3CN) δ (ppm): 7.59-7.55 (*m*, 2H, C<u>H</u>$_{Ph}$), 7.53-7.49 (*m*, 4H, C<u>H</u>$_{Ph}$), 7.44-7.42 (*m*, 4H, C<u>H</u>$_{Ph}$), 4.77 (*q*, $^3J_{H\text{-}H}$ = 7.2 Hz, 4H, NC<u>H</u>$_2$), 3.92 (*s*, 2H, C$_{trz}$C<u>H</u>$_2$), 1.61 (*t*, $^3J_{H\text{-}H}$ = 7.4 Hz, 6H, NCH$_2$C<u>H</u>$_3$). ^{13}C NMR (100 MHz, CD_3CN) δ (ppm): 223.15 (<u>C</u>O), 212.64 (<u>C</u>O), 177.65 (<u>C</u>$_{trz}$-Mo), 143.06 (<u>C</u>$_{trz}$CH$_2$), 135.72 (<u>C</u>$_{Ph}$), 131.79 (<u>C</u>H$_{\textit{para}}$-Ph), 130.60 (<u>C</u>H$_{\textit{orto}}$-Ph), 126.39 (<u>C</u>H$_{\textit{meta}}$-Ph), 68.22 (C$_{trz}$<u>C</u>H$_2$), 50.49 (N<u>C</u>H$_2$), 16.20 (NCH$_2$<u>C</u>H$_3$). Elem. anal. calcd. for $C_{25}H_{22}MoN_6O_4$: C 53.01; H 3.91; N 14.84%. Found: C 52.89; H 4.27; N 14.38%.

Mo6: L3b[Br]$_2$ (149 mg, 0.24 mmol), $Mo(CO)_6$ (83 mg, 0.31 mmol), KO^{t}Bu (62 mg, 0.55 mmol). Brown solid (151 mg, 95% yield). IR (KBr) υ CO (cm^{-1}): 1988, 1925, 1873, 1827. ^{1}H NMR (400 MHz, CD_3CN) δ (ppm): 7.75-7.73 (*m*, 4H, C<u>H</u>$_{Ph}$), 7.62-7.56 (*m*, 16H, C<u>H</u>$_{Ph}$), 4.12 (*s*, 2H, C$_{trz}$C<u>H</u>$_2$). ^{13}C NMR (100 MHz, CD_3CN) δ (ppm): 221.77 (<u>C</u>O), 213.51 (<u>C</u>O), 181.40 (<u>C</u>$_{trz}$-Mo), 142.85 (<u>C</u>$_{trz}$CH$_2$), 141.79 (<u>C</u>$_{Ph}$), 135.56 (<u>C</u>H$_{Ph}$), 132.06 (<u>C</u>H$_{Ph}$), 131.49 (<u>C</u>H$_{Ph}$), 130.72 (<u>C</u>H$_{Ph}$), 129.75 (<u>C</u>H$_{Ph}$), 127.74 (<u>C</u>H$_{Ph}$), 126.55 (<u>C</u>H$_{Ph}$), 123.01 (<u>C</u>H$_{Ph}$), 79.10 (C$_{trz}$<u>C</u>H$_2$), 66.22 (C$_{trz}$<u>C</u>H$_2$). ^{95}Mo NMR (26 MHz, CD_3CN) δ (ppm): -1677.36. Elem. anal. calcd. for $C_{33}H_{22}MoN_6O_4$: C 59.83; H 3.35; N 12.69%. Found: C 59.69; H 3.01; N 12.89%.

Mo7: L4[Br] (88 mg, 0.23 mmol), $Mo(CO)_6$ (80 mg, 0.30 mmol), KO^{t}Bu (34 mg, 0.30 mmol). Red crystals (60 mg, 51% yield). IR (KBr) υ CO (cm^{-1}): 2010, 1918, 1861, 1816. ^{1}H NMR (400 MHz, CD_3CN) δ (ppm): 8.96 (*d*, $^3J_{H\text{-}H}$ = 6.4 Hz, 1H, NC<u>H</u>$_{Py}$), 8.29 (*d*, $^3J_{H\text{-}H}$ = 8 Hz, 1H, C<u>H</u>$_{Py}$), 8.17-8.13 (*td*, $^3J_{H\text{-}H}$ = 7.8, 1.6 Hz, 1H, C<u>H</u>$_{Py}$), 7.65-7.61 (*m*, 1H, C<u>H</u>$_{Py}$), 7.57-7.50 (*m*, 7H, C<u>H</u>$_{Ph}$), 7.43-7.38 (*m*, 3H, C<u>H</u>$_{Ph}$). ^{13}C NMR (100 MHz, CD_3CN) δ (ppm): 225.69 (<u>C</u>O), 221.56 (<u>C</u>O), 208.25 (<u>C</u>O), 185.42 (<u>C</u>$_{trz}$-Mo), 154.40, 152.65, 149.44, 141.48, 136.54, 132.14, 131.30, 130.66, 130.27, 129.31, 129.08, 126.83, 126.12, 115.28. Elem. anal. calcd. for $C_{23}H_{14}MoN_4O_4.C_4H_{10}O$: C 55.87; H 4.17; N 9.65%. Found: C 56.30; H 4.31; N 9.81%.

2.5.3. Single Crystal X-Ray Diffraction Studies

A crystal of **Mo7** suitable for single-crystal X-ray analysis was selected, covered with Fomblin (polyfluoro ether oil) and mounted on a nylon loop. The data was collected at room temperature on a Bruker D8 Venture diffractometer equipped with a Photon II detector and an Oxford Cryostem Cooler,

using graphite monochromated Mo-Kα radiation (λ= 0.71073 Å). The data was processed using the APEX4 suite software package, which includes integration and scaling (SAINT), absorption corrections (SADABS)[31] and space group determination (XPREP). Structure solution and refinement were done using direct methods with the programs[32] SHELXT 2018/2 and SHELXL-2018/3 inbuilt in APEX and WinGX-Version 2021.3 software packages.[33] All non-hydrogen atoms were refined anisotropically and the hydrogen atoms were inserted in idealized positions and allowed to refine riding on the parent carbon atom. The molecular diagrams were drawn with Mercury.[34] Crystal and structure refinement data are given in **Table 1** (see Table 1 in Annexes – A.2.3).

2.6. Acknowledgements and Contributions

We thank FC&T for funding PTDC/QUI-QIN/0359/2021, PTDC/QUI-QOR/0712/2020, MOSTMICRO-ITQB, UIDB/04612/20220 and UIPD/04612/2020. M. C. Almeida and Elemental Analysis Service at ITQB NOVA are acknowledged for the elemental analysis of the compounds. The NMR data were acquired at CERMAX, ITQB NOVA, Oeiras, Portugal with equipment funded by FCT, project AAC 01/SAICT/2016. We thank the Crystallography Service of the LAQV, Department of Chemistry, NOVA School of Science and Technology, Portugal, and Dra. Clara Gomes for the structural determination of **Mo7**.

Beatriz Garcia performed all the experiments described in this Chapter. Beatriz Royo directed the research.

2.7. References

1. Friães, S., Realista, S., Gomes, C. S. B., Martinho, P. N., Royo, B. (**2021**). Click-derived triazoles and triazolylidenes of manganese for electrocatalytic reduction of CO_2. *Molecules*, 26(21). https://doi.org/10.3390/molecules26216325

2. Maity, R., Sarkar, B. (**2022**). Chemistry of Compounds Based on 1,2,3-Triazolylidene-Type Mesoionic Carbenes. *J. Am. Chem. Soc. Au*, 2(1), 22–57. https://doi.org/10.1021/jacsau.1c00338

3. Guisado-Barrios, G., Soleilhavoup, M., Bertrand, G. (**2018**). 1 H-1,2,3-Triazo.l-5-ylidenes: Readily Available Mesoionic Carbenes. *Acc. Chem. Res.* 51(12), 3236–3244. https://doi.org/10.1021/acs.accounts.8b00480

4. Sharpless, W. D., Wu, P., Vidar Hansen, T., Lindberg, J. G. (**2005**). Just Click It: Undergraduate Procedures for the Copper(I)-Catalyzed Formation of 1,2,3-Triazoles from Azides and Terminal Acetylenes. *J. Chem. Educ.*, 82(12), 1833. https://doi.org/10.1021/ed082p1833

5. Monkowius, U., Ritter, S., König, B., Zabel, M., Yersin, H. (**2007**). Synthesis, characterisation and ligand properties of novel Bi-1,2,3-triazole ligands. *Eur. J. Inorg. Chem.*, 29, 4597–4606. https://doi.org/10.1002/ejic.200700479

6. Schweinfurth, D., Hettmanczyk, L., Suntrup, L., Sarkar, B. (**2017**). Metal Complexes of Click-Derived Triazoles and Mesoionic Carbenes: Electron Transfer, Photochemistry, Magnetic Bistability, and Catalysis. *Z. Anorg. Allg. Chem.*, 643(9), 554–584. https://doi.org/10.1002/zaac.201700030

7. Kwok, S. W., Fotsing, J. R., Fraser, R. J., Rodionov, V. O., Fokin, V. v. (**2010**). Transition-metal-free catalytic synthesis of 1,5-diaryl-1,2,3-triazoles. *Org. Lett*, *12*(19), 4217–4219. https://doi.org/10.1021/ol101568d

8. Badawi, M. A. A. H., Abu-Orabi, S. T. (**2021**). Quantum mechanical investigations of base-catalyzed cycloaddition reaction between phenylacetylene and azidobenzene. *J. Chem. Res.*, *45*(5–6), 519–525. https://doi.org/10.1177/1747519820946253

9. Suntrup, L., Hohloch, S., Sarkar, B. (**2016**). Expanding the Scope of Chelating Triazolylidenes: Mesoionic Carbenes from the 1,5-"Click"-Regioisomer and Catalytic Synthesis of Secondary Amines from Nitroarenes. *Chem. Eur. J.*, *22*(50), 18009–18018. https://doi.org/10.1002/chem.201603901

10. Virant, M., Košmrlj, J. (**2019**). Arylation of Click Triazoles with Diaryliodonium Salts. *J. Org. Chem.*, *84*(21), 14030–14044. https://doi.org/10.1021/acs.joc.9b02197

11. Lalrempuia, R., McDaniel, N. D., Müller-Bunz, H., Bernhard, S., Albrecht, M. (**2010**). Water oxidation catalyzed by strong carbene-type donor-ligand complexes of iridium. *Angew. Chem. Int. Ed.*, 49(50), 9765–9768. https://doi.org/10.1002/anie.201005260

12. Petronilho, A., Woods, J. A., Bernhard, S., Albrecht, M. (**2014**). Bimetallic iridium-carbene complexes with mesoionic triazolylidene ligands for water oxidation catalysis. *Eur. J. of Inorg. Chem.*, 4, 708–714. https://doi.org/10.1002/ejic.201300843

13. Vivancos, Á., Albrecht, M. (**2017**). Influence of the Linker Length and Coordination Mode of (Di)Triazolylidene Ligands on the Structure and Catalytic Transfer Hydrogenation Activity of Iridium(III) Centers. *Organometallics*, *36*(8), 1580–1590. https://doi.org/10.1021/acs.organomet.7b00140

14. Delgado-Rebollo, M., Canseco-Gonzalez, D., Hollering, M., Mueller-Bunz, H., Albrecht, M. (**2014**). Synthesis and catalytic alcohol oxidation and ketone transfer hydrogenation activity of donor-functionalized mesoionic triazolylidene ruthenium(II) complexes. *Dalton Trans.*, 43(11), 4462–4473. https://doi.org/10.1039/c3dt53052c

15. Sarkar, B., Suntrup, L. (**2017**). Illuminating Iron: Mesoionic Carbenes as Privileged Ligands in Photochemistry. *Angew. Chem. Inter. Ed.*, 129(31), 9064–9066. https://doi.org/10.1002/ange.201704522

16. Chábera, P., Liu, Y., Prakash, O., Thyrhaug, E., Nahhas, A. el, Honarfar, A., Essén, S., Fredin, L. A., Harlang, T. C. B., Kjær, K. S., Handrup, K., Ericson, F., Tatsuno, H., Morgan, K., Schnadt, J., Häggström, L., Ericsson, T., Sobkowiak, A., Lidin, S., … Wärnmark, K. (**2017**). A low-spin Fe(III) complex with 100-ps ligand-to-metal charge transfer photoluminescence. *Nature*, 543(7647), 695–699. https://doi.org/10.1038/nature21430

17. Mejuto, C., Royo, B., Guisado-Barrios, G., Peris, E. (**2015**). Rhodium, iridium and nickel complexes with a 1,3,5-triphenylbenzene tris-MIC ligand. Study of the electronic properties and catalytic activities. *Beilstein J. Org. Chem.*, 11, 2584–2590. https://doi.org/10.3762/bjoc.11.278

18. Al-Shnani, F., Guisado-Barrios, G., Sainz, D., Peris, E. (**2019**). Tris-triazolium Salts as Anion Receptors and as Precursors for the Preparation of Cylinder-like Coordination Cages. *Organometallics*, 38(3), 697–701. https://doi.org/10.1021/acs.organomet.8b00874

19. van der Meer, M., Glais, E., Siewert, I., Sarkar, B. (**2015**). Electrocatalytic Dihydrogen Production with a Robust Mesoionic Pyridyl carbene Cobalt Catalyst. *Angew. Chem. Inter. Ed.,* 127(46), 13997–14000. https://doi.org/10.1002/ange.201506061

20. Suntrup, L., Stein, F., Klein, J., Wilting, A., Parlane, F. G. L., Brown, C. M., Fiedler, J., Berlinguette, C. P., Siewert, I., Sarkar, B. (**2020**). Rhenium Complexes of Pyridyl-Mesoionic Carbenes: Photochemical Properties and Electrocatalytic CO_2 Reduction. *Inorg. Chem.*, 59(7), 4215–4227. https://doi.org/10.1021/acs.inorgchem.9b02591

21. Scherpf, T., Carr, C. R., Donnelly, L. J., Dubrawski, Z. S., Gelfand, B. S., Piers, W. E. (**2022**). A Mesoionic Carbene-Pyridine Bidentate Ligand That Improves Stability in Electrocatalytic CO_2 Reduction by a Molecular Manganese Catalyst. *Inorg. Chem.*, 61(34), 13644–13656. https://doi.org/10.1021/acs.inorgchem.2c02689

22. Schaper, L. A., Graser, L., Wei, X., Zhong, R., Öfele, K., Pöthig, A., Cokoja, M., Bechlars, B., Herrmann, W. A., Kühn, F. E. (**2013**). Exploring the scope of a novel ligand class: Synthesis and catalytic examination of metal complexes with “normal” 1,2,3-triazolylidene ligands. *Inorg. Chem.*, 52(10), 6142–6152. https://doi.org/10.1021/ic400533u

23. Schmidt, A., Grover, N., Zimmermann, T. K., Graser, L., Cokoja, M., Pöthig, A., Kühn, F. E. (**2014**). Synthesis and characterization of novel cyclopentadienyl molybdenum imidazo[1,5-a]pyridine-3-ylidene complexes and their application in olefin epoxidation catalysis. *J. Catal.*, 319, 119–126. https://doi.org/10.1016/j.jcat.2014.08.013

24. Beerhues, J., Sen, S., Schowner, R., Mate Nagy, G., Wang, D., Buchmeiser, M. R. (**2017**). Tailored molybdenum imido alkylidene N-heterocyclic carbene complexes as latent catalysts for the polymerization of dicyclopentadiene. *J. Polym. Sci., Part A: Polymer Chemistry*, 55(18), 3028–3033. https://doi.org/10.1002/pola.28578

25. Baltrun, M., Watt, F. A., Schoch, R., Wölper, C., Neuba, A. G., Hohloch, S. (**2019**). A new bis-phenolate mesoionic carbene ligand for early transition metal chemistry. *Dalton Trans.*, 48(39), 14611–14625. https://doi.org/10.1039/c9dt03099a

26. Bens, T., Boden, P., di Martino-Fumo, P., Beerhues, J., Albold, U., Sobottka, S., Neuman, N. I., Gerhards, M., Sarkar, B. (**2020**). Chromium(0) and Molybdenum(0) Complexes with a Pyridyl-Mesoionic Carbene Ligand: Structural, (Spectro)electrochemical, Photochemical, and Theoretical Investigations. *Inorg. Chem.*, 59(20), 15504–15513. https://doi.org/10.1021/acs.inorgchem.0c02537

27. Bens, T., Marhöfer, D., Boden, P., Steiger, S. T., Suntrup, L., Niedner-Schatteburg, G., Sarkar, B. (**2023**). A Different Perspective on Tuning the Photophysical and Photochemical Properties: The Influence of Constitutional Isomers in Group 6 Carbonyl Complexes with Pyridyl-Mesoionic Carbenes. *Inorg. Chem.*, 62(39), 16182-16195. https://doi.org/10.1021/acs.inorgchem.3c02478

28. Friães, S., Gomes, C. S. B., Royo, B. (**2023**). Bis-Triazolylidenes of Manganese and Rhenium and Their Catalytic Application in N-Alkylation of Amines with Alcohols. *Organometallics*, 42(14), 1803–1809. https://doi.org/10.1021/acs.organomet.3c00046

29. Zhao, J. W., Guo, J. W., Huang, M. J., You, Y. Z., Wu, Z. H., Liu, H. M., Huang, L. H. (**2019**). Design, synthesis and biological evaluation of new steroidal β-triazoly enones as potent antiproliferative agents. *Steroids*, *150*. https://doi.org/10.1016/j.steroids.2019.108431

30. Merritt, E. A., Olofsson, B. (**2009**). Diaryliodonium Salts: A Journey from Obscurity to Fame. *Angew. Chem. Int. Ed.*, 48, 9052 – 9070. https://doi.org/10.1002/anie.200904689

31. SADABS 2016/2: Krause, L.; Herbst-Irmer, R.; Sheldrick, G. M.; Stalke, D. J. Appl. Cryst. 2015, 48, 3-10

32. (a) SHELXL: Sheldrick, G. M. Acta Crystallogr., Sect. C-Struct. Chem. 2015, 71, 3-8; (b) Hübschle, C. B.; Sheldrick, G. M.; Dittrich, B.; ShelXle: a Qt graphical user interface for SHELXL, J. Appl. Crystallogr. 2011, 44, 1281-1284

33. L. J. Farrugia, *J. Appl. Crystallogr*. 2012, 45, 849–854.

34. C. F. Macrae, I. Sovago, S. J. Cottrell, P. T. A. Galek, P. McCabe, E. Pidcock, M. Platings, G. P. Shields, J. S. Stevens, M. Towler and P. A. Wood, *J. Appl. Cryst*., 53, 226-235, 2020

Chapter 3

Catalytic Application of Molybdenum(0) Triazolylidene Complexes in Borrowing Hydrogen (BH) and Acceptorless Dehydrogenative Coupling (ADC) Reactions

3.1. Summary

In this chapter, we describe the first application of mesoionic carbenes of molybdenum in borrowing hydrogen (BH) and acceptorless dehydrogenative coupling (ADC) processes. In particular, in the synthesis of quinolines, *N*-alkylation of amines with alcohols, α-alkylation of ketones with alcohols, and β-alkylation between alcohols, and also in the oxidation of amines to amides. These methods are seen as atom-efficient and waste-free ways to access valuable chemical products like alkylated amines, imines, amides, *N*-heterocycles, and aldol condensation products, which have applications as pharmaceuticals, agrochemicals, materials, and in other fields.

In Chapter 3, we describe the excellent catalytic activity of complex **Mo2** for the synthesis of a wide variety of substituted quinolines (17 examples were isolated with good yields) from 2-aminobenzylalcohols and readily available secondary alcohols. In addition, the catalytic activity of **Mo2** in the *N*-alkylation of amines with alcohols have been explored and compared to that of the Mo related complex containing the bis-NHC^{Me} ligand. Furthermore, we have also obtained promising results in the α-alkylation of ketones with alcohols, β-alkylation between alcohols, and in the oxidation of amines to amides using our novel Mo complexes. Interestingly, we have observed that variation of the substituents of the triazolylidene ring in complexes [Mo(CO)$_4$(bis-trz)] has a significative impact in the catalytic efficiency of their Mo complexes.

3.2. Introduction

The Borrowing Hydrogen (BH) and Acceptorless Dehydrogenative Coupling (ADC) processes mediated by Earth-abundant transition-metal complexes have recently attracted enormous interest as promising, atom-efficient and waste-free strategies to access high-value products – alkylated amines, imines, amides, *N*-heterocycles, and aldol condensation products (important building blocks for the synthesis of pharmaceuticals, agrochemicals, materials, among others).[1-6]

For these transformations, a wide range of catalytic systems have been developed. Many of these systems are based on the use of expensive metals (*e.g.* Ir, Rh). In terms of sustainability, the development of Mo-based catalysts for these processes is particularly attractive. However, as mentioned in Chapter 1, there are very few examples of homogeneous Mo catalytic systems for BH and ADC processes.[7-10] On the other hand, the catalytic applications of Mo complexes bearing 1,2,3-triazolylidene ligands are limited to the epoxidation of alkenes and the polymerization of dicyclopentadiene (DCPD), as previously stated in Chapter 2. In continuation with the interest of our group in developing phosphine-free catalytic systems with inexpensive metals, we report here in Chapter 3, the catalytic applications of our new family of bis-triazolylidene molybdenum(0) complexes in the synthesis of quinolines through acceptorless dehydrogenative coupling (ADC) reactions, in the *N*-alkylation of amines with alcohols, α-alkylation of ketones with alcohols, and β-alkylation between alcohols through borrowing hydrogen (BH) reactions. Preliminary studies have also shown the potential of Mo-triazolylidenes in the catalytic oxidation of primary amines to amides (**Scheme 3.1**).

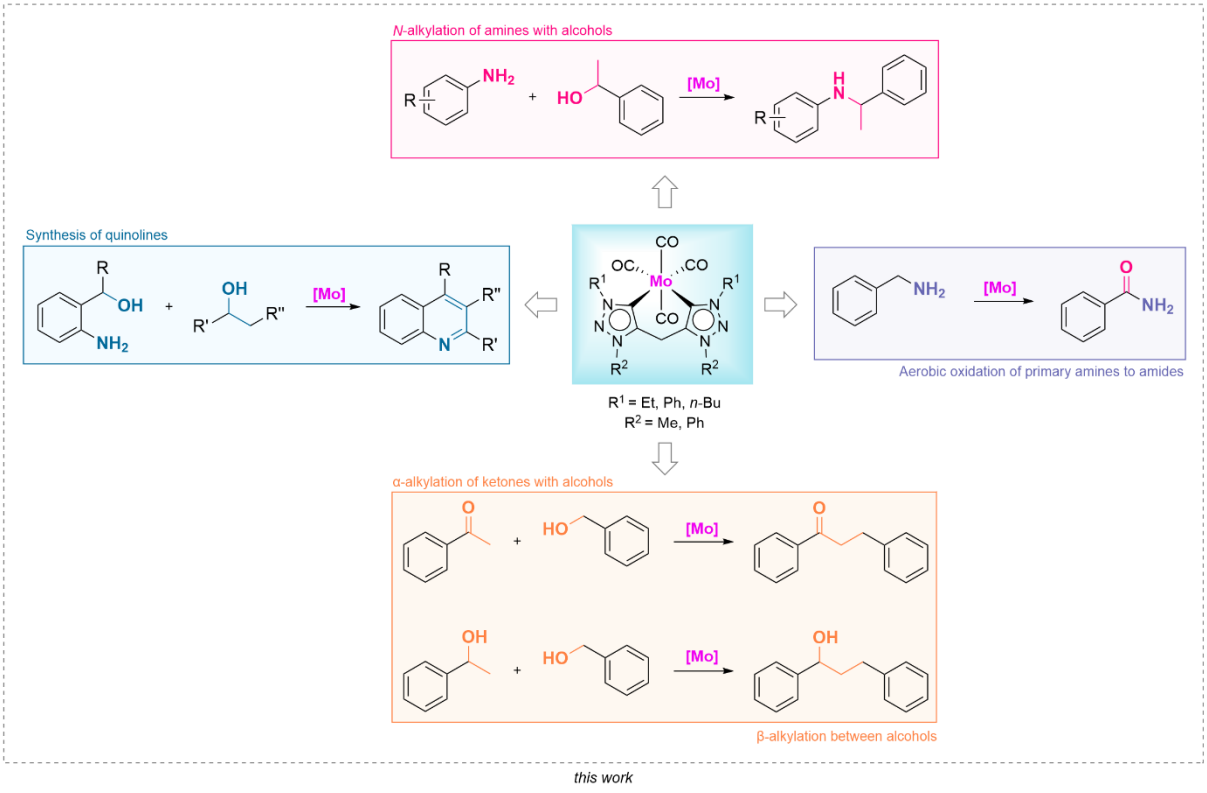

Scheme 3.1. Catalytic applications of our novel Mo triazolylidene complexes described in this work.

3.3. Results and Discussion

3.3.1. Catalytic Application in the Synthesis of Quinolines

The dehydrogenative cross-coupling of 2-aminobenzyl alcohol (**1a**) with 1-phenylethanol (**2a**) was selected as model reaction to explore the reactivity of the Mo complexes synthesized in Chapter 2 for the synthesis of quinolines through acceptorless dehydrogenative coupling (ADC) processes. Initially, the reaction was carried out in toluene using a stoichiometric ratio between **1a** and **2a**, in the presence of **Mo2** as catalyst and a base (**Scheme 3.2**).

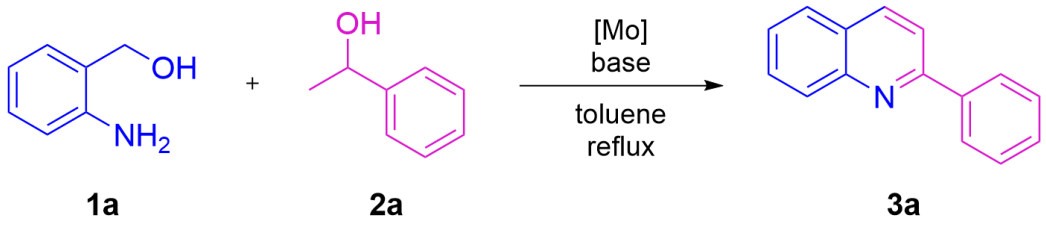

Scheme 3.2. Dehydrogenative cross-coupling formation of 2-phenylquinoline (**3a**) catalyzed by complex **Mo2**.

Optimization of the reaction conditions was performed by varying the amount and type of base, catalyst loading, temperature, and reaction time. Results are summarized in **Table 3.1**. Initially, when **1a** was reacted with an equimolar amount of **2a** (0.5 mmol) in the presence of *t*-BuOK (0.1 equiv.) and 2 mol% of **Mo2** in toluene at 150 ºC for 24 h, no reaction occurred, and formation of **3a** was not observed (Table 3.1, entry 1). Increasing the amount of catalyst to 4 and 5 mol%, produced the formation of **3a** in very low yield (5% yield, Table 3.1, entries 2 and 3). The use of NaOH and KOH instead of *t*-BuOK did not improve the efficiency of the reaction (Table 3.1, entries 4 and 5). When the amount of *t*-BuOK was increased to 0.2 equivalents, formation of **3a** in 30% yield was obtained (Table 3.1, entry 6). Gratifyingly, further increasing of the amount of base to 0.5 equivalents led to complete consumption of the starting materials and formation of **3a** in quantitative yield (Table 3.1, entry 7). It was observed that after 17 h of reaction, the conversion of **1a** and **2a** in **3a** was already completed, while in 6 h, a yield of 58% for **3a** was obtained (Table 3.1, entries 9 and 8, respectively). Attempts to reduce the amount of *t*-BuOK (0.3 equiv.) or the amount of catalyst (2.5 mol%), as well as the temperature to 110 °C, resulted in lower yields of **3a** (40, 60, and 25%, respectively, Table 3.1, entries 10-12). If the reaction is performed in neat conditions instead of using toluene, a decrease of the yield of **3a** was obtained (80%, Table 3.1, entry 13). In addition, the blank reactions performed in the absence of catalyst or base indicated that the presence of **Mo2** and base is necessary for the ADC reaction, since no detectable formation of **3a** was detected in the blank reactions (Table 3.1, entries 14 and 15). It was also found that no reaction occurred in the presence of $Mo(CO)_6$, indicating that the introduction of the MIC ligand in the coordination sphere of Mo is crucial for its reactivity (entry 16).

Table 3.1. Optimization of the reaction conditions for the dehydrogenative cross-coupling of 2-aminobenzyl alcohol (**1a**) with 1-phenylethanol (**2a**) using complex **Mo2**.[a]

Entry	Cat. [mol%]	Base [equiv.]	Time (h)	Temp. (°C)	Yield (%)[b]
1	2	*t*-BuOK [0.1]	24	150	~0
2	4	*t*-BuOK [0.1]	24	150	<5
3	5	*t*-BuOK [0.1]	24	150	~5
4	5	NaOH [0.1]	24	150	0
5	5	KOH [0.1]	24	150	0
6	5	*t*-BuOK [0.2]	24	150	30
7	**5**	***t*-BuOK [0.5]**	**24**	**150**	**>99**
8	5	*t*-BuOK [0.5]	6	150	58
9	**5**	***t*-BuOK [0.5]**	**17**	**150**	**>99**
10	5	*t*-BuOK [0.3]	17	150	40
11	2.5	*t*-BuOK [0.5]	17	150	60
12	5	*t*-BuOK [0.5]	17	110	25
13[c]	5	*t*-BuOK [0.5]	17	150	80
14	5	--	17	150	0
15	--	*t*-BuOK [0.5]	17	150	<5
16	$Mo(CO)_6$ [5]	*t*-BuOK [0.5]	17	150	~0

[a] General conditions: catalyst **Mo2**, **1a** (0.5 mmol), **2a** (0.5 mmol), base, and dry toluene (2 mL), reaction performed under N_2. [b] Yields determined by ^1H NMR spectroscopy using 1,3,5-trimethoxybenzene as an internal standard. [c] Under neat conditions.

Next, screening of the catalytic activity of complexes **Mo1**-**Mo7** was investigated using the optimized conditions shown in Table 3.1, entry 9 (0.5 mmol of **1a**, 0.5 mmol of **2a**, 0.5 equiv. of *t*-BuOK, and 5 mol% of catalyst at 150 ºC for 17 h in toluene) (**Table 3.2**). Under these conditions, complexes **Mo2** and **Mo4** displayed the highest catalytic activities, reaching quantitative yield of the corresponding quinoline **3a** (Table 3.2, entries 2 and 4). Complex **Mo1** bearing the N,N-chelating bis-triazole ligand **L1a** gave only 5% yield (Table 3.2, entry 1), showing that the presence of the bis-triazolylidene ligand **L2a** is responsible for the activity of its complex (**Mo2**). On the other hand, complexes **Mo3**, **Mo5,** and **Mo6** afforded significantly lower yields (6, 31 and 18%, respectively) (Table 3.2, entries 3 and 5-6) than **Mo2** and **Mo4**, which indicates that the presence of aromatic groups at the N1 and N3 positions of the triazolylidene ligands have a detrimental effect in the catalytic activity. Interestingly, complex **Mo7** with a pyridine ring directly linked to the triazolylidene fragment exhibited no activity (Table 3.2, entry 7).

These results showed an interesting trend, complexes **Mo2** and **Mo4** bearing stronger σ-donating bis-triazolylidene ligands resulted to be the most effective pre-catalysts.

Table 3.2. Catalyst Screening for the dehydrogenative cross-coupling of 2-aminobenzyl alcohol (**1a**) with 1-phenylethanol (**2a**) using **Mo1**-**Mo7** complexes.[a]

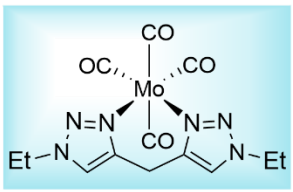

Mo1

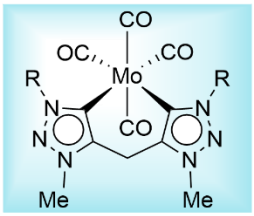

Mo2 (R = Et)
Mo3 (R = Ph)
Mo4 (R = *n*-Bu)

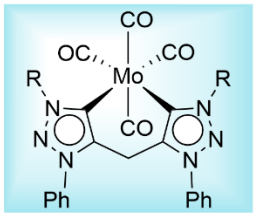

Mo5 (R = Et)
Mo6 (R = Ph)

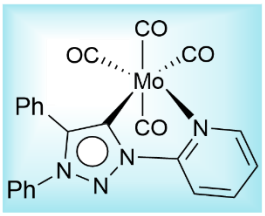

Mo7

Entry	Complex	Yield (%)[b]
1	**Mo1**	5
2	**Mo2**	>99
3	**Mo3**	6
4	**Mo4**	>99
5	**Mo5**	31
6	**Mo6**	18
7	**Mo7**	0

[a] Reaction conditions: 5 mol % of catalyst, **1a** (0.5 mmol), **2a** (0.5 mmol), *t*-BuOK (0.5 equiv.), dry toluene (2 mL), 17 h, 150 ºC. [b] Yields determined by ^{1}H NMR spectroscopy using 1,3,5-trimethoxybenzene as an internal standard.

As shown in Table 3.2, complexes **Mo2** and **Mo4** showed the best catalytic performances. In order to compare further the reactivity between both **Mo2** and **Mo4** complexes, the use of **Mo4** was explored using less amount of base, less catalyst loading, and lower temperature. Results are summarized in **Table 3.3**. Comparable yields of **3a** were obtained with both **Mo2** and **Mo4** catalysts using different conditions. Therefore, it was proved that the length of the aliphatic chain (ethyl vs *n*-butyl) at the N1 position of the triazolylidene ligands had no effect on the catalytic efficiency.

Table 3.3. Dehydrogenative cross-coupling of 2-aminobenzyl alcohol (**1a**) with 1-phenylethanol (**2a**) using **Mo2** and **Mo4**.[a]

Entry	Cat.	Cat. (mol%)	Base [equiv.]	Temp. (°C)	Yield (%)[b]
1	**Mo2**	5	*t*-BuOK [0.2]	150	30
2	**Mo4**	5	*t*-BuOK [0.2]	150	32
3	**Mo2**	2.5	*t*-BuOK [0.5]	150	60
4	**Mo4**	2.5	*t*-BuOK [0.5]	150	59
5	**Mo2**	5	*t*-BuOK [0.5]	110	25
6	**Mo4**	5	*t*-BuOK [0.5]	110	33

[a] General conditions: catalyst, **1a** (0.5 mmol), **2a** (0.5 mmol), *t*-BuOK, dry toluene (2 mL) for 17 h under N_2. [b] Yields determined by ^{1}H NMR spectroscopy using 1,3,5-trimethoxybenzene as an internal standard.

To demonstrate the scope of the reaction, a wide variety of quinolines (**3**) were synthesized from several 2-aminobenzyl alcohols and secondary alcohols using **Mo2** under the optimized reaction conditions (5 mol% of complex **Mo2**, 0.5 mmol of amine, 0.5 mmol of alcohol, and 0.5 equiv. *t*-BuOK in toluene at 150 ºC for 17 h). Starting with 2-aminobenzyl alcohol (**1a**), a series of secondary aromatic alcohols and aliphatic ketones were used as coupling partners. The substrate scope screening results (**3a-o**) are presented in **Table 3.4**. The reaction proceeded smoothly for various substituted 1-phenylethanol derivatives (Table 3.4, entries 1-7). Gratifyingly, 1-(2-naphthyl)ethanol (**2b**) afforded full conversion, and the corresponding quinoline **3b** was isolated in excellent yield (98%, entry 2) without the need for purification by column chromatography. Both, electron-donating (**3c**) and -withdrawing substituents (**3d-f**) at the *para*-position of the phenyl ring were well tolerated (50-70% yield, entries 3-6), but the electron-withdrawing fluoro-substituted substrate 1-(4-fluorophenyl)ethanol (**2f**) showed lower conversion (entry 6). With bromo as a substituent at the *ortho*-position (**2g**), the coupling cyclization processed with relatively lower efficiency (34%, Table 3.4, entry 7). Furthermore, 1,2,3,4-tetrahydro-1-naphthol (**2h**) was successfully converted to desired product **3h** in 78% yield (Table 3.4, entry 8). Although the conversion was complete in this case, the yield value of 78% is the consequence of the generation of additional derivatives of the intended quinoline (benz[c]acridine). In addition, 4-phenyl-2-butanol (**2i**) was a suitable substrate for this transformation, affording the corresponding product **3i** in good yield (77%, Table 3.4, entry 9). Unfortunately, heteroaromatic 1-(2-pyridinyl)ethanol (**2j**) reacted giving low yield (22% yield, Table 3.4, entry 10), probably due to the more difficult dehydrogenation reaction of this alcohol due to the metal chelating properties of the pyridine moiety.

In the case of aliphatic alcohols, when 1-cyclopropylethanol was employed in the reaction, the corresponding product **3k** could be obtained, albeit in moderate yield (43%, Table 3.4, entry 11). The dehydrogenative oxidation of aliphatic and cyclic alcohols is anticipated to be more challenging than that of 1-phenylethanol derivatives, which leads to relatively stable aryl ketone intermediates. Therefore, by replacing the aliphatic alcohol **2** with its ketone derivative (**2k**), higher conversion (>99%) and yield (87%,

Table 3.4, entry 12) were obtained because only the dehydrogenation of **1a** was needed in this case. Likewise, the coupling of cyclohexanone (**2l**) with **1a** led to a maximum yield of **3l** (Table 3.4, entry 13). In the reaction of 2-heptanone (**2m**) with **1a**, the corresponding quinoline was obtained as a regioisomeric mixture (55% yield of **3m** and 14% yield of 3-butyl-2-methylquinoline), favoring cyclization at less-hindered position over α-methylene, that is, the aldol condensation taking place at the methyl position of the ketone **2m** rather than at the methylenic one (Table 3.4, entry 14). Finally, 1,3 and 2,6-diketones such as **2n** and **2o** afforded di-quinolinyl (hetero)-arene products in quantitative yields (98% of **3n** and 80% of **3o**, Table 3.4, entries 15 and 16).

Table 3.4. Synthesis of quinolines through annulation of 2-aminobenzyl alcohol (**1a**) with aromatic alcohols and aliphatic ketones catalyzed by **Mo2**.[a]

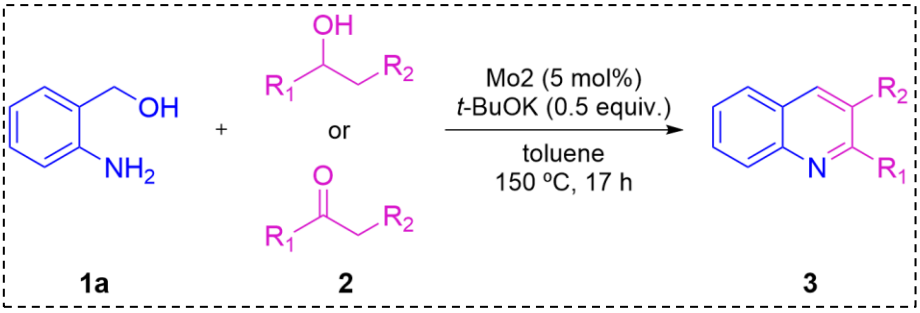

Entry	2		3	Conv. (%)	Yield (%)
1	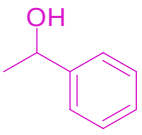 **2a**		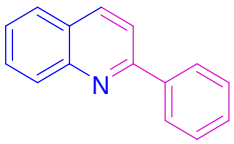 **3a**	>99	97
2	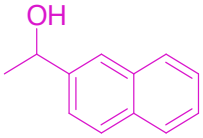 **2b**		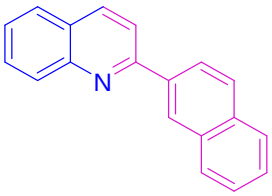 **3b**	>99	98
3	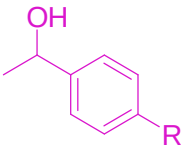 **2c - 2f**	**2c**, **3c**, R= Me **2d**, **3d**, R= Br **2e**, **3e**, R= Cl **2f**, **3f**, R= F	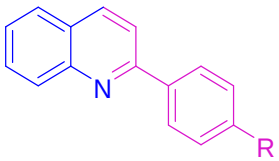 **3c - 3f**	77	66
4				88	68
5				86	70
6				86	50
7[j]	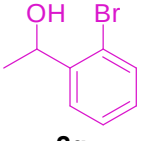 **2g**		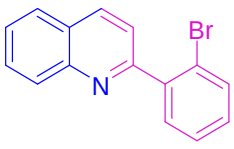 **3g**	-	34[b]

8	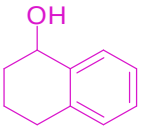 **2h**	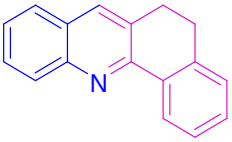 **3h**	>99	78
9	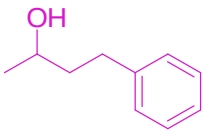 **2i**	 **3i**	90	77
10	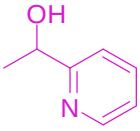 **2j**	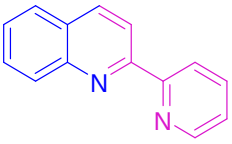 **3j**	-	22[b]
11[c] **12**	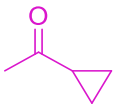 **2k**	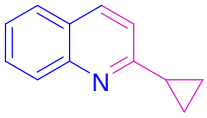 **3k**	62 >99	43 87
13	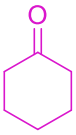 **2l**	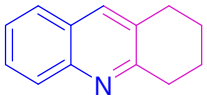 **3l**	>99	99
14[d]	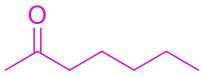 **2m**	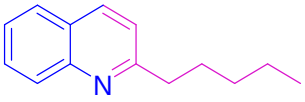 **3m**	>99	55
15[e]	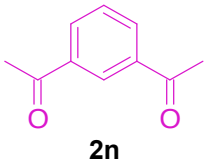 **2n**	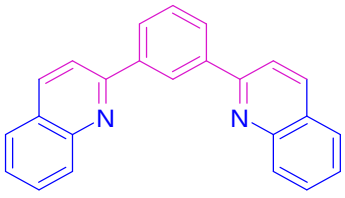 **3n**	>99	98
16[e]	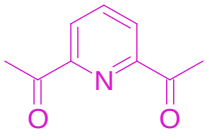 **2o**	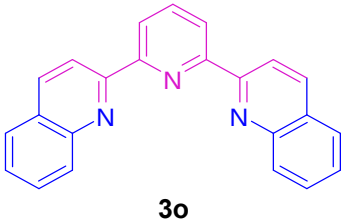 **3o**	-	80

[a] General reaction conditions: Catalyst **Mo2** (5 mol%), **1a** (0.5 mmol), **2** (0.5 mmol), KO^{t}Bu (0.5 equiv.), toluene (2 mL) at 150°C for 17 h; Conversion determined by ^{1}H NMR spectroscopy based on substrate **2**; Yields refer to

isolated yields. [b] Yield determined by ^{1}H NMR spectroscopy using 1,3,5-trimethoxybenzene as an internal standard. [c] 1-Cyclopropylethanol was used instead of cyclopropyl methyl ketone. [d] 3-Butyl-2-methylquinoline was also formed in 14% yield. [e] 1.0 mmol of **1a** was used.

In addition, annulation of γ-amino alcohols with 1-phenylethanol (**2a**) was explored (**Table 3.5**). The reaction of 2-aminobenzyl alcohol bearing an electron-donating substituent at the 3-position of the phenyl ring (**1b**) with 1-phenylethanol (**2a**) afforded complete conversion, and the corresponding quinoline **3p** was isolated in excellent yield (99%, Table 3.5, entry 1). Furthermore, 1-(2-aminophenyl)ethanol (**1c**) was coupled with **2a** and the expected quinoline **3q** was isolated in moderate yield (66%, Table 3.5, entry 2), which shows that the ADC reaction under our conditions is not restricted to primary benzyl alcohols. However, self-coupling cyclization of **1c** was observed, and 2-(4-methylquinolin-2-yl)aniline was isolated in 17% yield along with **3q**.

Table 3.5. Synthesis of quinolines through annulation of γ-amino alcohols with 1-phenylethanol (**2a**) catalyzed by molybdenum complex **Mo2**.[a]

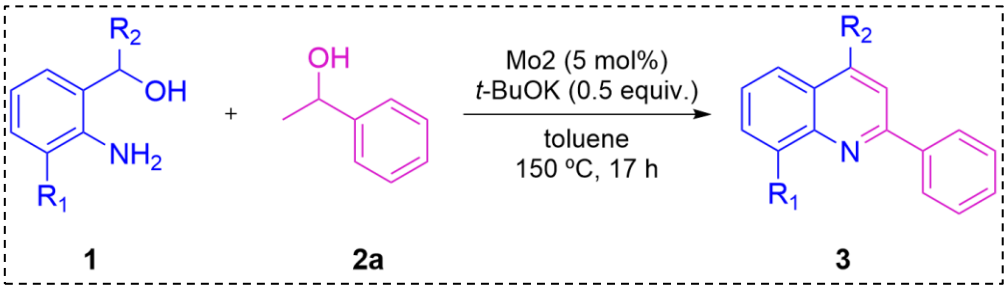

Entry	1	3	Conv. (%)[b]	Yield (%)[c]
1	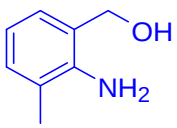 **1b**	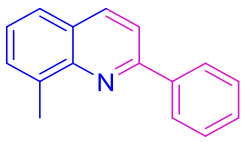 **3p**	>99	99
2[d]	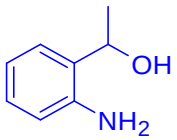 **1c**	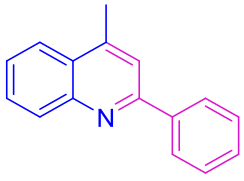 **3q**	-	66

[a] General reaction conditions: Catalyst **Mo2** (5 mol%), **1** (0.5 mmol), **2a** (0.5 mmol), KO^{t}Bu (0.5 equiv.), and toluene (2 mL) were heated at 150°C for 17 h. [b] Conversion determined by ^{1}H NMR spectroscopy based on substrate **2a**. [c] Isolated yields. [d] 2-(4-Methylquinolin-2-yl)aniline was formed in 17% yield along with **3q**.

3.3.2. Catalytic Application in Borrowing Hydrogen (BH) Processes

3.3.2.1. *N*-Alkylation of Amines with Alcohols

As part of our interest in investigating the catalytic activity of our novel molybdenum(0) complexes in BH processes, we decided to test complexes **Mo2** and **Mo5** in the *N*-alkylation of amines with secondary alcohols, using aniline (**4a**) and 1-phenylethanol (**2a**) as substrates and in the presence of *t*-BuOK under the conditions depicted in **Scheme 3.3**.

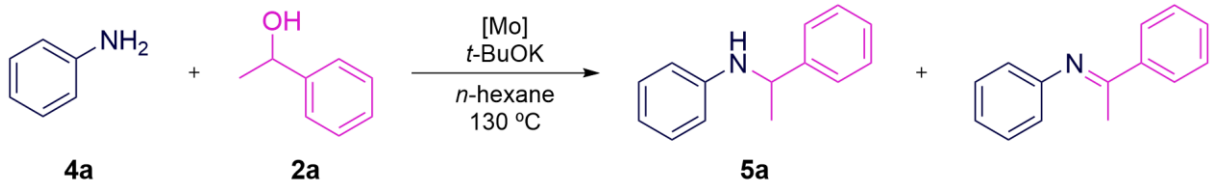

Scheme 3.3. *N*-alkylation of aniline (**4a**) with 1-phenylethanol (**2a**) catalyzed by different Mo(0) complexes.

We also tested complex [Mo(bis-NHC^{Me})(CO)$_4$][10], which was used as a benchmark, and it allowed us to compare the activity of triazolylidene *vs* imidazolylidene molybdenum complexes. As shown in **Table 3.6**, when the reaction of aniline (0.5 mmol) with 1-phenylethanol (0.65 mmol) was performed in *n*-hexane at 130 ºC for 24 h using 1.1 equiv. of *t*-BuOK and 2 mol% of catalyst, the catalytic efficiencies of all complexes were comparable (73-76% yield of *N*-alkylated amine **5a**, Table 3.6, entries 1 and 5-6). Notably, the solvent had a significant influence on the reactivity and selectivity of the reaction; when the reaction was carried out in toluene under the same conditions (Table 3.6, entry 2), complex **Mo2** afforded low yield of the amine **5a** (39% yield) and formation of a secondary imine as a byproduct (11% yield) was detected. Hence, *n*-hexane as a solvent is required for the selective formation of the secondary amine. Following that, using complexes **Mo2** and the related [Mo(bis-NHC^{Me})(CO)$_4$] (2 mol%) in *n*-hexane at 130 ºC for 24 h and decreasing the amount of base to 0.5 equiv. produced the corresponding amine **5a** in 66% and 68% yield, respectively (Table 3.6, entries 3 and 7). The reaction under these conditions was also completely selective for the amine, with no presence of the secondary imine, and just a ~10% loss in yield value when compared to the results obtained using 1.1 equiv. of *t*BuOK. However, it was observed that if the reactions were left for shorter reaction times (16 h), the yield significantly decreased to 39% (Table 3.6, entries 4 and 8), and traces of the secondary imine were detected (9% and 16% yield, respectively).

Therefore, it was feasible to conclude that molybdenum complexes bearing bis-triazolylidene (**Mo2**) and bis-imidazolylidene ([Mo(bis-NHC^{Me})(CO)$_4$]) ligands displayed comparable catalytic activity in the *N*-alkylation of aniline (**4a**) with 1-phenylethanol (**2a**) under all of the aforementioned conditions. It must be highlighted that the Mo(0) complexes **Mo2** and **Mo5** were found capable of catalyzing the *N*-alkylation of anilines with secondary alcohols, which are more challenging substrates and far less frequently reported in the literature than with primary alcohols.

Table 3.6. *N*-alkylation of aniline (**4a**) with 1-phenylethanol (**2a**) catalyzed by complexes **Mo2**, **Mo5** and [Mo(bis-NHC^{Me})(CO)$_4$].[a]

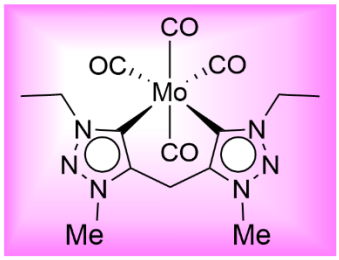

Mo2

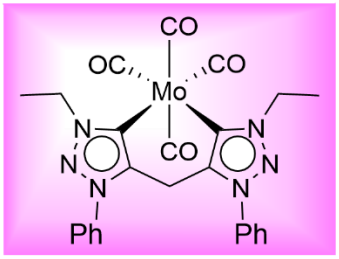

Mo5

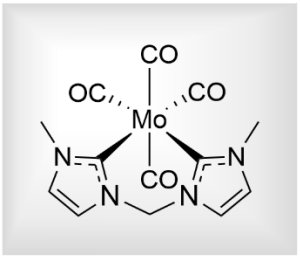

[Mo(bis-NHC^{Me})(CO)$_4$]

Entry	Complex	*t*-BuOK (equiv.)	Time (h)	Yield amine (%)[b]	Yield imine (%)[b]
1	**Mo2**	1.1	24	76	0
2[c]		1.1	24	39	11
3		0.5	24	66	0
4		0.5	16	39	9
5	**Mo5**	1.1	24	73	0
6	**[Mo(bis-NHC^{Me})(CO)$_4$]**	1.1	24	76	0
7		0.5	24	68	0
8		0.5	16	39	16

[a] Reaction conditions: aniline (0.5 mmol), 1-phenylethanol (0.65 mmol), 2 mol% of catalyst, *t*-BuOK, and dry *n*-hexane (0.5 mL), seal tube under N_2, 130 ºC. [b] Yields determined by ^{1}H NMR spectroscopy using 1,3,5-trimethoxybenzene as an internal standard. [c] 0.5 mL of dry toluene was used.

Next, the influence of different substrates on this type of reaction was briefly explored using different anilines (0.5 mmol) and alcohols (0.65 mmol) in the presence of 5 mol% of complex **Mo2** and *t*-BuOK (1.1 equiv.) in *n*-hexane at 130 ºC for 24 h (**Scheme 3.4**). The *N*-alkylation of aniline with benzyl alcohol was conducted, and 55% yield of the corresponding primary amine **5b** was obtained. Surprisingly, a lower yield was observed using the primary alcohol than with the secondary one (55% vs 76%, respectively). In addition, 1-phenylethanol reacted with different halide-substituted anilines, and the corresponding *N*-alkylated secondary amines were successfully obtained. In this manner, the products from 2-iodoaniline (**5c**) and 2,6-dibromoaniline (**5d**) were isolated in 71% and 66% yield, respectively. It is worth mentioning that, to the best of our knowledge, the latter substrate has never been employed in the *N*-alkylation of amines with alcohols. Considering that halide-substituted anilines at the *ortho*-position frequently provide lower yields, these are promising results. The presence of imine was not observed in any of the cases, so all reactions were selective for the formation of the corresponding amine.

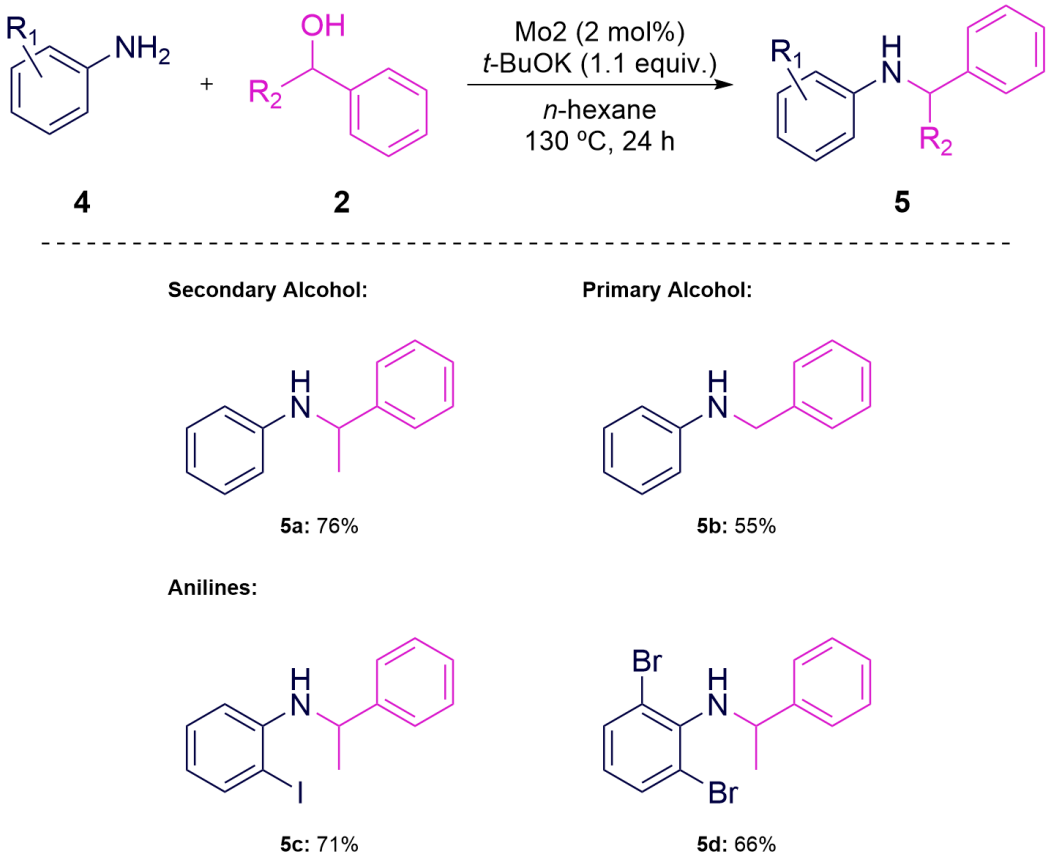

Scheme 3.4. Scope of *N*-alkylation of anilines with alcohols. General reaction conditions: aniline (0.5 mmol), alcohol (0.65 mmol), 2 mol% of catalyst, *t*-BuOK (1.1 equiv.), and dry *n*-hexane (0.5 mL), seal tube under N_2, 130 ºC, 24h. Yields determined by ^{1}H NMR spectroscopy using 1,3,5-trimethoxybenzene as an internal standard.

Finally, as illustrated in **Scheme 3.5**, we decided to test the activity of complex **Mo4** in the *N*-alkylation of aniline (**4a**) with benzyl alcohol (**2p**). In this case, complex **Mo4** was investigated at a catalyst loading of 3 mol% in toluene at 130 ºC for 14 h in the presence of catalytic amounts of *t*-BuOK. Instead of *n*-hexane, toluene was used as a solvent. When the reaction was carried out under such conditions using 1.0 equiv. of *t*-BuOK, only 35% yield of *N*-alkylated primary amine was obtained. Interestingly, when the amount of base was reduced to 0.5 equiv., the yield of **5b** increased significantly (75%). That is, complex **Mo4** displayed significant higher activity when a smaller amount of base was present.

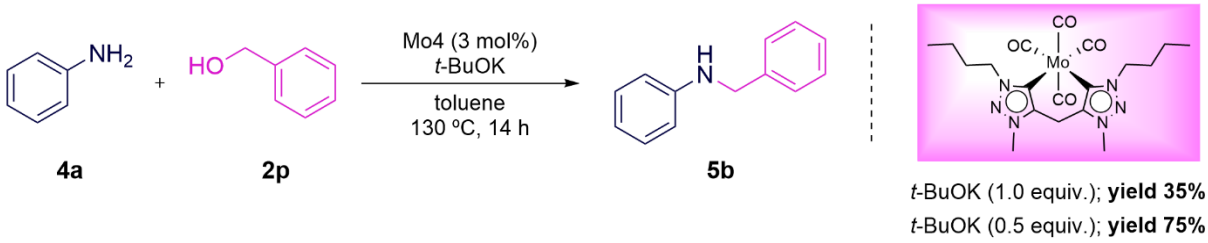

Scheme 3.5. *N*-alkylation of aniline (**4a**) with benzyl alcohol (**2p**) catalyzed by **Mo4**. Reaction conditions: aniline (0.5 mmol), benzyl alcohol (0.65 mmol), **Mo4** (3 mol%), *t*-BuOK, and dry toluene (1 mL), seal tube under N_2, 130 ºC, 14 h. Yields determined by ^{1}H NMR spectroscopy using 1,3,5-trimethoxybenzene as an internal standard.

3.3.2.2. α-Alkylation of Ketones with Alcohols

The catalytic activity of complexes **Mo2** and **Mo5** in the α-alkylation of ketones with alcohols was also investigated (**Scheme 3.6**). Preliminary studies conducted with acetophenone (0.5 mmol) and benzyl alcohol (0.6 mmol) as model substrates in toluene at 110 ºC for 2 h showed promising results as the formation of the alkylated product **7** was observed by ^{1}H NMR spectroscopy.

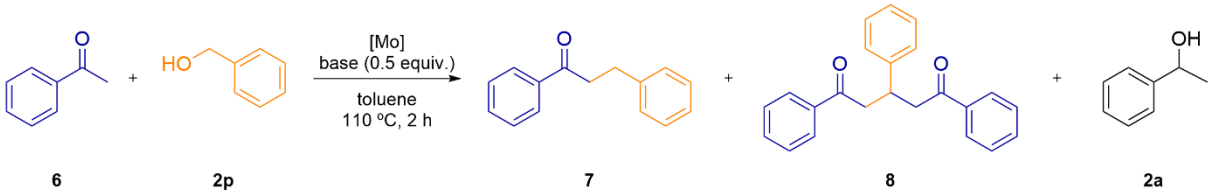

Scheme 3.6. α-Alkylation of acetophenone (**6**) with benzyl alcohol (**2p**) catalyzed by different Mo(0) complexes.

When **Mo2** (4 mol%) was used as a pre-catalyst and NaOH (0.5 equiv.) as a base under N_2 atmosphere, the reaction afforded 1,3-diphenylpropan-1-one (**7**) in 29% yield along with the formation of 1-phenylethanol (**2a**) in 34% yield, which resulted from the reduction of acetophenone, indicating that hydrogen transfer occurred during the reaction. Moreover, under these conditions, the reaction formed an additional product in 26% yield along with the corresponding alkylated product of acetophenone, which was found to be 1,3,5-triphenyl-1,5-pentanedione (**8**) (**Table 3.7**, entry 1). Surprisingly, in the presence of 5 mol% of catalyst **Mo2** under an inert atmosphere, lower conversion (67% vs 89%, entries 2 and 1, respectively) and lower selectivity (**7**: 10%, **8**: 28%, and **2a**: 29%, entry 2) were observed. Yet, when the reaction was performed under air, the reactivity (96%) and chemoselectivity were significantly improved, and 65% of the desired α-alkylated product **7** was obtained with 31% of **2a** (entry 3). In this case, there was no formation of **8**. On the other hand, complex **Mo5** catalyzed the reaction under the same conditions affording full conversion and selectivity to product **7** (Table 3.7, entry 4). That is, using 5 mol% of catalyst and 0.5 equiv. of NaOH in toluene at 110 ºC for 2 h, and performing the reaction under air, the catalytic activity and selectivity of **Mo5** were higher than that of **Mo2**. With *t*-BuOK (0.5 equiv.), an excellent conversion of about 93% was achieved with complex **Mo5** under air, however, the reaction afforded 1,3-diphenylpropan-1-one (**7**) in 47% yield coupled with 1-phenylethanol (**2a**) in 46% yield (entry 5). This indicates that the reaction is no longer selective when *t*-BuOK is used as a base.

Table 3.7. α-Alkylation of acetophenone (**6**) with benzyl alcohol (**2p**) catalyzed by complexes **Mo2** and **Mo5**.[a]

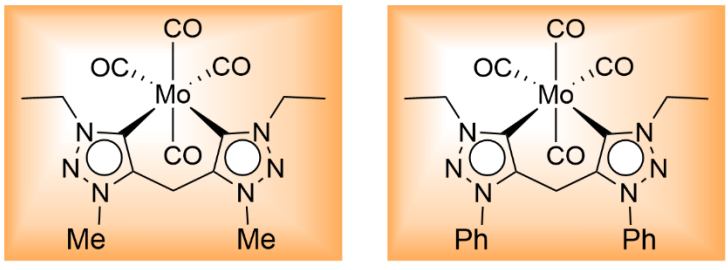

Mo2 **Mo5**

Entry	Complex	Cat. (mol%)	Base [equiv.]	Conv. (%)[b]	Yield (%) 7 / 8 / 2a[b]
1[c]	Mo2	4	NaOH [0.5]	89	29 / 26 / 34
2[c]		5	NaOH [0.5]	67	10 / 28 / 29
3[d]		5	NaOH [0.5]	96	65 / 0 / 31
4[d]	Mo5	5	NaOH [0.5]	>99	99 / 0 / 1
5[d]		5	*t*-BuOK [0.5]	93	47 / 0 / 46

[a] Reaction conditions: acetophenone (0.5 mmol), benzyl alcohol (0.6 mmol), catalyst, base, and dry toluene (1 mL), seal tube, 110 ºC, 2 h. [b] Yields determined by ^{1}H NMR spectroscopy. [c] Under N_2. [d] Under air.

Taking into consideration the results obtained, we believe that the reaction conditions could be further optimized to achieve higher yields. However, due to a limitation of time, further optimization was not performed in this work. We also believe that is possible to prepare 1,3,5-triphenyl-1,5-pentanedione (**8**) as a major product by optimizing the reaction conditions under an inert atmosphere (the molar ratio of reactants, temperature, reaction time, the amount of catalyst used, etc.). Synthesis of **8** through an α-alkylation of ketones with alcohols was recently reported by Rajasekaran et al.[11] for the first time using Ru(II)-thioamide complexes as metal catalysts.

3.3.2.3. β-Alkylation Between Alcohols

Encouraged by the above results, we anticipated that **Mo2** might be active in cross-coupling of secondary and primary alcohols (**Scheme 3.7**). Therefore, we explored the model reaction of 1-phenylethanol (0.5 mmol) with benzyl alcohol (0.5 mmol) using **Mo2** (5 mol%) as catalyst in the presence of *t*-BuOK (0.5 equiv.) in toluene at 150 ºC for 24 h. Under these conditions, 80% yield of 1,3-diphenylpropan-1-ol (**9**) and 20% yield of 1,3-diphenylpropan-1-one (**7**) were obtained. Although the conversion was complete, the presence of product **7** was most likely due to the reaction being carried out under reflux, which allows H_2 to be released from the catalyst. If the reaction is carried out in a closed reaction vessel, hydrogen transfer from the catalyst to compound **7** is favored, which could make the reaction selective for the hydrogenated product **9**. In the case of quinoline synthesis, it is critical to carry out the reaction under reflux in order to promote coupling cyclization of γ-amino alcohols with secondary alcohols via hydrogen release from the catalyst (ADC reaction).

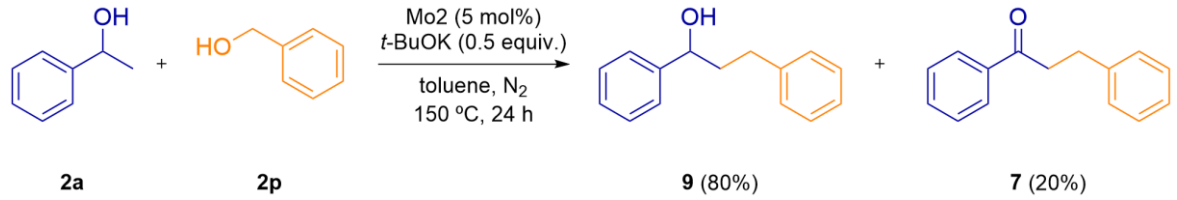

Scheme 3.7. β-Alkylation of 1-phenylethanol (**2a**) with benzyl alcohol (**2p**) catalyzed by complex **Mo2**.

3.3.3. Catalytic Application in the Aerobic Oxidation of Primary Amines to Amides

There are few reports on the direct oxygenation of the α-methylene group of primary amines to produce the corresponding amides in high yield or selectivity employing homogeneous systems, owing to the significantly higher reactivity of the -NH_2 group compared to the methylene α-carbon. Most homogeneous catalytic methods for primary amine oxidation require harsh conditions as well as high amount of catalyst and base. Further, the oxygenation of primary amines often requires a stoichiometric amount of different oxidants. Using O_2/air as the terminal oxidant for the selective α-oxygenation of amines to amides where H_2O is the only byproduct provides an attractive green synthetic alternative. Recently, Yadav and co-workers[12] demonstrated the use of an annulated mesoionic carbene (MIC) Ru complex for the aerobic oxidation of benzylamine to the corresponding amide using ambient air as an oxidant in the presence of a sub-stoichiometric amount of *t*-BuOK in *t*-butanol.

Mesoionic carbene (MIC) ligands of the 1,2,3-triazolylidene (trz) type have strong σ-donor properties, and their transition metal complexes have shown excellent activities in oxidation chemistry. Based on this, we decided to explore the activity of the Mo complexes reported in Chapter 2 in the aerobic oxidation of primary amines to amides. It is worth to mention that this reaction has never been reported using a Mo-based catalytic system. Gratifyingly, we present in this work, the first example of a Mo catalytic system for the challenging oxidation of amines to amides. The catalytic utility of complexes **Mo2** and **Mo5** was evaluated using benzylamine (**10**) as a model substrate. As shown in **Scheme 3.8**, several products can be formed in this reaction, benzylamide (**11**), benzonitrile (**12**), and *N*-benzylidenebenzylamine (**13).**

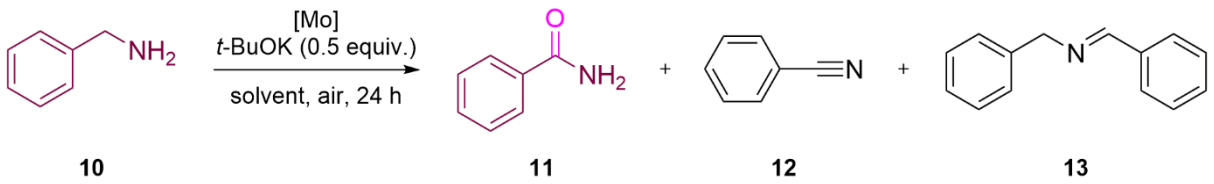

Scheme 3.8. Aerobic oxidation of benzylamine (**10**) catalyzed by different Mo(0) complexes.

An initial experiment using benzylamine (0.5 mmol), *t*-BuOK (0.5 equiv.), and catalyst **Mo2** (2 mol%) in *t*-BuOH (2 mL) at 80 °C for 24 h under air resulted in no conversion (**Table 3.8**, entry 1). However, replacing *t*-BuOH by toluene, increasing the catalyst loading to 5 mol%, and raising the temperature to 110 ºC resulted in complete conversion of **10** (entry 2). Benzylamide (**11**) was produced in 63% yield, with benzonitrile (**12**) (17% yield) and *N*-benzylidenebenzylamine (**13**) (20% yield) as minor side products. Under such conditions, **Mo5** was completely inactive (entry 3).

Table 3.8. Aerobic oxidation of benzylamine (**10**) catalyzed by molybdenum complexes **Mo2** and **Mo5**.[a]

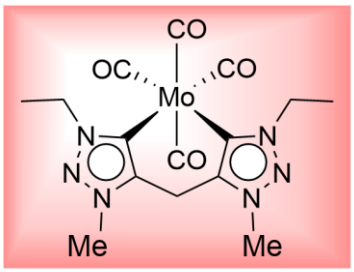

Mo2

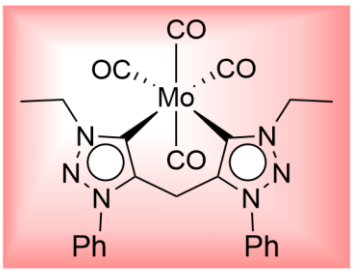

Mo5

Entry	Complex	Cat. (mol%)	Solvent	Temp. (°C)	Conv. (%)[b]	Yield (%) 11 / 12 / 13[b]
1	**Mo2**	2	^{t}BuOH	80	0	-
2		5	Toluene	110	>99	63 / 17 / 20
3	**Mo5**	5	Toluene	110	0	-

[a] Reaction conditions: catalyst, benzylamine (0.5 mmol), *t*-BuOK (0.5 equiv.), and solvent (1 mL), 24 h. [b] Conversion and yields determined by ^{1}H NMR spectroscopy.

The results reported here are highly encouraging, and we hope that by adjusting the reaction conditions, we will be able to improve the catalytic activity and selectivity of our molybdenum complex **Mo2**. This work is ongoing in our laboratory.

3.4. Conclusions

Up to now, the chemistry and catalysis of 1,2,3-triazolylidene of Mo has remained poorly developed. We report here for the first time, the impact of the presence of mesoionic triazolylidene ligands on the catalytic performance of Mo tetracarbonyl complexes in BH and ADC processes.

Interestingly, complexes **Mo2** and **Mo4** has shown an excellent performance in the synthesis of quinolines through ADC reactions. We have demonstrated that Mo complexes bearing triazolylidene ligands with different alkyl groups (Et, *n*-Bu) as substituents displayed comparable catalytic activity and were significantly more active than those complexes bearing triazolylidene ligands with aromatic groups (Ph) as substituents. In contrast, a Mo complex bearing a mixed-pyridine triazolylidene ligand exhibited no activity in this reaction. A sustainable synthesis of a wide variety of substituted quinolines was achieved through the annulation of 2-aminobenzyl alcohols and 1-(2-aminophenyl)ethanol with a variety of secondary alcohols. The reaction proceeds in the presence of *t*-BuOK (0.5 equiv.) through a sequence of dehydrogenation and condensation steps that results in selective C–C and C–N bond formation, using complex **Mo2** as the catalyst (5 mol%). Under the same reaction conditions, **Mo2** was also capable to mediate the catalytic β-alkylation of alcohols.

In addition, preliminary investigations have shown that Mo complexes bearing bis-triazolylidene (**Mo2**) or bis-imidazolylidene ([Mo(bis-NHC^{Me})(CO)$_4$]) ligands displayed comparable catalytic activity in the *N*-alkylation of amines with secondary alcohols. On the other hand, the catalytic activity and selectivity of **Mo5** were higher than those of **Mo2** in the α-alkylation of ketones with alcohols using 5 mol% of catalyst and 0.5 equiv. of NaOH and performing the reaction under air.

Gratifyingly, we have disclosed the excellent catalytic performance of **Mo2** in the aerobic oxidation of primary amines to amides. Further optimization of the reaction conditions and investigation of the scope of the reaction is undergoing in our laboratories.

In summary, this thesis has contributed to expand the area of organometallic chemistry and catalysis with molybdenum complexes bearing triazolylidene derived ligands.

3.5. Experimental Details

3.5.1. General Considerations

All reactions and manipulations, except for the aerobic oxidation of primary amines, were carried out under nitrogen atmosphere using standard Schlenk techniques, and solvents were purified from appropriate drying agents. Deuterated solvents were degassed and stored over molecular sieves. All other reagents were purchased from commercial suppliers and used without further purification. Analytical TLC was performed on ALUGRAM Xtra SIL G/UV_{254} silica gel plates (0.20 mm thickness). Column chromatography was performed on Honeywell's Fluka™ silica gel (230-400 mesh particle size (flash), 60 Å). Preparation of complex [Mo(bis-NHC^{Me})$(CO)_4$] was performed following the procedure reported in the literature.[10] ^1H, ^{13}C and ^{19}F NMR spectra were recorded on a Bruker Avance III 400 MHz. In the description of each spectrum, the data are described as follows: deuterated solvent; chemical shift δ (in ppm); signal multiplicity [singlet (*s*), broad singlet (*br s*), doublet (*d*), triplet (*t*), quartet (*q*), quintet (*quint.*), sextet (*sext.*), multiplet (*m*)]; coupling constant value (*J*, in Hz); relative area (nH, number of protons); assignment to protons of the molecule. The signal of the deuterated solvent itself was used as a reference.

3.5.2. Synthesis of Quinolines

3.5.2.1. General Procedure for Catalyst Screening and Optimization of the Reaction Conditions

To a Schlenk tube, in an inert atmosphere, the appropriate catalyst, 2-aminobenzyl alcohol **1a** (0.5 mmol), 1-phenylethanol **2a** (0.5 mmol), base, and dry toluene (2 mL) were added in that order. The reaction mixture was heated at the appropriate temperature during the corresponding reaction time. After cooled to room temperature, the solution was diluted with $CHCl_3$ (5 mL), and filtered through a short pad of celite. The yield of 2-phenylquinoline **3a** was determined by ^1H NMR spectroscopy using 1,3,5-trimethoxybenzene (0.25 mmol) as an internal standard.

3.5.2.2. General Procedure for the Synthesis of Quinolines

To a Schlenk tube, in an inert atmosphere, catalyst **Mo2** (5 mol%), γ-amino alcohol **1** (0.5 mmol), alcohol or ketone **2** (0.5 mmol), *t*-BuOK (0.25 mmol), and dry toluene (2 mL) were added in that order, and the reaction mixture was heated at 150 ºC for 17 h. After cooled to room temperature, the solution was diluted with ethyl acetate (5 mL), and filtered through a short pad of celite. The filtrate was evaporated and the crude residue was purified by column chromatography.

3.5.2.3. Characterization of Quinolines

2-Phenylquinoline (**3a**)

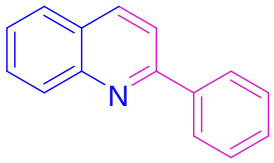

According to the general procedure, 2-aminobenzyl alcohol **1a** (62 mg, 0.5 mmol) and 1-phenylethanol **2a** (60 µL, 0.5 mmol) gave the title compound **3a** as a white solid (100 mg, 97%). Eluent: hexane/ethyl acetate (3:1). **^{1}H NMR (400 MHz, $CDCl_3$) δ (ppm):** 8.23 (*d*, *J* = 8.8 Hz, 1H), 8.20-8.17 (*m*, 3H), 7.89 (*d*, *J* = 8.8 Hz, 1H), 7.83 (*d*, *J* = 8.4 Hz, 1H), 7.74 (*ddd*, *J* = 8.4, 6.9, 1.3 Hz, 1H), 7.56-7.52 (*m*, 3H), 7.49-7.45 (*m*, 1H). **^{13}C NMR (100 MHz, $CDCl_3$) δ (ppm):** 157.52, 148.44, 139.84, 136.91, 129.89, 129.79, 129.45, 128.98, 127.71, 127.60, 127.32, 126.42, 119.16.

2-(Naphthalen-2-yl)quinoline (**3b**)

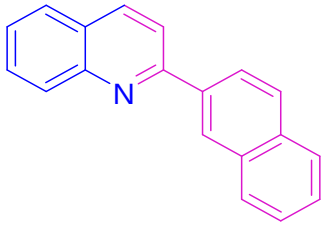

According to the general procedure, 2-aminobenzyl alcohol **1a** (62 mg, 0.5 mmol) and 1-(2-naphthyl)ethanol **2b** (86 mg, 0.5 mmol) gave the title compound **3b** as a yellow solid (125 mg, 98%). Acetone was used to precipitate the product. **^{1}H NMR (400 MHz, $CDCl_3$) δ (ppm):** 8.63 (*s*, 1H), 8.39 (*d*, *J* = 7.6 Hz, 1H), 8.25 (*dd*, *J* = 12.1, 8.6 Hz, 1H), 8.06-8.00 (*m*, 3H), 7.92-7.90 (*m*, 1H), 7.86 (d, *J* = 8.0 Hz, 1H), 7.76 (*t*, *J* = 7.6 Hz, 1H), 7.57-7.53 (*m*, 3H). **^{13}C NMR (100 MHz, $CDCl_3$) δ (ppm):** 157.32, 148.53, 137.12, 136.95, 134.01, 133.65, 129.89, 129.87, 128.97, 128.72, 127.87, 127.64, 127.38, 127.29, 126.85, 126.48, 125.21, 119.30.

2-(*p*-Tolyl)quinoline (**3c**)

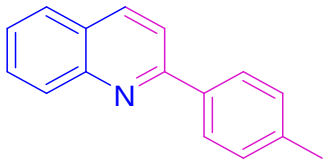

According to the general procedure, 2-aminobenzyl alcohol **1a** (62 mg, 0.5 mmol) and 1-(4-methylphenyl)ethanol **2c** (86 mg, 0.5 mmol) gave the title compound **3c** as a white solid (72 mg, 66%). Eluent: petroleum ether/$CHCl_3$ (1:2). **^{1}H NMR (400 MHz, $CDCl_3$) δ (ppm):** 8.19 (*d*, *J* = 8.8 Hz, 2H), 8.09 (*d*, *J* = 8.4 Hz, 2H), 7.86 (*d*, *J* = 8.8 Hz, 1H), 7.81 (*d*, *J* = 8.0 Hz, 1H), 7.73 (*t*, *J* = 7.8 Hz, 1H), 7.52 (*t*, *J*

= 7.4 Hz, 1H), 7.35 (*d*, *J* = 8.0 Hz, 2H), 2.45 (*s*, 3H). **^{13}C NMR (100 MHz, $CDCl_3$) δ (ppm):** 157.48, 148.44, 139.54, 137.02, 136.79, 129.80, 129.71, 127.58, 127.24, 126.22, 119.00, 21.48.

2-(4-Bromophenyl)quinoline (**3d**)

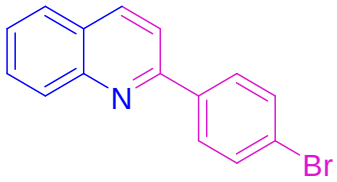

According to the general procedure, 2-aminobenzyl alcohol **1a** (62 mg, 0.5 mmol) and 4-bromo-α-methyl benzyl alcohol **2d** (69 μL, 0.5 mmol) gave the title compound **3d** as a yellow solid (97 mg, 68%). Eluent: petroleum ether/ethyl acetate (19:1). **^{1}H NMR (400 MHz, $CDCl_3$) δ (ppm):** 8.21 (*d*, *J* = 8.6 Hz, 1H), 8.16 (*d*, *J* = 8.5 Hz, 1H), 8.06 (*d*, *J* = 8.4 Hz, 2H), 7.82 (*d*, *J* = 8.5 Hz, 2H), 7.74 (*t*, *J* = 7.5 Hz, 1H), 7.65 (*d*, *J* = 8.4 Hz, 2H), 7.54 (*t*, *J* = 7.6 Hz, 1H). **^{13}C NMR (100 MHz, $CDCl_3$) δ (ppm):** 156.15, 148.36, 138.62, 137.09, 132.09, 129.97, 129.83, 129.21, 127.61, 127.36, 126.64, 124.05, 118.61.

2-(4-Chlorophenyl)quinoline (**3e**)

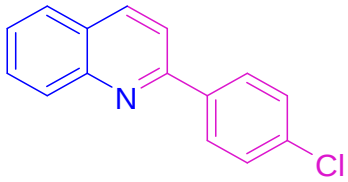

According to the general procedure, 2-aminobenzyl alcohol **1a** (62 mg, 0.5 mmol) and 1-(4-chlorophenyl)ethanol **2e** (67 μL, 0.5 mmol) gave the title compound **3e** as a yellow solid (84 mg, 70%). Eluent: hexane/ethyl acetate (9:1). **^{1}H NMR (400 MHz, $CDCl_3$) δ (ppm):** 8.23 (*d*, *J* = 8.8 Hz, 1H), 8.16 (*d*, *J* = 8.8 Hz, 1H), 8.13 (*d*, *J* = 8.4 Hz, 2H), 7.86-7.82 (*m*, 2H), 7.74 (*t*, *J* = 7.6 Hz, 1H), 7.55 (*d*, *J* = 7.6 Hz, 1H), 7.52-7.49 (*m*, 2H). **^{13}C NMR (100 MHz, $CDCl_3$) δ (ppm):** 156.17, 148.39, 138.21, 137.11, 135.69, 129.99, 129.85, 129.16, 128.96, 127.63, 127.37, 126.65, 118.71.

2-(4-Fluorophenyl)quinoline (**3f**)

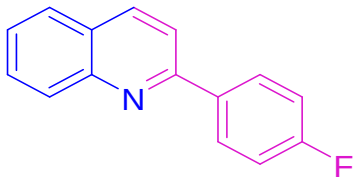

According to the general procedure, 2-aminobenzyl alcohol **1a** (62 mg, 0.5 mmol) and 1-(4-fluorophenyl)ethanol **2f** (63 μL, 0.5 mmol) gave the title compound **3f** as a light yellow solid (56 mg, 50%). Eluent: hexane/ethyl acetate (19:1). **^{1}H NMR (400 MHz, $CDCl_3$) δ (ppm):** 8.23-8.15 (*m*, 4H), 7.83 (*d*, *J* = 8.8 Hz, 2H), 7.76-7.71 (*m*, 1H), 7.53 (*t*, *J* = 7.4 Hz, 1H), 7.21 (*t*, *J* = 8.6 Hz, 2H). **^{13}C NMR (100**

MHz, $CDCl_3$) δ (ppm): 163.81 (*d*, *J* = 247.6 Hz), 156.24, 148.24, 136.91, 135.82 (*d*, *J* = 1.8 Hz), 129.79, 129.65, 129.41 (*d*, *J* = 8.3 Hz), 127.48, 127.08, 126.35, 118.63, 115.78 (*d*, *J* = 21.4 Hz). **^{19}F NMR (565 MHz, $CDCl_3$) δ (ppm):** -112.50.

2-(2-Bromophenyl)quinoline (**3g**)

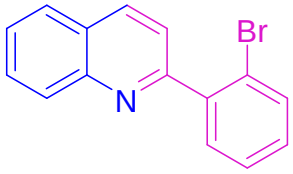

According to the general procedure, 2-aminobenzyl alcohol **1a** (62 mg, 0.5 mmol) and 1-(2-bromophenyl)ethanol **2g** (68 µL, 0.5 mmol) gave the title compound **3g** (34%). The yield was determined by ^{1}H NMR spectroscopy using 1,3,5-trimethoxybenzene as an internal standard.

5,6-Dihydrobenzo[c]acridine (**3h**)

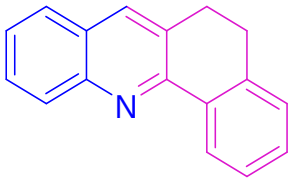

According to the general procedure, 2-aminobenzyl alcohol **1a** (62 mg, 0.5 mmol) and 1,2,3,4-tetrahydro-1-naphthol **2h** (68 µL, 0.5 mmol) gave the title compound **3h** as colorless crystals (90 mg, 78%). Eluent: petroleum ether/$CHCl_3$ (1:1). **^{1}H NMR (400 MHz, $CDCl_3$) δ (ppm):** 8.59 (*dd*, *J* = 7.6, 1.2 Hz, 1H), 8.14 (*d*, *J* = 8.4 Hz, 1H), 7.92 (*s*, 1H), 7.75 (*d*, *J* = 8.4 Hz, 1H), 7.65 (*ddd*, *J* = 8.4, 6.9, 1.4 Hz, 1H), 7.50-7.41 (*m*, 2H), 7.38 (*td*, *J* = 7.4, 1.5 Hz, 1H), 7.28 (*d*, *J* = 7.2 Hz, 1H), 3.15-3.12 (*m*, 2H), 3.04-3.00 (*m*, 2H). **^{13}C NMR (100 MHz, $CDCl_3$) δ (ppm):** 153.54, 147.78, 139.55, 134.87, 133.83, 130.73, 129.81, 129.57, 128.78, 128.08, 128.01, 127.47, 127.06, 126.20, 28.98, 28.55.

2-Phenethylquinoline (**3i**)

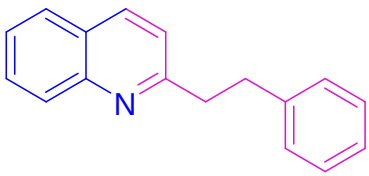

According to the general procedure, 2-aminobenzyl alcohol **1a** (62 mg, 0.5 mmol) and 4-phenyl-2-butanol **2i** (77 µL, 0.5 mmol) gave the title compound **3i** as a white solid (90 mg, 77%). Eluent: hexane/$CHCl_3$ (1:3) then AcOEt. **^{1}H NMR (400 MHz, $CDCl_3$) δ (ppm):** 8.09 (*d*, *J* = 8.4 Hz, 1H), 8.05 (*d*, *J* = 8.4 Hz, 1H), 7.79 (*d*, *J* = 8.4 Hz, 1H), 7.71 (*ddd*, *J* = 8.4, 6.9, 1.4 Hz, 1H), 7.53-7.48 (*m*, 1H), 7.31-7.23 (*m*, 6H), 3.33-3.29 (*m*, 2H), 3.19-3.15 (*m*, 2H). **^{13}C NMR (100 MHz, $CDCl_3$) δ (ppm):** 161.96,

148.10, 141.65, 136.40, 129.57, 128.99, 128.66, 128.54, 127.67, 126.95, 126.14, 125.96, 121.71, 41.11, 36.08.

2-(Pyridin-2-yl)quinoline (**3j**)

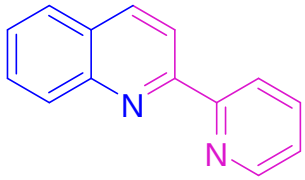

According to the general procedure, 2-aminobenzyl alcohol **1a** (62 mg, 0.5 mmol) and 1-(2-pyridinyl)ethanol **2j** (57 µL, 0.5 mmol) gave the title compound **3j** (22%). The yield was determined by ^{1}H NMR spectroscopy using 1,3,5-trimethoxybenzene as an internal standard.

2-Cyclopropylquinoline (**3k**)

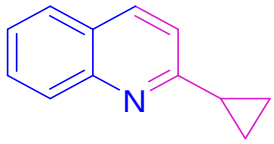

According to the general procedure, 2-aminobenzyl alcohol **1a** (62 mg, 0.5 mmol) and 1-cyclopropylethanol (50 µL, 0.5 mmol) gave the title compound **3k** as a brownish oil (36 mg, 43%). Eluent: *n*-hexane/ethyl acetate (10:1).

According to the general procedure, 2-aminobenzyl alcohol **1a** (62 mg, 0.5 mmol) and cyclopropyl methyl ketone **2k** (50 µL, 0.5 mmol) gave the title compound **3k** as a brownish oil (73 mg, 87%). The product was obtained without purification. **^{1}H NMR (400 MHz, $CDCl_3$) δ (ppm):** 8.00 (*d*, *J* = 8.4 Hz, 1H), 7.96 (*d*, *J* = 8.4 Hz, 1H), 7.74 (*d*, *J* = 8.0 Hz, 1H), 7.66-7.62 (*m*, 1H), 7.45-7.41 (*m*, 1H), 7.17 (*d*, *J* = 8.4 Hz, 1H), 2.28-2.21 (*m*, 1H), 1.18-1.14 (*m*, 2H), 1.13-1.07 (*m*, 2H). **^{13}C NMR (100 MHz, $CDCl_3$) δ (ppm):** 163.55, 148.14, 135.94, 129.40, 128.81, 127.58, 126.87, 125.30, 119.46, 18.24, 10.39.

1,2,3,4-Tetrahydroacridine (**3l**)

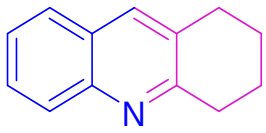

According to the general procedure, 2-aminobenzyl alcohol **1a** (62 mg, 0.5 mmol) and cyclohexanone **2l** (52 µL, 0.5 mmol) gave the title compound **3l** as a yellow solid (91 mg, 99%). The product was obtained without purification. **^{1}H NMR (400 MHz, $CDCl_3$) δ (ppm):** 7.97 (*d*, *J* = 8.4 Hz, 1H), 7.81 (*s*, 1H), 7.70 (*d*, *J* = 8.0 Hz, 1H), 7.62-7.58 (*m*, 1H), 7.43 (*t*, *J* = 7.6 Hz, 1H), 3.13 (*t*, *J* = 6.6 Hz, 2H), 2.98 (*t*, *J* = 6.4 Hz, 2H), 2.03-1.97 (*m*, 2H), 1.93-1.87 (*m*, 2H). **^{13}C NMR (100 MHz, $CDCl_3$) δ (ppm):** 159.49, 146.79, 135.11, 131.12, 128.62, 128.44, 127.36, 127.03, 125.67, 33.74, 29.42, 23.39, 23.07.

2-Pentylquinoline (**3m**)

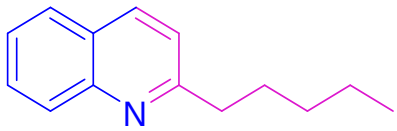

According to the general procedure, 2-aminobenzyl alcohol **1a** (62 mg, 0.5 mmol) and 2-heptanone **2m** (71 µL, 0.5 mmol) gave the title compound **3m** as a yellowish oil (55 mg, 55%) and **3m'** as colorless crystals (14 mg, 14%). Eluent: petroleum ether/ethyl acetate (10:1). **^{1}H NMR (400 MHz, $CDCl_3$) δ (ppm):** 8.05 (*dd*, *J* = 8.4, 3.7 Hz, 2H), 7.77 (*d*, *J* = 8.1 Hz, 1H), 7.70-7.66 (*m*, 1H), 7.49-7.46 (*m*, 1H), 7.30 (*d*, *J* = 8.4 Hz, 1H), 2.99-2.95 (*m*, 2H), 1.86-1.78 (*m*, 2H), 1.43-1.35 (*m*, 4H), 0.90 (*t*, *J* = 7.0 Hz, 3H). **^{13}C NMR (100 MHz, $CDCl_3$) δ (ppm):** 163.27, 148.05, 136.29, 129.43, 128.96, 127.60, 126.84, 125.75, 121.50, 39.50, 31.90, 29.91, 22.71, 14.16.

3-Butyl-2-methylquinoline (**3m'**)

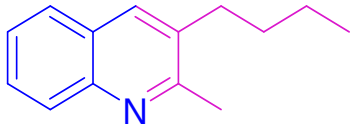

^{1}H NMR (400 MHz, $CDCl_3$) δ (ppm): 7.99 (*d*, *J* = 8.4 Hz, 1H), 7.83 (*s*, 1H), 7.72 (*d*, *J* = 8.1 Hz, 1H), 7.61 (*t*, *J* = 7.6 Hz, 1H), 7.45 (*t*, *J* = 7.5 Hz, 1H), 2.77 (*t*, *J* = 8.0 Hz, 2H), 2.73 (*s*, 3H), 1.68 (*quint.*, *J* = 7.6 Hz, 2H), 1.46 (*sext.*, *J* = 7.4 Hz, 2H), 0.99 (*t*, *J* = 7.2 Hz, 3H). **^{13}C NMR (100 MHz, $CDCl_3$) δ (ppm):** 158.78, 146.49, 134.65, 134.54, 128.55, 128.40, 127.55, 127.03, 125.75, 32.74, 31.98, 23.34, 22.76, 14.11.

1,3-Di(quinolin-2-yl)benzene (**3n**)

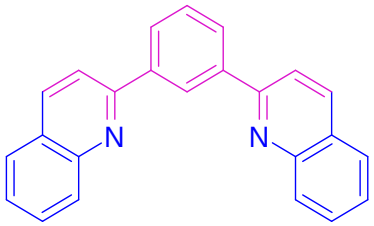

According to the general procedure, 2-aminobenzyl alcohol **1a** (123 mg, 1.0 mmol) and 1,3-diacetylbenzene **2n** (81 mg, 0.5 mmol) gave the title compound **3n** as a yellow solid (163 mg, 98%). Acetone was used to precipitate the product. **^{1}H NMR (400 MHz, $CDCl_3$) δ (ppm):** 8.97 (*s*, 1H), 8.29 (*t*, *J* = 8.0 Hz, 4H), 8.23 (*d*, *J* = 8.8 Hz, 2H), 8.04 (*d*, *J* = 8.4 Hz, 2H), 7.87 (*d*, *J* = 8.4 Hz, 2H), 7.76 (*t*, *J* = 7.6 Hz, 2H), 7.71 (*t*, *J* = 7.8 Hz, 1H), 7.56 (*t*, *J* = 7.4 Hz, 2H). **^{13}C NMR (100 MHz, $CDCl_3$) δ (ppm):** 157.28, 148.46, 140.42, 137.01, 129.94, 129.86, 129.57, 128.67, 127.65, 127.45, 126.94, 126.53, 119.31.

2,6-Di(quinolin-2-yl)pyridine (**3o**)

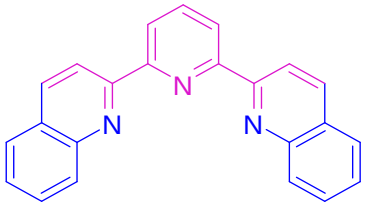

According to the general procedure, 2-aminobenzyl alcohol **1a** (123 mg, 1.0 mmol) and 2,6-diacetylpyridine **2o** (82 mg, 0.5 mmol) gave the title compound **3o** as a white solid (134 mg, 80%). Acetone was used to precipitate the product. **^{1}H NMR (400 MHz, $CDCl_3$) δ (ppm):** 8.85 (*d*, *J* = 8.4 Hz, 2H), 8.78 (*d*, *J* = 8.0 Hz, 2H), 8.34 (*d*, *J* = 8.8 Hz, 2H), 8.22 (*d*, *J* = 8.4 Hz, 2H), 8.07 (*t*, *J* = 7.8 Hz, 1H), 7.89 (*d*, *J* = 8.0 Hz, 2H), 7.76 (*ddd*, *J* = 8.3, 7.0, 1.3 Hz, 2H), 7.58 (*t*, *J* = 7.4 Hz, 2H). **^{13}C NMR (100 MHz, $CDCl_3$) δ (ppm):** 156.36, 155.68, 148.11, 138.09, 136.85, 130.00, 129.71, 128.50, 127.78, 126.91, 122.22, 119.24.

8-Methyl-2-phenylquinoline (**3p**)

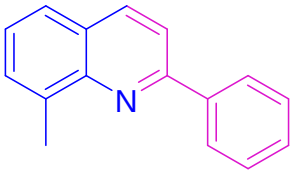

According to the general procedure, (2-amino-3-methylphenyl)methanol **1b** (69 mg, 0.5 mmol) and 1-phenylethanol **2a** (60 µL, 0.5 mmol) gave the title compound **3p** as a yellow solid (109 mg, 99%). Diethyl ether was added to precipitate impurities. **^{1}H NMR (400 MHz, $CDCl_3$) δ (ppm):** 8.28 (*d*, *J* = 7.2 Hz, 2H), 8.19 (*d*, *J* = 8.6 Hz, 1H), 7.91 (*d*, *J* = 8.6 Hz, 1H), 7.67 (*d*, *J* = 8.1 Hz, 1H), 7.58 (*d*, *J* = 7.0 Hz, 1H), 7.54 (*t*, *J* = 7.4 Hz, 2H), 7.48 (*d*, *J* = 7.2 Hz, 1H), 7.42 (*t*, *J* = 7.4 Hz, 1H), 2.92 (*s*, 3H). **^{13}C NMR (100 MHz, $CDCl_3$) δ (ppm):** 155.67, 147.31, 140.00, 137.82, 137.08, 129.82, 129.36, 128.91, 127.61, 127.23, 126.17, 125.52, 118.34, 18.04.

4-Methyl-2-phenylquinoline (**3q**)

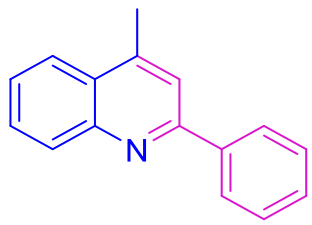

According to the general procedure, 1-(2-aminophenyl)ethanol **1c** (69 mg, 0.5 mmol) and 1-phenylethanol **2a** (60 µL, 0.5 mmol) gave the title compound **3q** as yellowish crystals (72 mg, 66%) and **3q'** as a yellow solid (20 mg, 17%). Eluent: petroleum ether/ethyl acetate (10:1). **^{1}H NMR (400 MHz, $CDCl_3$) δ (ppm):** 8.21-8.16 (*m*, 3H), 8.00 (*d*, *J* = 8.3 Hz, 1H), 7.75-7.72 (*m*, 2H), 7.57-7.52 (*m*, 3H), 7.47

(*t*, *J* = 7.2 Hz, 1H), 2.76 (*s*, 3H). **^{13}C NMR (100 MHz, $CDCl_3$) δ (ppm):** 157.18, 148.24, 144.90, 139.94, 130.40, 129.42, 129.29, 128.88, 127.64, 127.36, 126.12, 123.72, 119.87, 19.11.

2-(4-Methylquinolin-2-yl)aniline (**3q'**)

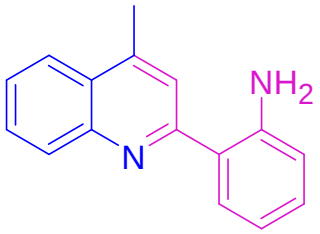

^{1}H NMR (400 MHz, $CDCl_3$) δ (ppm): 8.06 (*d*, *J* = 8.4 Hz, 1H), 7.99 (*dd*, *J* = 8.3, 0.8 Hz, 1H), 7.72-7.69 (*m*, 2H), 7.68 (*s*, 1H), 7.54 (*ddd*, *J* = 8.1, 6.9, 1.2 Hz, 1H), 7.23-7.19 (*m*, 1H), 6.85-6.80 (*m*, 2H), 6.16 (*br s*, 2H), 2.75 (*s*, 3H). **^{13}C NMR (100 MHz, $CDCl_3$) δ (ppm):** 159.04, 147.51, 146.83, 144.78, 130.24, 129.89, 129.47, 129.37, 126.58, 125.99, 123.68, 121.85, 121.20, 117.49, 117.37, 19.15.

3.5.3. Typical Procedure for *N*-Alkylation of Amines with Alcohols

To a Schlenk tube with a Teflon cap under N_2, was added amine **4** (0.5 mmol), alcohol **2** (0.65 mmol), Mo catalyst, base, and the appropriate dry solvent. The mixture was then stirred at 130 °C during the corresponding reaction time. After cooled to room temperature, the solution was diluted with $CHCl_3$ (5 mL), and filtered through a short pad of celite. The yield of the *N*-alkylated product **5** was determined by ^{1}H NMR spectroscopy using 1,3,5-trimethoxybenzene (0.25 mmol) as an internal standard.

3.5.4. Typical Procedure for α-Alkylation of Ketones with Alcohols

In a Schlenk tube with a Teflon cap, Mo catalyst, base (0.25 mmol), acetophenone **6** (0.5 mmol) and benzyl alcohol **2p** (0.6 mmol) were mixed with toluene (1 mL). The mixture was then stirred at 110 °C for 2 h. After completion of the reaction, the reaction mixture was cooled to ambient temperature, and 5 mL of water was added. The aqueous solution was extracted with CH_2Cl_2 (3 ×5 mL) and the combined organic layers were dried over anhydrous Na_2SO_4, and filtered. The solvent was removed and the crude residue was analyzed by ^{1}H NMR spectroscopy.

3.5.5. Typical Procedure for β-Alkylation Between Alcohols

To a Schlenk tube, in an inert atmosphere, catalyst **Mo2** (5 mol%), benzyl alcohol **2p** (0.5 mmol), 1-phenylethanol **2a** (0.5 mmol), *t*-BuOK (0.25 mmol), and dry toluene (2 mL) were added in that order, and the reaction mixture was heated at 150 ºC for 24 h. After cooled to room temperature, the solution was diluted with $CHCl_3$ (5 mL), and filtered through a short pad of celite. The filtrate was evaporated and the crude residue was analyzed by ^{1}H NMR spectroscopy.

3.3.6. Typical Procedure for Aerobic Oxidation of Primary Amines to Amides

Benzylamine **10** (0.5 mmol) and *t*-BuOK (0.25 mmol) were sequentially added to a solution of Mo catalyst in 1 mL of the appropriate solvent. The mixture was stirred at the appropriate temperature for 24 h in air. After completion of the reaction, the solvent was evaporated under reduced pressure and the residue was analyzed by ^{1}H NMR spectroscopy.

3.6. Acknowledgements and Contributions

We thank FC&T for funding PTDC/QUI-QIN/0359/2021, PTDC/QUI-QOR/0712/2020, MOSTMICRO-ITQB, UIDB/04612/20220 and UIPD/04612/2020. The NMR data were acquired at CERMAX, ITQB NOVA, Oeiras, Portugal with equipment funded by FCT, project AAC 01/SAICT/2016.

Beatriz Garcia performed all the experiments described in this Chapter. Beatriz Royo directed the research.

3.7. References

1. Hofmann, N., & Hultzsch, K. C. (**2021**). Borrowing Hydrogen and Acceptorless Dehydrogenative Coupling in the Multicomponent Synthesis of N-Heterocycles: A Comparison between Base and Noble Metal Catalysis. *Eur. J. Org. Chem*. 2021(46) 6206–6223. https://doi.org/10.1002/ejoc.202100695

2. Ding, K. (**2021**). Switching between borrowing hydrogen and acceptorless dehydrogenative coupling by base transition-metal catalysts. *Tetrahedron*, 99, 132451. https://doi.org/10.1016/j.tet.2021.132451

3. Paul, B., Maji, M., Chakrabarti, K., & Kundu, S. (**2020**). Tandem transformations and multicomponent reactions utilizing alcohols following dehydrogenation strategy. *Org. Biomol. Chem.*, 18(12), 2193–2214. https://doi.org/10.1039/c9ob02760b

4. Hakim Siddiki, S. M. A., Toyao, T., & Shimizu, K. I. (**2018**). Acceptorless dehydrogenative coupling reactions with alcohols over heterogeneous catalysts. *Green Chem.*, 20(13), 2933–2952. https://doi.org/10.1039/c8gc00451j

5. Wang, Y., Wang, M., Li, Y., & Liu, Q. (**2021**). Homogeneous manganese-catalyzed hydrogenation and dehydrogenation reactions. *Chem*, 7(5), 1180–1223. https://doi.org/10.1016/j.chempr.2020.11.013

6. Corma, A., Navas, J., & Sabater, M. J. (**2018**). Advances in One-Pot Synthesis through Borrowing Hydrogen Catalysis. *Chem. Rev.,* 118(4), 1410–1459. https://doi.org/10.1021/acs.chemrev.7b00340

7. Azizi, K., & Madsen, R. (**2018**). Molybdenum-Catalyzed Dehydrogenative Synthesis of Imines from Alcohols and Amines. *ChemCatChem*, 10(17), 3703–3708. https://doi.org/10.1002/cctc.201800677

8. Wu, D., Bu, Q., Guo, C., Dai, B., & Liu, N. (**2021**). Cooperative catalysis of molybdenum with organocatalysts for distribution of products between amines and imines. *Mol. Catal.*, 503. https://doi.org/10.1016/j.mcat.2021.111415

9. Liu, J., Li, W., Li, Y., Liu, Y., & Ke, Z. (**2021**). Selective C-alkylation Between Alcohols Catalyzed by N-Heterocyclic Carbene Molybdenum. *Chem. Asian J.*, 16(20), 3124–3128. https://doi.org/10.1002/asia.202100959

10. Li, W., Huang, M., Liu, J., Huang, Y. L., Lan, X. B., Ye, Z., Zhao, C., Liu, Y., & Ke, Z. (**2021**). Enhanced Hydride Donation Achieved Molybdenum Catalyzed Direct N-Alkylation of Anilines or Nitroarenes with Alcohols: From Computational Design to Experiment. *ACS Catal.*, 11, 10377–10382. https://doi.org/10.1021/acscatal.1c02956

11. Rajasekaran, H., Peter, J., Eliseenkov, E. v., Boyarskiy, V. P., Bhuvanesh, N., & Karvembu, R. (**2022**). Half-sandwich Ru(II)-thioamide complexes as catalysts for one pot synthesis of aromatic 1,5-diketones. *J. Organomet. Chem.*, 965–966. https://doi.org/10.1016/j.jorganchem.2022.122322

12. Yadav, S., Reshi, N. U. D., Pal, S., & Bera, J. K. (**2021**). Aerobic oxidation of primary amines to amides catalyzed by an annulated mesoionic carbene (MIC) stabilized Ru complex. *Catal. Sci. Technol.*, 11(21), 7018–7028. https://doi.org/10.1039/d1cy01541a

Chapter 4

Conclusions and Future Work

The chemistry and catalysis of Mo triazolylidene complexes remain rather unexplored. This thesis was dedicated to explore the potential of Mo triazolylidene complexes in catalysis. To meet this goal, a new family of Mo complexes bearing bidentate bis-triazolylidene ligands containing different wingtips have been prepared, and their catalytic activity in a variety of catalytic applications has been screened.

A new family of molybdenum(0) tetracarbonyl complexes with triazolylidene/triazole/pyridine ligands of general formula $[Mo(CO)_4(L)]$ (L = bis-1,2,3-triazole (**L1**), bis-1,2,3-triazol-5-ylidene (**L2** and **L3**), pyridyl-1,2,3-triazol-4-ylidene (**L4**)) were successfully synthesized and fully characterized by NMR (^{1}H, ^{13}C, and ^{95}Mo) and IR spectroscopy, and by elemental analysis. The NMR and IR data of all complexes (**Mo1**-**Mo7**) provided valuable insights of the donor capacity of the bidentate mesoionic ligands; **L2** and **L3** exhibited higher σ-donor ability compared to **L1** and **L4**. In addition, the introduction of aromatic groups at the N3 and N1 positions of the triazolylidene rings decreased the overall donor capacity of the bis-triazolylidene ligands. Therefore, ligands containing alkyl groups at the N1 and N3 positions (**L2a** and **L2c**) were shown to have the highest σ-donor capacity.

It was explored, for the first time, the impact of the presence of mesoionic triazolylidene ligands on the catalytic performance of Mo tetracarbonyl complexes in borrowing hydrogen (BH) and acceptorless dehydrogenative coupling (ADC) processes, and in the aerobic oxidation of amines to amides. Interestingly, when applied for the synthesis of quinolines through ADC, complexes **Mo2** and **Mo4** bearing strong σ-donating bis-triazolylidene ligands (**L2a** and **L2c**, respectively) resulted to be the most effective pre-catalysts. In contrast, Mo complexes containing triazolylidene ligands with aromatic groups as substituents displayed significantly less activity than **Mo2** and **Mo4**, and the Mo complex bearing a mixed-pyridine triazolylidene ligand (**L4**) was completely inactive. Gratifyingly, we have developed a sustainable, efficient, and practical synthesis of a wide variety of substituted quinolines using complex **Mo2** as catalyst, through the annulation of 2-aminobenzyl alcohols and 1-(2-aminophenyl)ethanol with a variety of secondary alcohols. The coupling reactions occurred at 5 mol% catalyst loading and 150 ºC in the presence of *t*-BuOK (0.5 equiv.), and tolerated a wide range of functional groups (17 examples), allowing to isolate the corresponding quinolines in moderate to excellent yields (22% to 99%). Under the same reaction conditions, **Mo2** was also capable to mediate the catalytic β-alkylation of alcohols. Furthermore, preliminary investigations have shown that Mo complexes bearing bis-triazolylidene (**Mo2**) or bis-imidazolylidene ($[Mo(bis\text{-}NHC^{Me})(CO)_4]$) ligands displayed comparable catalytic activity in the *N*-alkylation of amines with secondary alcohols under the same hydrogen-borrowing conditions. On the other hand, we have demonstrated that **Mo5** displayed the best catalytic performance for the α-alkylation of ketones with alcohols, achieving 100% of selectivity for the formation of the corresponding α-alkylated product. Excitingly, we have also disclosed the

excellent catalytic performance of **Mo2** in the aerobic oxidation of primary amines to amides, using 5 mol% of catalyst and 0.5 equiv of *t*-BuOK in toluene at 110 ºC for 24 h.

The protocols developed in this thesis provide concise and environmentally friendly methods for the construction of C-C and C-N bonds giving access to high-value compounds, such as alkylated amines, imines, amides, and *N*-heterocycles. The use of a catalyst based on a phosphine-free inexpensive metal complex makes these methodologies particularly appealing and meaningful. Overall, this thesis opens up new possibilities for the application of molybdenum(0) complexes with mesoionic carbene (MIC) ligands in a wide range of catalytic processes and holds promise for the development of more efficient and sustainable synthetic methodologies.

Currently, our research is focused on the optimization of the catalytic conditions for the aerobic oxidation of primary amines to amides mediated by **Mo2**, which represents the first Mo catalytic system for this type of reaction.

Annexes

Chapter 2 - Annex

Synthesis and Characterization of Molybdenum(0) Complexes with Triazolylidene Ligands

A2.1. Characterization of **L1**-**L4**

A2.2. Characterization of **Mo1**-**Mo7**

A2.3. X-Ray Structure and Crystallographic Details of Complex **Mo7**

A2.1. Characterization of **L1**-**L4**

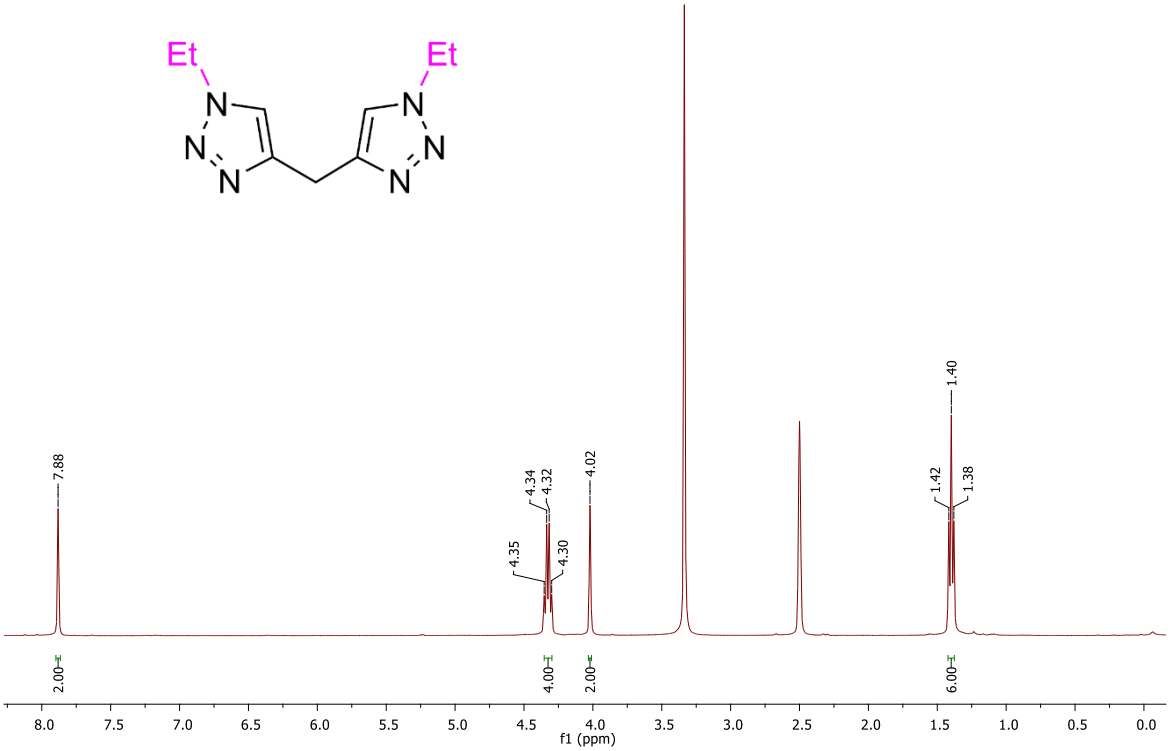

Figure A2.1. ^{1}H NMR spectrum in DMSO-d_6 of **L1a**.

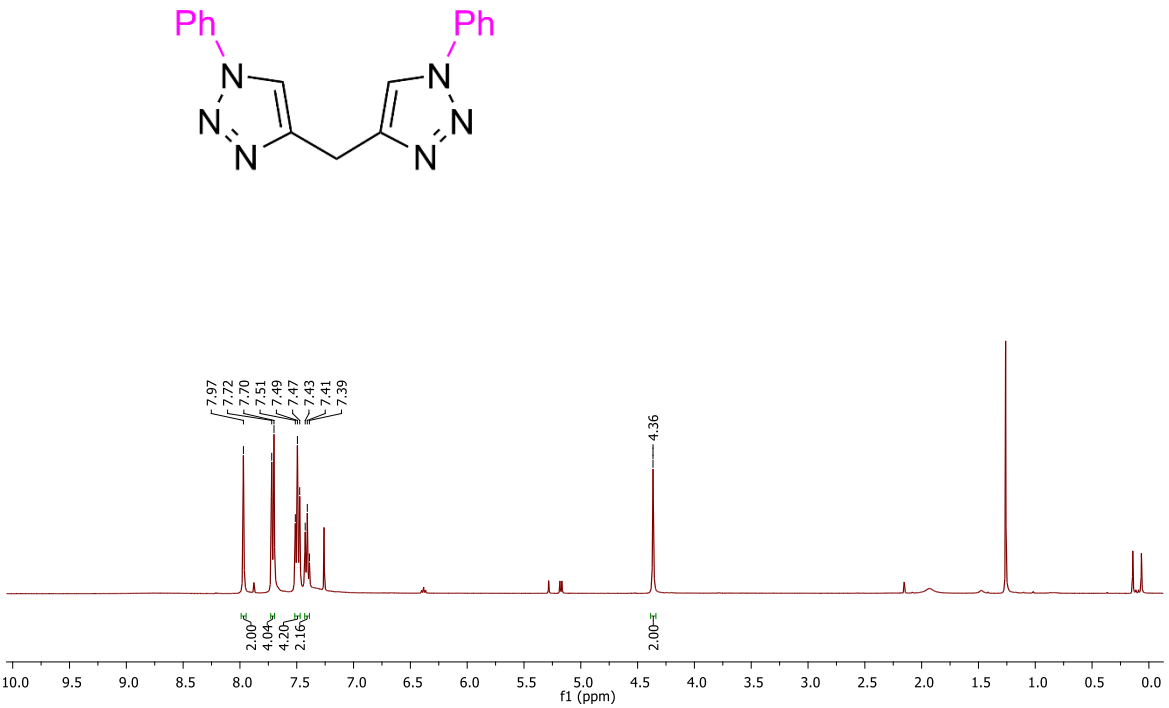

Figure A2.2. ^{1}H NMR spectrum in $CDCl_3$ of **L1b**.

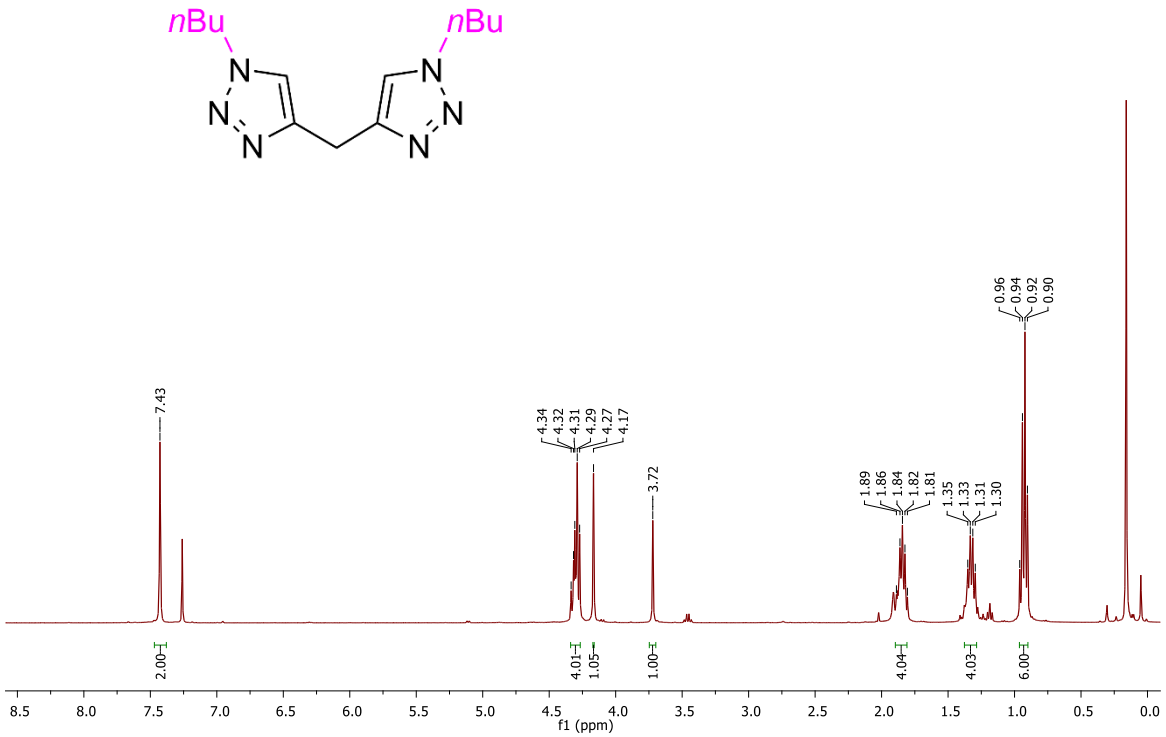

Figure A2.3. ^{1}H NMR spectrum in $CDCl_3$ of **L1c**.

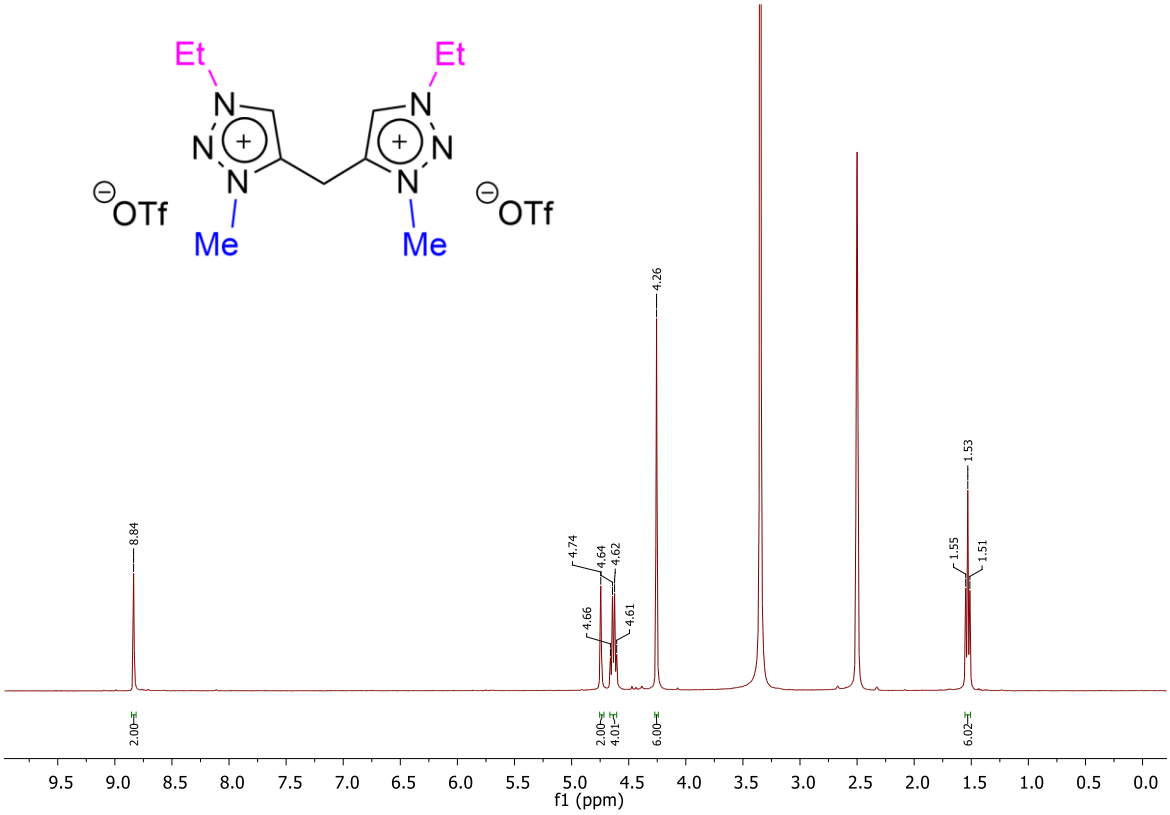

Figure A2.4. ^{1}H NMR spectrum in DMSO-d_6 of **L2a[OTf]$_2$**.

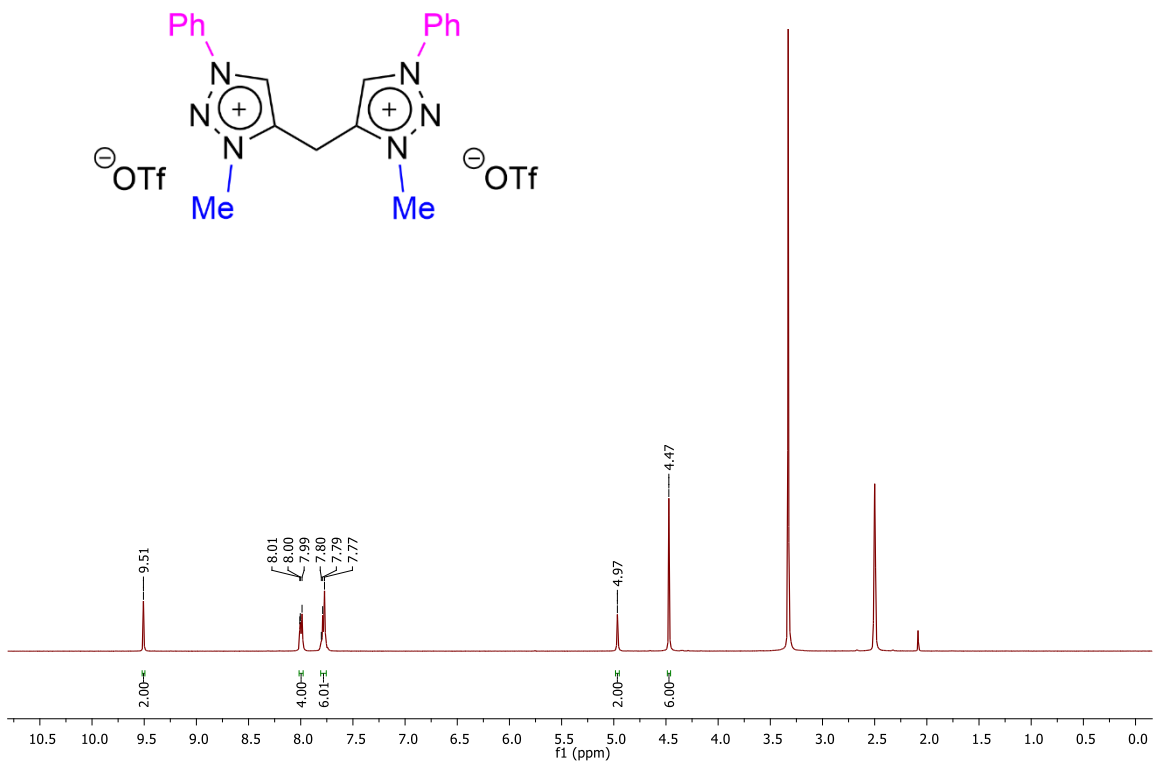

Figure A2.5. ^{1}H NMR spectrum in DMSO-d_6 of **L2b[OTf]$_2$**.

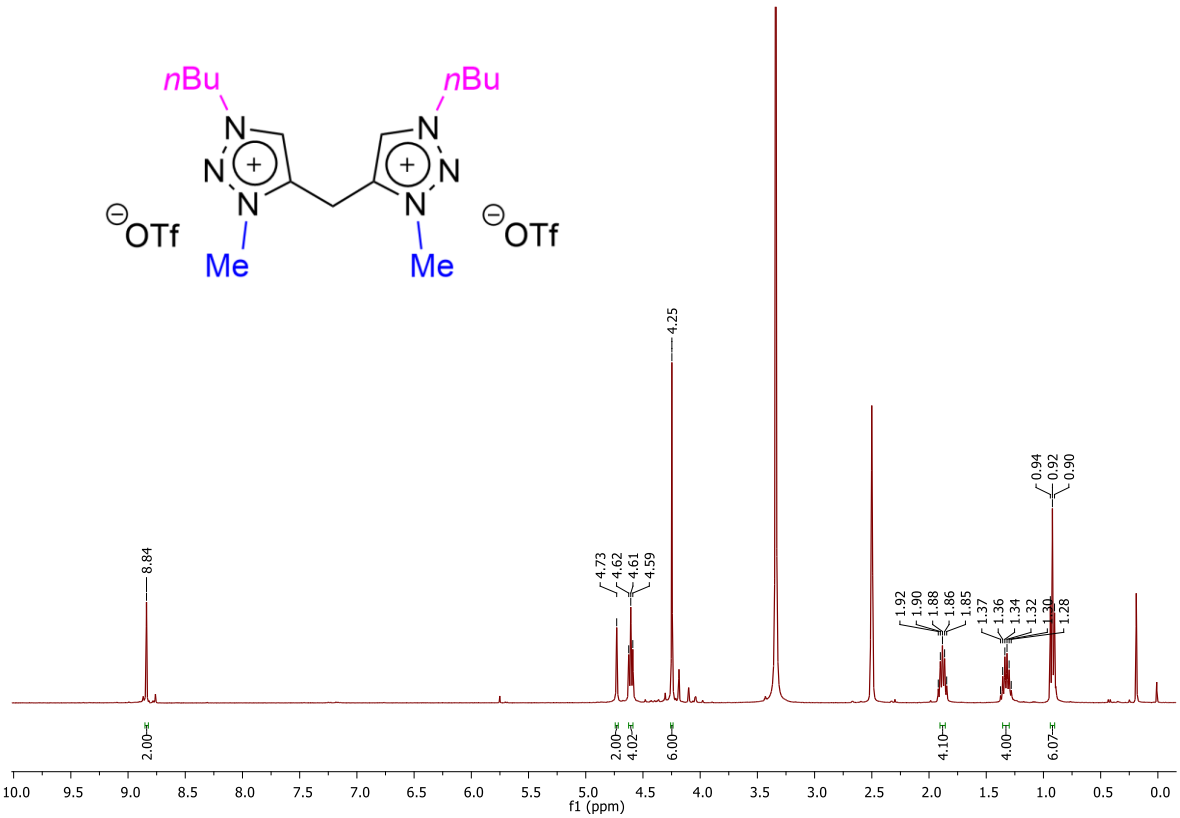

Figure A2.6. ^{1}H NMR spectrum in DMSO-d_6 of **L2c[OTf]$_2$**.

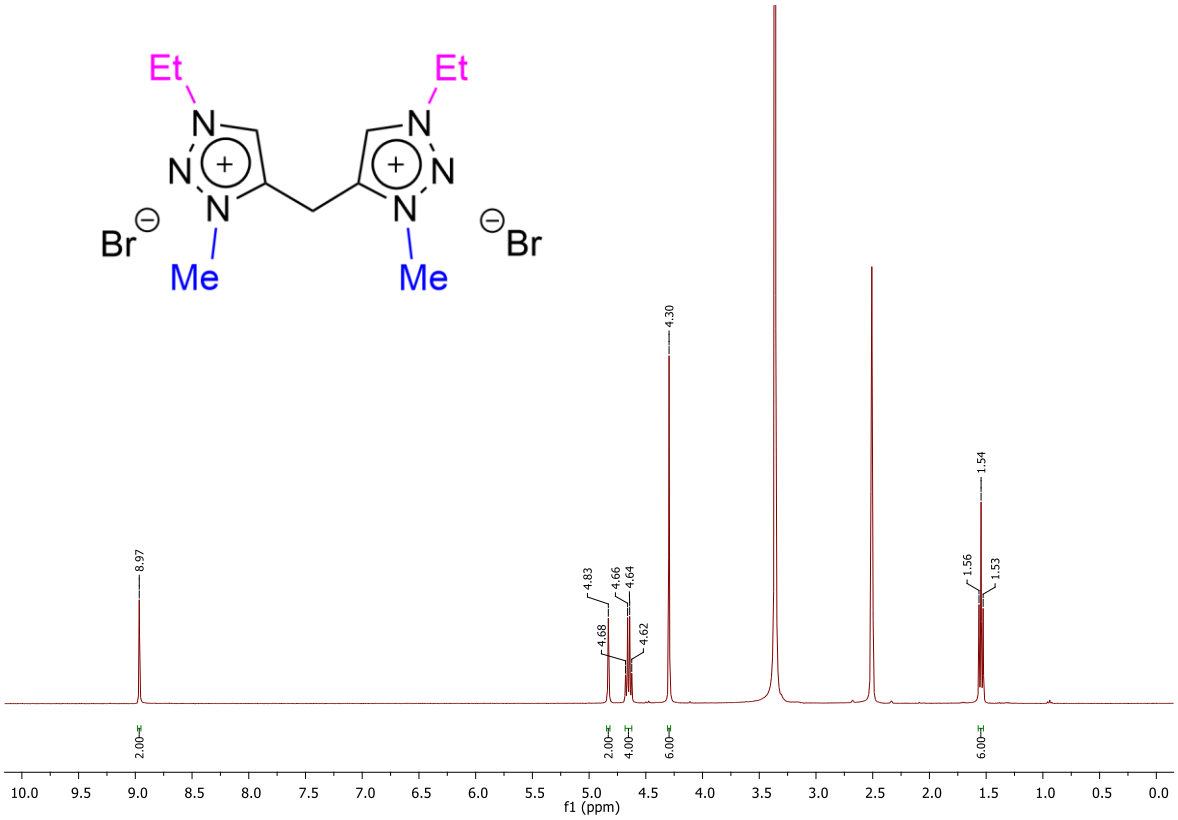

Figure A2.7. ^{1}H NMR spectrum in DMSO-d_6 of **L2a[Br]$_2$**.

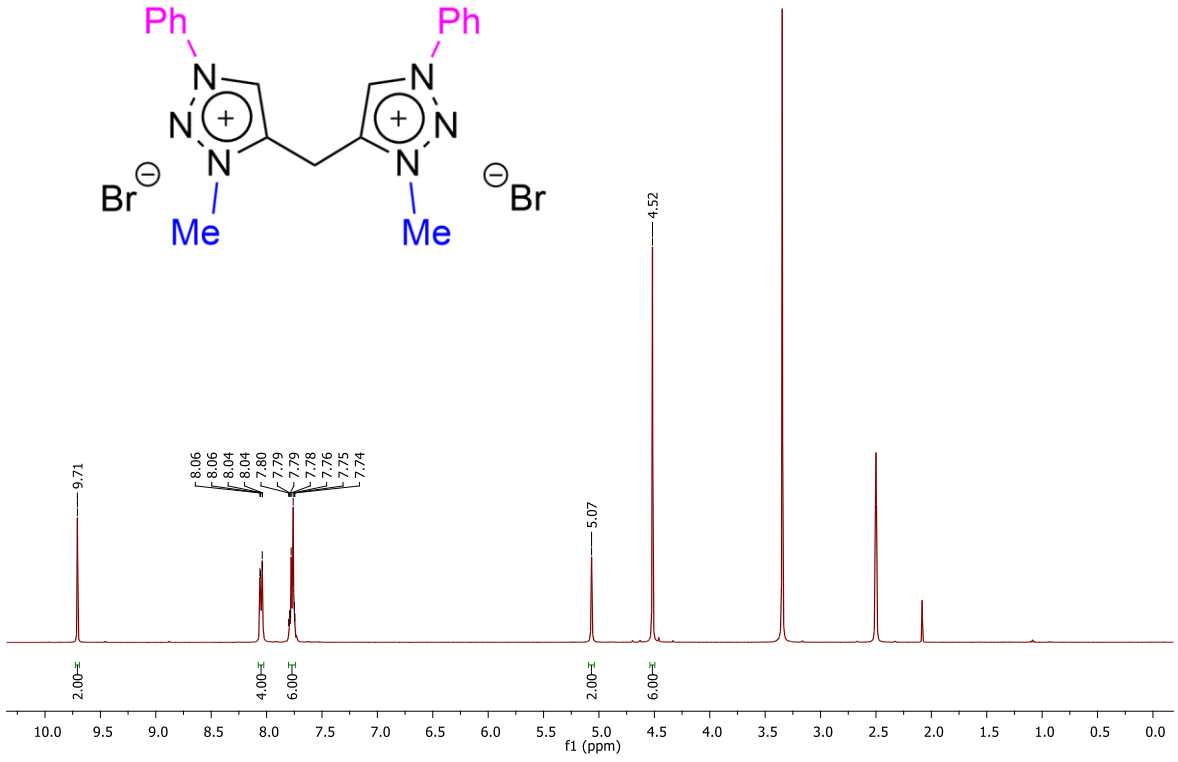

Figure A2.8. ^{1}H NMR spectrum in DMSO-d_6 of **L2b[Br]$_2$**.

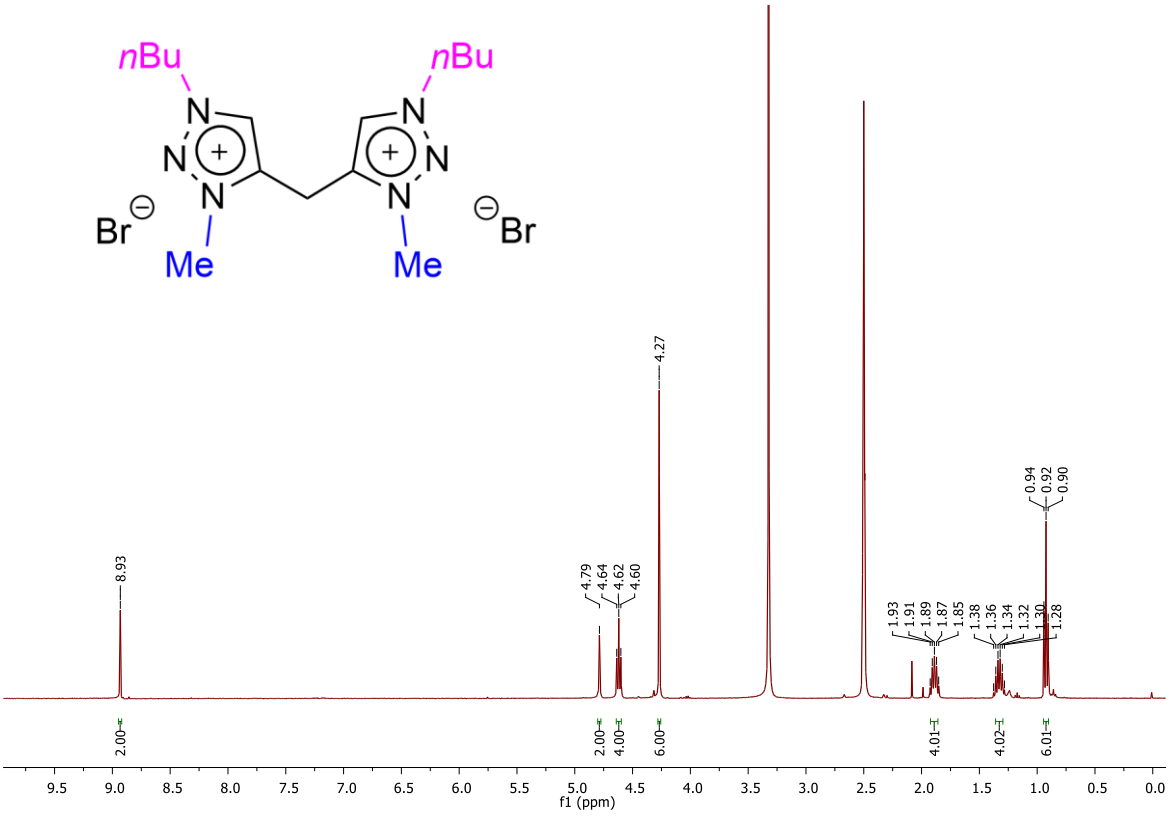

Figure A2.9. ^{1}H NMR spectrum in DMSO-d_6 of **L2c[Br]$_2$**.

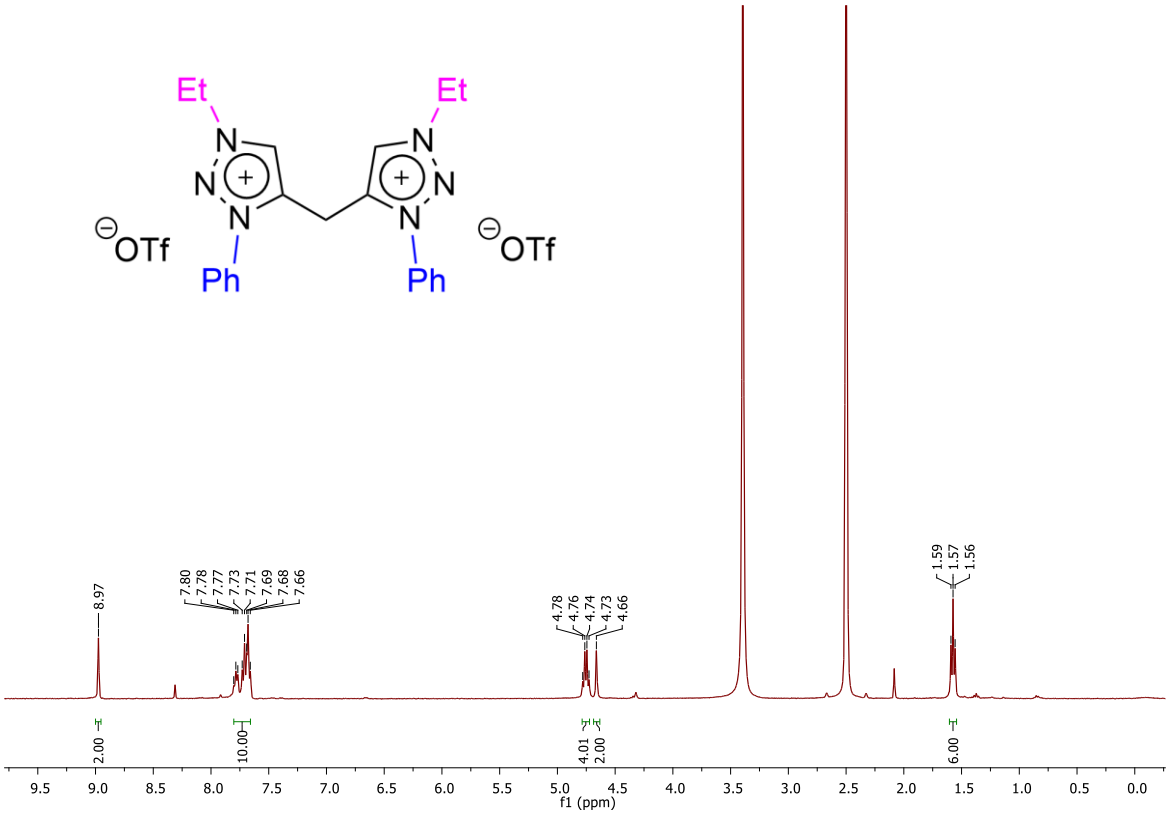

Figure A2.10. ^{1}H NMR spectrum in DMSO-d_6 of **L3a[OTf]$_2$**.

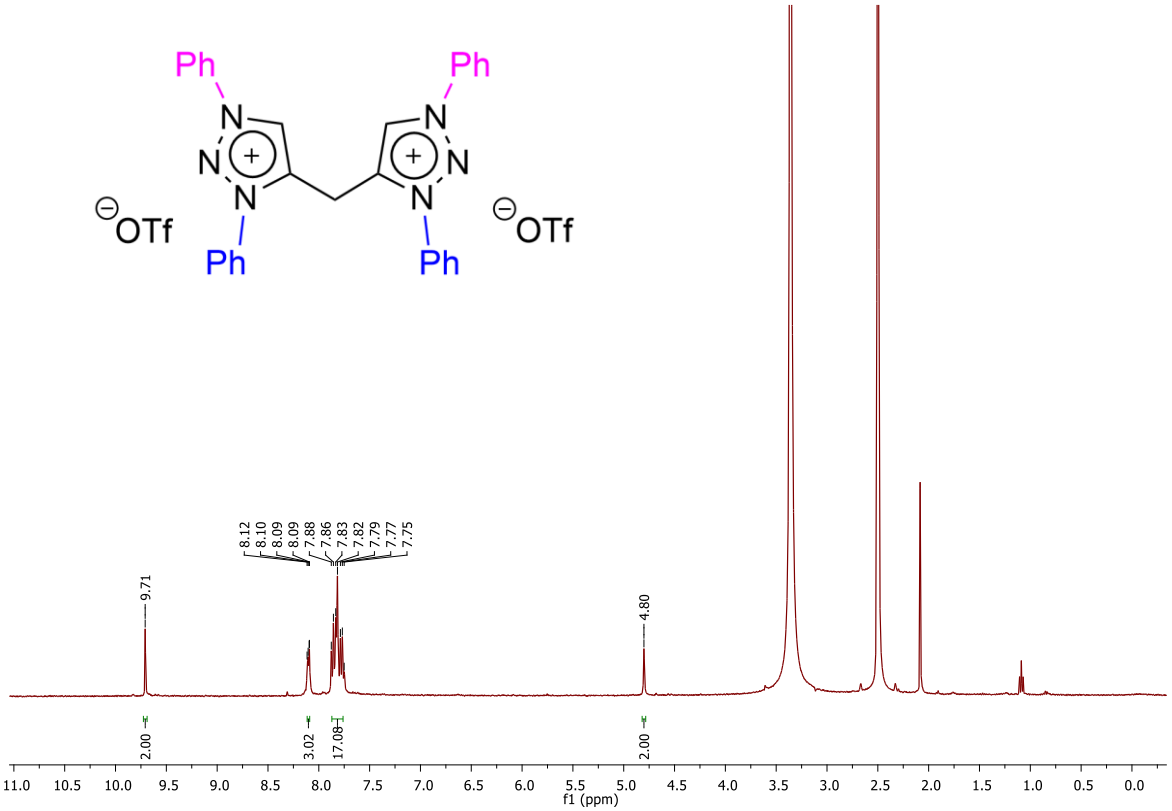

Figure A2.11. ^{1}H NMR spectrum in DMSO-d_6 of **L3b[OTf]$_2$**.

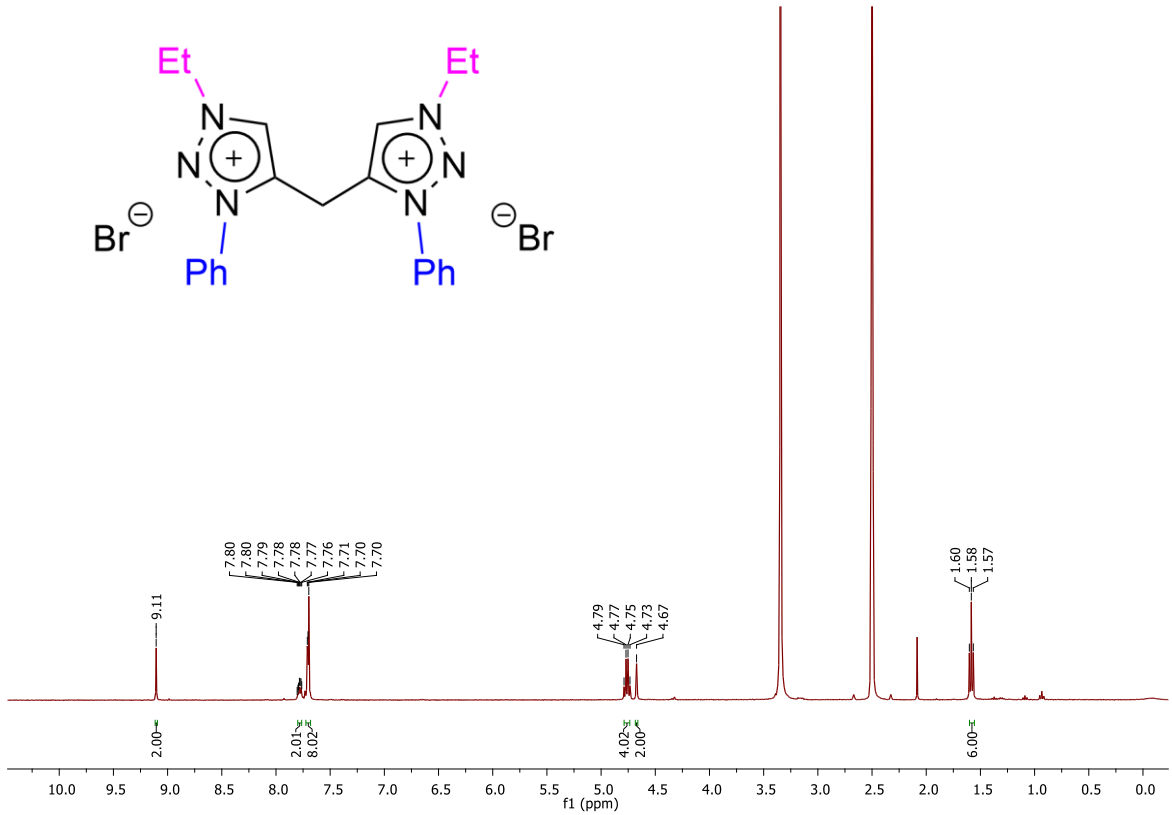

Figure A2.12. ^{1}H NMR spectrum in DMSO-d_6 of **L3a[Br]$_2$**.

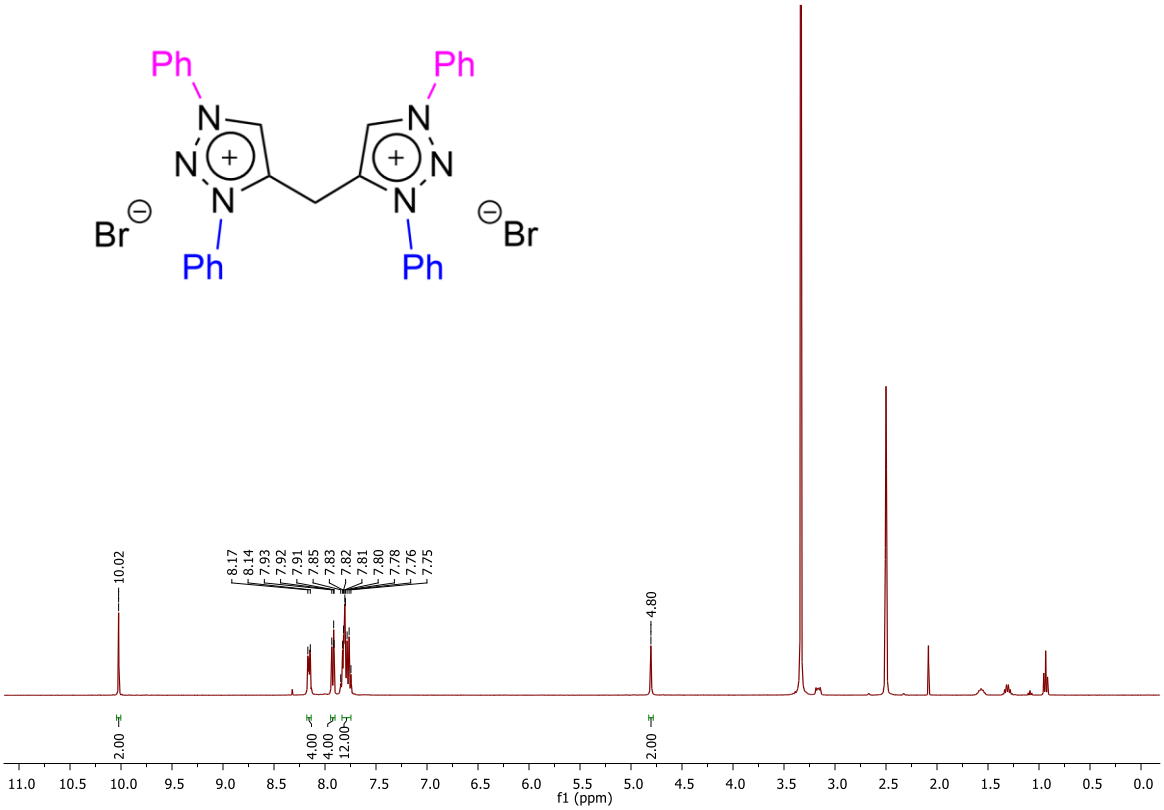

Figure A2.13. ^{1}H NMR spectrum in DMSO-d_6 of **L3b[Br]$_2$**.

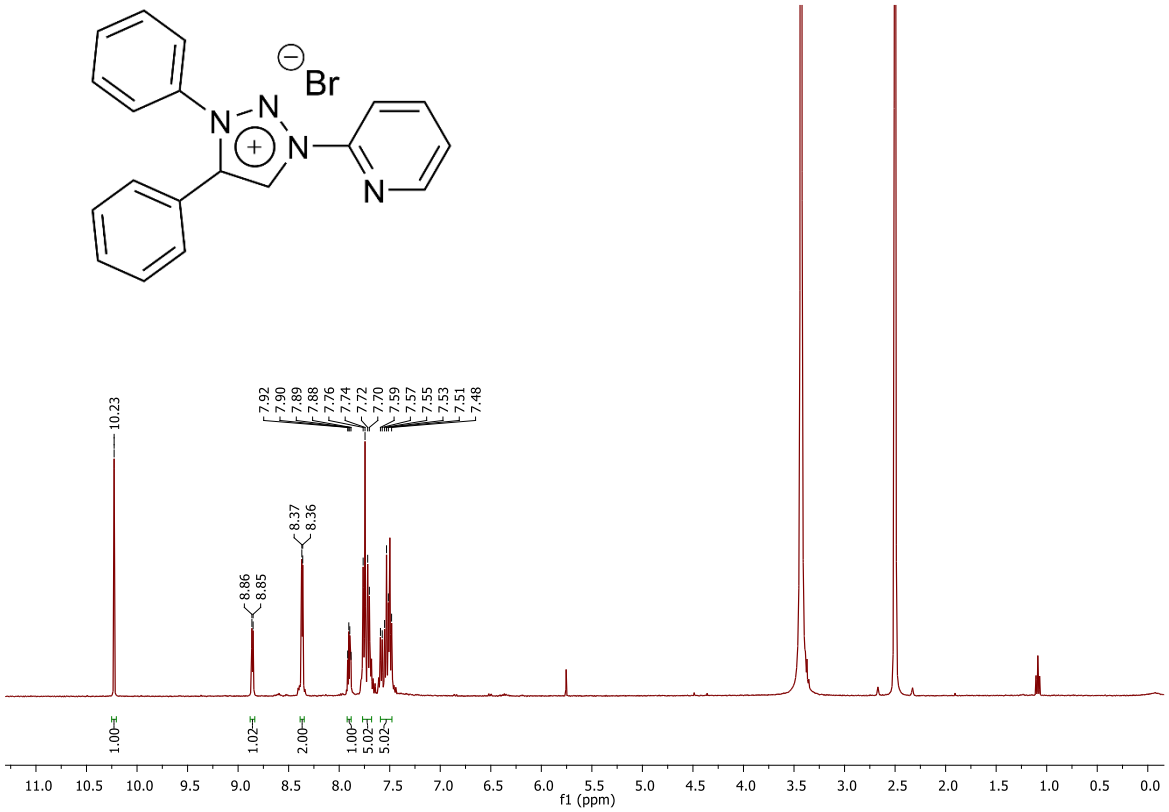

Figure A2.14. ^{1}H NMR spectrum in DMSO-d_6 of **L4[Br]**.

A2.2. Characterization of **Mo1**-**Mo7**

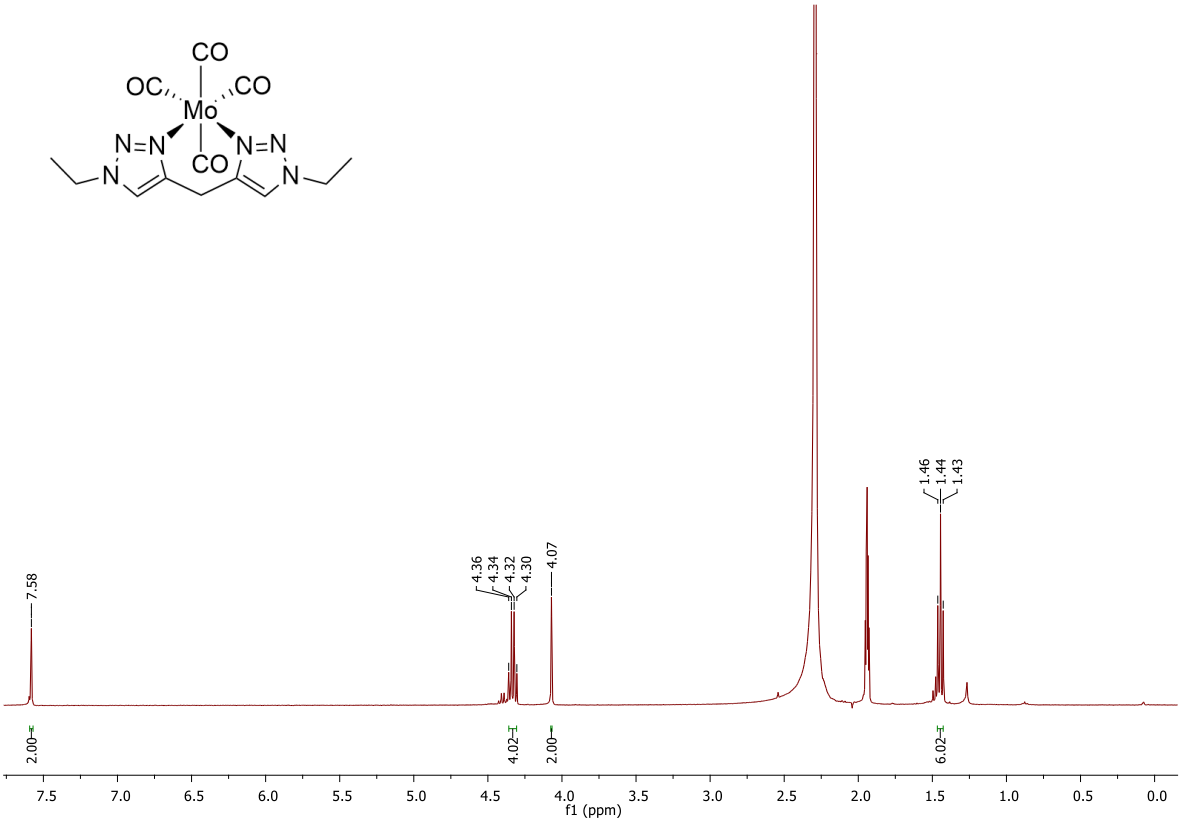

Figure A2.15. ^{1}H NMR spectrum in CD_3CN of **Mo1**.

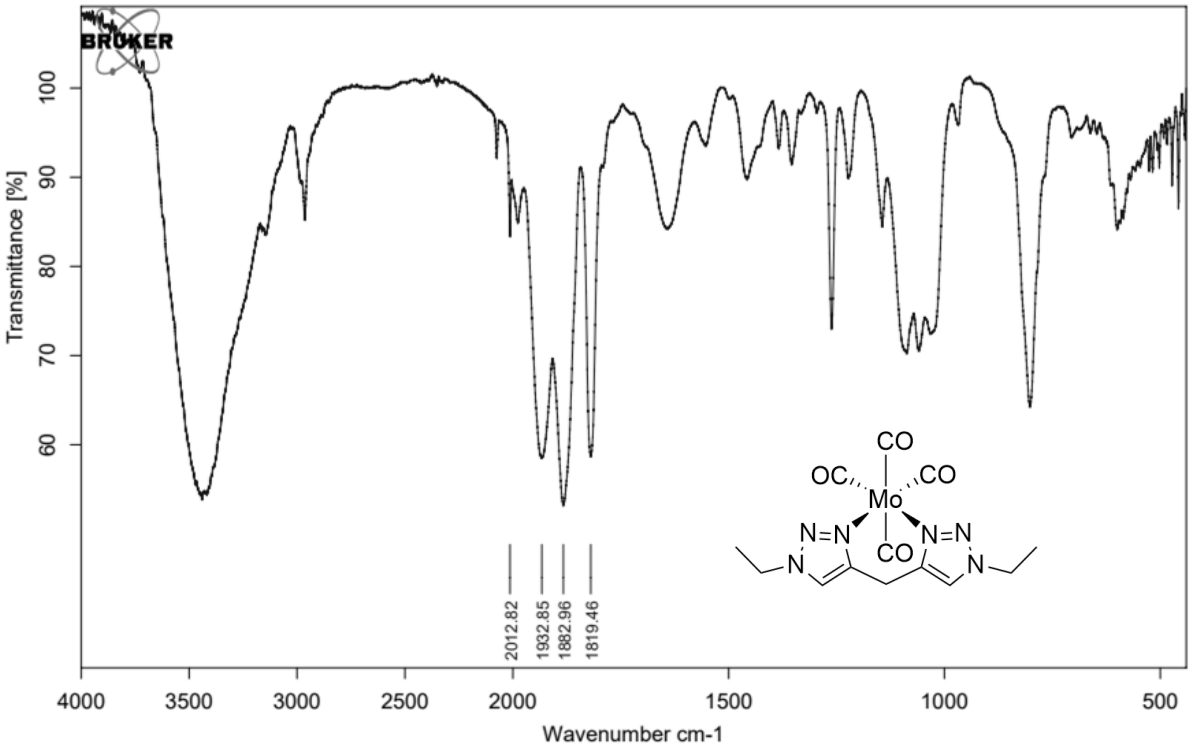

Figure A2.16. IR spectrum of **Mo1** in KBr.

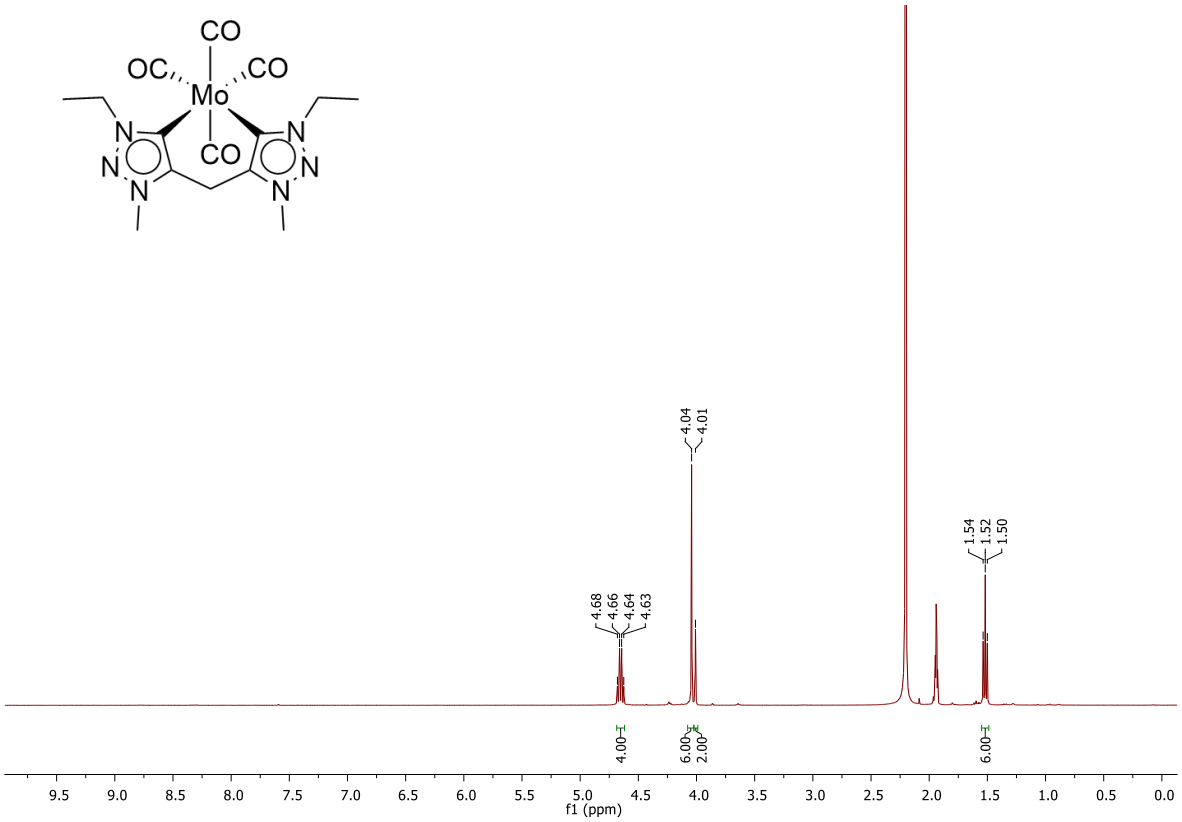

Figure A2.17. ^{1}H NMR spectrum in CD_3CN of **Mo2**.

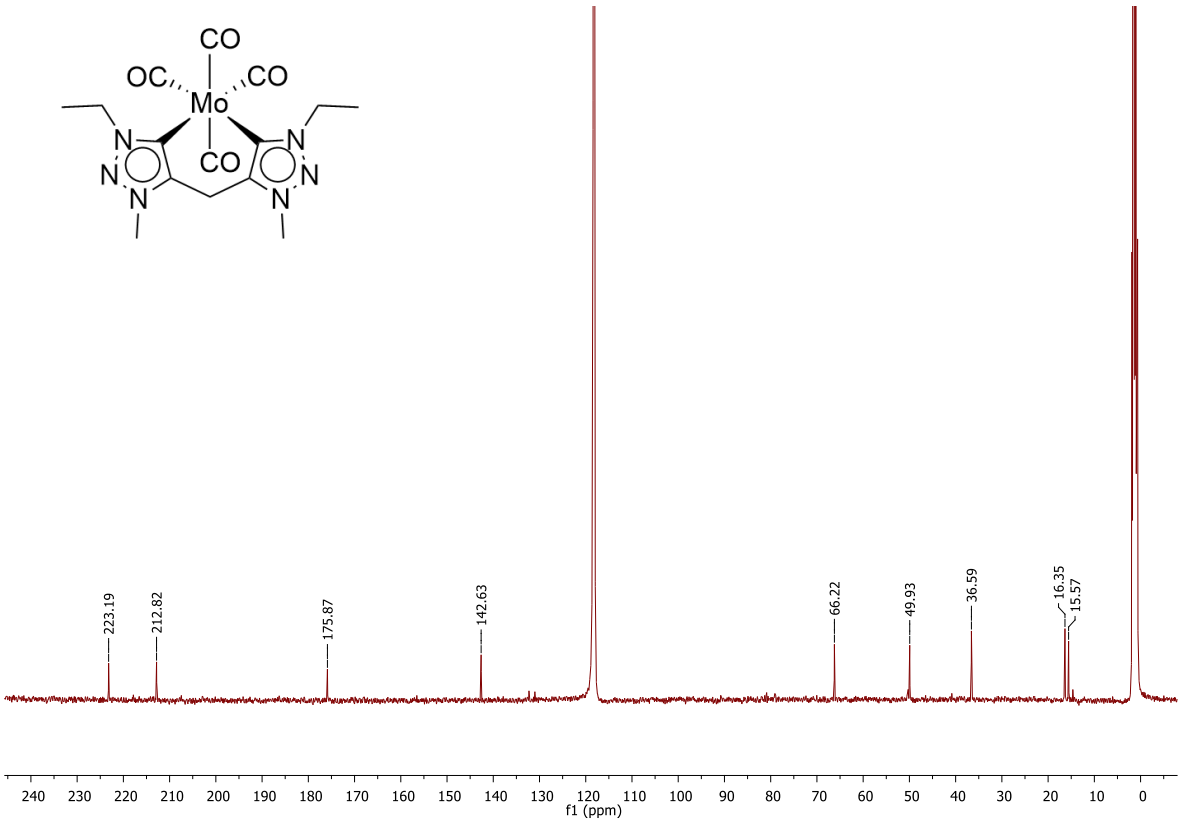

Figure A2.18. ^{13}C NMR spectrum in CD_3CN of **Mo2**.

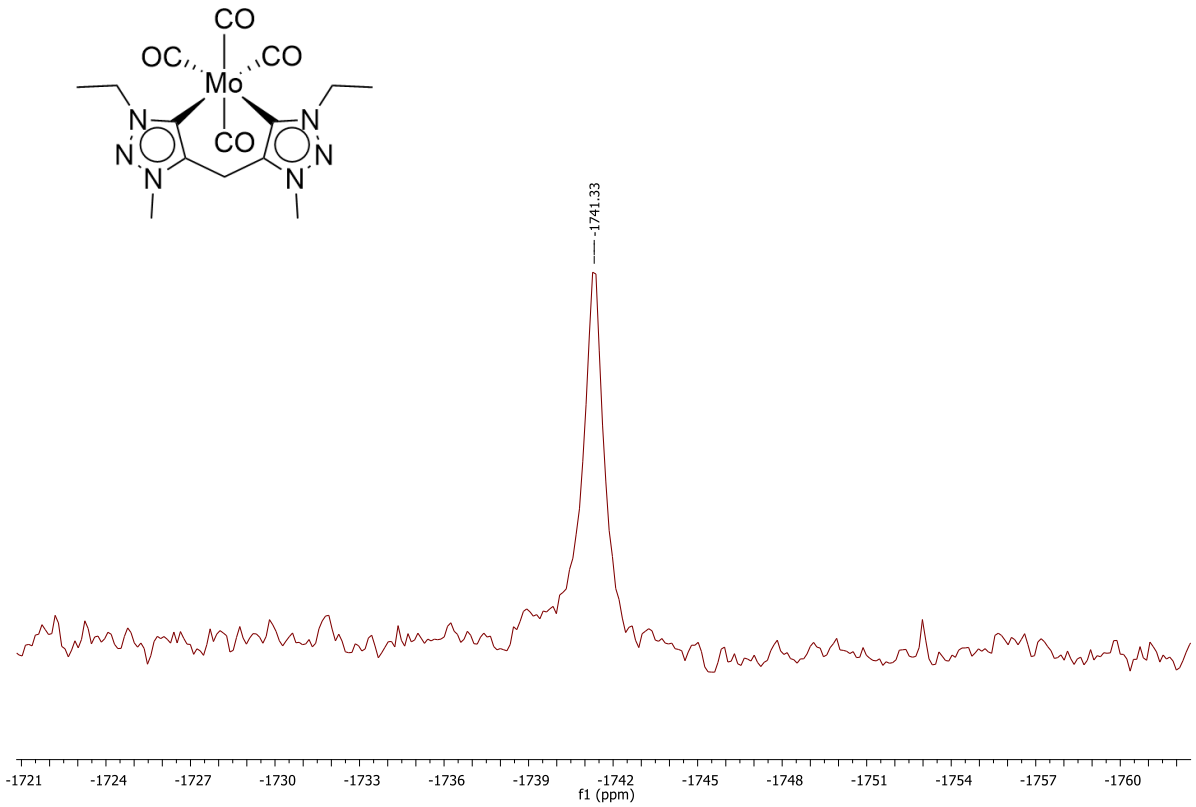

Figure A2.19. ^{95}Mo NMR spectrum in CD_3CN of **Mo2**.

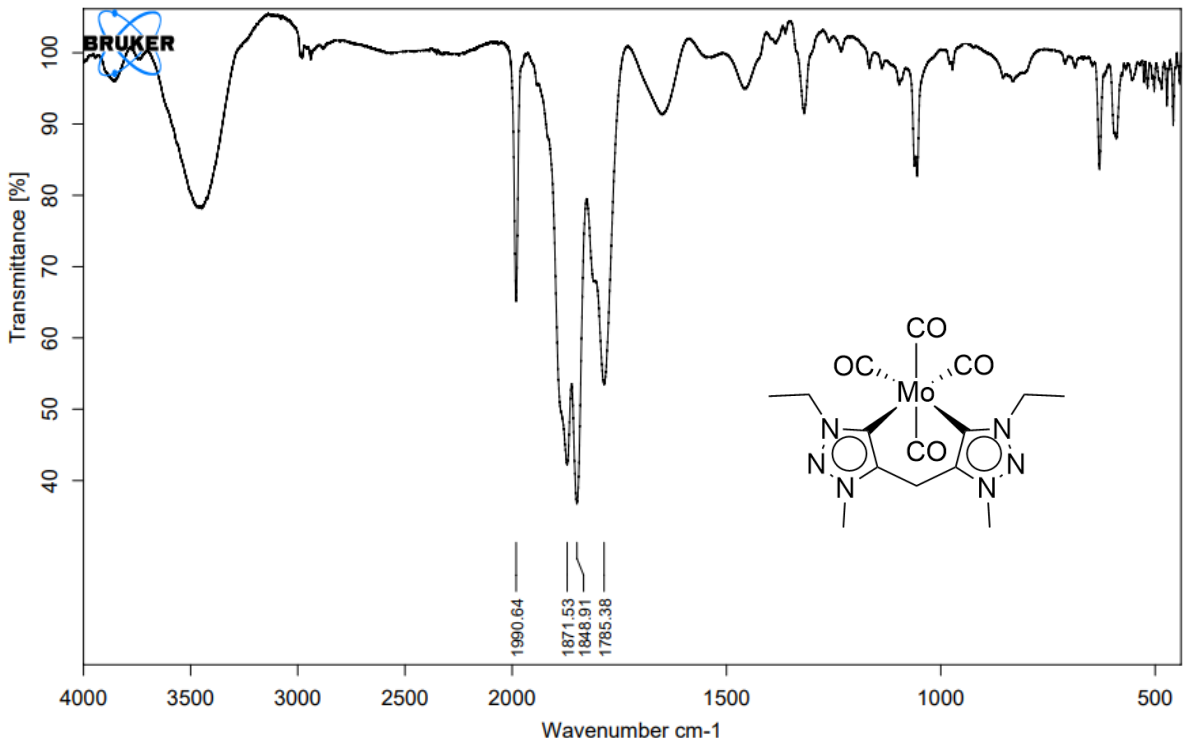

Figure A2.20. IR spectrum of **Mo2** in KBr.

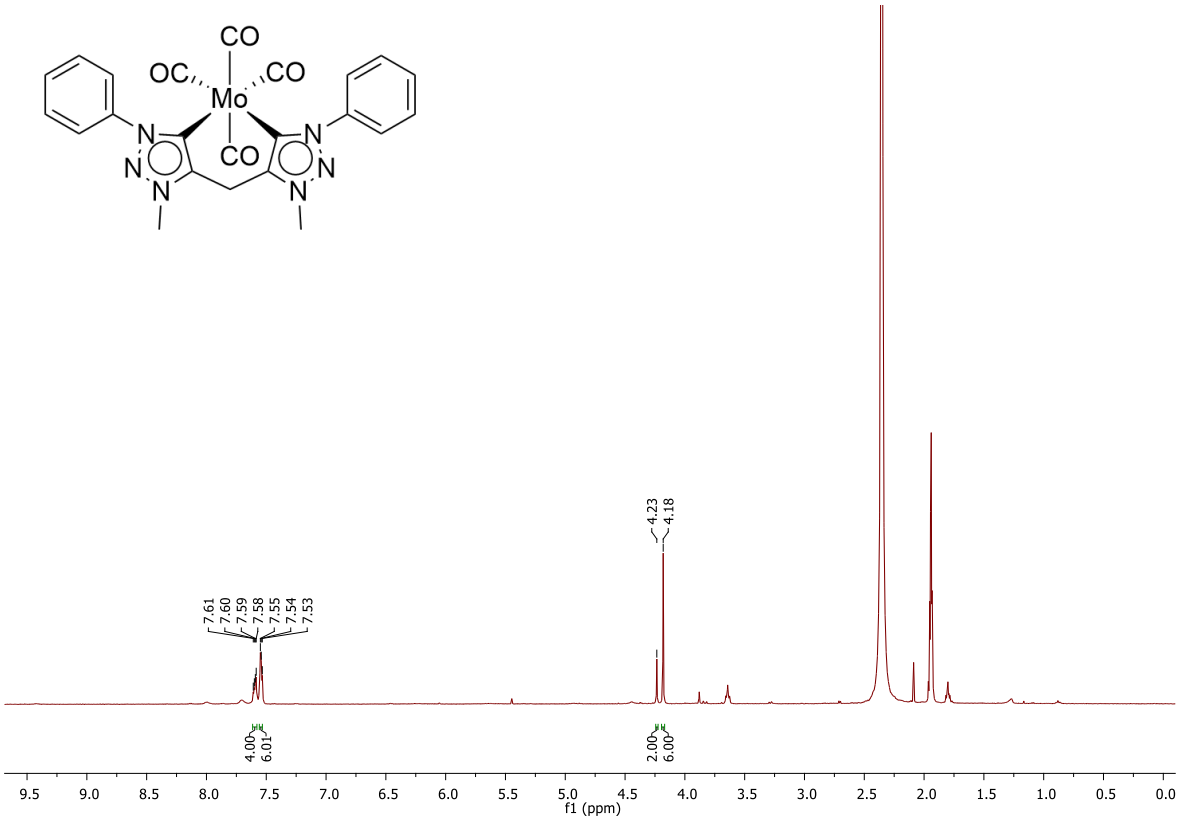

Figure A2.21. ^{1}H NMR spectrum in CD_3CN of **Mo3**.

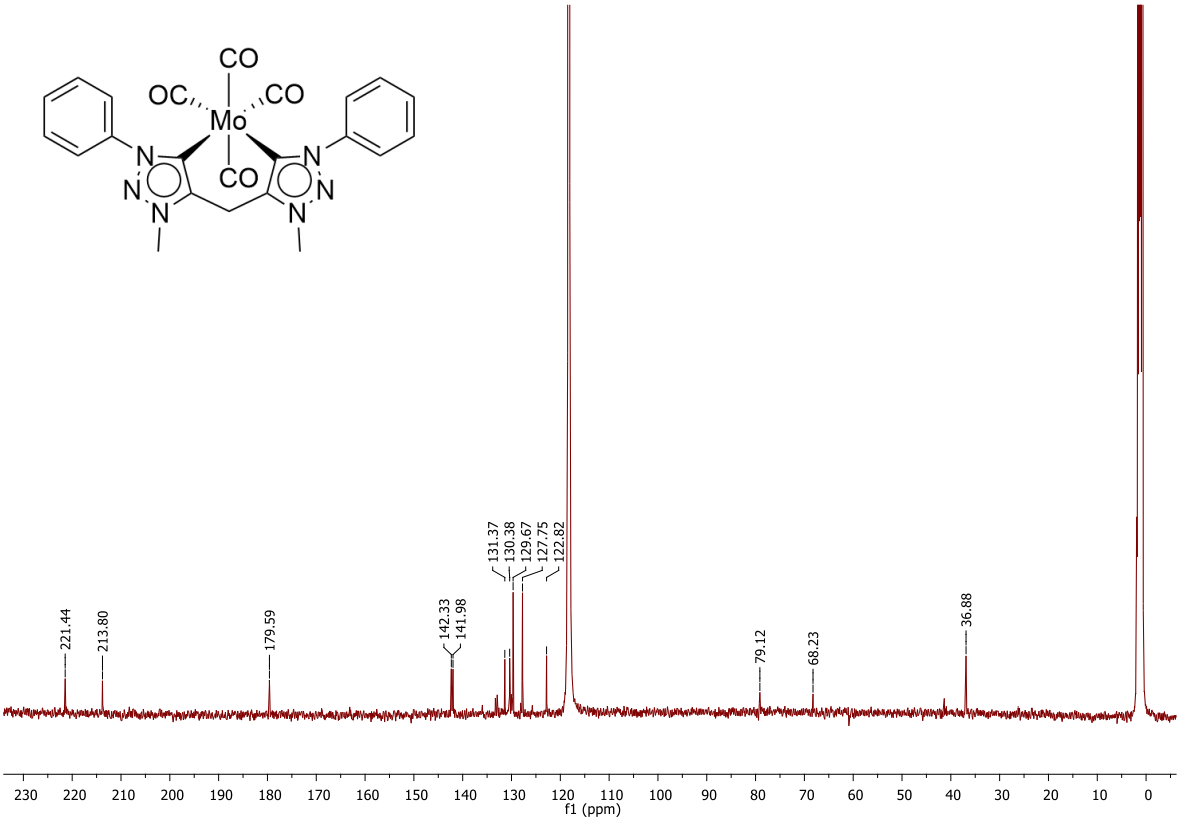

Figure A2.22. ^{13}C NMR spectrum in CD_3CN of **Mo3**.

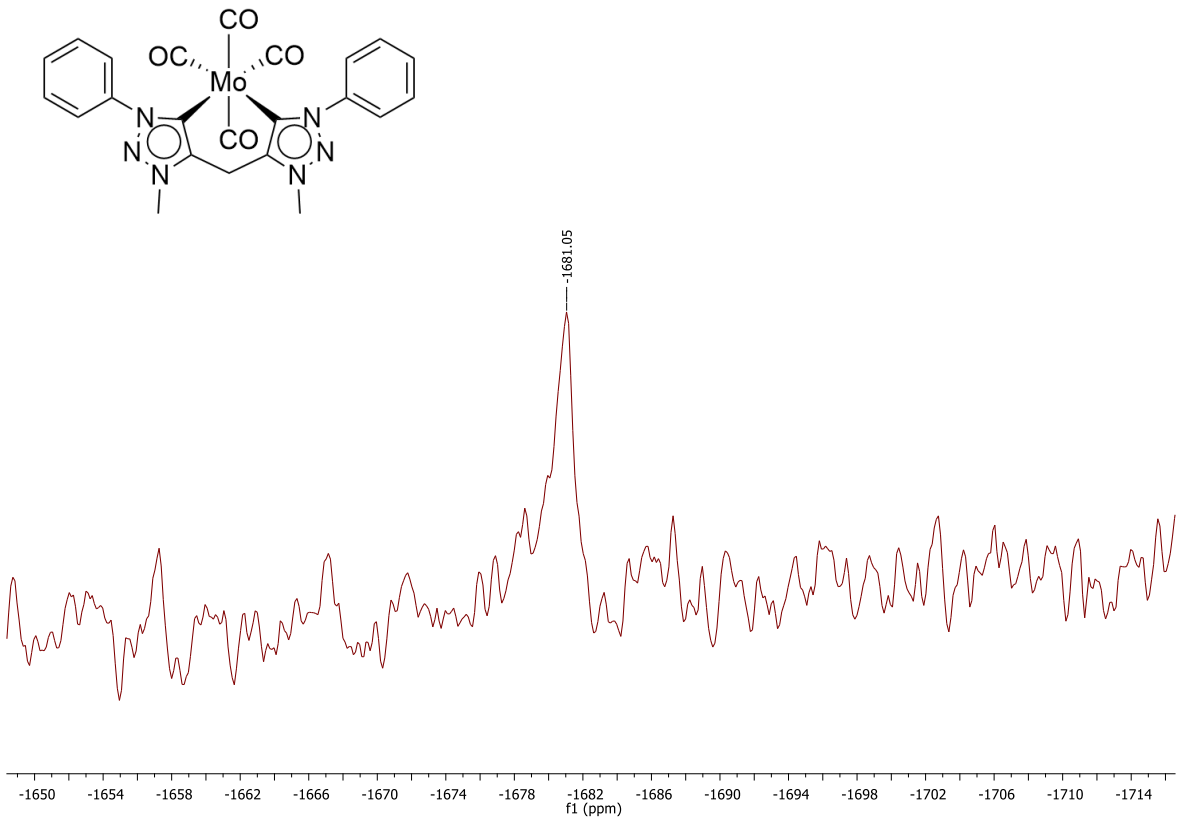

Figure A2.23. ^{95}Mo NMR spectrum in CD_3CN of **Mo3**.

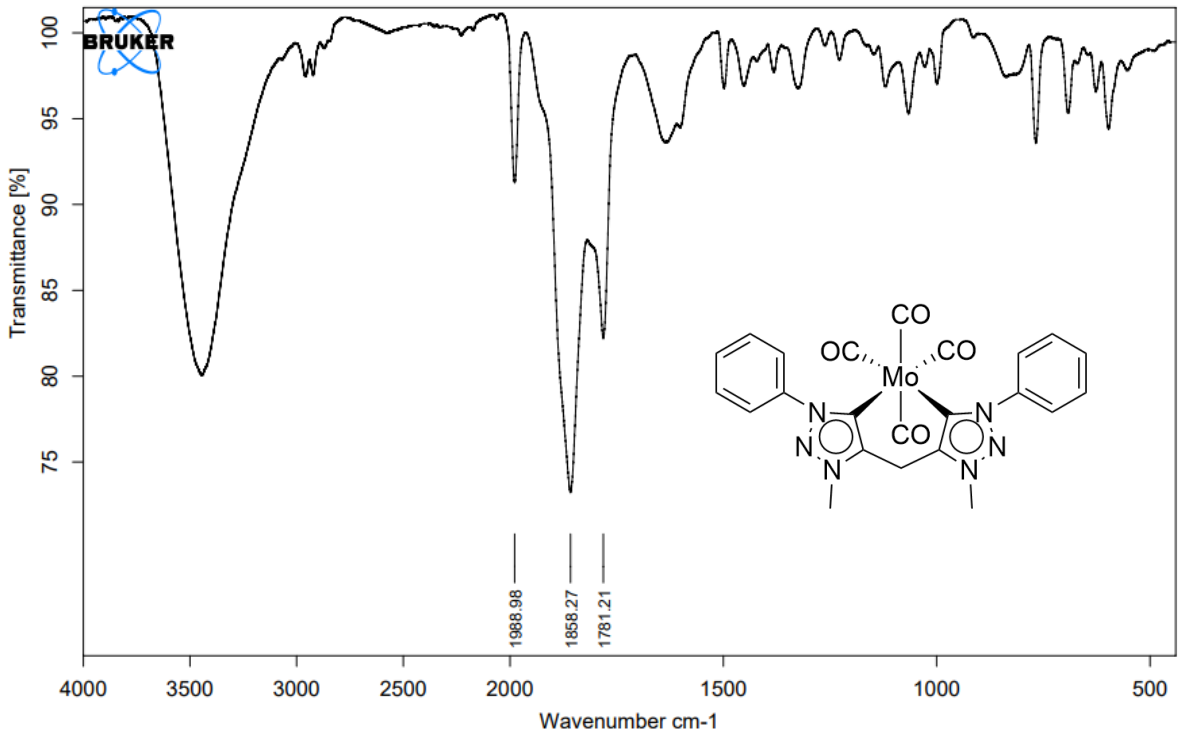

Figure A2.24. IR spectrum of **Mo3** in KBr.

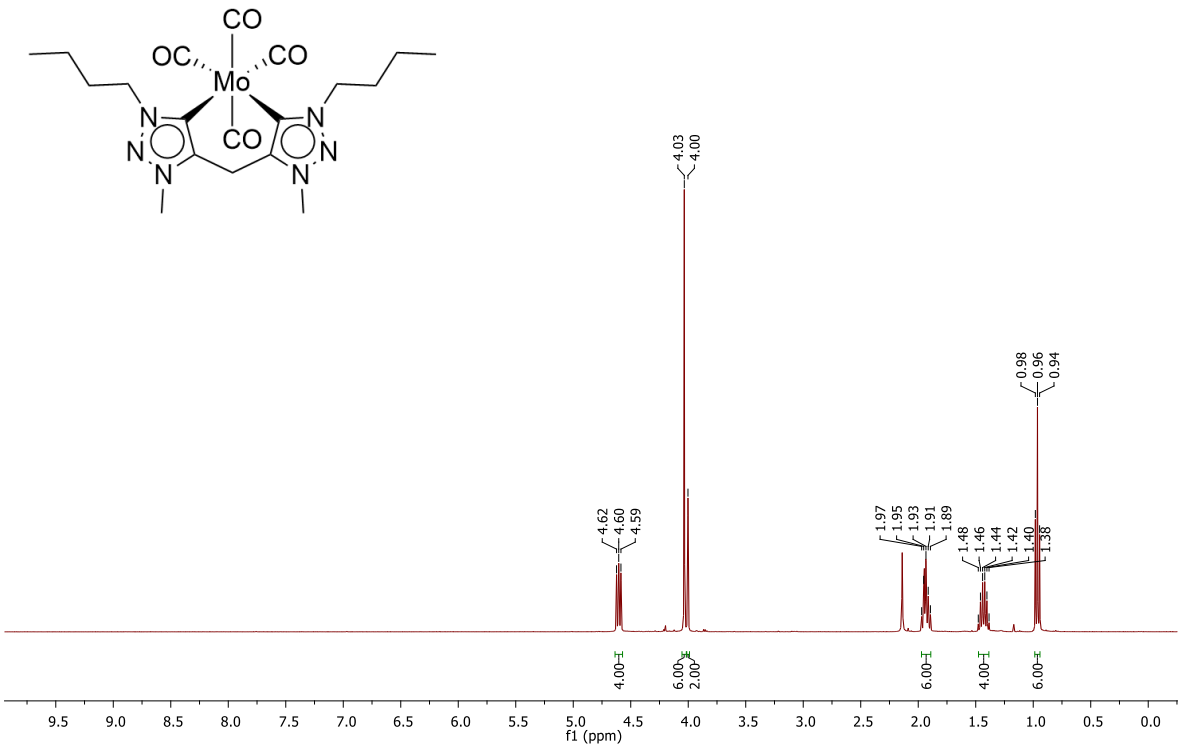

Figure A2.25. ^{1}H NMR spectrum in CD_3CN of **Mo4**.

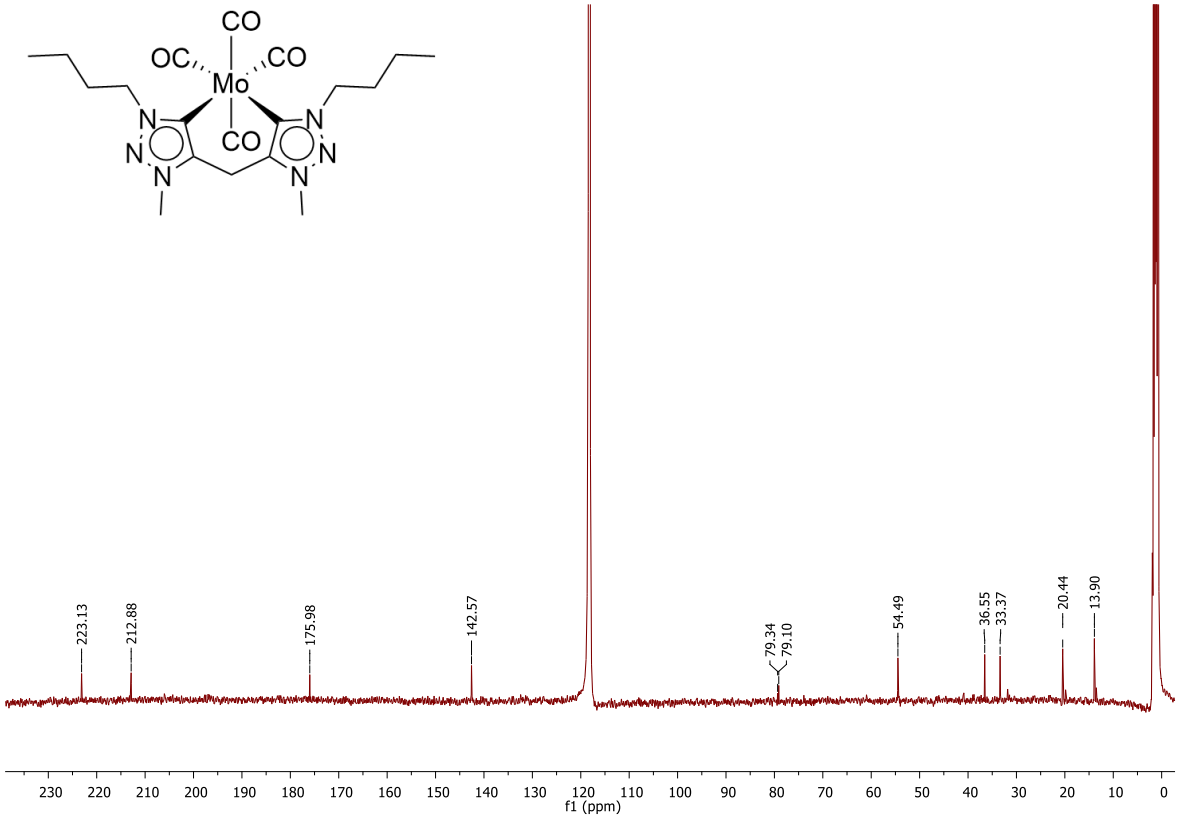

Figure A2.26. ^{13}C NMR spectrum in CD_3CN of **Mo4**.

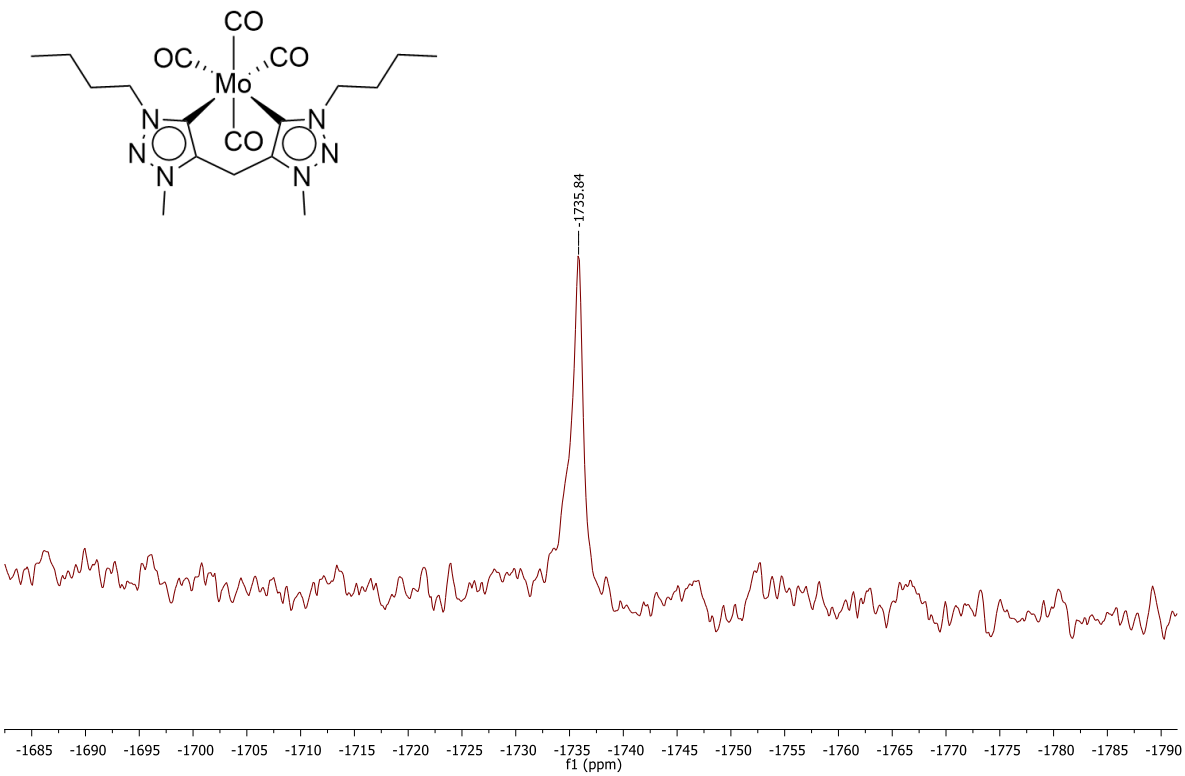

Figure A2.27. ^{95}Mo NMR spectrum in CD_3CN of **Mo4**.

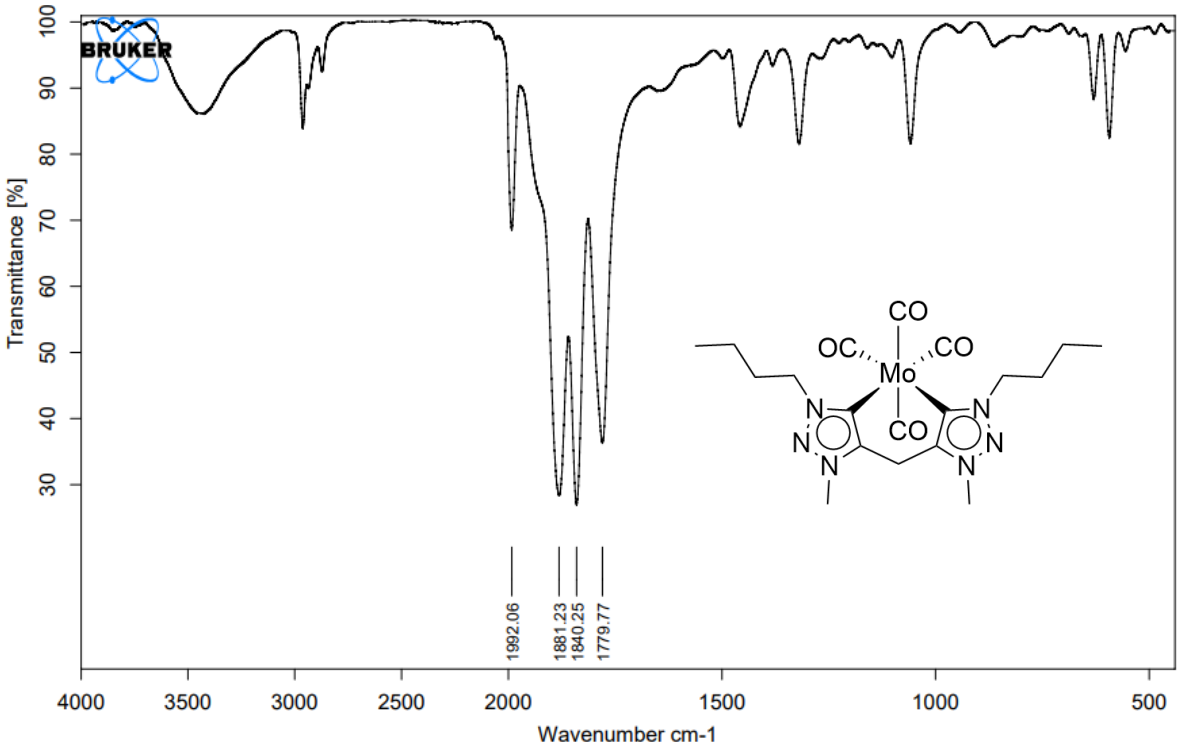

Figure A2.28. IR spectrum of **Mo4** in KBr.

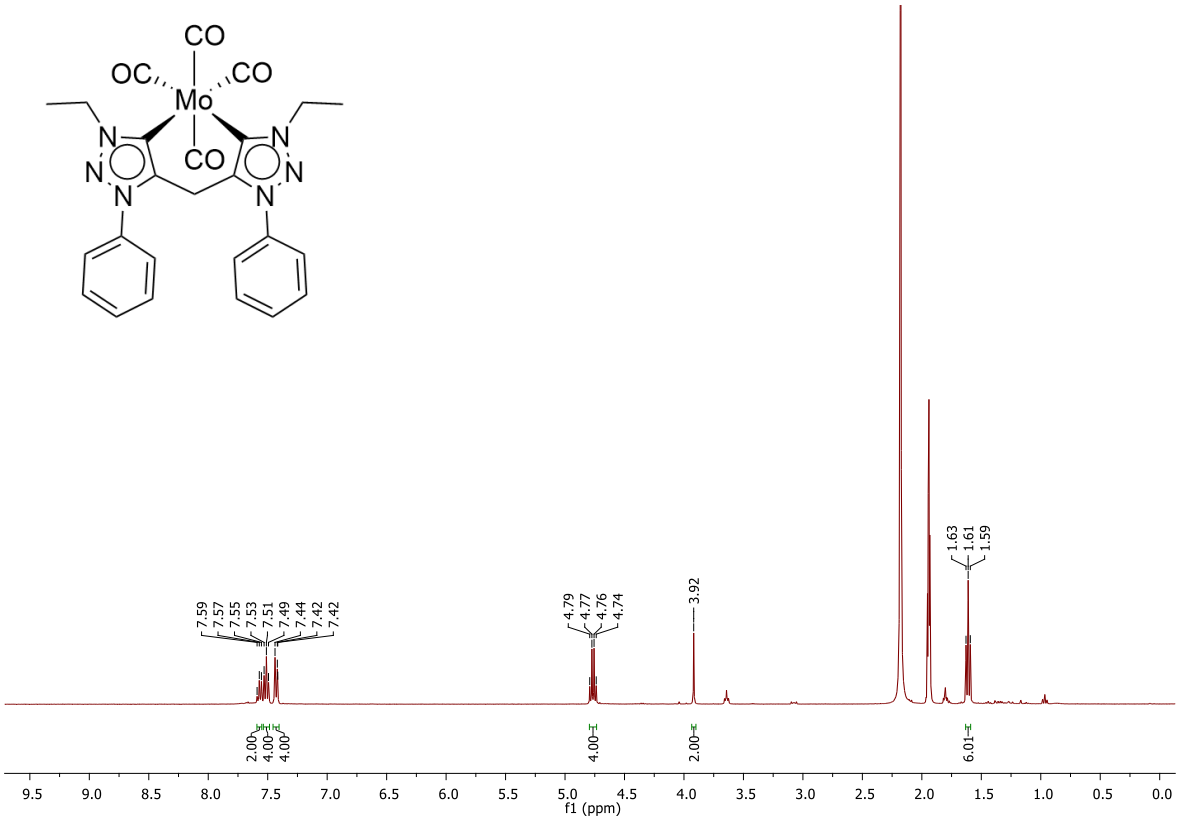

Figure A2.29. ^{1}H NMR spectrum in CD_3CN of **Mo5**.

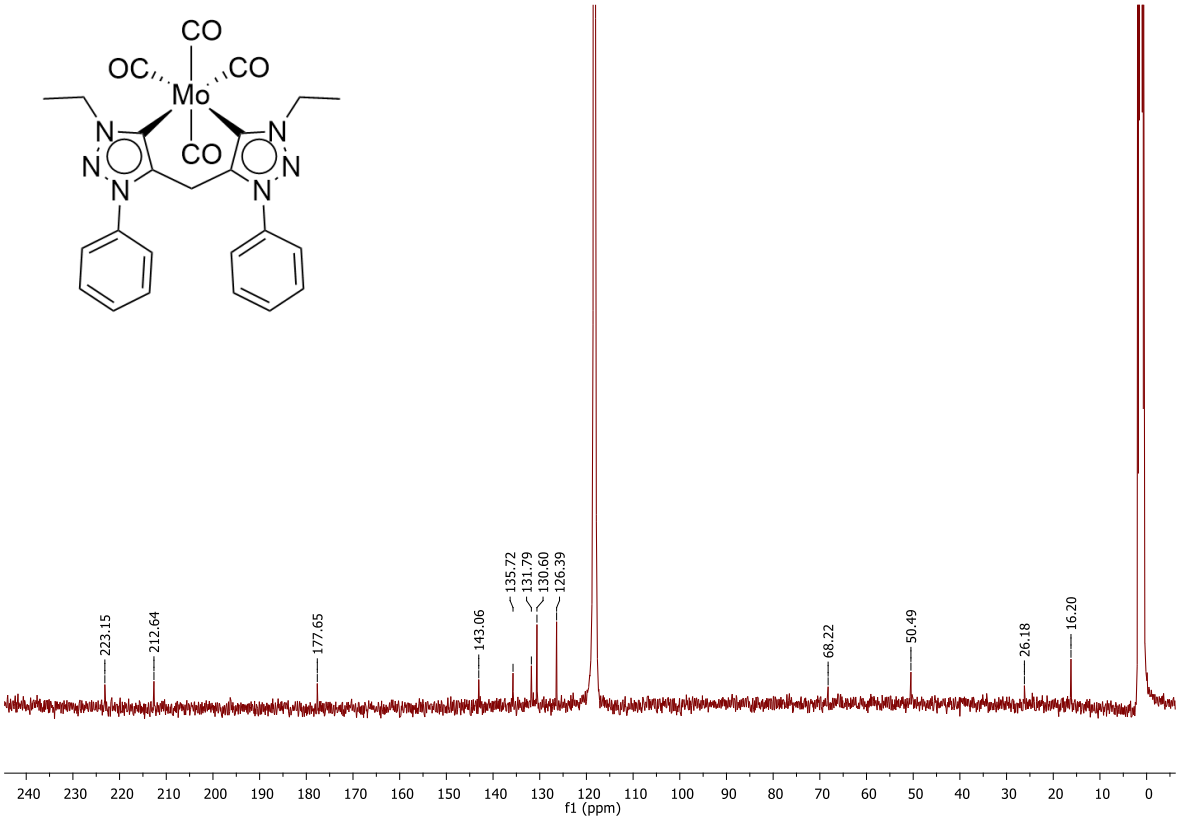

Figure A2.30. ^{13}C NMR spectrum in CD_3CN of **Mo5**.

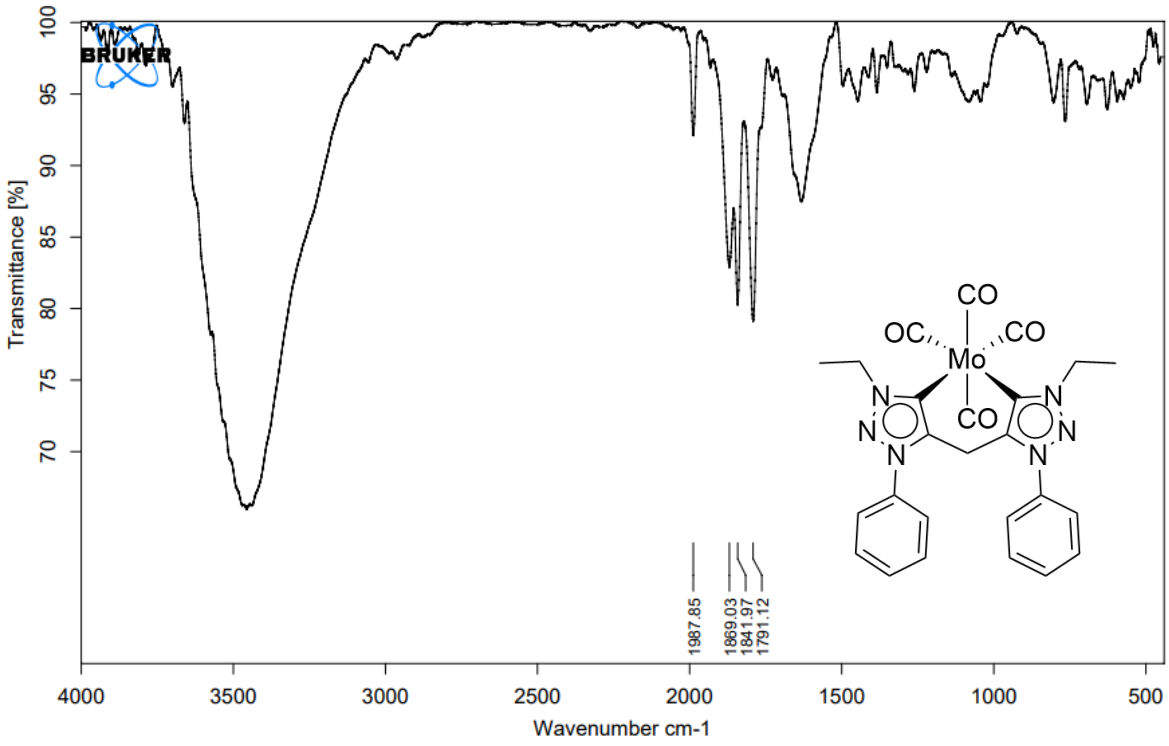

Figure A2.31. IR spectrum of **Mo5** in KBr.

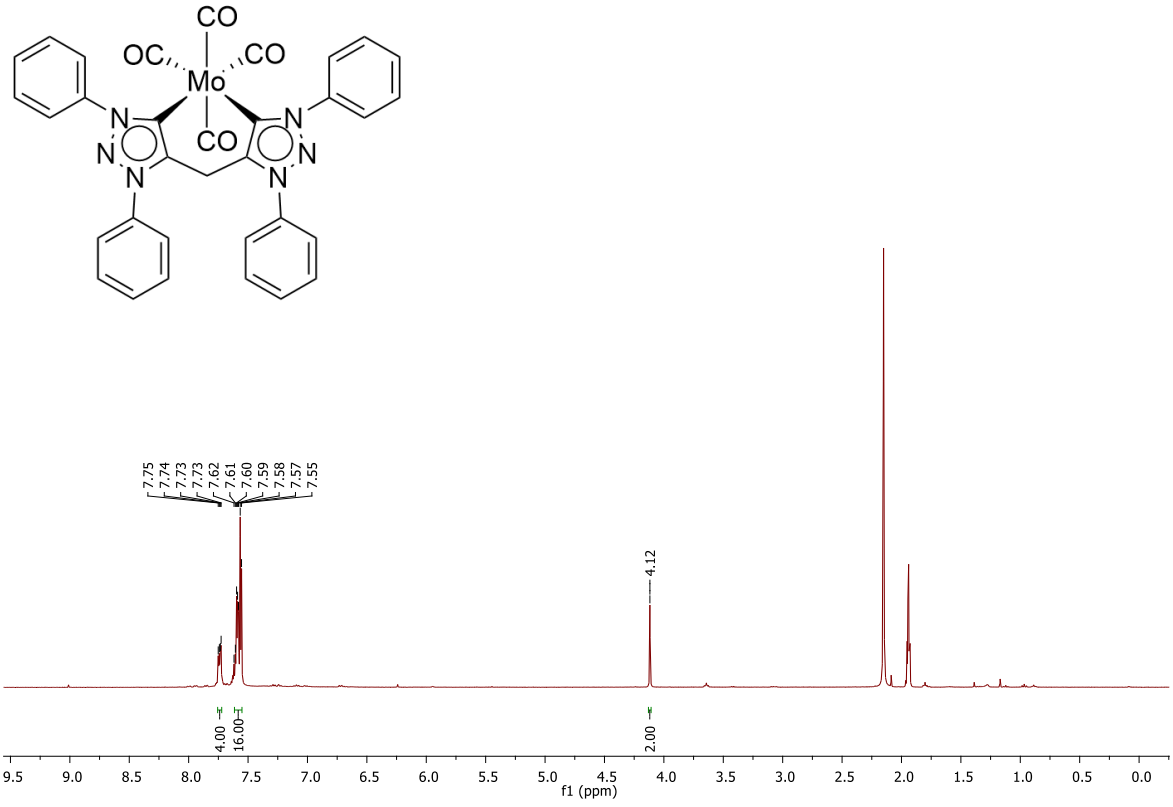

Figure A2.32. ^{1}H NMR spectrum in CD_3CN of **Mo6**.

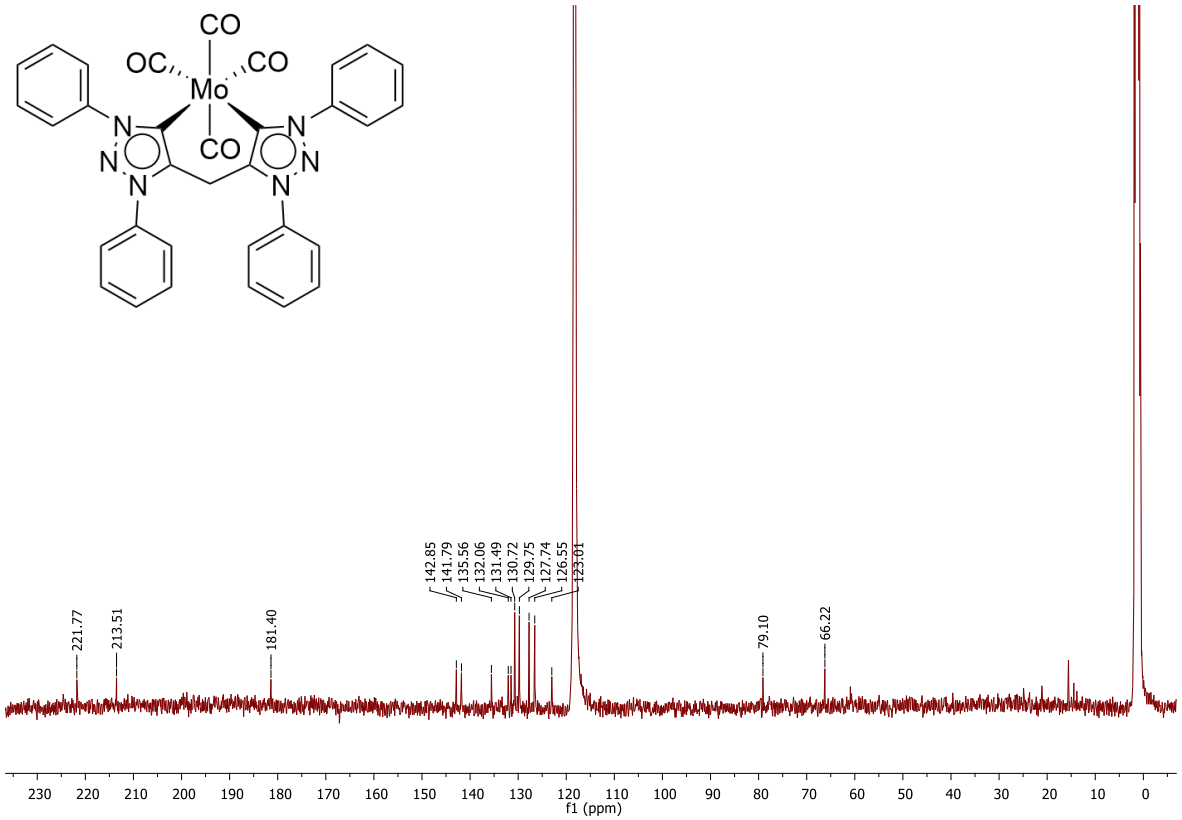

Figure A2.33. ^{13}C NMR spectrum in CD_3CN of **Mo6**.

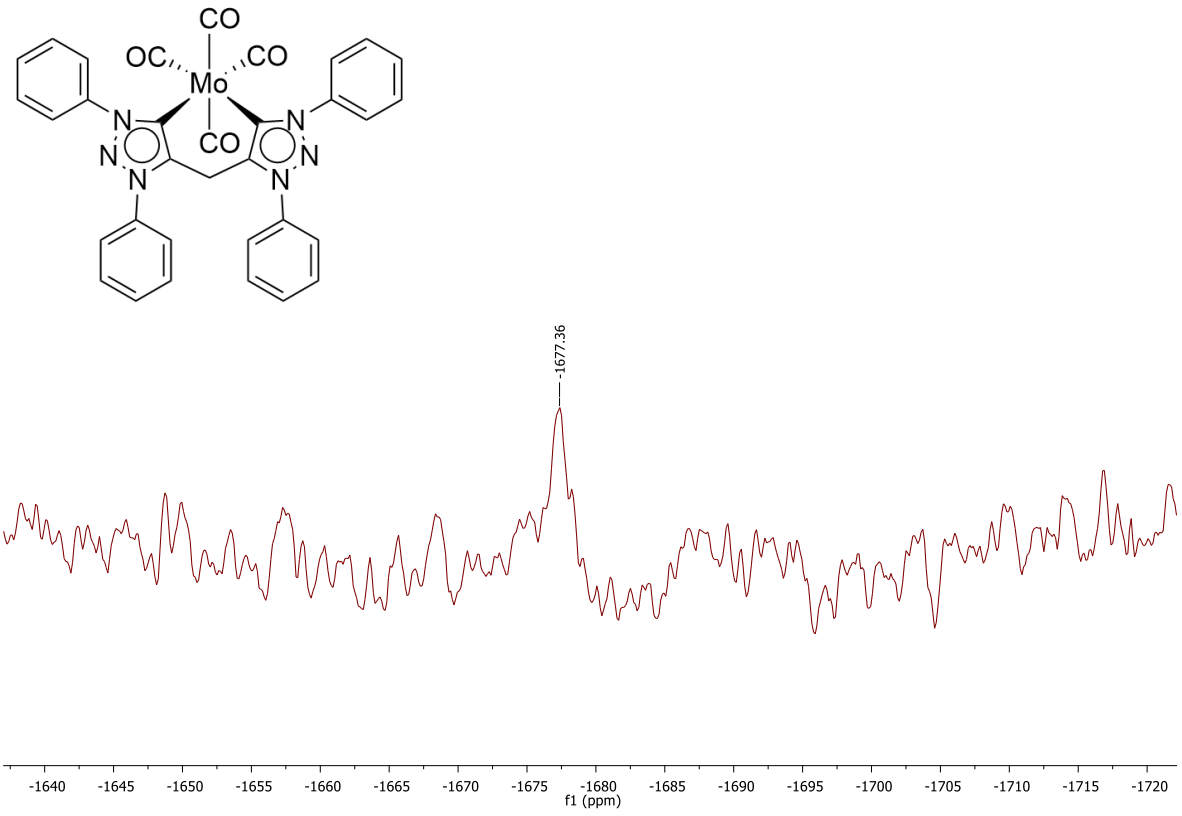

Figure A2.34. ^{95}Mo NMR spectrum in CD_3CN of **Mo6**.

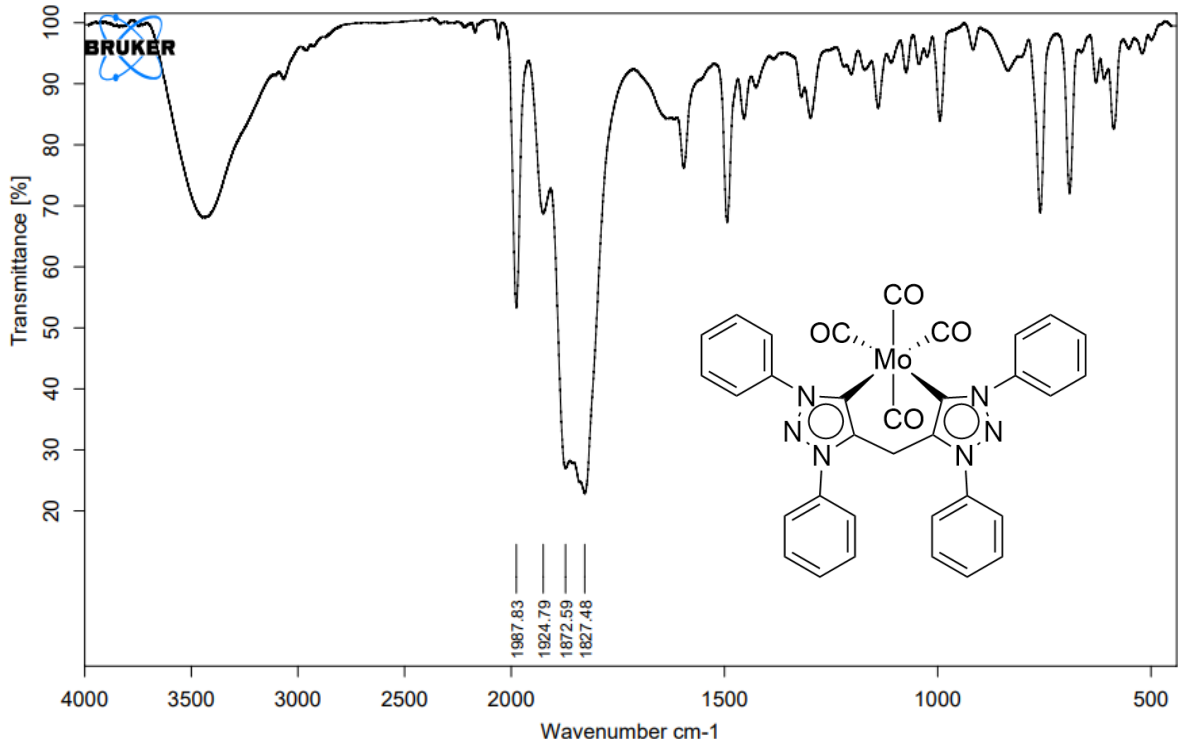

Figure A2.35. IR spectrum of **Mo6** in KBr.

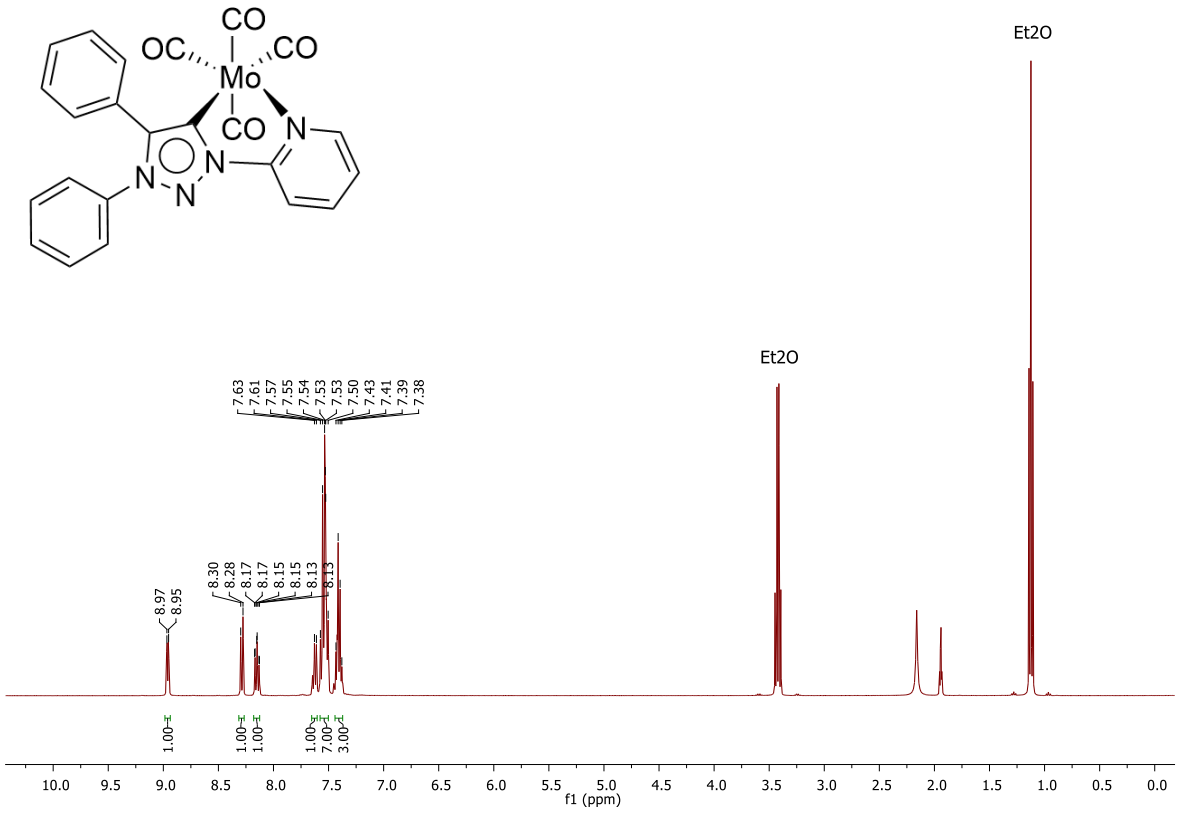

Figure A2.36. ^{1}H NMR spectrum in CD_3CN of **Mo7**.

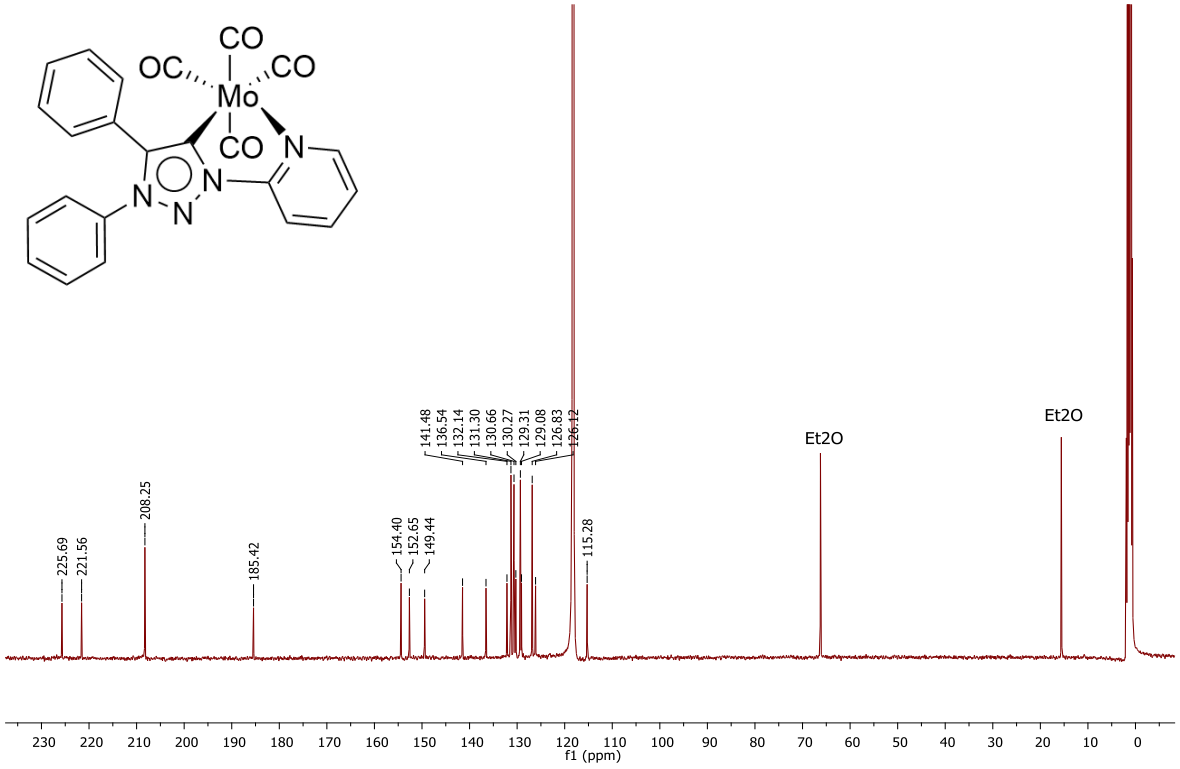

Figure A2.37. ^{13}C NMR spectrum in CD_3CN of **Mo7**.

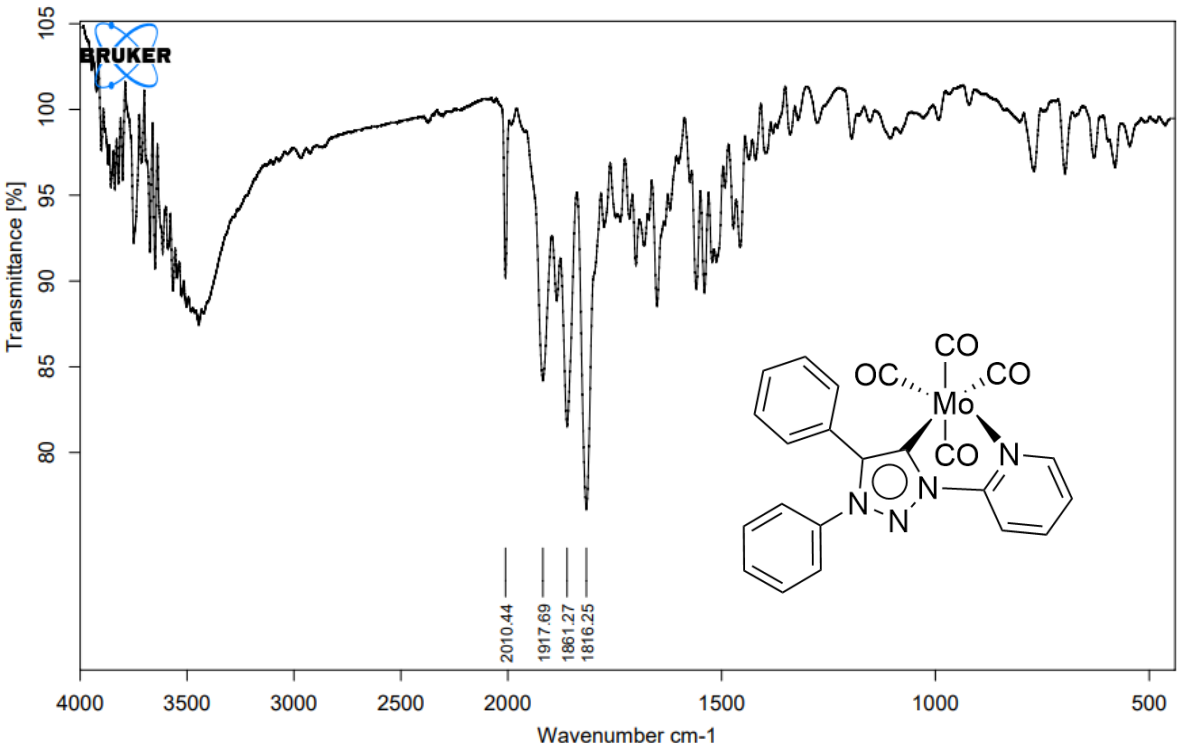

Figure A2.38. IR spectrum of **Mo7** in KBr.

A2.3. X-Ray Structure and Crystallographic Details of Complex **Mo7**

Table 1. Crystal data and structure refinement for the title compound.

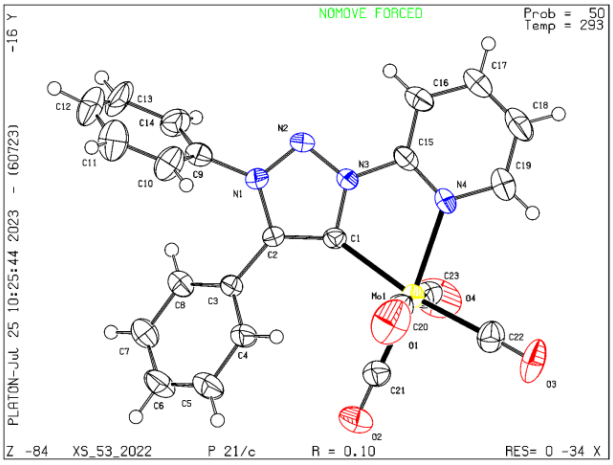

Empirical formula	C23 H14 Mo N4 O4	
Formula weight	506.32	
Temperature	293(2) K	
Wavelength	0.71073 Å	
Crystal system	Monoclinic	
Space group	P 21/c	
Unit cell dimensions	a = 9.4144(3) Å	α= 90°.
	b = 12.9795(5) Å	β= 101.8700(10)°.
	c = 22.3460(7) Å	γ = 90°.
Volume	2672.16(16) Å^3	
Z	4	
Density (calculated)	1.259 Mg/m^3	
Absorption coefficient	0.521 mm^{-1}	
F(000)	1016	
Crystal size	0.200 x 0.160 x 0.100 mm^3	
Theta range for data collection	2.581 to 28.305°.	
Index ranges	-12<=h<=12, -17<=k<=17, -29<=l<=29	
Reflections collected	185729	
Independent reflections	6644 [R(int) = 0.3724]	
Completeness to theta = 25.242°	99.8 %	
Refinement method	Full-matrix least-squares on F^2	
Data / restraints / parameters	6644 / 0 / 289	
Goodness-of-fit on F^2	1.172	
Final R indices [I>2sigma(I)]	R1 = 0.0985, wR2 = 0.2788	
R indices (all data)	R1 = 0.1815, wR2 = 0.3140	
Extinction coefficient	n/a	
Largest diff. peak and hole	3.093 and -1.019 e.Å^{-3}	

Table 2. Atomic coordinates (x 104) and equivalent isotropic displacement parameters (Å2x 103) for the title compound. U(eq) is defined as one third of the trace of the orthogonalized Uij tensor.

	x	y	z	U(eq)
C(1)	5782(6)	4502(5)	6452(2)	27(1)
C(2)	5490(6)	5375(5)	6083(3)	27(1)
C(3)	4091(6)	5732(5)	5722(3)	28(1)
C(4)	2882(7)	5637(7)	5963(3)	40(2)
C(5)	1496(8)	5881(8)	5623(4)	55(2)
C(6)	1379(8)	6244(8)	5039(4)	51(2)
C(7)	2586(9)	6378(7)	4787(3)	43(2)
C(8)	3951(7)	6115(6)	5124(3)	36(1)
C(9)	7028(7)	6858(6)	5843(3)	34(1)
C(10)	6509(11)	7731(7)	6076(4)	50(2)
C(11)	6744(13)	8678(8)	5831(4)	62(3)
C(12)	7551(13)	8710(7)	5373(4)	61(3)
C(13)	8019(13)	7859(9)	5141(5)	66(3)
C(14)	7775(9)	6888(7)	5376(4)	48(2)
C(15)	8072(7)	3882(6)	7062(3)	35(1)
C(16)	9573(8)	3909(8)	7215(4)	50(2)
C(17)	10272(10)	3154(9)	7602(5)	69(3)
C(18)	9488(11)	2443(10)	7825(5)	68(3)
C(19)	7965(10)	2436(8)	7644(4)	53(2)
C(20)	4208(9)	4160(7)	7471(3)	43(2)
C(21)	2789(8)	3276(6)	6426(4)	40(2)
C(22)	4242(10)	2003(7)	7339(4)	46(2)
C(23)	5152(9)	2146(7)	6208(4)	45(2)
N(1)	6778(6)	5881(5)	6107(2)	30(1)
N(2)	7888(5)	5413(5)	6459(2)	31(1)
N(3)	7259(5)	4595(4)	6652(2)	27(1)
N(4)	7260(6)	3174(5)	7257(3)	38(1)
O(1)	3732(11)	4669(8)	7791(4)	83(3)
O(2)	1583(7)	3340(6)	6188(3)	61(2)
O(3)	3877(10)	1359(7)	7605(4)	74(2)
O(4)	5261(10)	1516(8)	5863(4)	84(3)
Mo(1)	4819(1)	3184(1)	6857(1)	31(1)

Table 3. Bond lengths [Å] and angles [°] for the title compound.

C(1)-N(3)	1.376(7)	C(19)-N(4)	1.369(10)
C(1)-C(2)	1.394(8)	C(19)-H(19)	0.9300
C(1)-Mo(1)	2.215(6)	C(20)-O(1)	1.131(11)
C(2)-N(1)	1.370(7)	C(20)-Mo(1)	2.035(8)
C(2)-C(3)	1.471(8)	C(21)-O(2)	1.153(10)
C(3)-C(4)	1.361(9)	C(21)-Mo(1)	1.959(8)
C(3)-C(8)	1.406(9)	C(22)-O(3)	1.120(11)
C(4)-C(5)	1.405(9)	C(22)-Mo(1)	2.011(9)
C(4)-H(4)	0.9300	C(23)-O(4)	1.142(12)
C(5)-C(6)	1.370(13)	C(23)-Mo(1)	2.051(9)
C(5)-H(5)	0.9300	N(1)-N(2)	1.320(7)
C(6)-C(7)	1.380(12)	N(2)-N(3)	1.331(7)
C(6)-H(6)	0.9300	N(4)-Mo(1)	2.288(6)
C(7)-C(8)	1.392(9)		
C(7)-H(7)	0.9300	N(3)-C(1)-C(2)	100.6(5)
C(8)-H(8)	0.9300	N(3)-C(1)-Mo(1)	113.9(4)
C(9)-C(14)	1.375(11)	C(2)-C(1)-Mo(1)	145.3(4)
C(9)-C(10)	1.378(11)	N(1)-C(2)-C(1)	107.6(5)
C(9)-N(1)	1.438(9)	N(1)-C(2)-C(3)	123.7(6)
C(10)-C(11)	1.382(13)	C(1)-C(2)-C(3)	128.7(5)
C(10)-H(10)	0.9300	C(4)-C(3)-C(8)	119.0(6)
C(11)-C(12)	1.395(15)	C(4)-C(3)-C(2)	118.8(6)
C(11)-H(11)	0.9300	C(8)-C(3)-C(2)	122.1(6)
C(12)-C(13)	1.333(16)	C(3)-C(4)-C(5)	121.7(7)
C(12)-H(12)	0.9300	C(3)-C(4)-H(4)	119.2
C(13)-C(14)	1.403(12)	C(5)-C(4)-H(4)	119.2
C(13)-H(13)	0.9300	C(6)-C(5)-C(4)	118.4(8)
C(14)-H(14)	0.9300	C(6)-C(5)-H(5)	120.8
C(15)-N(4)	1.325(9)	C(4)-C(5)-H(5)	120.8
C(15)-C(16)	1.384(9)	C(5)-C(6)-C(7)	121.4(7)
C(15)-N(3)	1.410(8)	C(5)-C(6)-H(6)	119.3
C(16)-C(17)	1.381(12)	C(7)-C(6)-H(6)	119.3
C(16)-H(16)	0.9300	C(6)-C(7)-C(8)	119.6(7)
C(17)-C(18)	1.340(15)	C(6)-C(7)-H(7)	120.2
C(17)-H(17)	0.9300	C(8)-C(7)-H(7)	120.2
C(18)-C(19)	1.407(12)	C(7)-C(8)-C(3)	119.8(7)
C(18)-H(18)	0.9300	C(7)-C(8)-H(8)	120.1

C(3)-C(8)-H(8)	120.1	N(4)-C(19)-H(19)	119.7
C(14)-C(9)-C(10)	122.7(8)	C(18)-C(19)-H(19)	119.7
C(14)-C(9)-N(1)	119.3(7)	O(1)-C(20)-Mo(1)	173.2(8)
C(10)-C(9)-N(1)	118.0(7)	O(2)-C(21)-Mo(1)	178.0(8)
C(9)-C(10)-C(11)	118.9(8)	O(3)-C(22)-Mo(1)	177.7(9)
C(9)-C(10)-H(10)	120.6	O(4)-C(23)-Mo(1)	174.5(9)
C(11)-C(10)-H(10)	120.6	N(2)-N(1)-C(2)	112.9(5)
C(10)-C(11)-C(12)	118.3(9)	N(2)-N(1)-C(9)	118.3(5)
C(10)-C(11)-H(11)	120.8	C(2)-N(1)-C(9)	128.7(5)
C(12)-C(11)-H(11)	120.8	N(1)-N(2)-N(3)	102.1(5)
C(13)-C(12)-C(11)	122.2(9)	N(2)-N(3)-C(1)	116.9(5)
C(13)-C(12)-H(12)	118.9	N(2)-N(3)-C(15)	121.0(5)
C(11)-C(12)-H(12)	118.9	C(1)-N(3)-C(15)	122.1(6)
C(12)-C(13)-C(14)	120.5(9)	C(15)-N(4)-C(19)	117.2(7)
C(12)-C(13)-H(13)	119.8	C(15)-N(4)-Mo(1)	117.9(4)
C(14)-C(13)-H(13)	119.8	C(19)-N(4)-Mo(1)	124.6(6)
C(9)-C(14)-C(13)	117.3(9)	C(21)-Mo(1)-C(22)	88.0(3)
C(9)-C(14)-H(14)	121.4	C(21)-Mo(1)-C(20)	84.9(3)
C(13)-C(14)-H(14)	121.4	C(22)-Mo(1)-C(20)	88.2(4)
N(4)-C(15)-C(16)	124.3(7)	C(21)-Mo(1)-C(23)	88.2(3)
N(4)-C(15)-N(3)	113.3(5)	C(22)-Mo(1)-C(23)	88.6(4)
C(16)-C(15)-N(3)	122.3(7)	C(20)-Mo(1)-C(23)	172.4(3)
C(17)-C(16)-C(15)	118.0(9)	C(21)-Mo(1)-C(1)	101.0(3)
C(17)-C(16)-H(16)	121.0	C(22)-Mo(1)-C(1)	170.4(3)
C(15)-C(16)-H(16)	121.0	C(20)-Mo(1)-C(1)	89.5(3)
C(18)-C(17)-C(16)	119.5(8)	C(23)-Mo(1)-C(1)	94.8(3)
C(18)-C(17)-H(17)	120.2	C(21)-Mo(1)-N(4)	172.9(3)
C(16)-C(17)-H(17)	120.2	C(22)-Mo(1)-N(4)	98.5(3)
C(17)-C(18)-C(19)	120.4(9)	C(20)-Mo(1)-N(4)	98.1(3)
C(17)-C(18)-H(18)	119.8	C(23)-Mo(1)-N(4)	89.2(3)
C(19)-C(18)-H(18)	119.8	C(1)-Mo(1)-N(4)	72.6(2)
N(4)-C(19)-C(18)	120.6(9)		

Table 4. Torsion angles [°] for the title compound.

N(3)-C(1)-C(2)-N(1)	-0.5(6)	N(3)-C(1)-C(2)-C(3)	179.4(6)
Mo(1)-C(1)-C(2)-N(1)	173.4(6)	Mo(1)-C(1)-C(2)-C(3)	-6.8(12)
N(1)-C(2)-C(3)-C(4)	-140.9(7)	C(3)-C(2)-N(1)-N(2)	-179.8(6)
C(1)-C(2)-C(3)-C(4)	39.3(10)	C(1)-C(2)-N(1)-C(9)	-174.8(6)
N(1)-C(2)-C(3)-C(8)	42.6(10)	C(3)-C(2)-N(1)-C(9)	5.4(10)
C(1)-C(2)-C(3)-C(8)	-137.2(7)	C(14)-C(9)-N(1)-N(2)	72.5(9)
C(8)-C(3)-C(4)-C(5)	2.0(12)	C(10)-C(9)-N(1)-N(2)	-107.2(8)
C(2)-C(3)-C(4)-C(5)	-174.6(8)	C(14)-C(9)-N(1)-C(2)	-112.9(8)
C(3)-C(4)-C(5)-C(6)	-1.4(15)	C(10)-C(9)-N(1)-C(2)	67.4(9)
C(4)-C(5)-C(6)-C(7)	-0.4(16)	C(2)-N(1)-N(2)-N(3)	0.4(7)
C(5)-C(6)-C(7)-C(8)	1.6(15)	C(9)-N(1)-N(2)-N(3)	175.8(5)
C(6)-C(7)-C(8)-C(3)	-1.0(12)	N(1)-N(2)-N(3)-C(1)	-0.7(7)
C(4)-C(3)-C(8)-C(7)	-0.8(11)	N(1)-N(2)-N(3)-C(15)	-178.5(6)
C(2)-C(3)-C(8)-C(7)	175.7(7)	C(2)-C(1)-N(3)-N(2)	0.8(7)
C(14)-C(9)-C(10)-C(11)	0.0(13)	Mo(1)-C(1)-N(3)-N(2)	-175.4(4)
N(1)-C(9)-C(10)-C(11)	179.7(8)	C(2)-C(1)-N(3)-C(15)	178.5(6)
C(9)-C(10)-C(11)-C(12)	-2.5(15)	Mo(1)-C(1)-N(3)-C(15)	2.3(8)
C(10)-C(11)-C(12)-C(13)	4.2(17)	N(4)-C(15)-N(3)-N(2)	173.4(6)
C(11)-C(12)-C(13)-C(14)	-3.3(17)	C(16)-C(15)-N(3)-N(2)	-9.3(11)
C(10)-C(9)-C(14)-C(13)	0.9(13)	N(4)-C(15)-N(3)-C(1)	-4.2(9)
N(1)-C(9)-C(14)-C(13)	-178.7(7)	C(16)-C(15)-N(3)-C(1)	173.0(7)
C(12)-C(13)-C(14)-C(9)	0.7(15)	C(16)-C(15)-N(4)-C(19)	1.2(12)
N(4)-C(15)-C(16)-C(17)	-0.7(14)	N(3)-C(15)-N(4)-C(19)	178.4(7)
N(3)-C(15)-C(16)-C(17)	-177.6(9)	C(16)-C(15)-N(4)-Mo(1)	-173.2(6)
C(15)-C(16)-C(17)-C(18)	-1.4(18)	N(3)-C(15)-N(4)-Mo(1)	3.9(8)
C(16)-C(17)-C(18)-C(19)	3(2)	C(18)-C(19)-N(4)-C(15)	0.3(14)
C(17)-C(18)-C(19)-N(4)	-2.3(18)	C(18)-C(19)-N(4)-Mo(1)	174.3(8)
C(1)-C(2)-N(1)-N(2)	0.1(8)		

Chapter 3 - Annex

Catalytic Application of Molybdenum(0) Triazolylidene Complexes in Borrowing Hydrogen (BH) and Acceptorless Dehydrogenative Coupling (ADC) Reactions

A3.1. Characterization of Quinolines

A3.2. NMR data of the *N*-Alkylation of Amines with Alcohols

A3.3. NMR data of the α-Alkylation of Ketones with Alcohols

A3.4. NMR data of the β-Alkylation Between Alcohols

A3.5. NMR data of the Aerobic Oxidation of Primary Amines to Amides

A3.1. Characterization of Quinolines

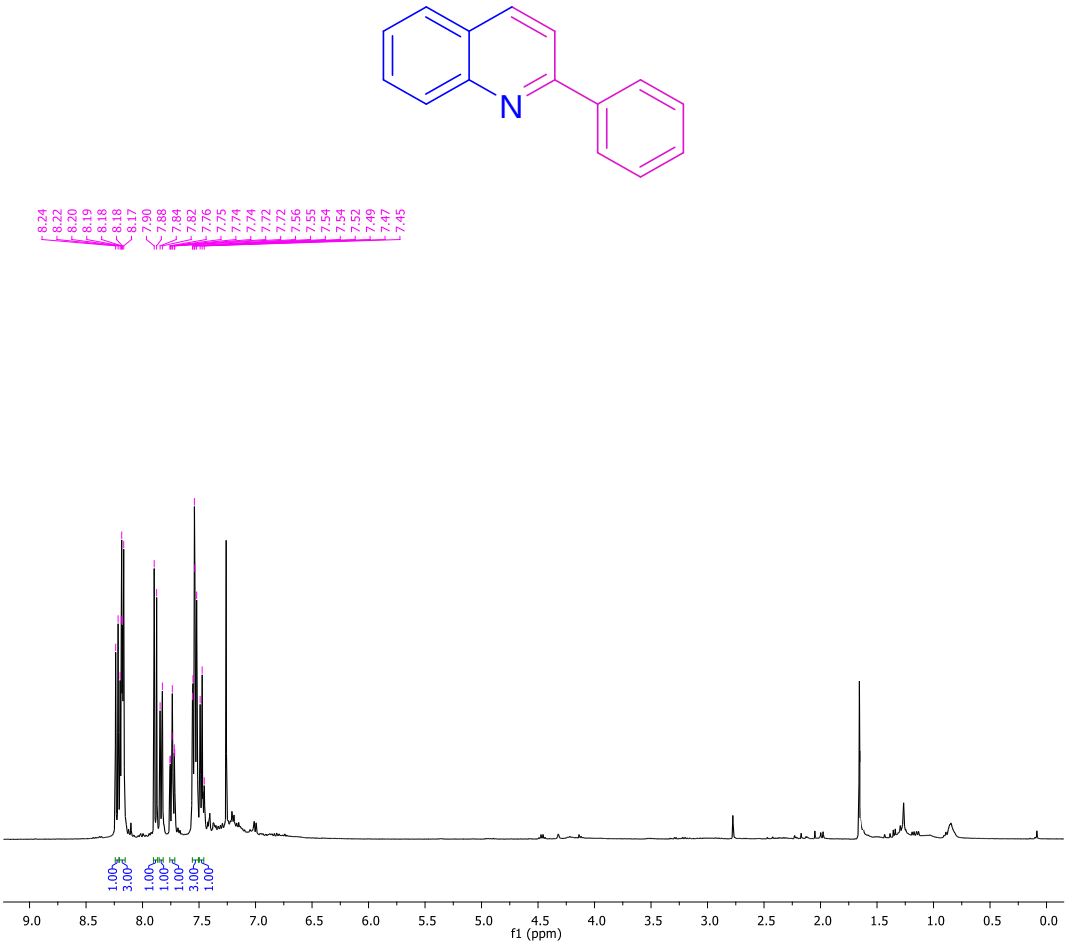

Figure A3.1. ^{1}H NMR spectrum of the compound **3a** in $CDCl_3$.

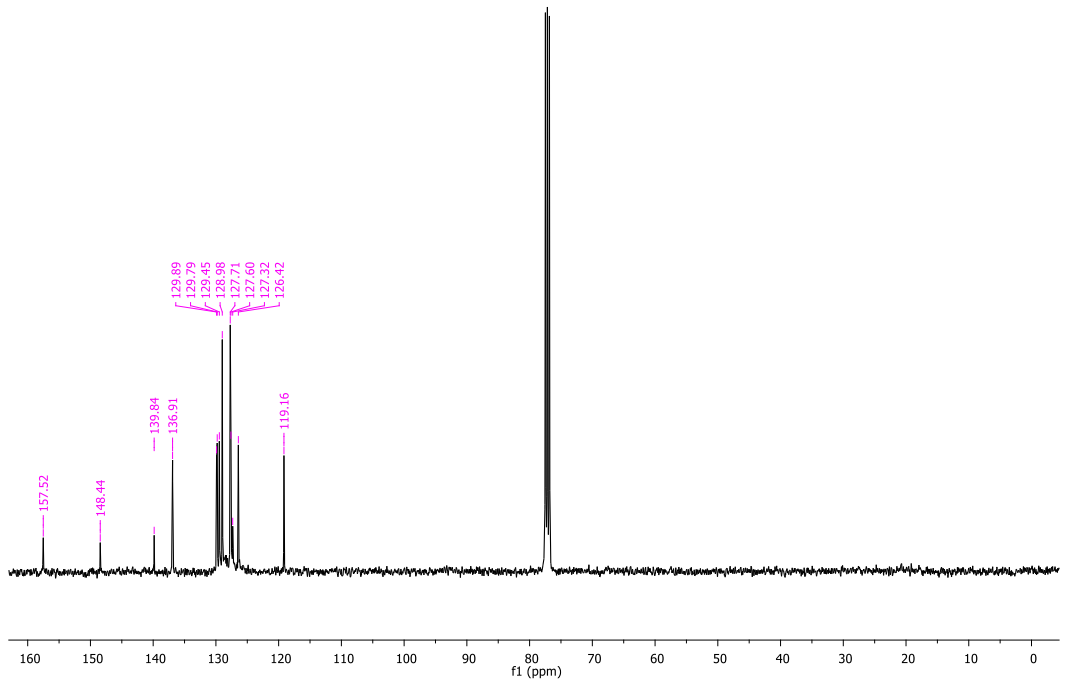

Figure A3.2. ^{13}C NMR spectrum of the compound **3a** in $CDCl_3$.

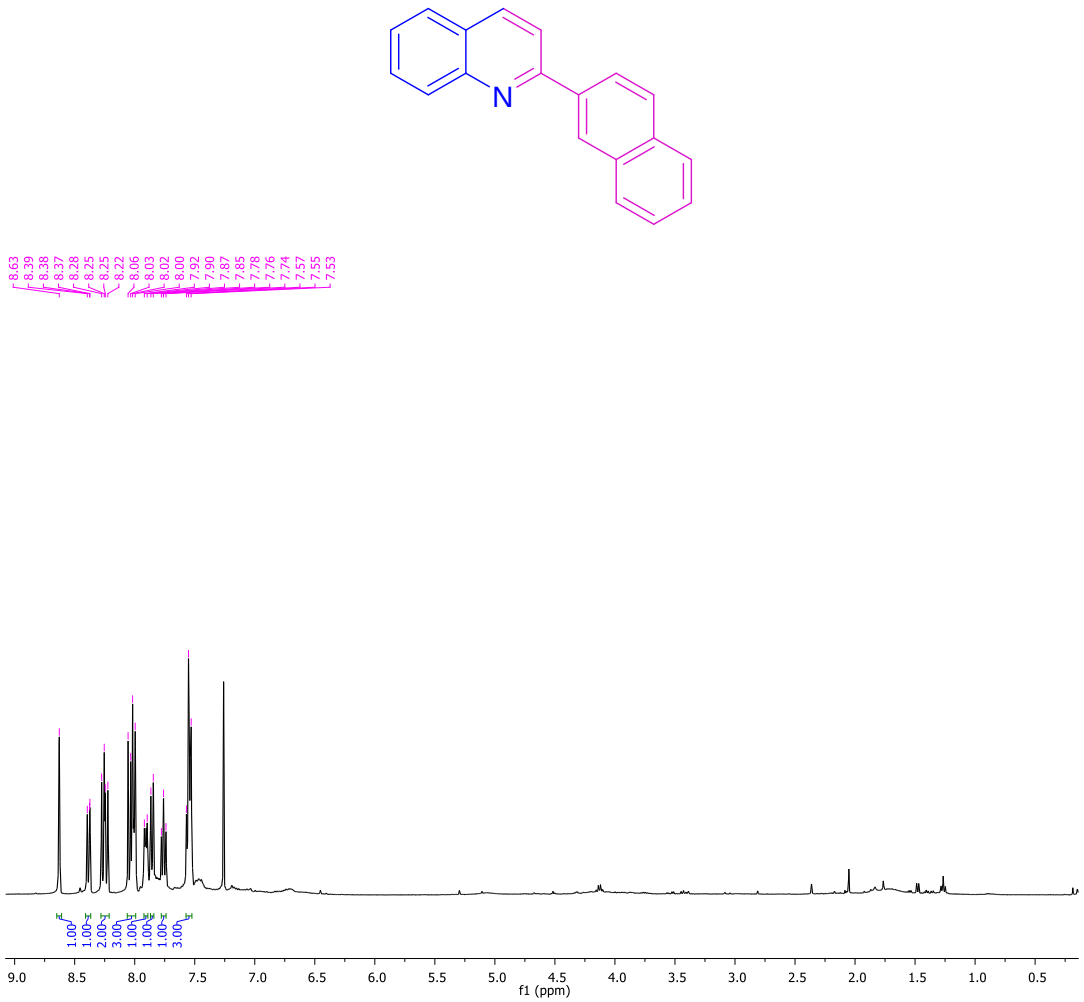

Figure A3.3. ^{1}H NMR spectrum of the compound **3b** in $CDCl_3$.

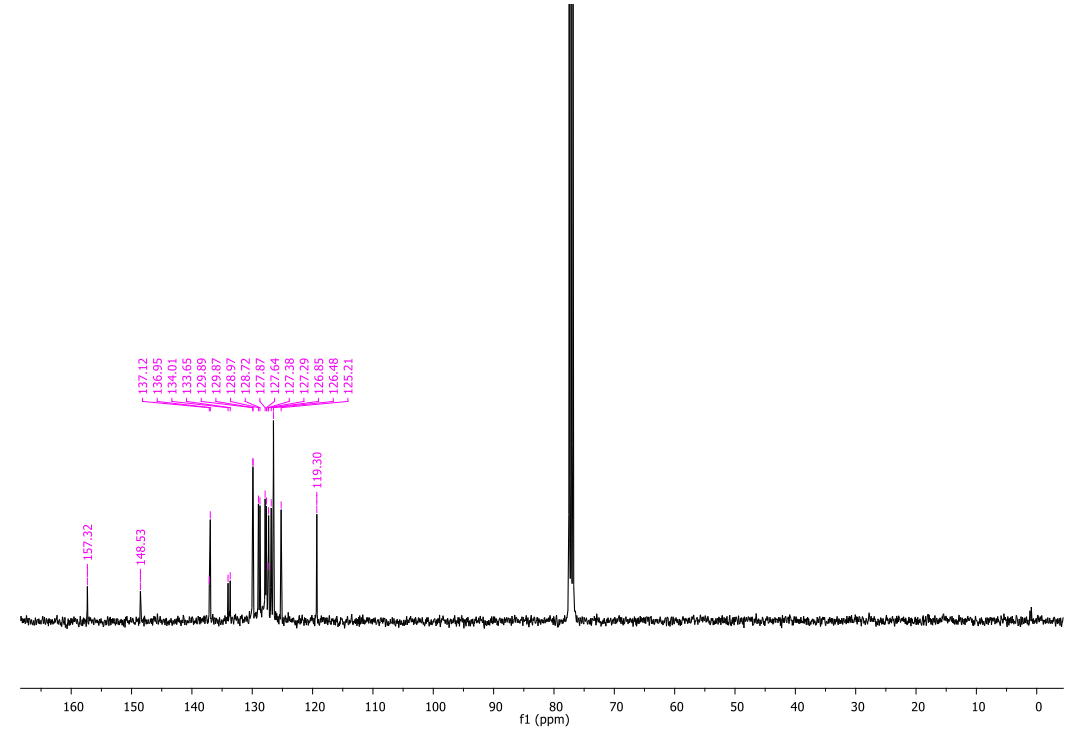

Figure A3.4. ^{13}C NMR spectrum of the compound **3b** in $CDCl_3$.

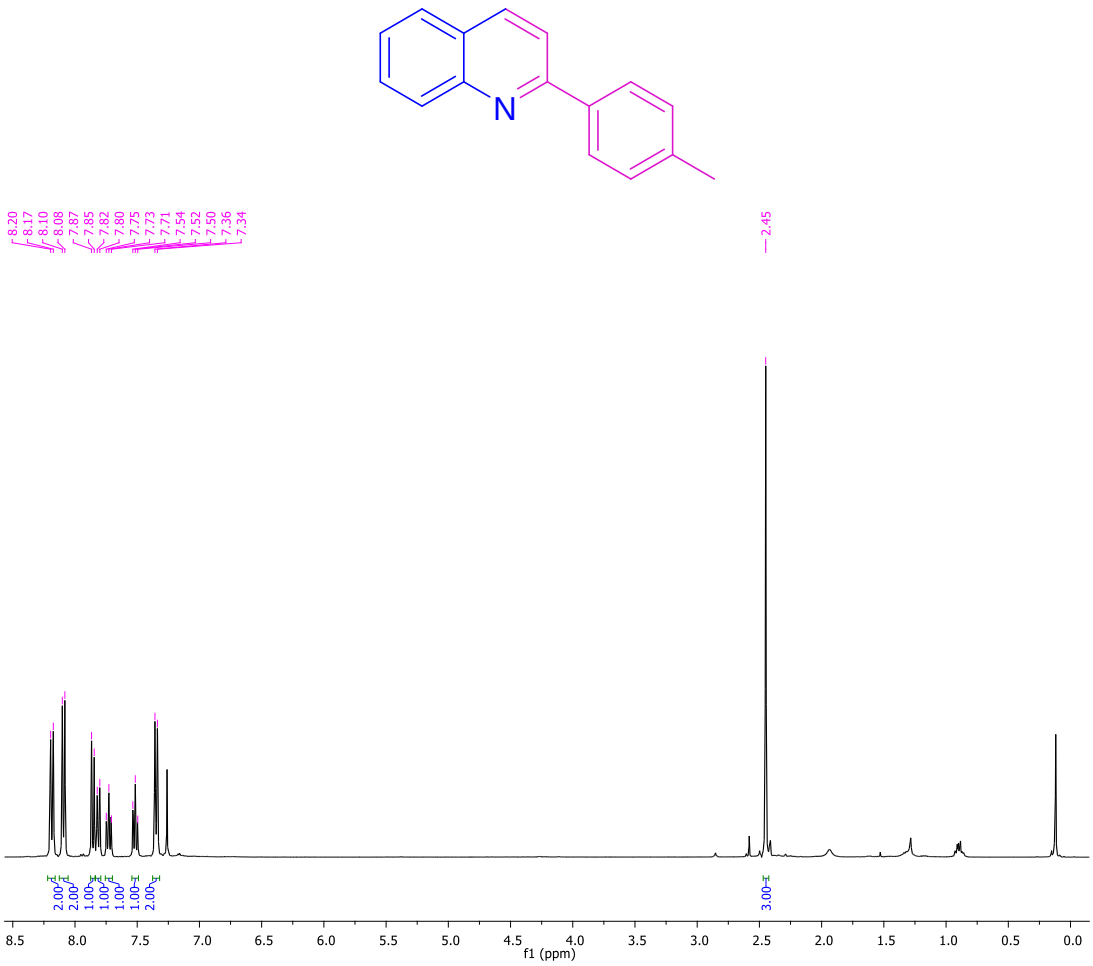

Figure A3.5. ^{1}H NMR spectrum of the compound **3c** in $CDCl_3$.

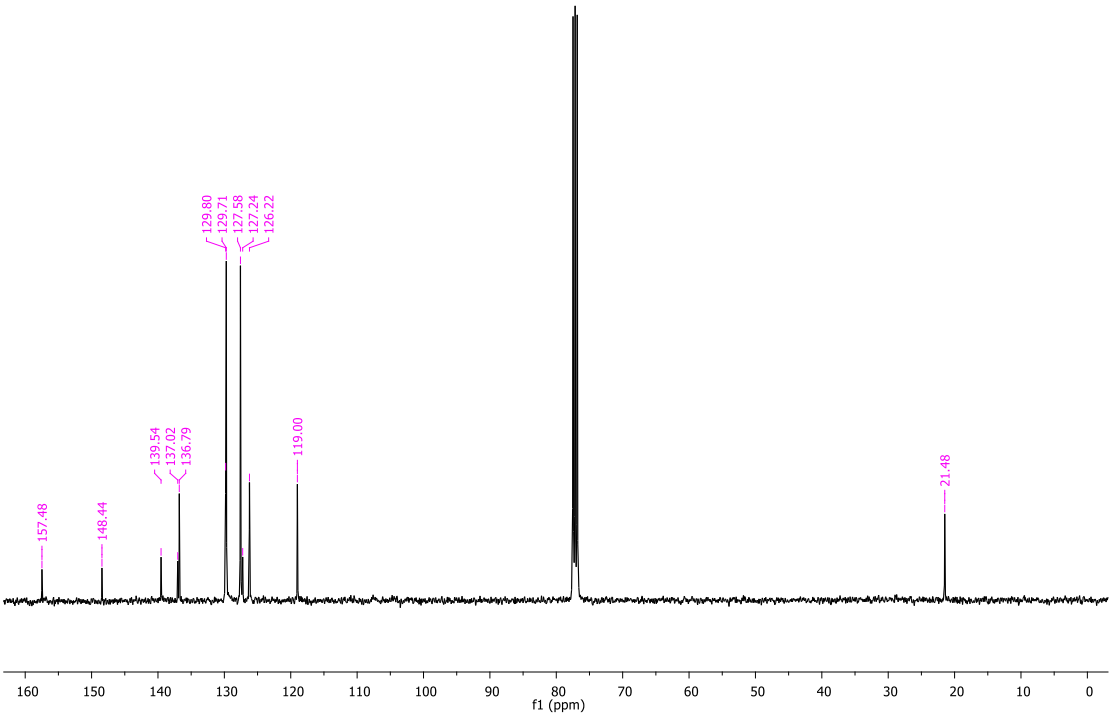

Figure A3.6. ^{13}C NMR spectrum of the compound **3c** in $CDCl_3$.

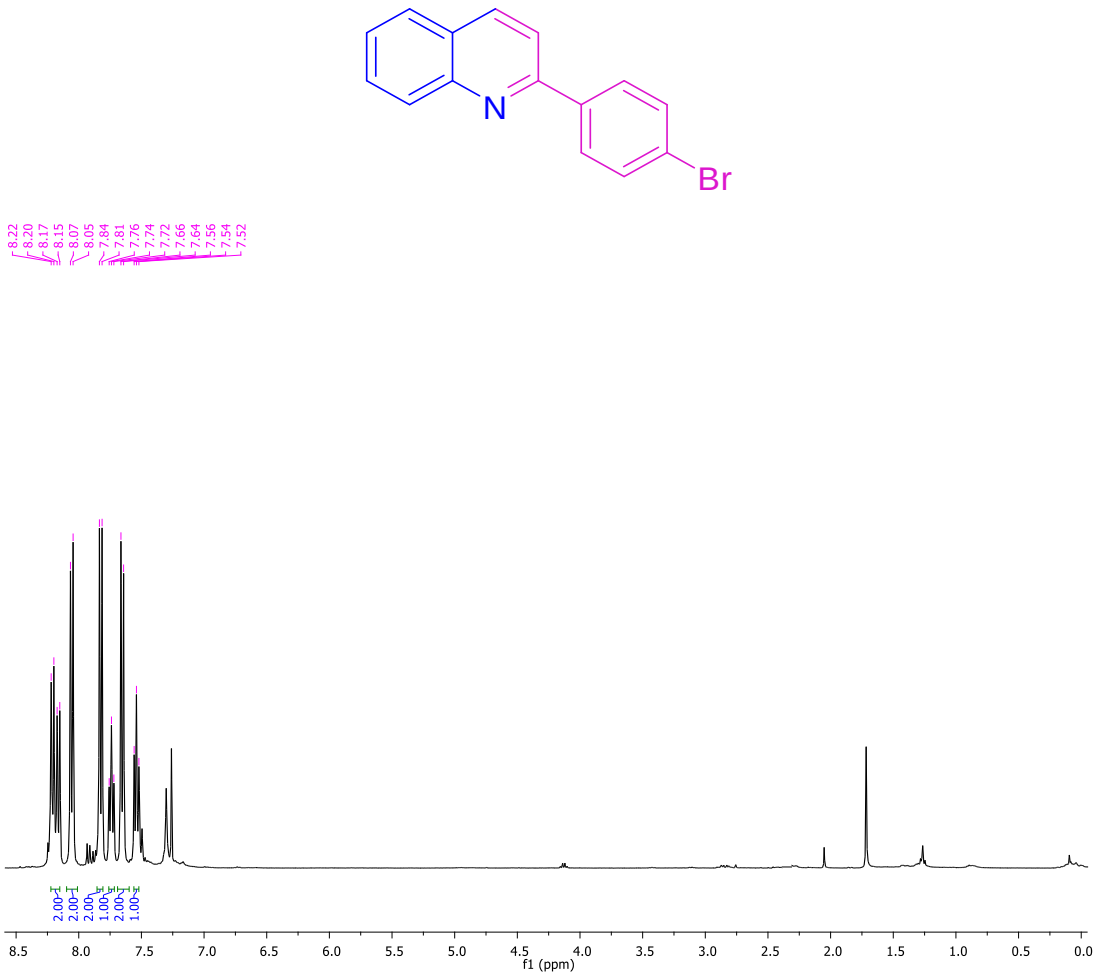

Figure A3.7. ^{1}H NMR spectrum of the compound **3d** in $CDCl_3$.

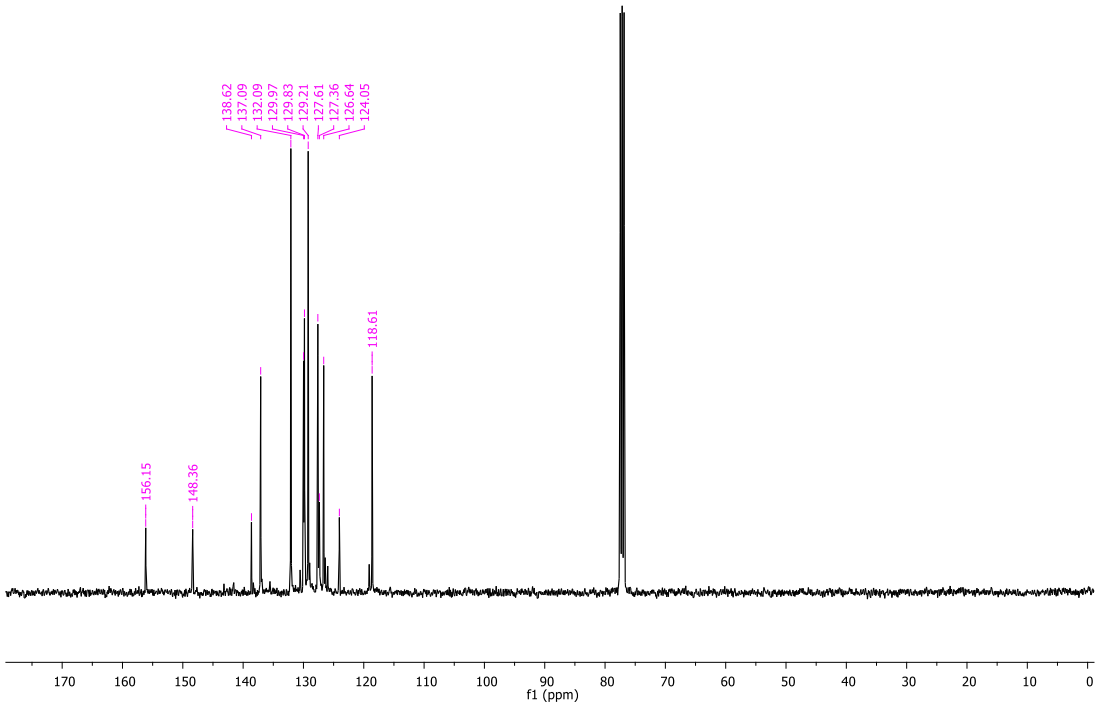

Figure A3.8. ^{13}C NMR spectrum of the compound **3d** in $CDCl_3$.

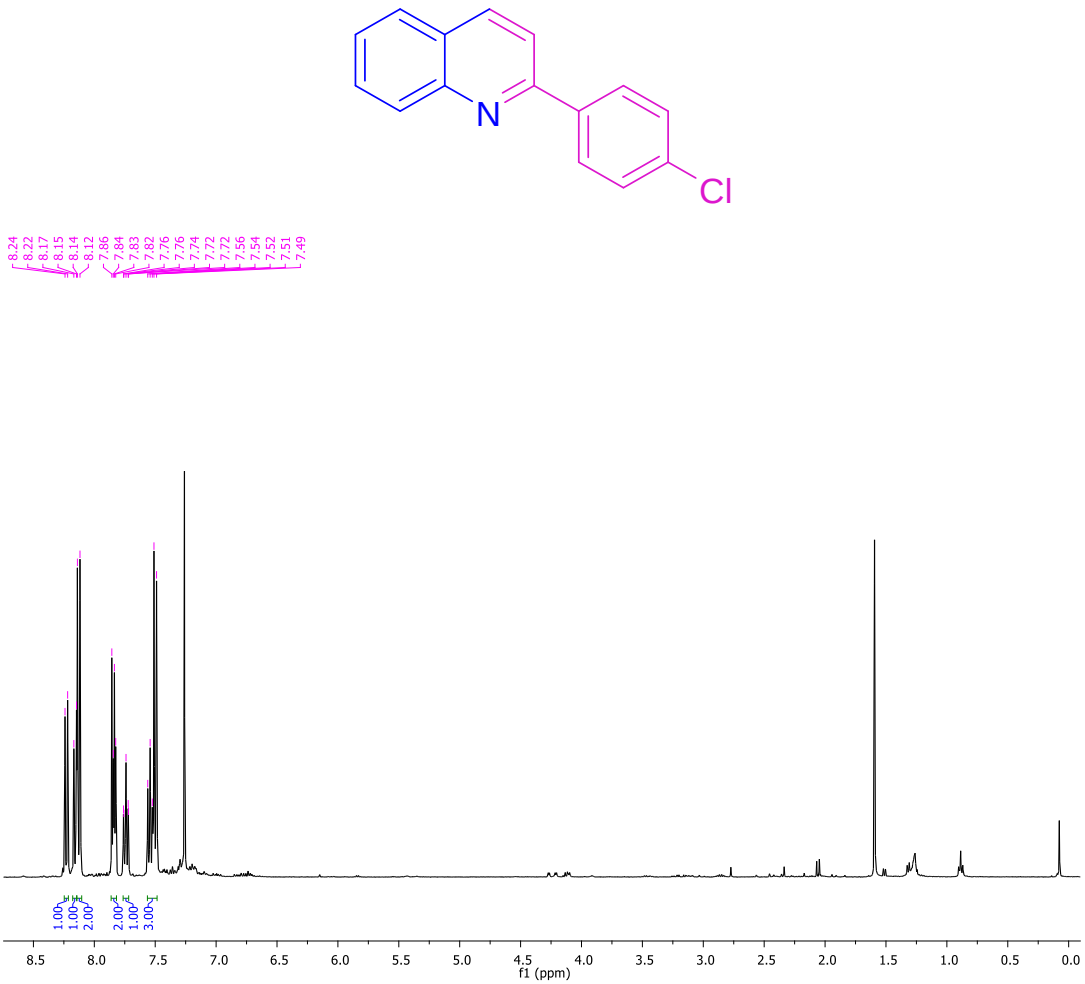

Figure A3.9. ^{1}H NMR spectrum of the compound **3e** in $CDCl_3$.

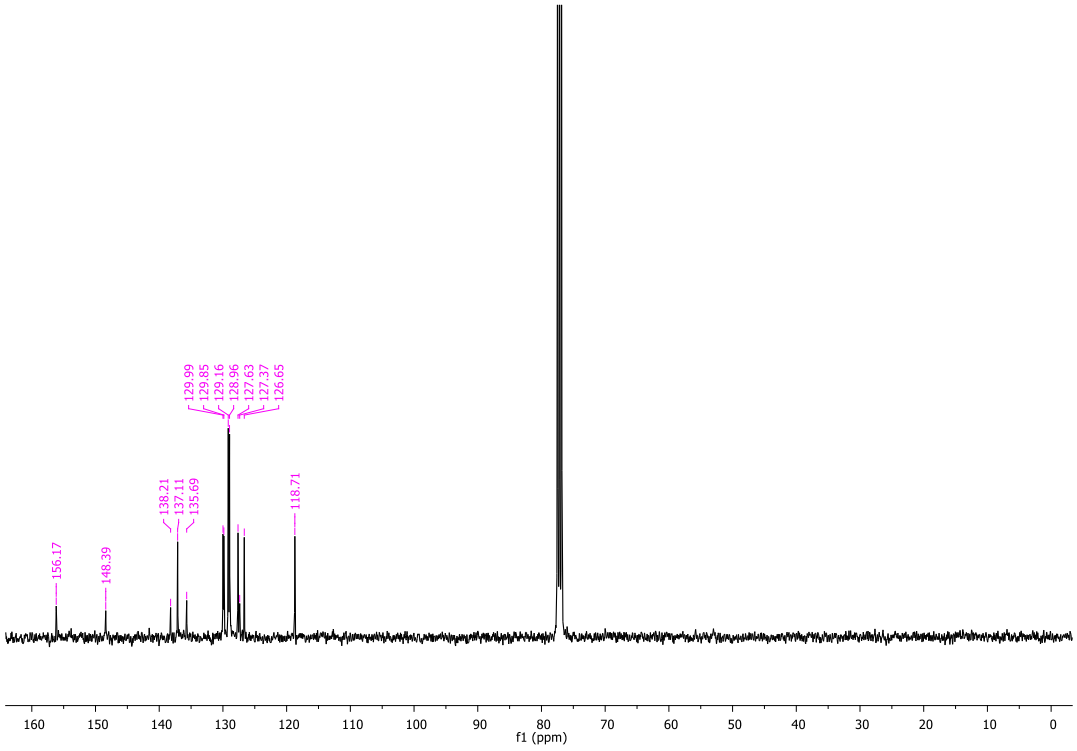

Figure A3.10. ^{13}C NMR spectrum of the compound **3e** in $CDCl_3$.

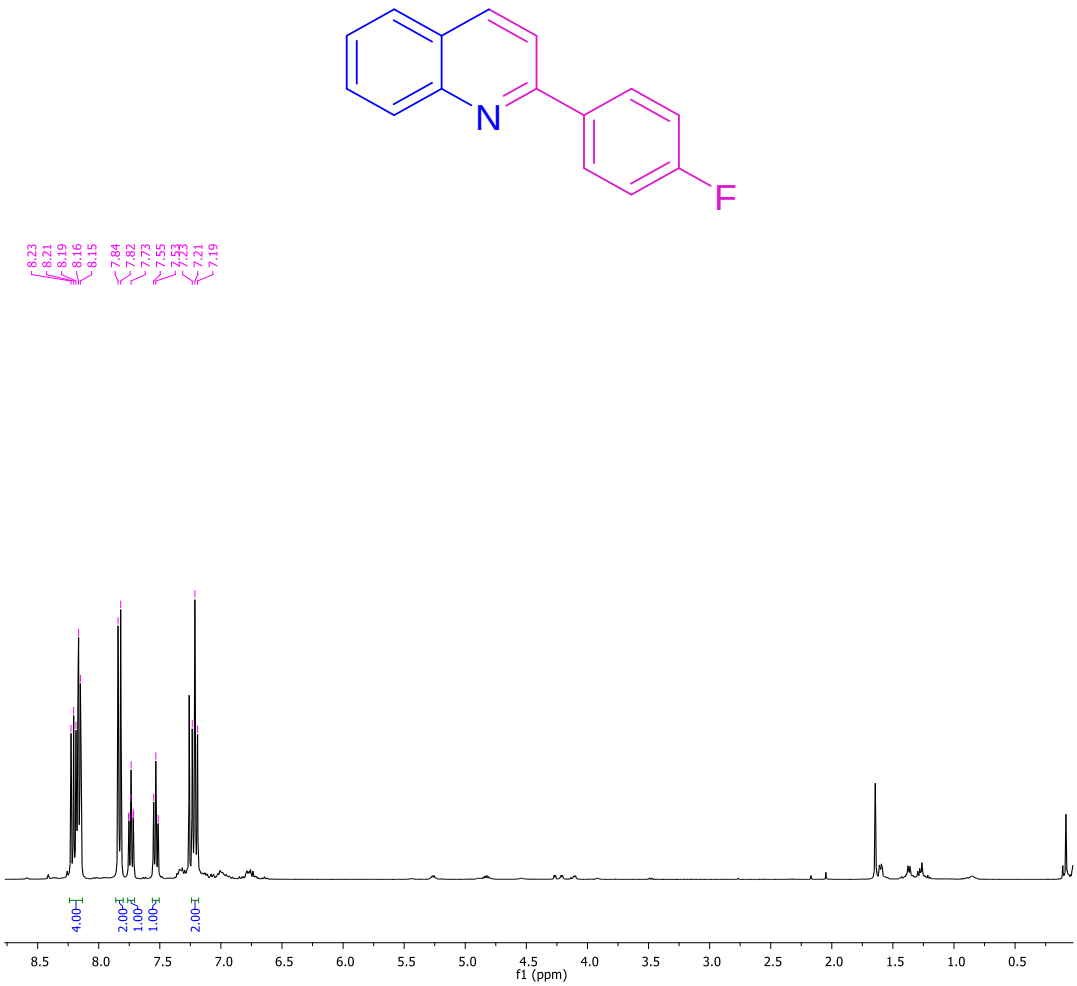

Figure A3.11. ^{1}H NMR spectrum of the compound **3f** in $CDCl_3$.

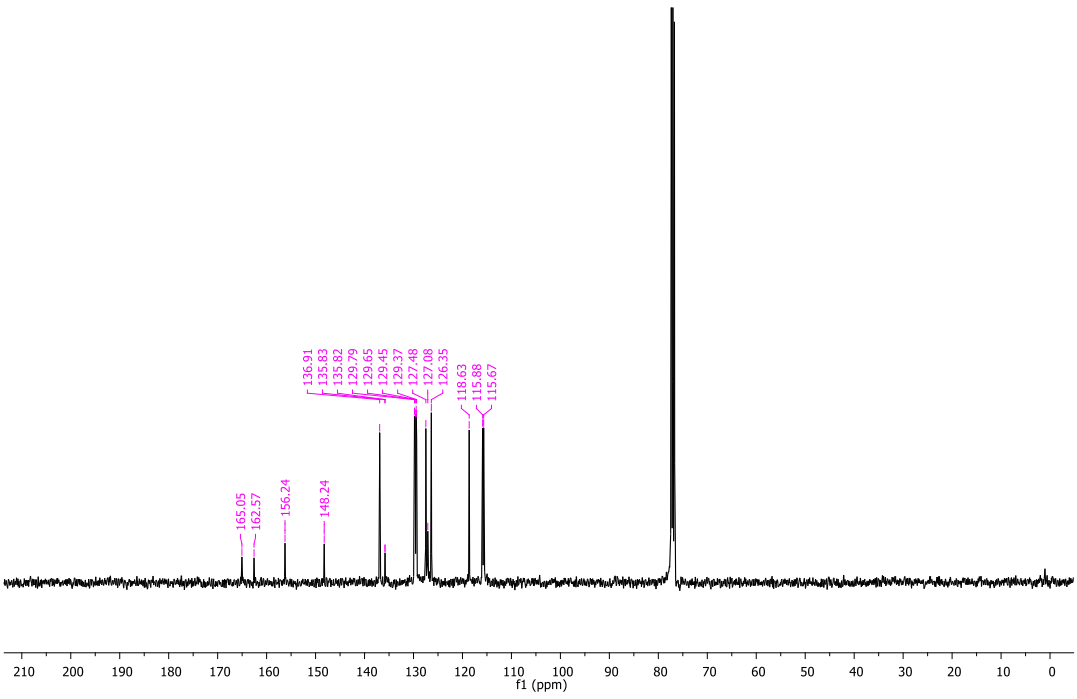

Figure A3.12. ^{13}C NMR spectrum of the compound **3f** in $CDCl_3$.

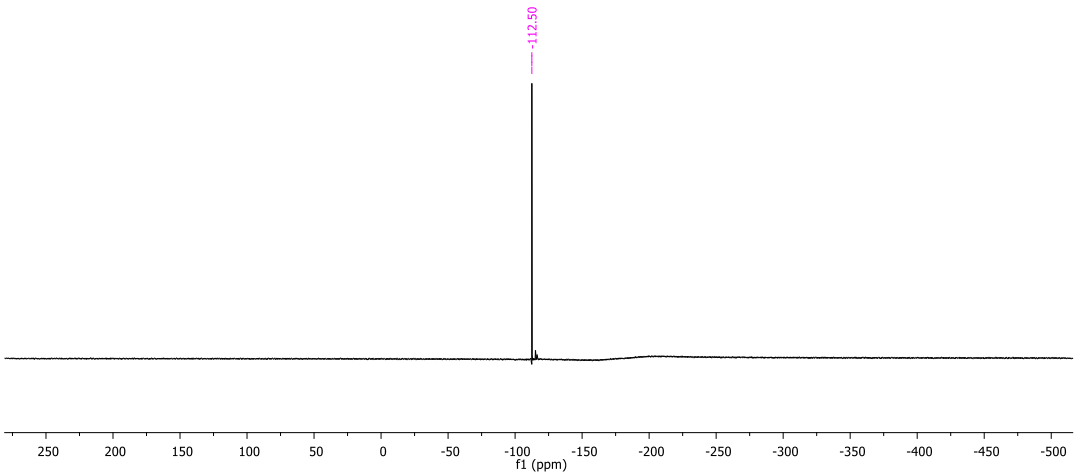

Figure A3.13. ^{19}F NMR spectrum of the compound **3f** in $CDCl_3$.

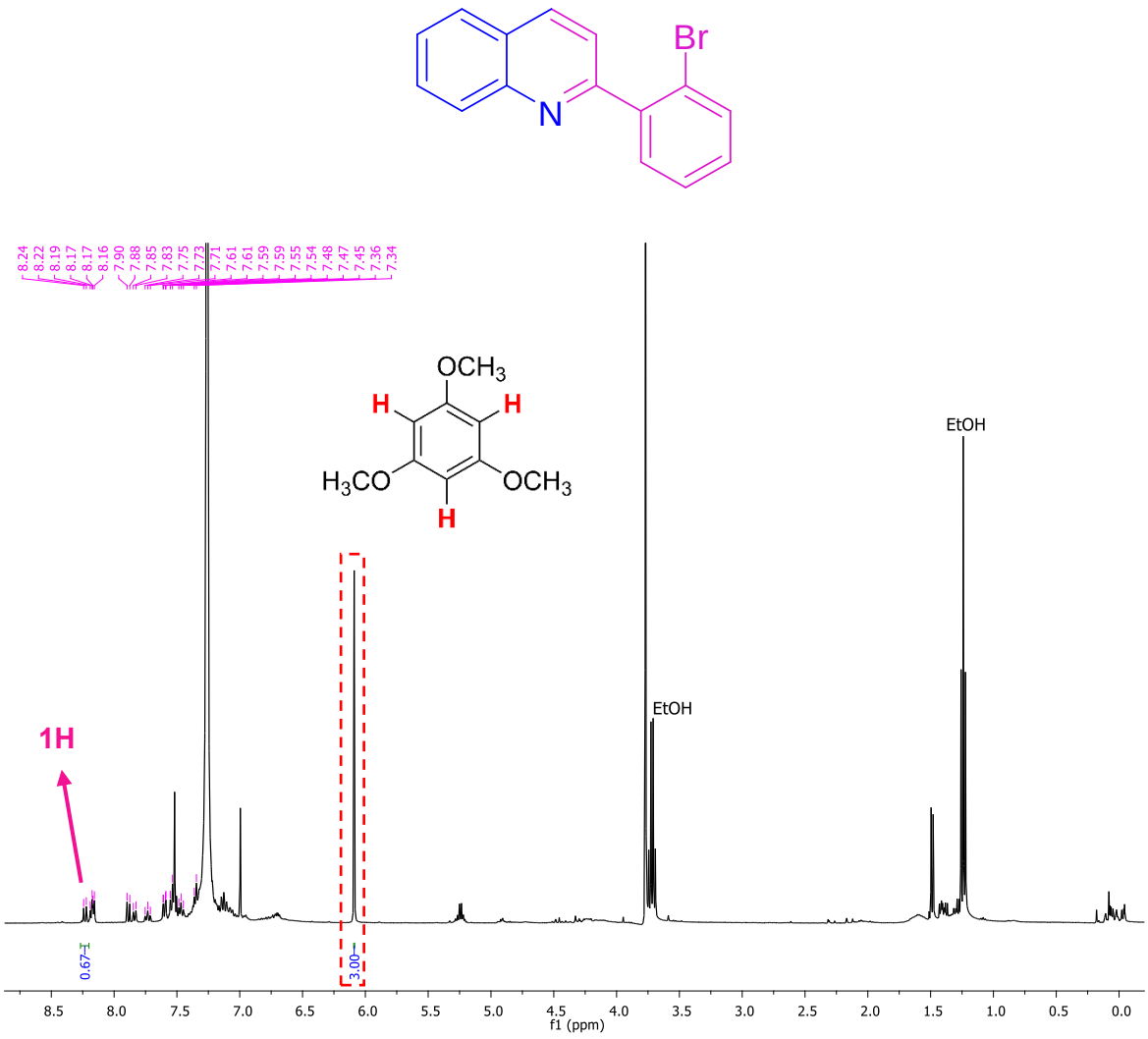

Figure A3.14. ^{1}H NMR spectrum of the compound **3g** in $CDCl_3$.

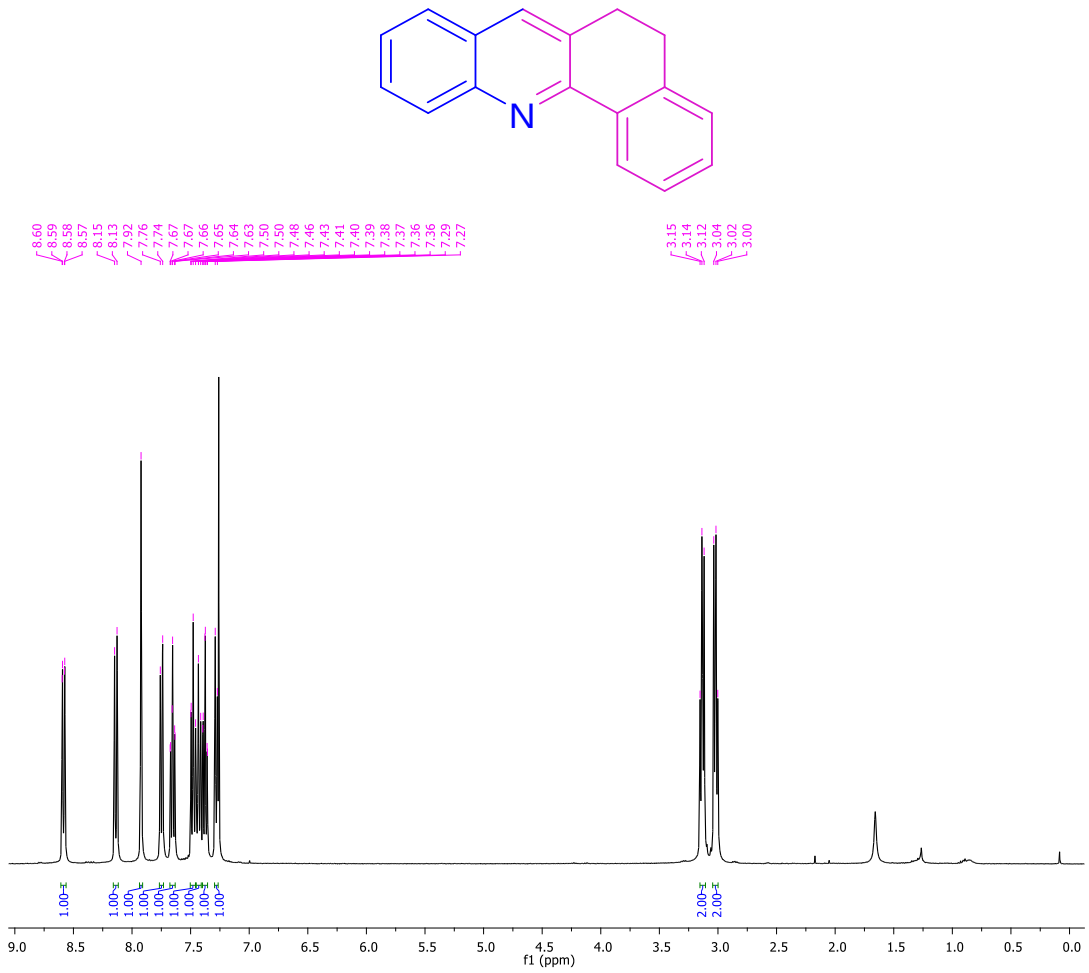

Figure A3.15. ^{1}H NMR spectrum of the compound **3h** in $CDCl_3$.

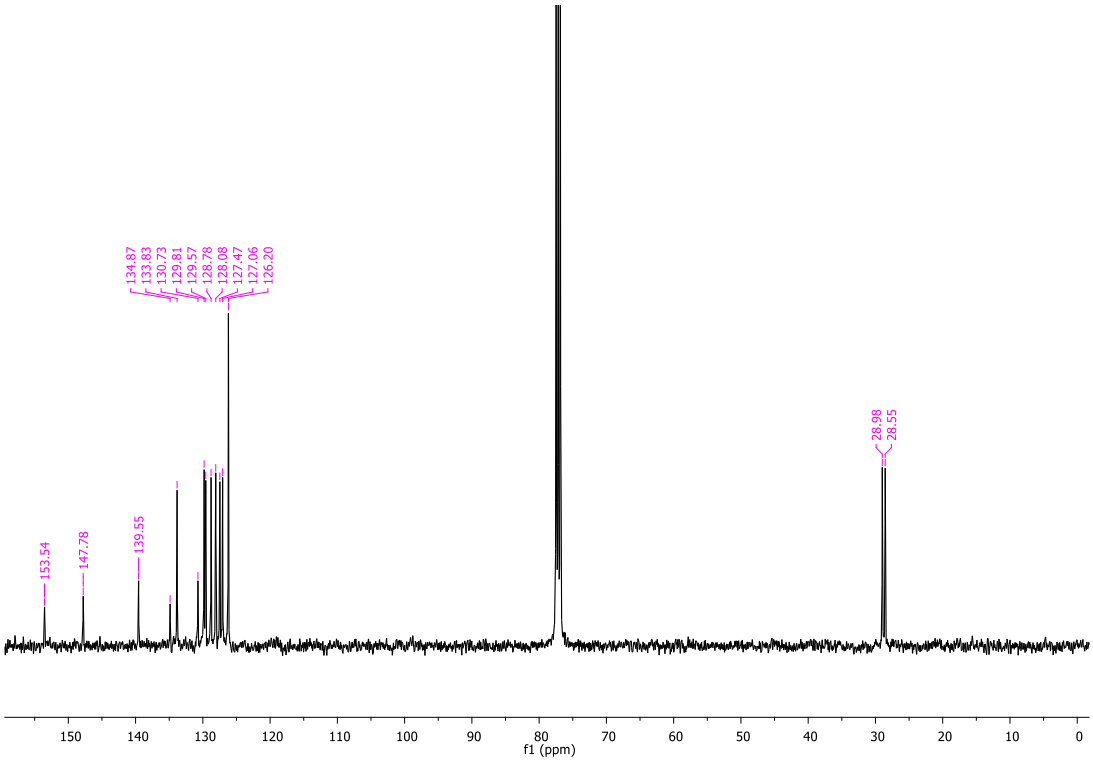

Figure A3.16. ^{13}C NMR spectrum of the compound **3h** in $CDCl_3$.

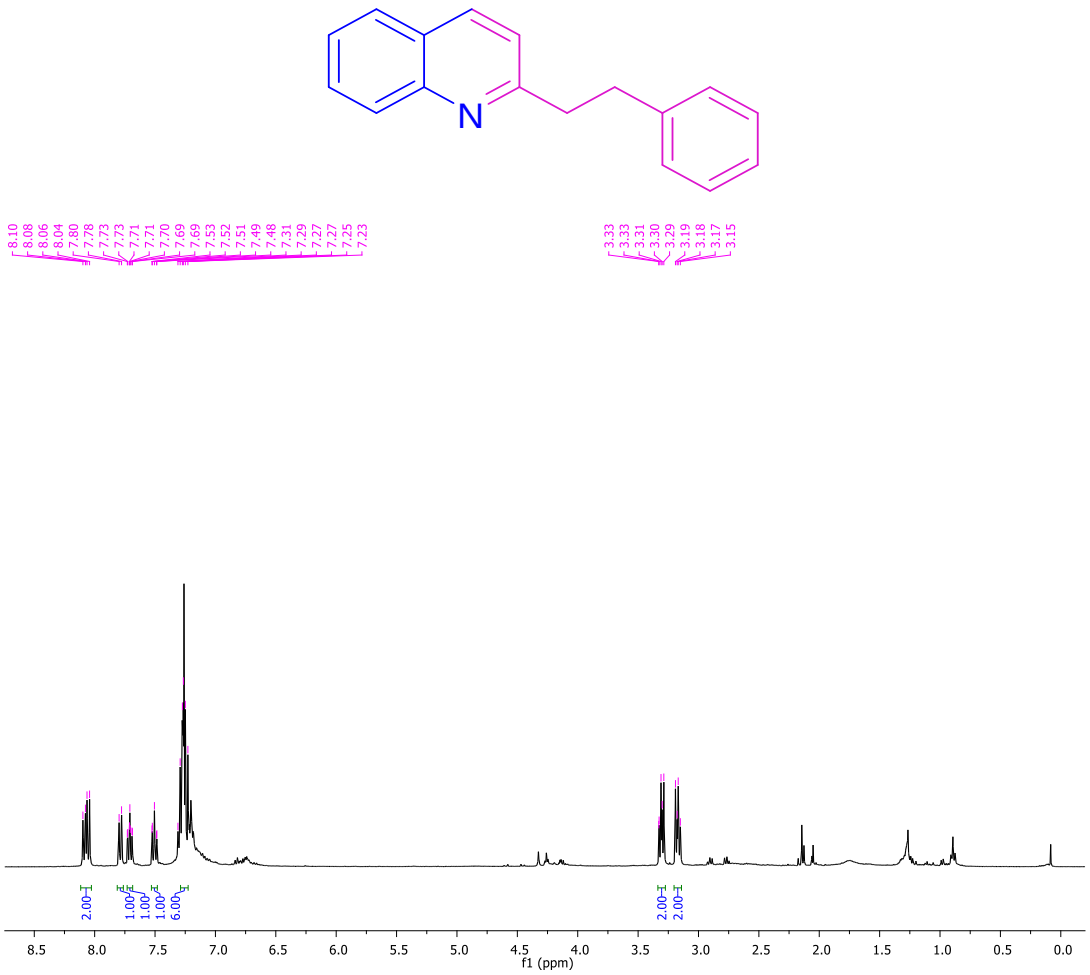

Figure A3.17. ^{1}H NMR spectrum of the compound **3i** in $CDCl_3$.

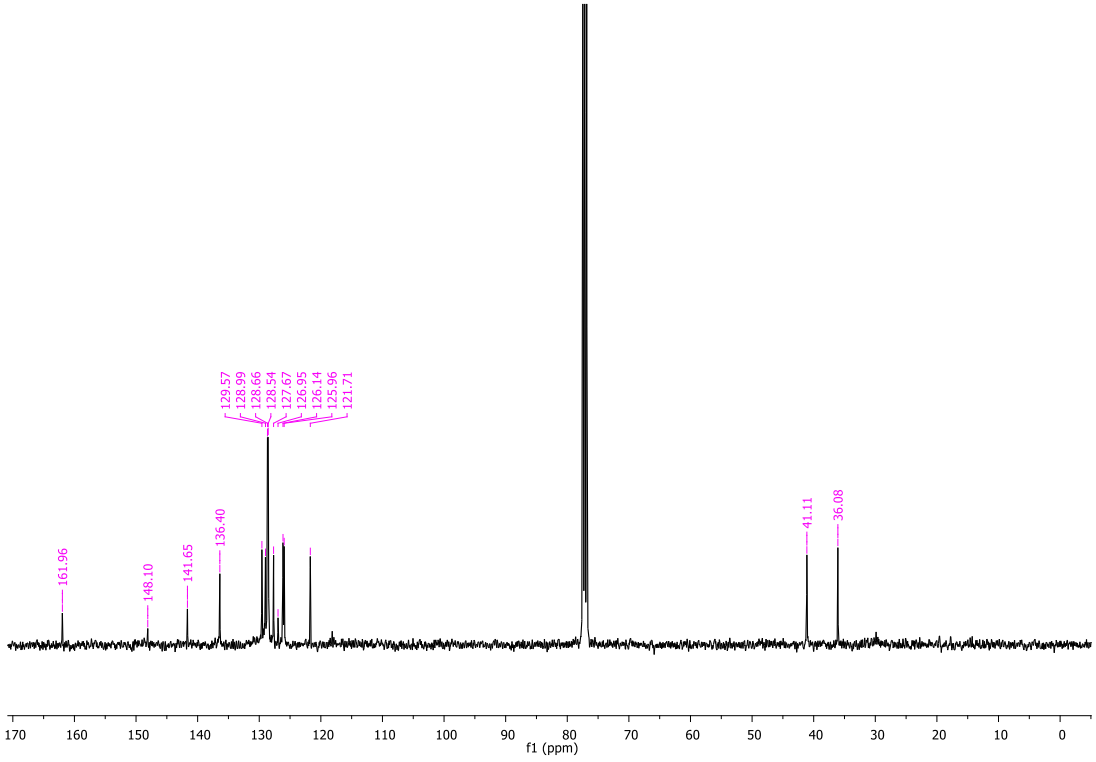

Figure A3.18. ^{13}C NMR spectrum of the compound **3i** in $CDCl_3$.

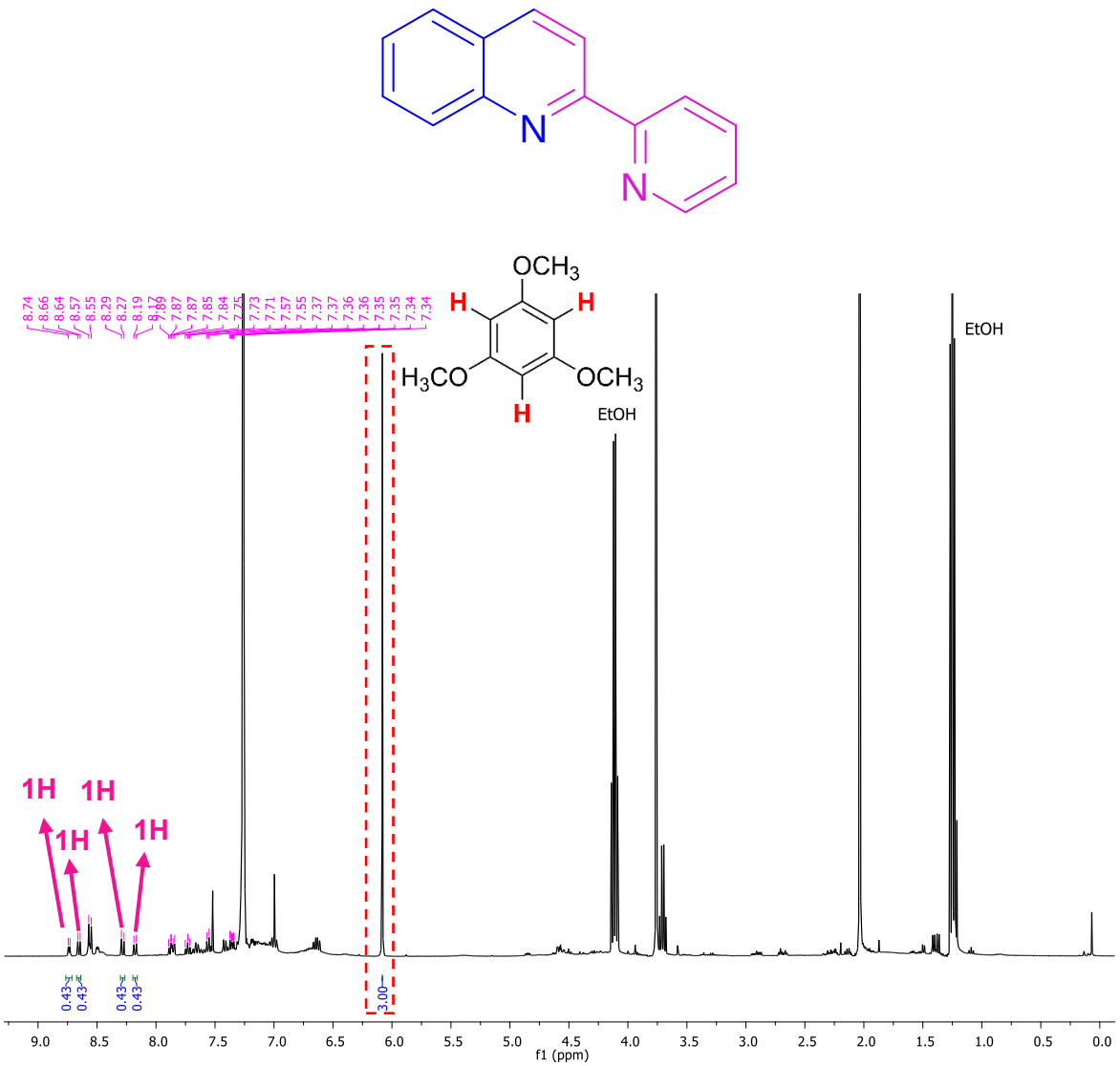

Figure A3.19. ^{1}H NMR spectrum of the compound **3j** in $CDCl_3$.

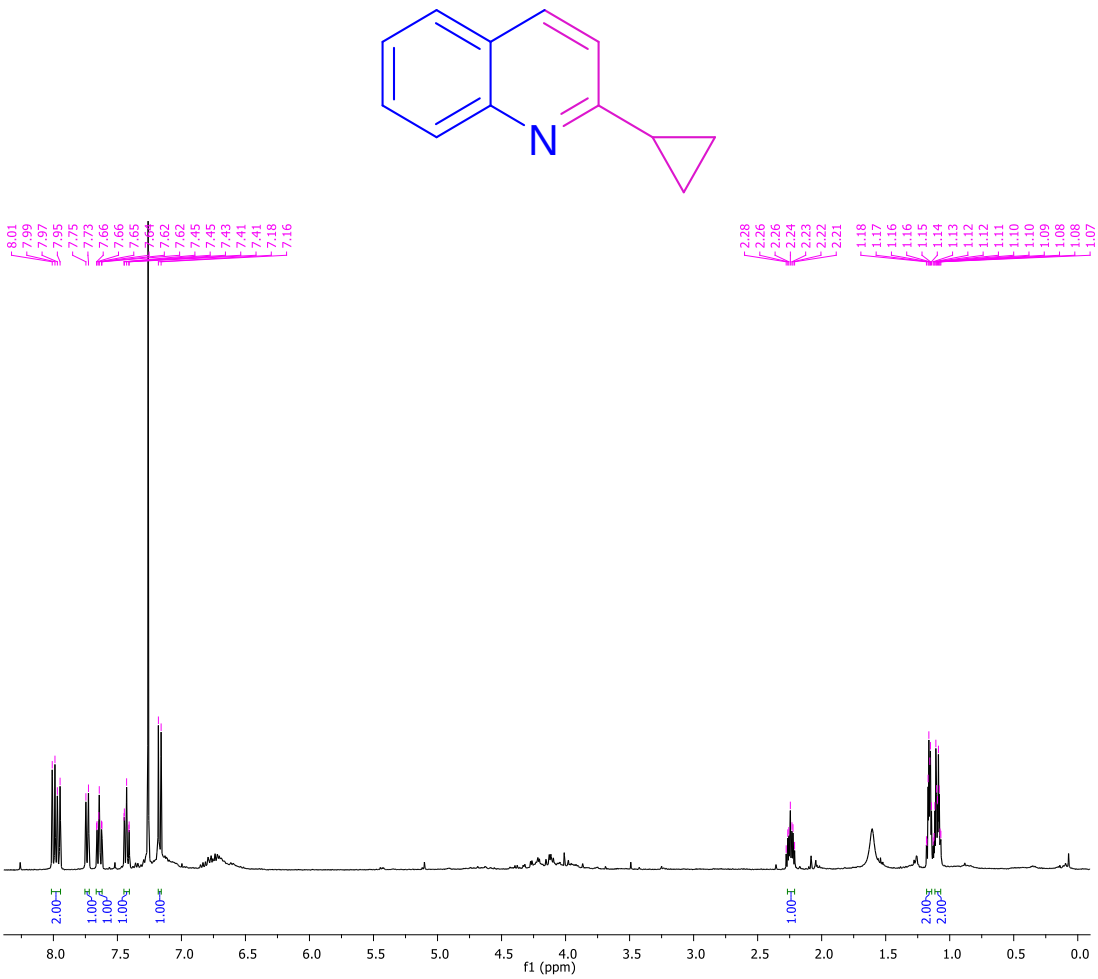

Figure A3.20. ^{1}H NMR spectrum of the compound **3k** in $CDCl_3$.

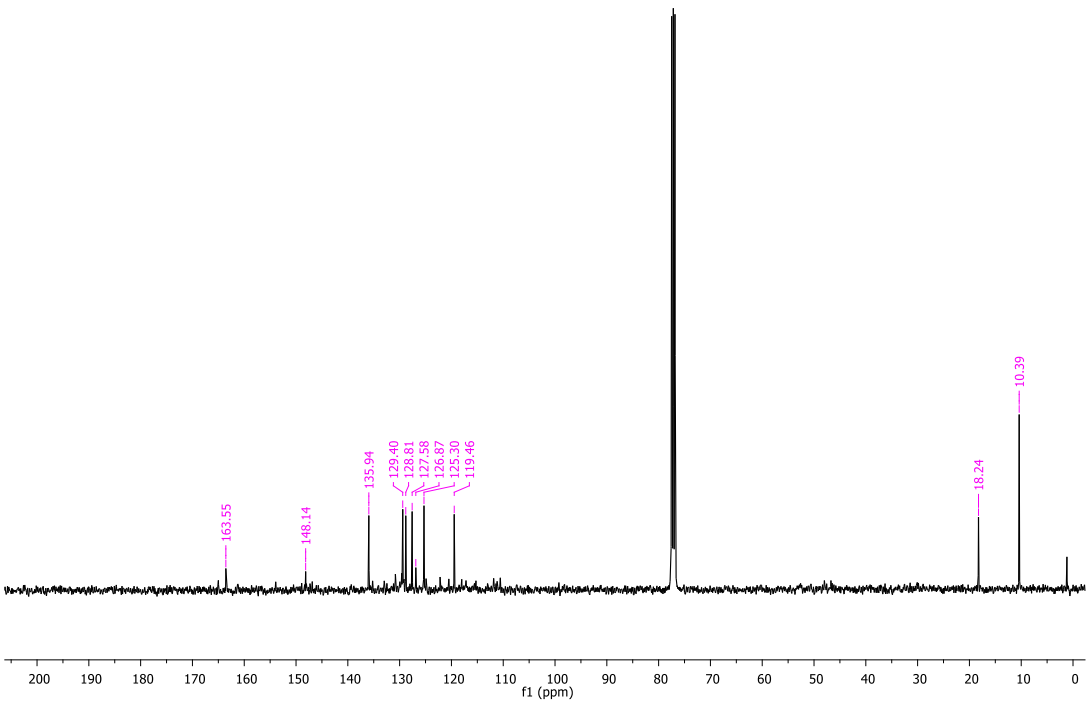

Figure A3.21. ^{13}C NMR spectrum of the compound **3k** in $CDCl_3$.

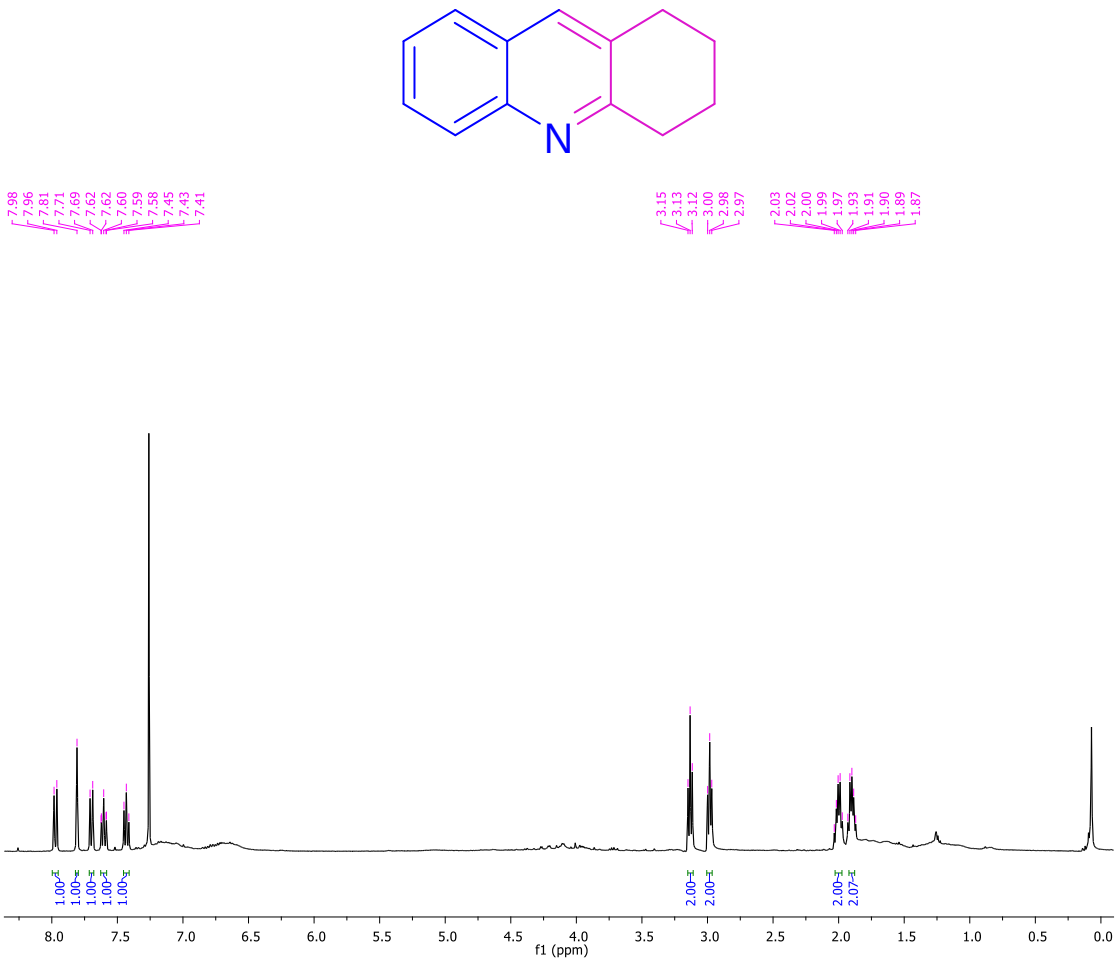

Figure A3.22. ^{1}H NMR spectrum of the compound **3l** in $CDCl_3$.

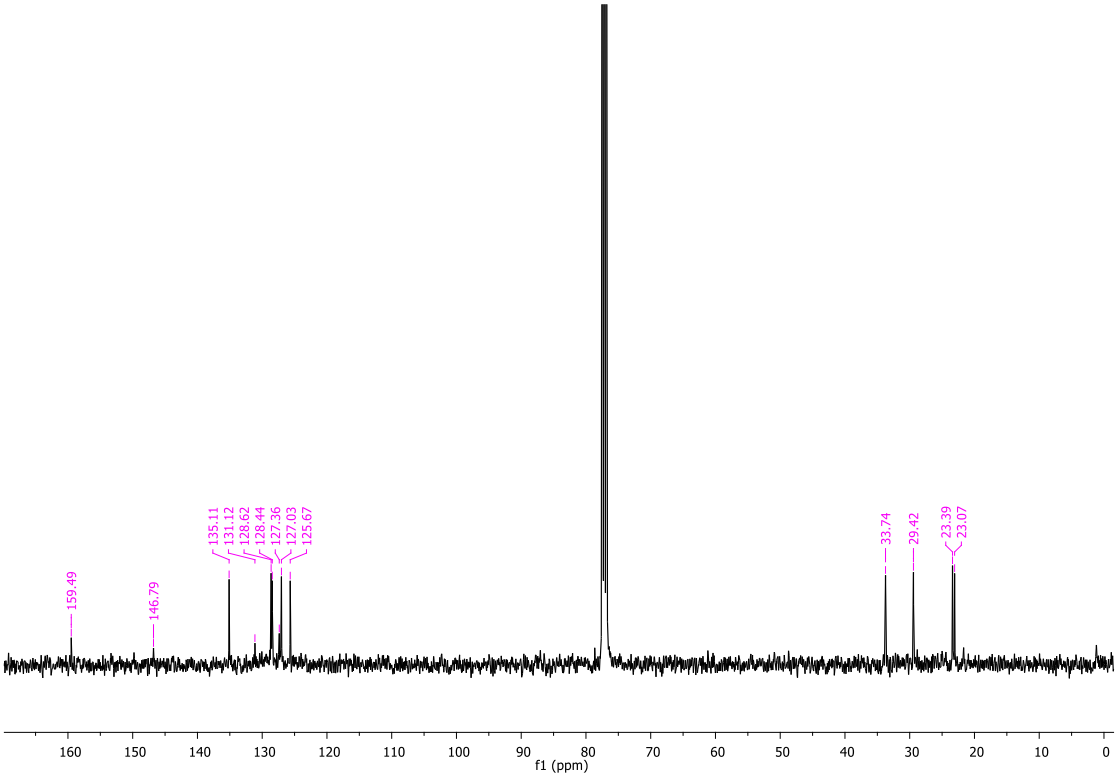

Figure A3.23. ^{13}C NMR spectrum of the compound **3l** in $CDCl_3$.

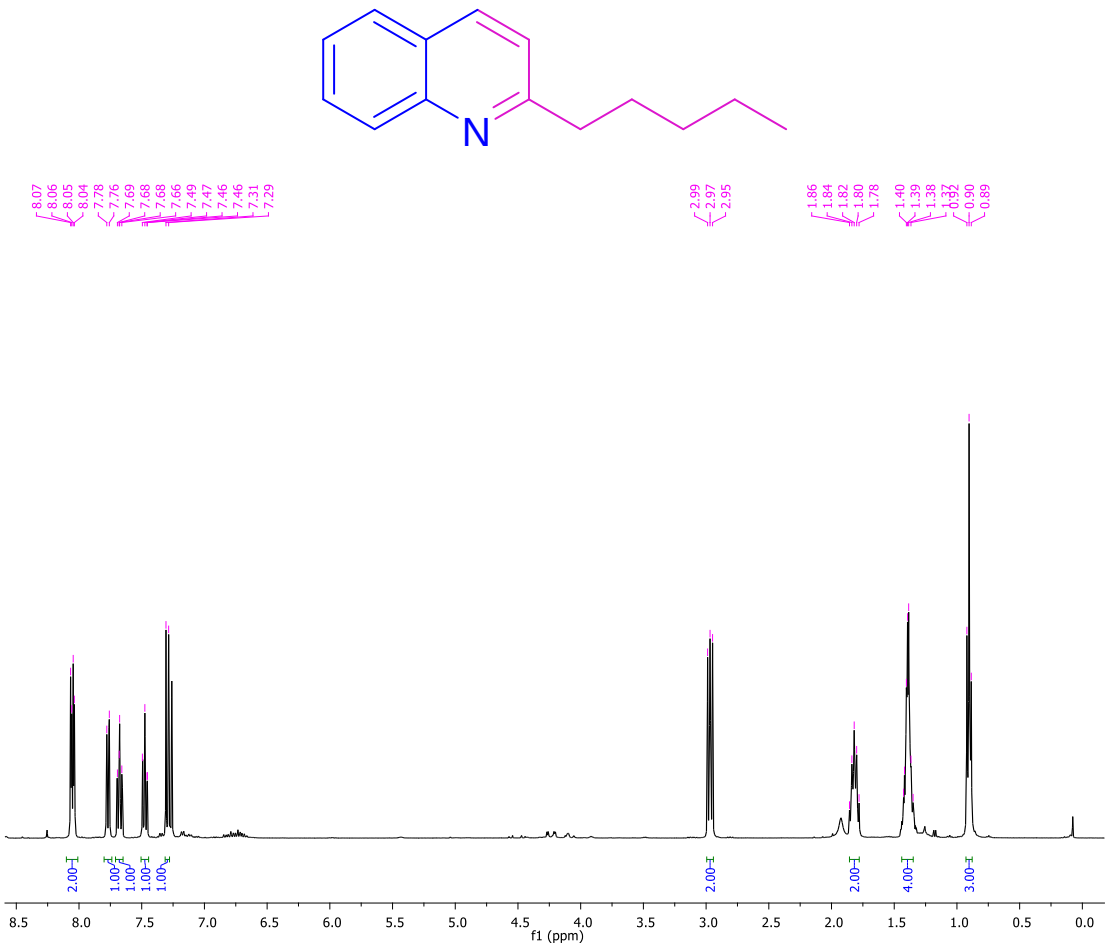

Figure A3.24. ^{1}H NMR spectrum of the compound **3m** in $CDCl_3$.

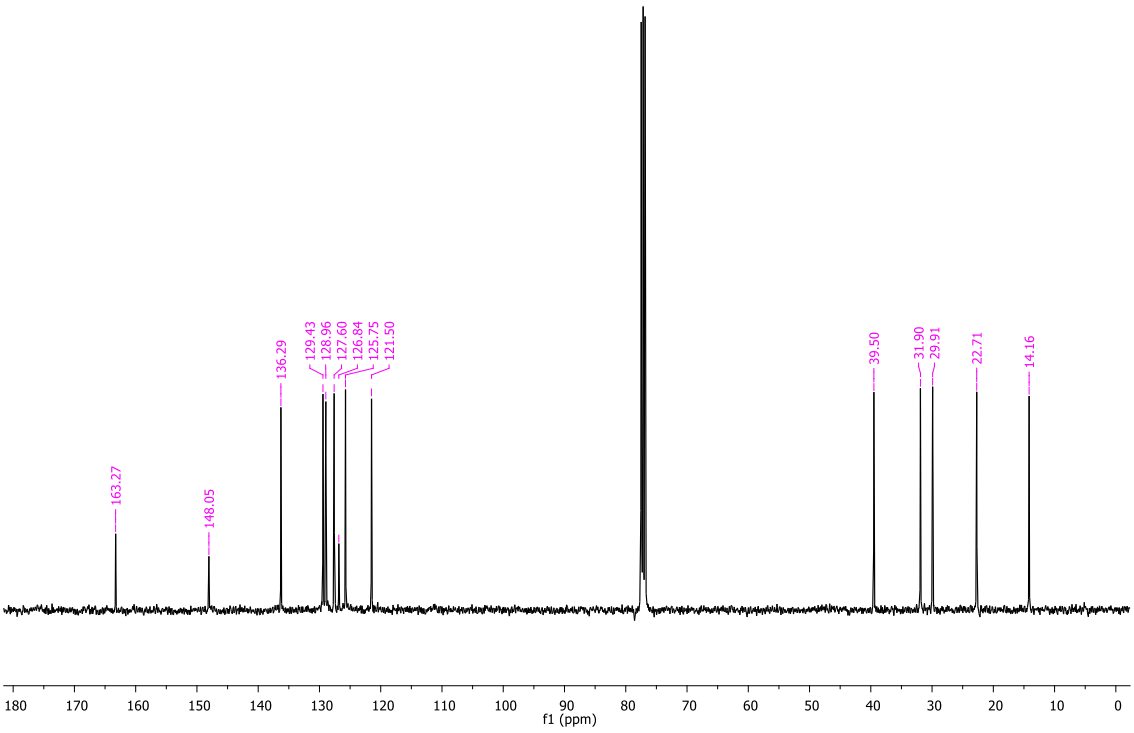

Figure A3.25. ^{13}C NMR spectrum of the compound **3m** in $CDCl_3$.

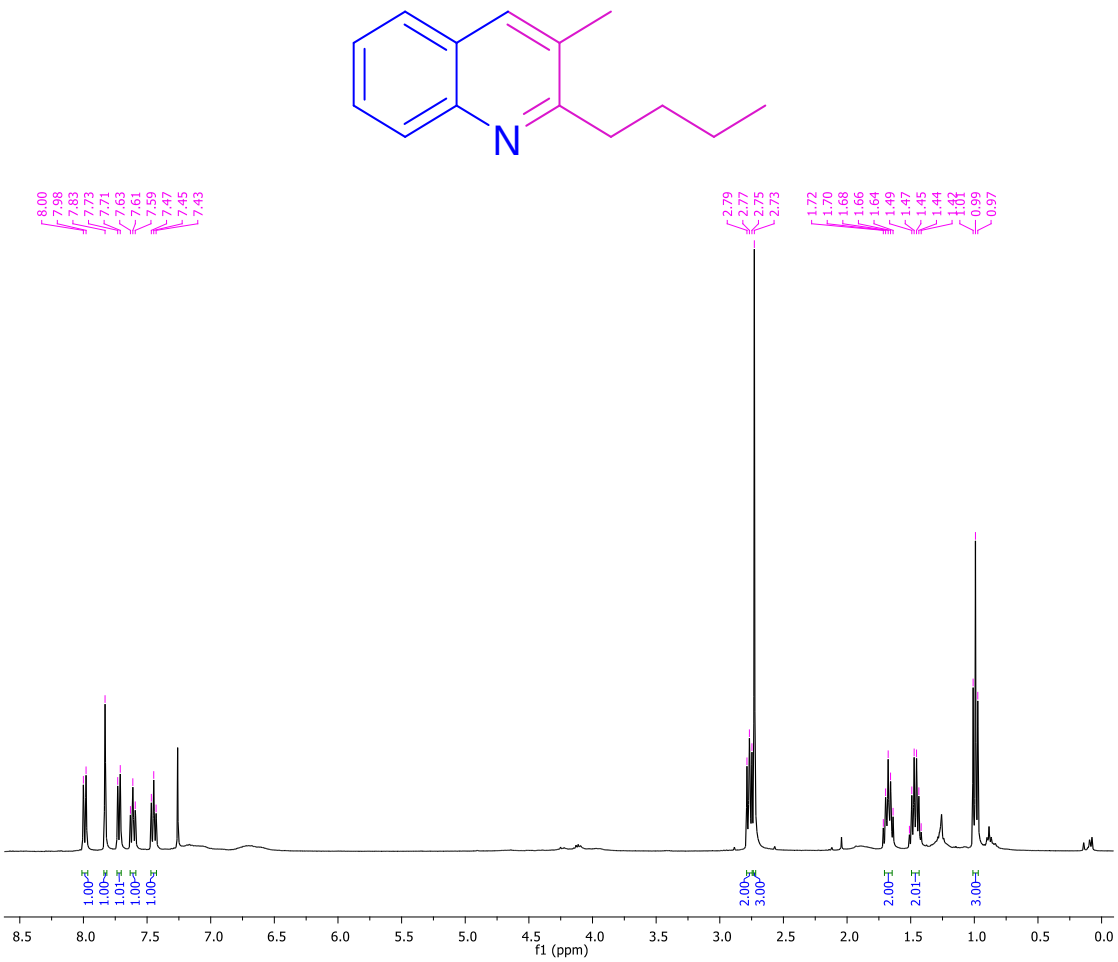

Figure A3.26. ^{1}H NMR spectrum of the compound **3m'** in $CDCl_3$.

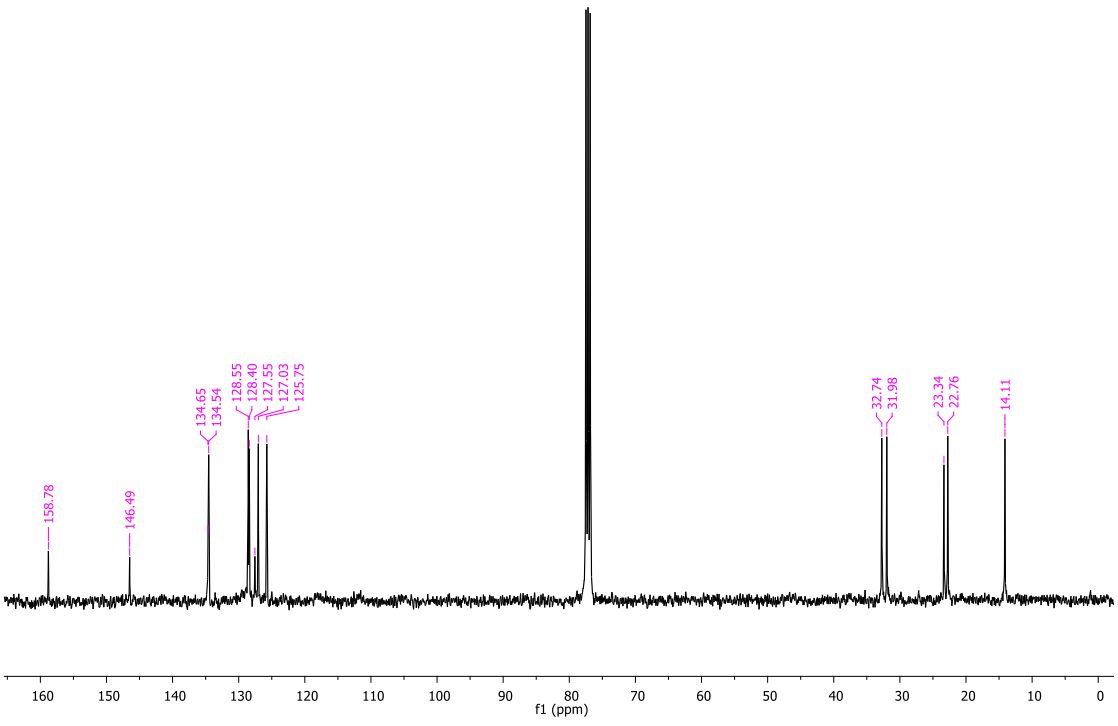

Figure A3.27. ^{13}C NMR spectrum of the compound **3m'** in $CDCl_3$.

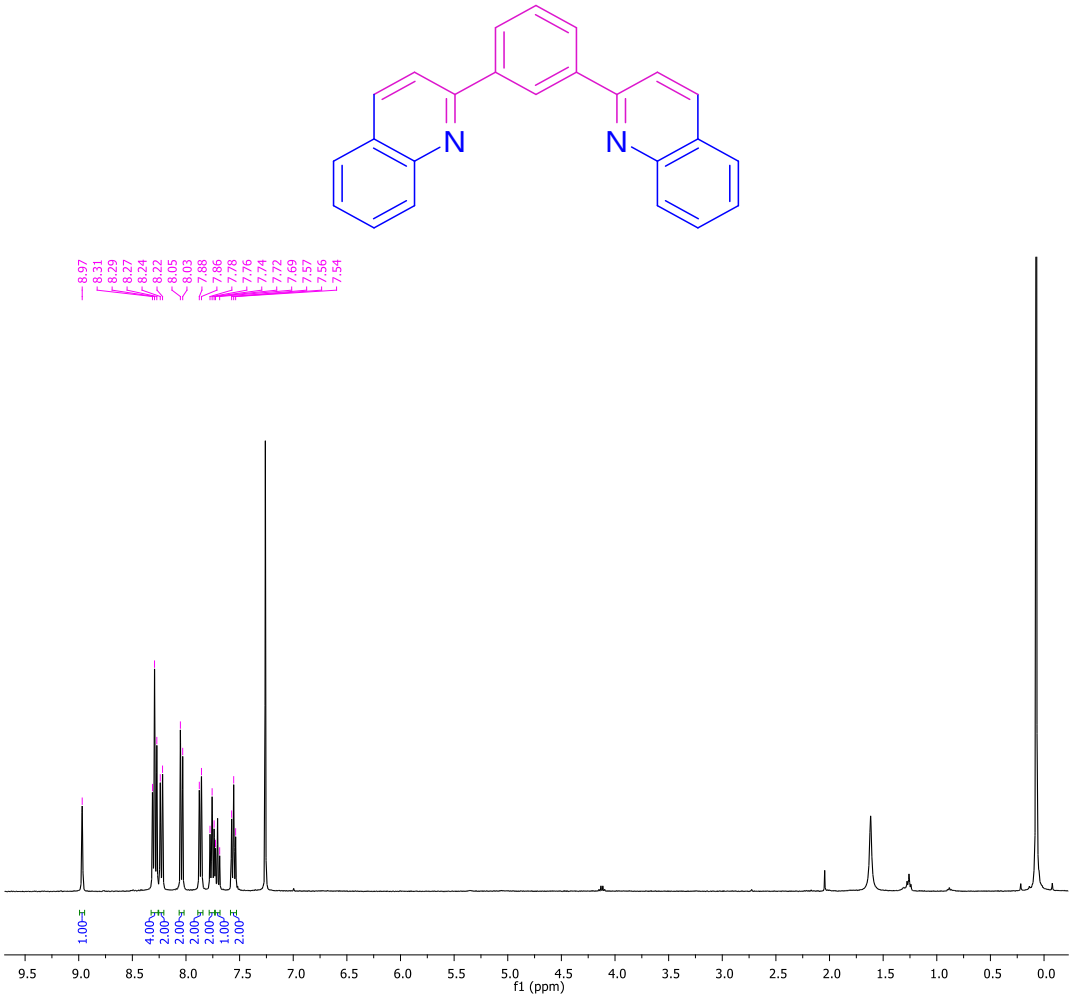

Figure A3.28. ^{1}H NMR spectrum of the compound **3n** in $CDCl_3$.

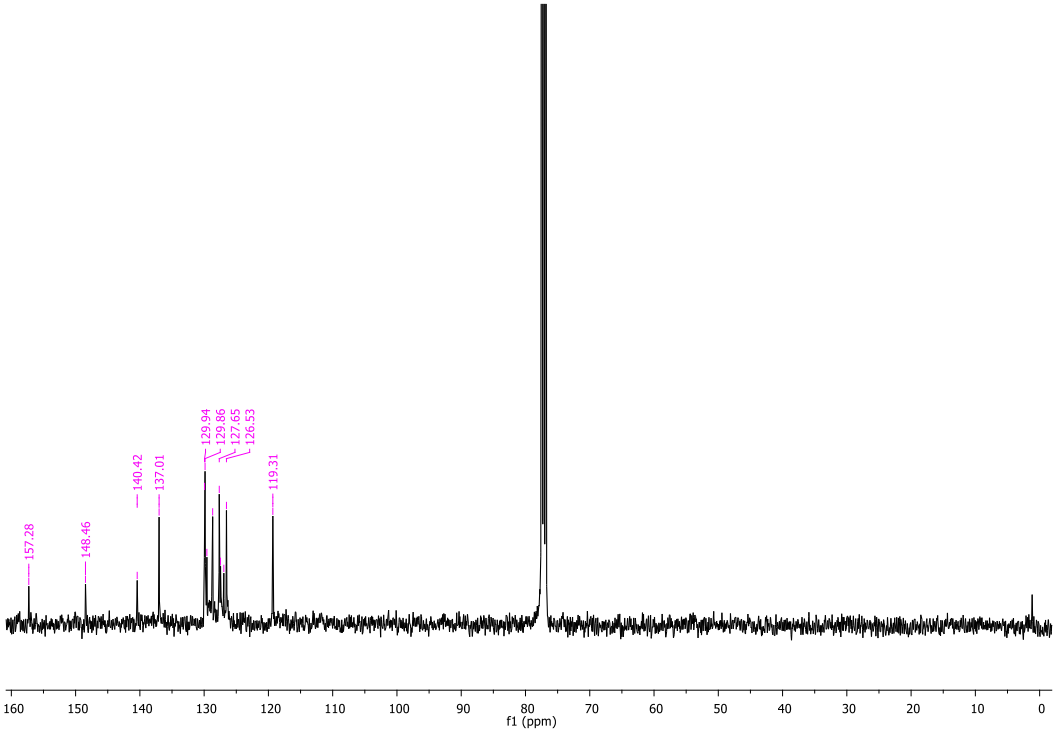

Figure A3.29. ^{13}C NMR spectrum of the compound **3n** in $CDCl_3$.

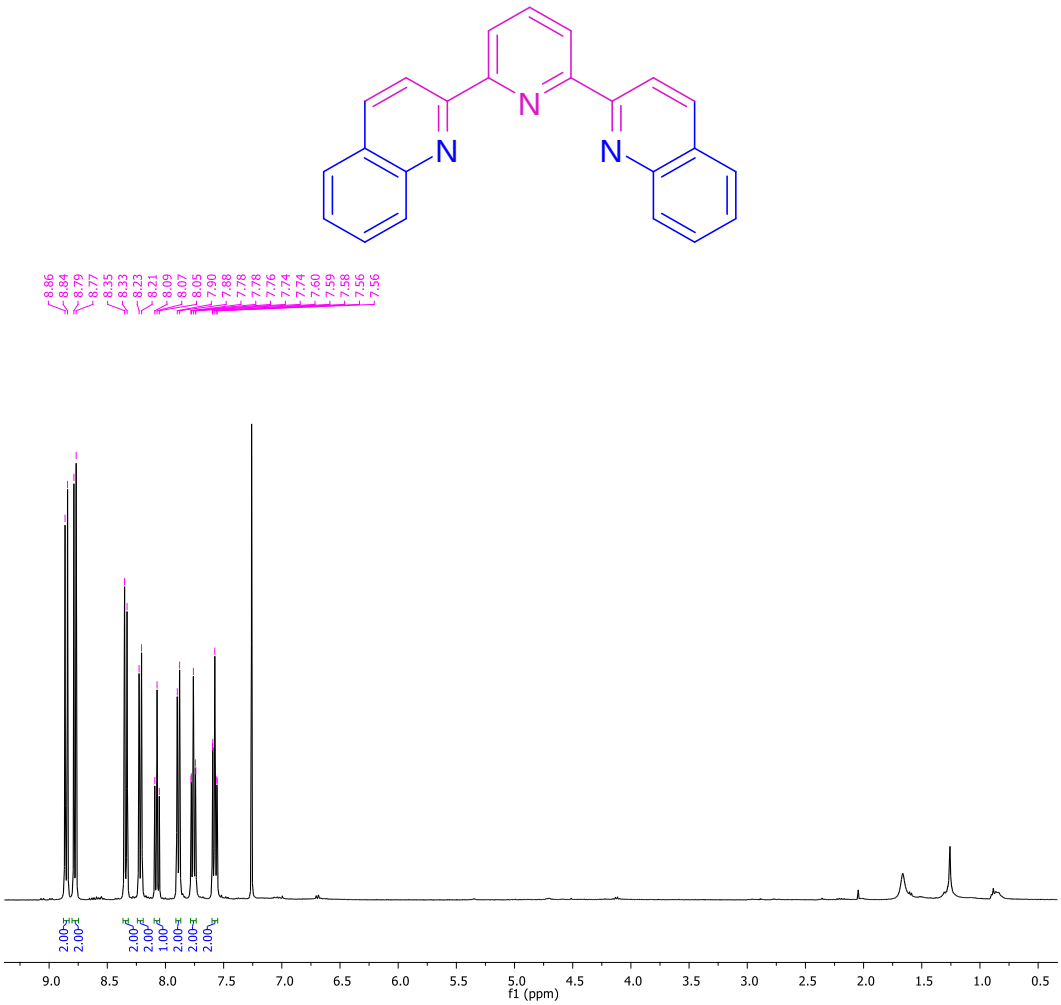

Figure A3.30. ^{1}H NMR spectrum of the compound **3o** in $CDCl_3$.

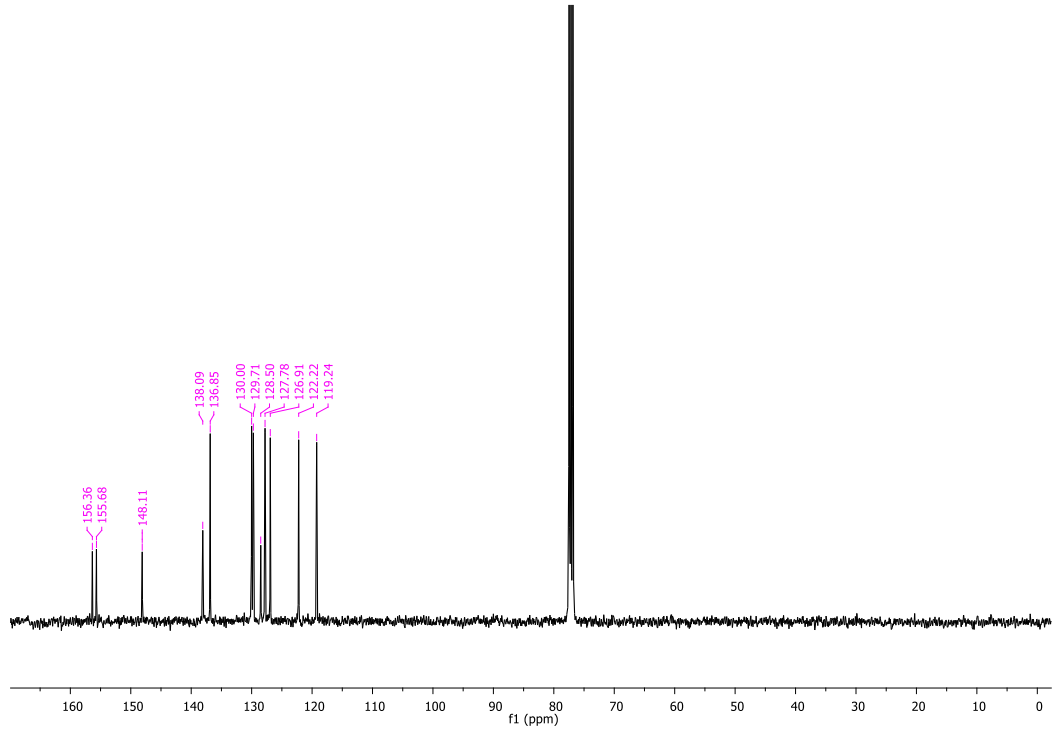

Figure A3.31. ^{13}C NMR spectrum of the compound **3o** in $CDCl_3$.

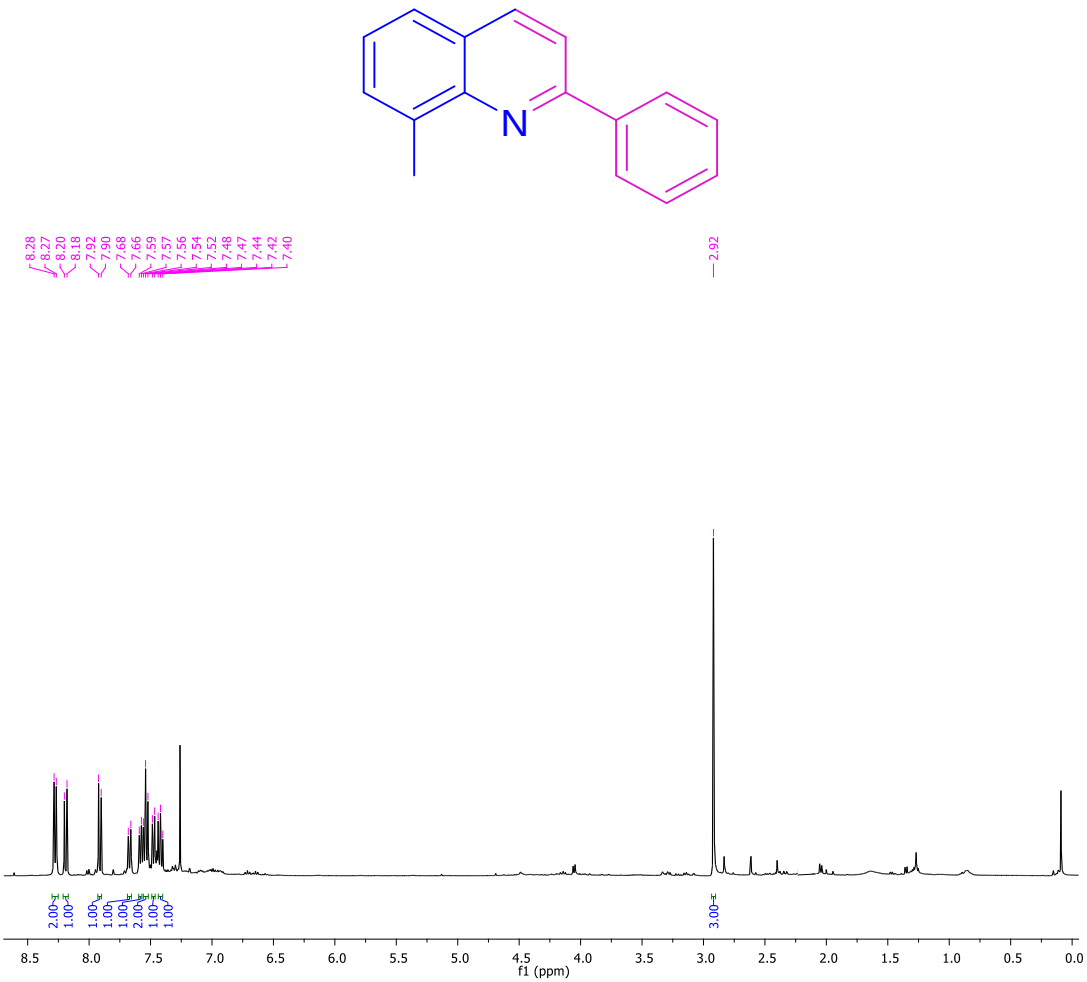

Figure A3.32. ^{1}H NMR spectrum of the compound **3p** in $CDCl_3$.

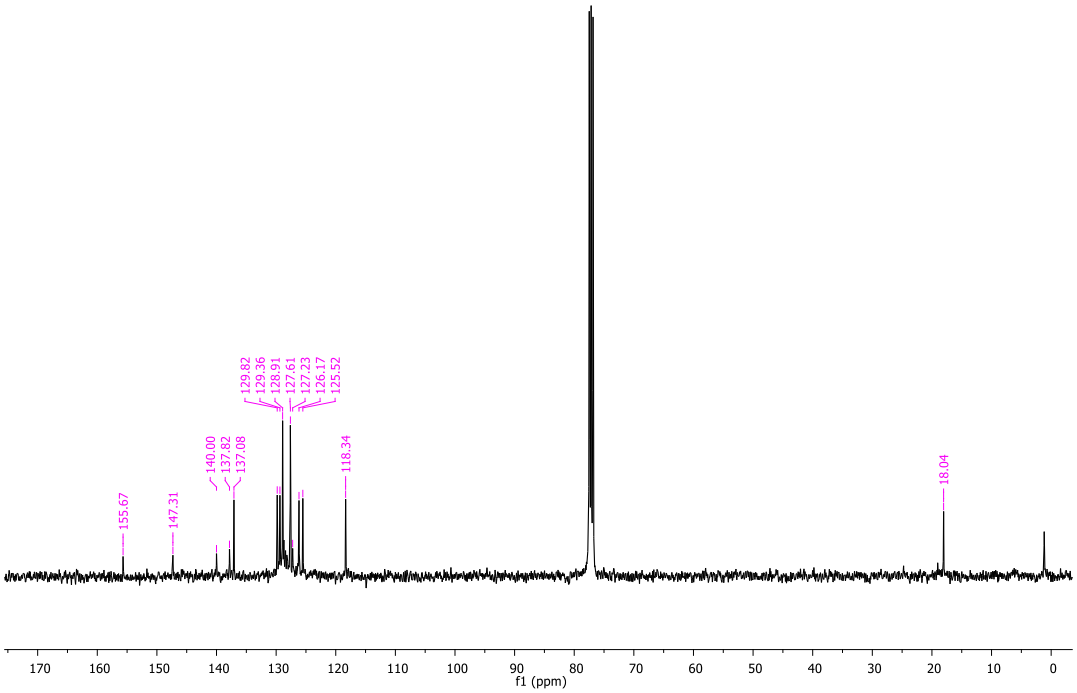

Figure A3.33. ^{13}C NMR spectrum of the compound **3p** in $CDCl_3$.

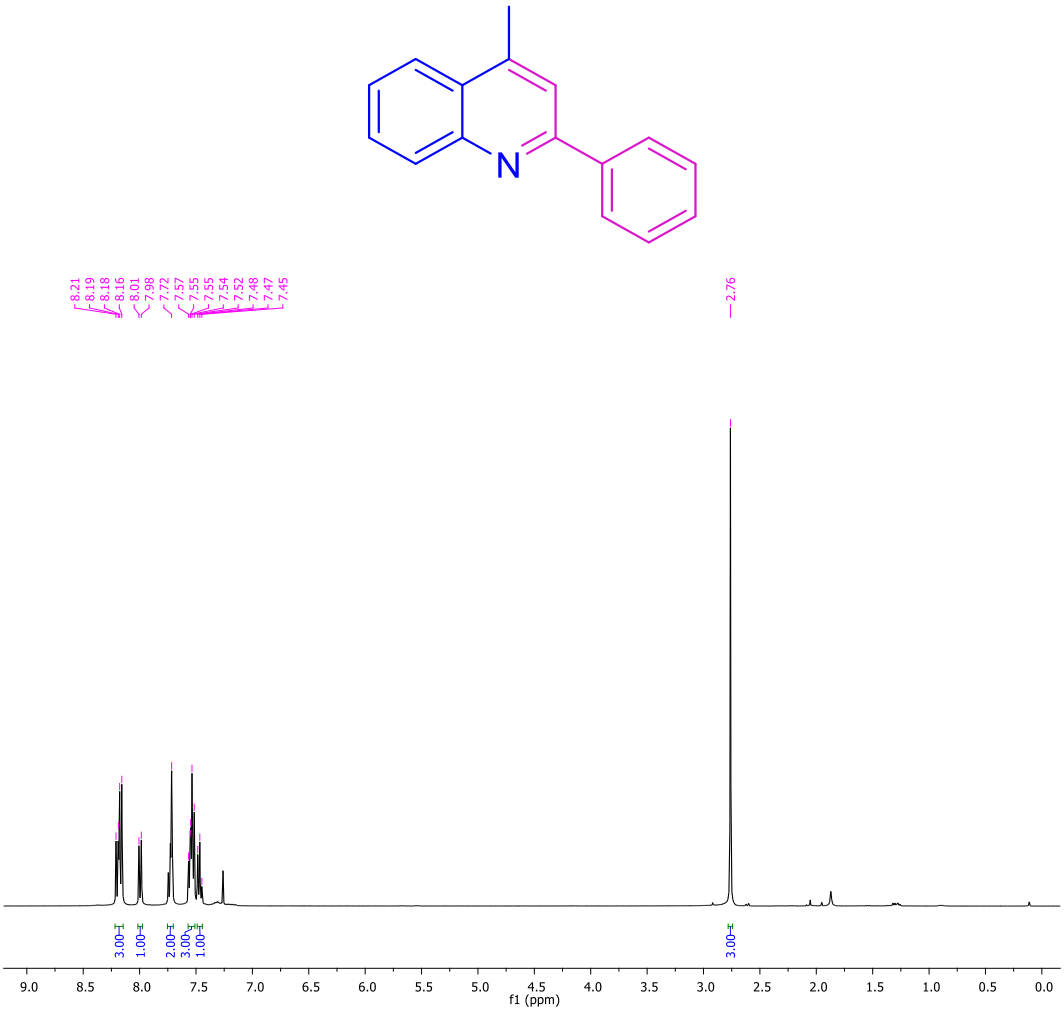

Figure A3.34. ^{1}H NMR spectrum of the compound **3q** in $CDCl_3$.

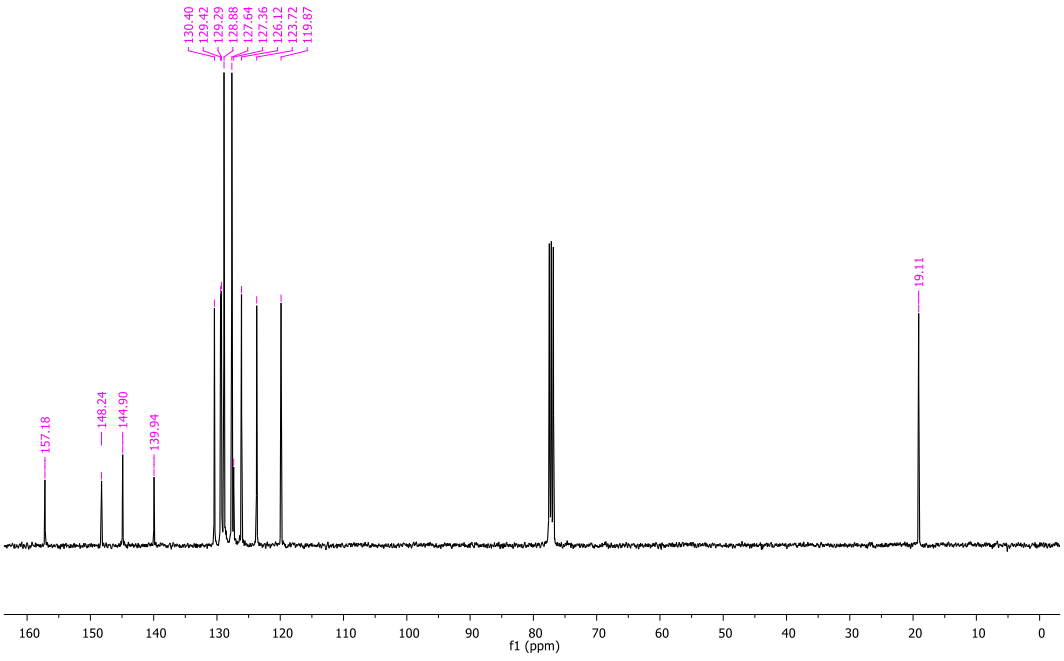

Figure A3.35. ^{13}C NMR spectrum of the compound **3q** in $CDCl_3$.

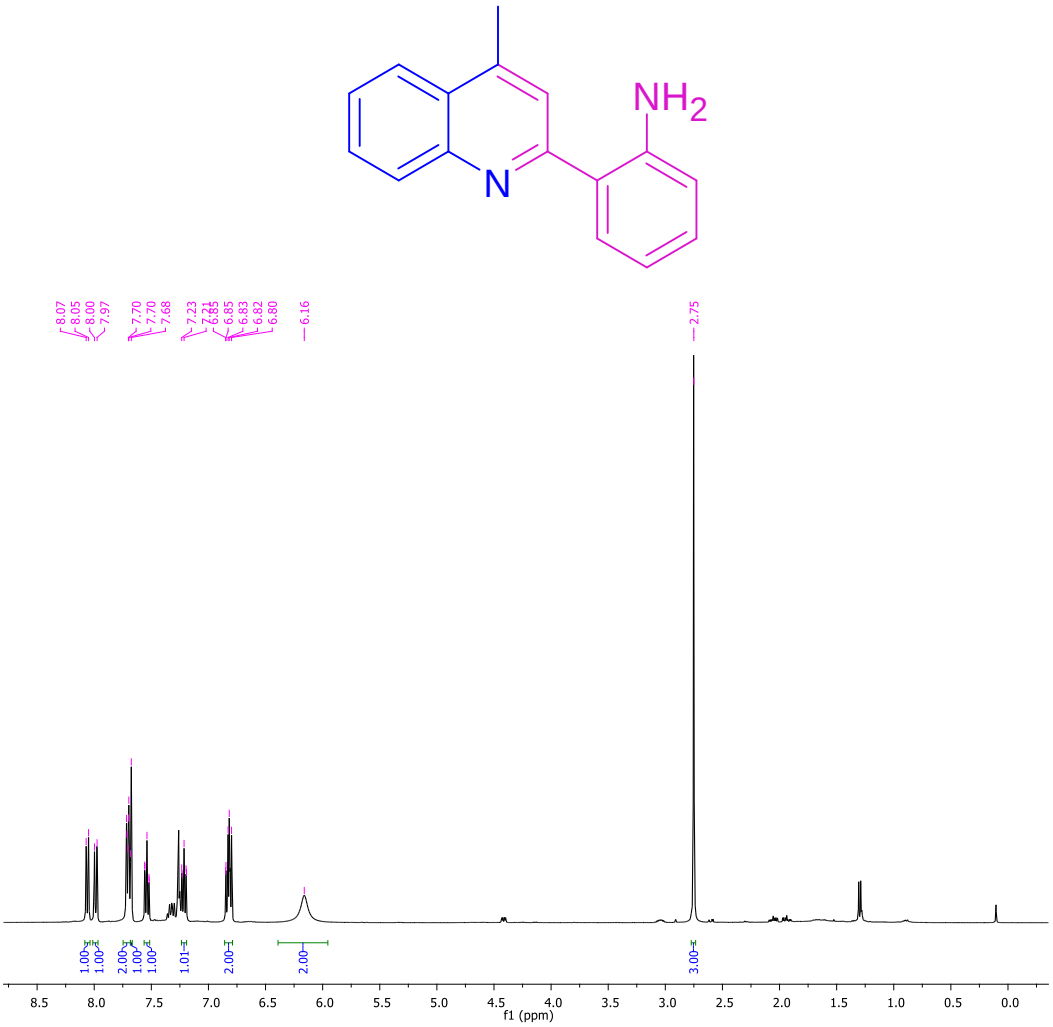

Figure A3.36. ^{1}H NMR spectrum of the compound **3q'** in $CDCl_3$.

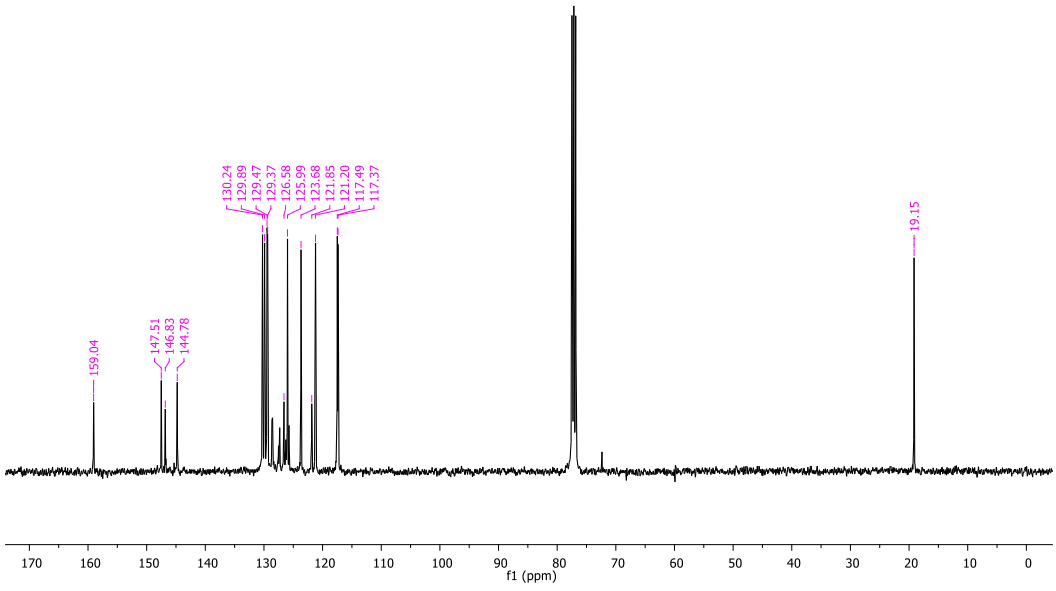

Figure A3.37. ^{13}C NMR spectrum of the compound **3q'** in $CDCl_3$.

A3.2. NMR data of the *N*-Alkylation of Amines with Alcohols

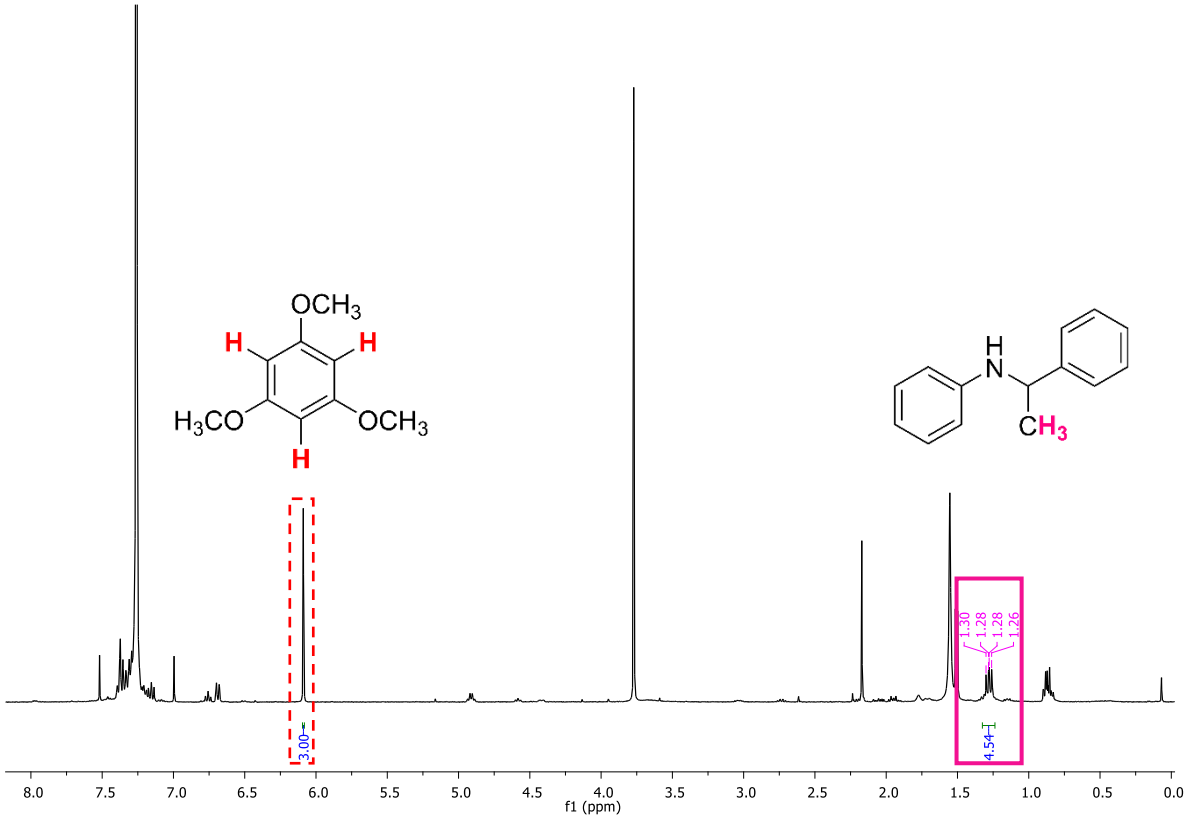

Figure A3.38. ^{1}H NMR spectrum of the reaction presented in Scheme 3.4, 5a.

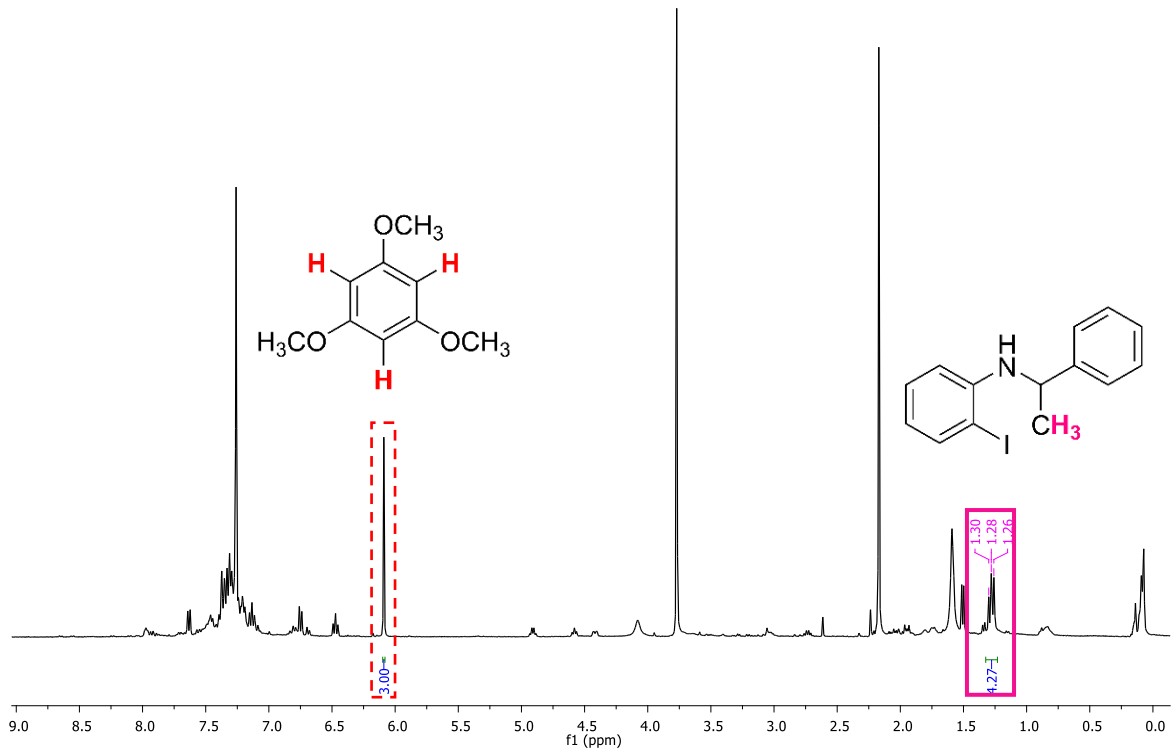

Figure A3.39. ^{1}H NMR spectrum of the reaction presented in Scheme 3.4, 5c.

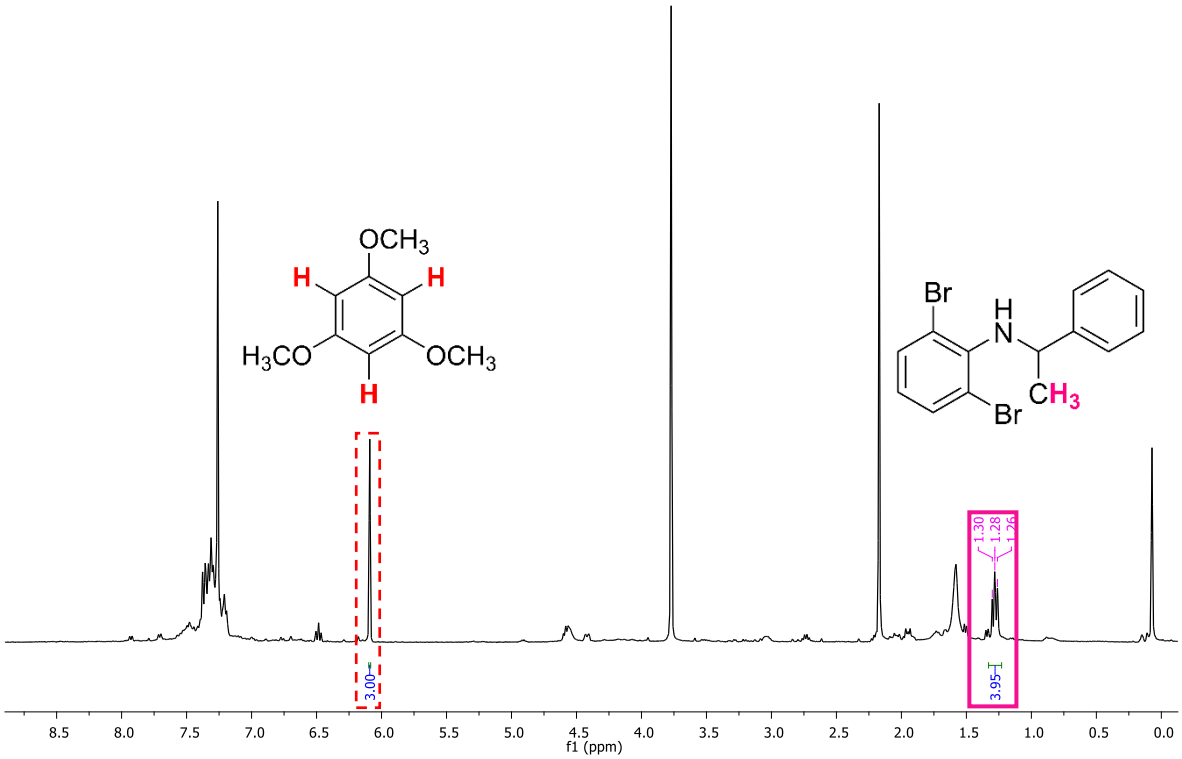

Figure A3.40. ^{1}H NMR spectrum of the reaction presented in Scheme 3.4, 5d.

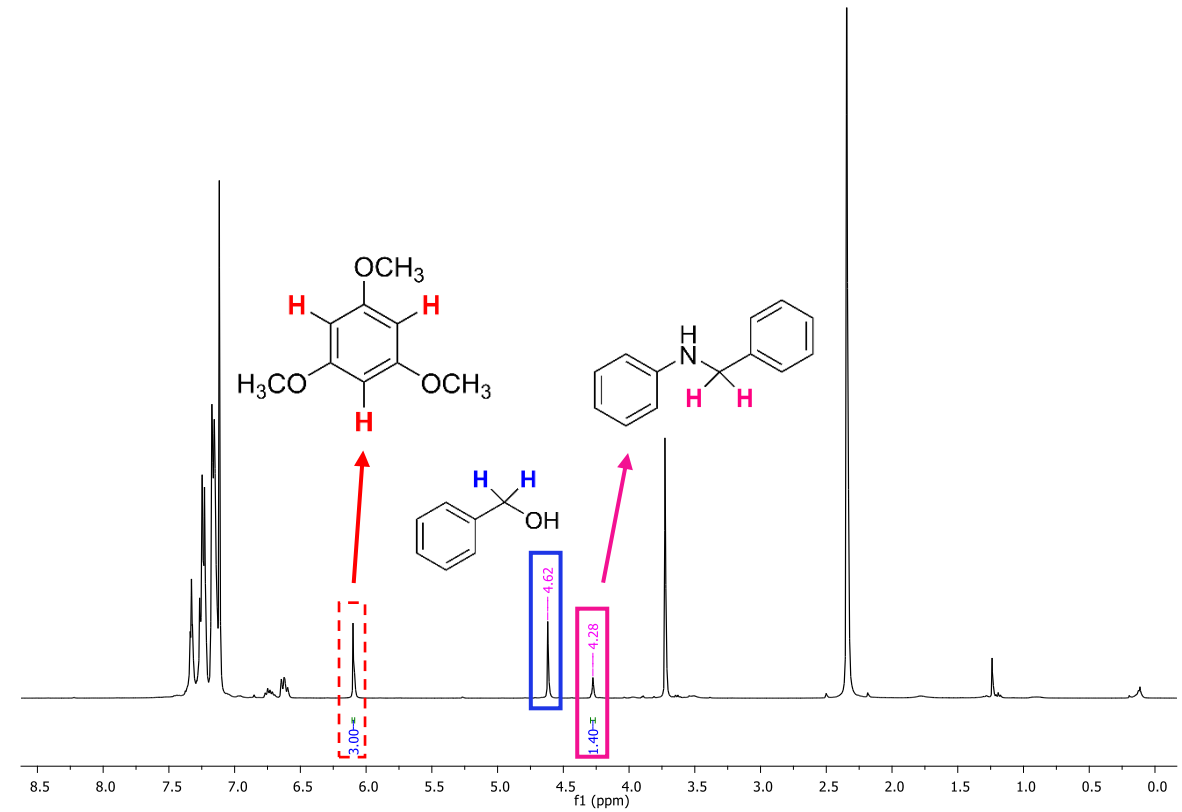

Figure A3.41. ^{1}H NMR spectrum of the reaction presented in Scheme 3.5, 1.0 equiv *t*-BuOK.

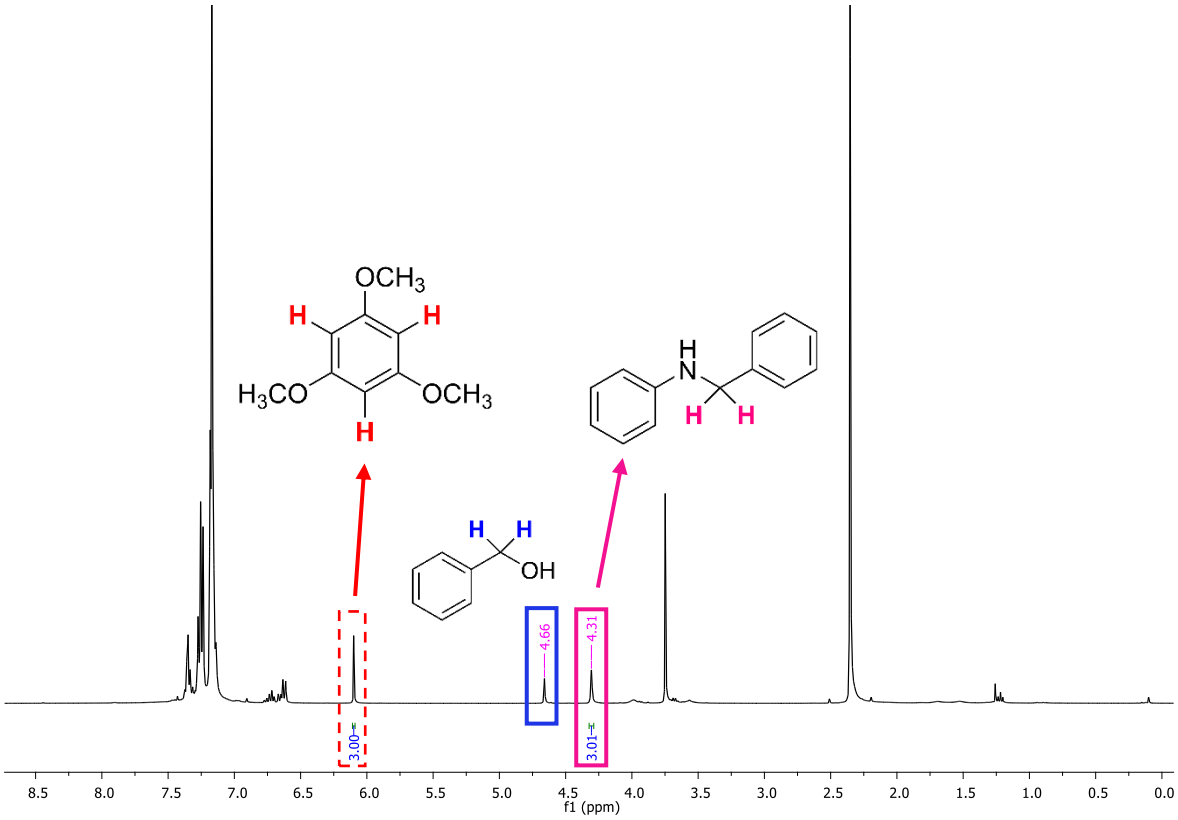

Figure A3.42. ^{1}H NMR spectrum of the reaction presented in Scheme 3.5, 0.5 equiv *t*-BuOK.

A3.3. NMR data of the α-Alkylation of Ketones with Alcohols

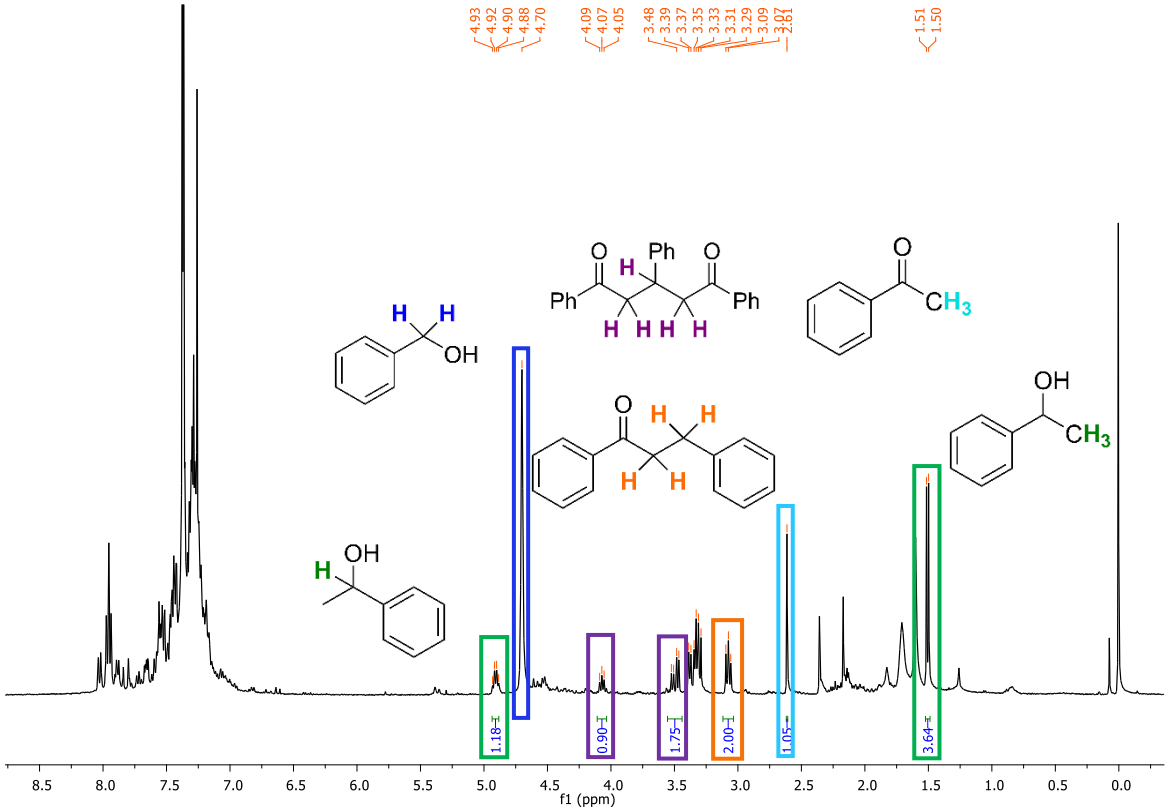

Figure A3.43. ^{1}H NMR spectrum of the reaction presented in Table 3.7, entry 1.

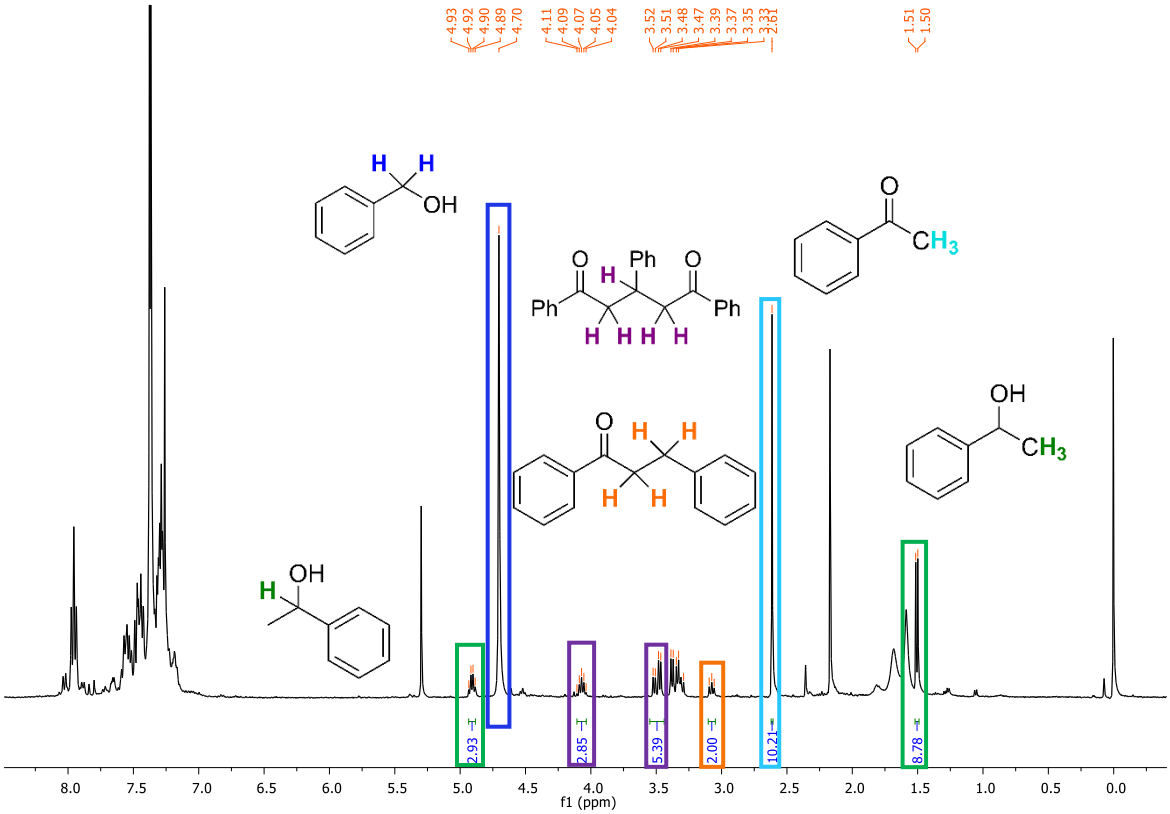

Figure A3.44. ^{1}H NMR spectrum of the reaction presented in Table 3.7, entry 2.

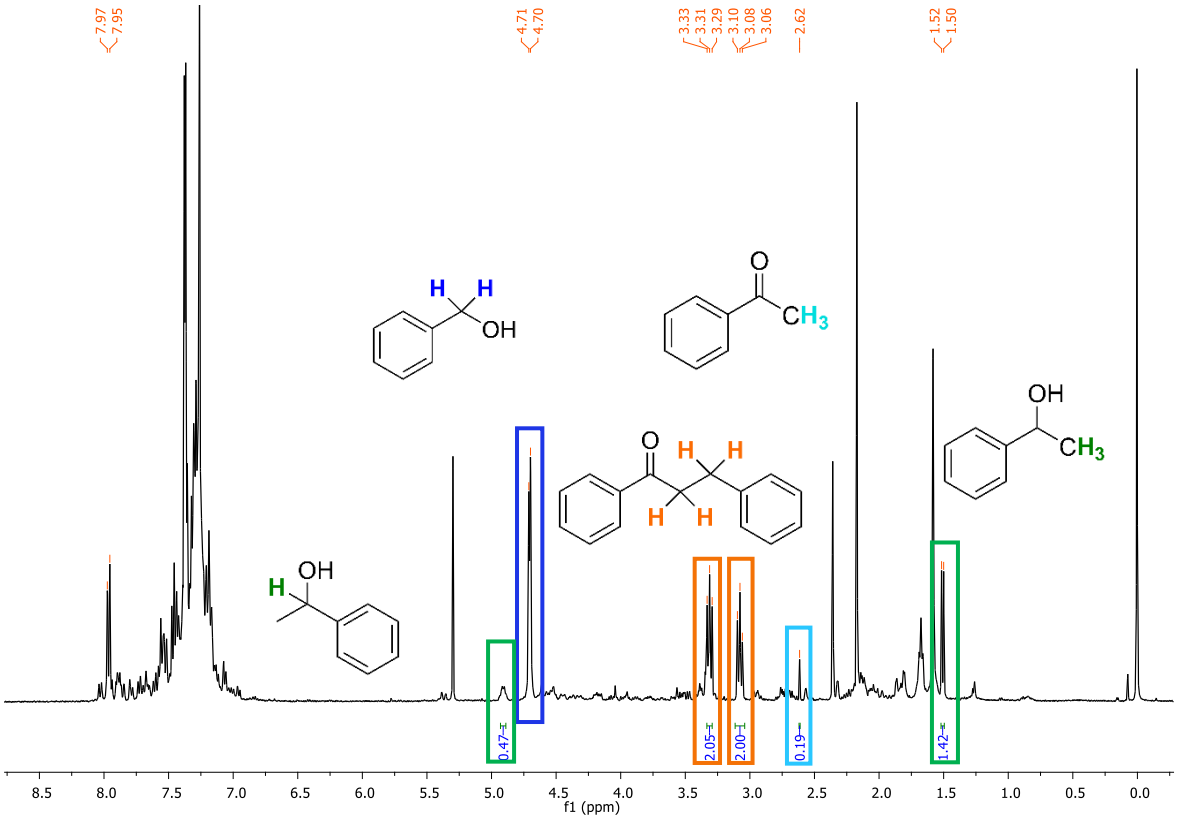

Figure A3.45. ^{1}H NMR spectrum of the reaction presented in Table 3.7, entry 3.

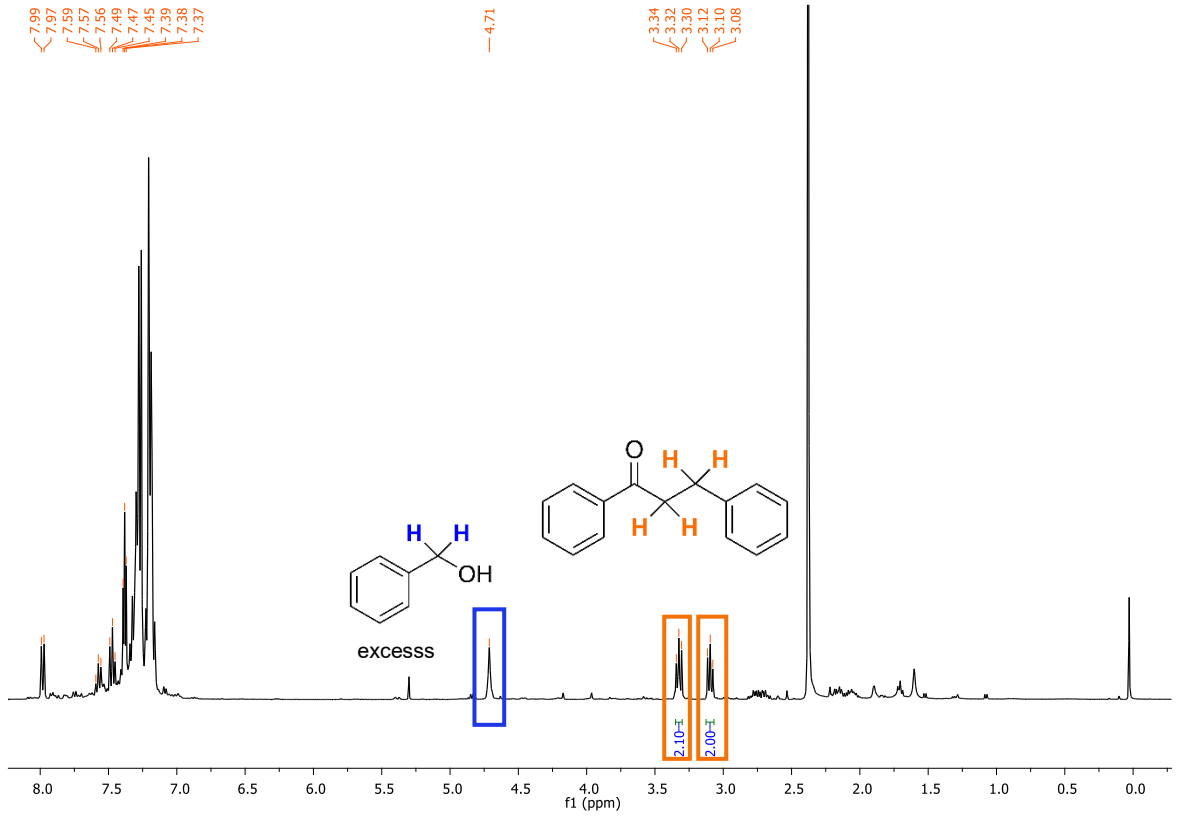

Figure A3.46. ^{1}H NMR spectrum of the reaction presented in Table 3.7, entry 4.

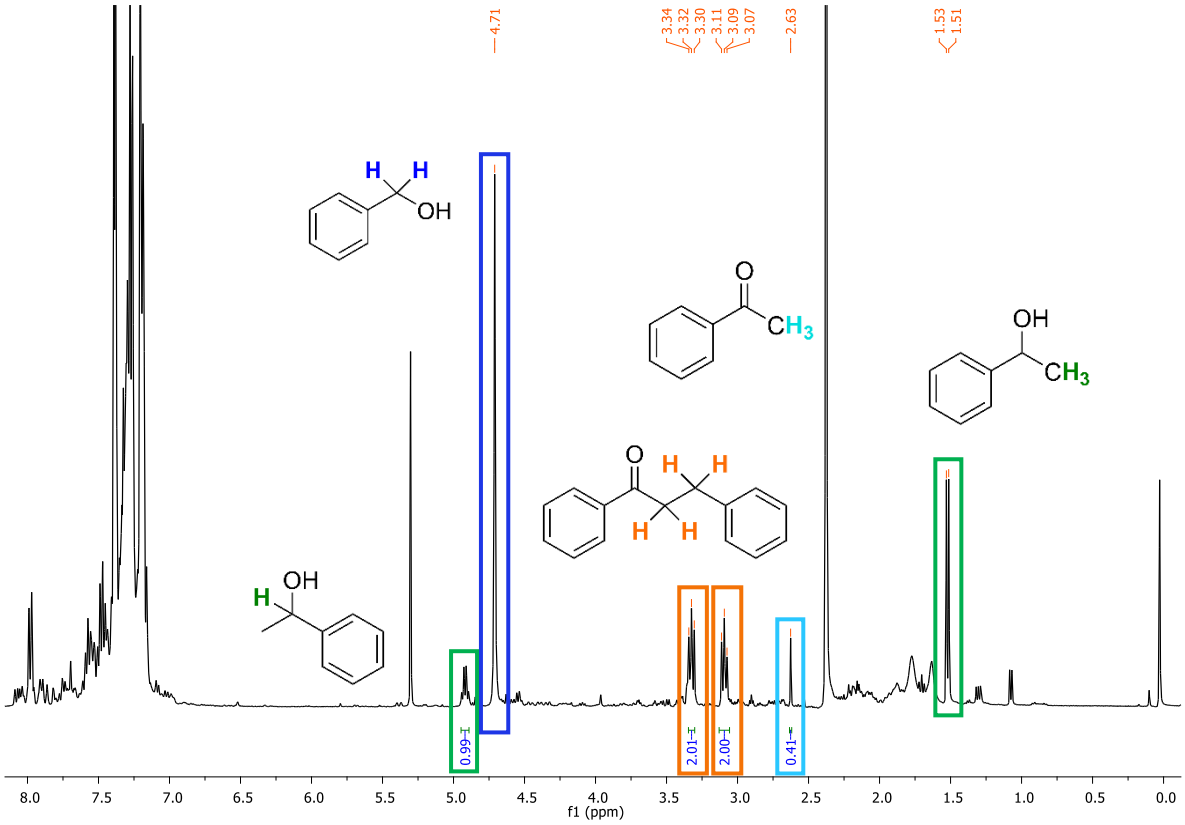

Figure A3.47. ^{1}H NMR spectrum of the reaction presented in Table 3.7, entry 5.

A3.4. NMR data of the β-Alkylation Between Alcohols

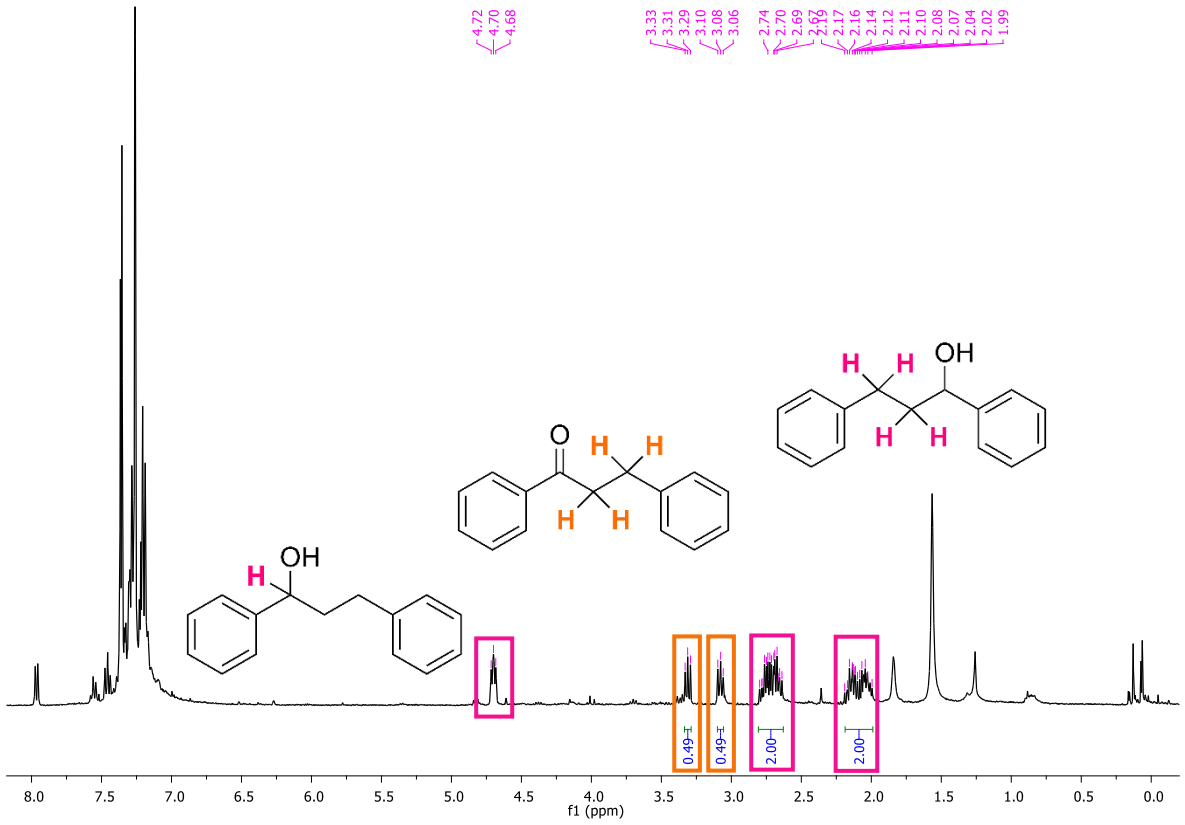

Figure A3.48. ^{1}H NMR spectrum of the reaction presented in Scheme 3.7.

A3.5. NMR data of the Aerobic Oxidation of Primary Amines to Amides

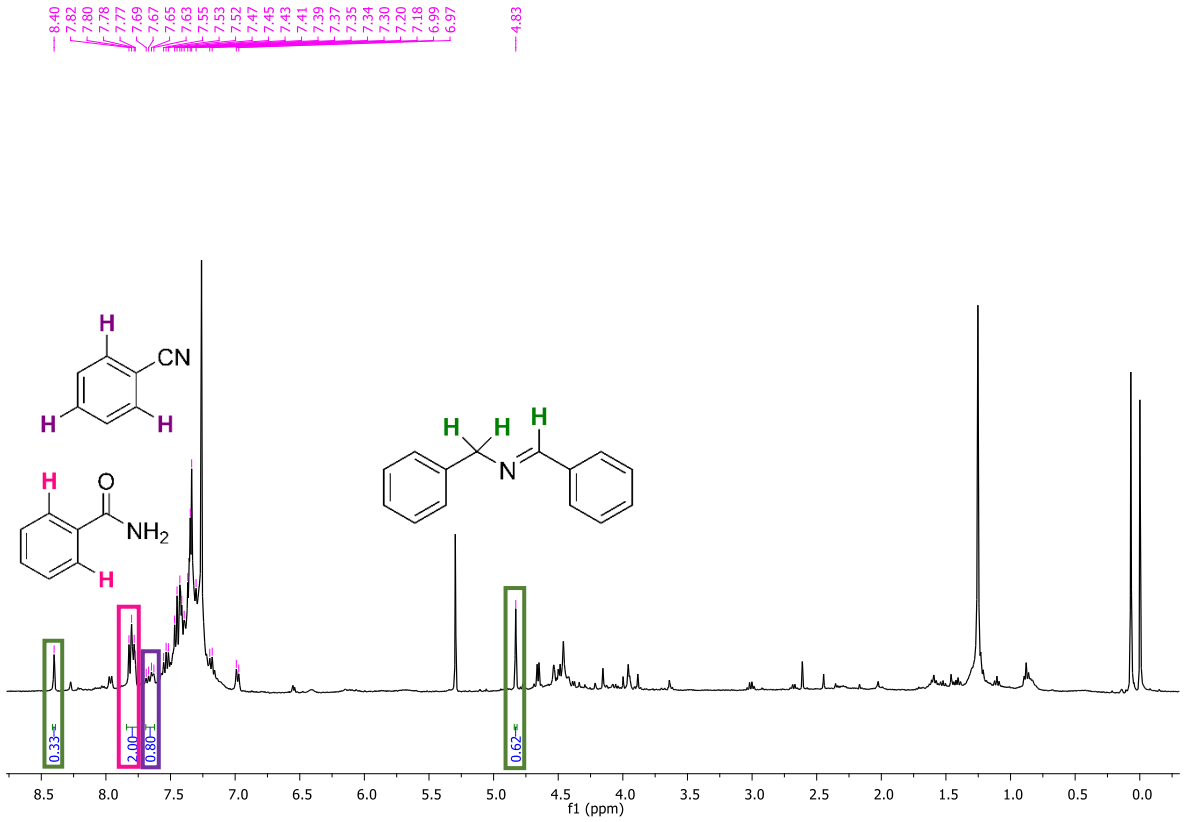

Figure A3.49. ^{1}H NMR spectrum of the reaction presented in Table 3.8, entry 2.